

**ERNEST ORLANDO LAWRENCE
BERKELEY NATIONAL LABORATORY**

LBNL-PUB--5440

**Laboratory Directed Research
and Development Program
FY 1997**

March 1998

RECEIVED
JUL 23 1998
OSTI

MASTER

DISTRIBUTION OF THIS DOCUMENT IS UNLIMITED

DISCLAIMER

This document was prepared as an account of work sponsored by the United States Government. While this document is believed to contain correct information, neither the United States Government nor any agency thereof, nor The Regents of the University of California, nor any of their employees, makes any warranty, express or implied, or assumes any legal responsibility for the accuracy, completeness, or usefulness of any information, apparatus, product, or process disclosed, or represents that its use would not infringe privately owned rights. Reference herein to any specific commercial product, process, or service by its trade name, trademark, manufacturer, or otherwise, does not necessarily constitute or imply its endorsement, recommendation, or favoring by the United States Government or any agency thereof, or The Regents of the University of California. The views and opinions of authors expressed herein do not necessarily state or reflect those of the United States Government or any agency thereof, or The Regents of the University of California.

Ernest Orlando Lawrence Berkeley National Laboratory
is an equal opportunity employer.

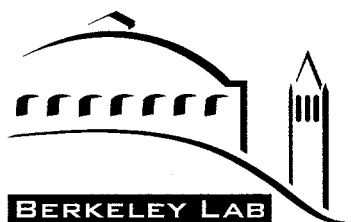
DISCLAIMER

**Portions of this document may be illegible
in electronic image products. Images are
produced from the best available original
document.**

**Report on
Ernest Orlando Lawrence
Berkeley National Laboratory**

**Laboratory Directed
Research and Development
Program**

FY 1997



**ERNEST ORLANDO LAWRENCE
BERKELEY NATIONAL LABORATORY
UNIVERSITY OF CALIFORNIA
BERKELEY, CALIFORNIA 94720**

Table of Contents

| | | |
|---|--|----|
| Introduction | | ix |
| Accelerator and Fusion Research Division | | 1 |
| Christine Celata Richard Donahue K. Leung Paul Luke Peter Zawislanski | A Neutron Logging Instrument for the Detection of Water and Chemical Waste | 1 |
| William Fawley Edward Lee | End-to-End Accelerator Modeling in the Presence of Strong, Collective Beam Fields | 2 |
| Alan Jackson Clyde Taylor | "Superbend"—A 5 T Bending Magnet Design for the ALS | 3 |
| Wim Leemans Jonathan Wurtele Swapan Chattopadhyay | Laser-Driven Acceleration of Particles | 5 |
| Jacques Millaud Howard Padmore Thomas Earnest David Nygren | Advance Towards the Next Generation of Pixellated Detectors for Protein Crystallography | 6 |
| Howard Padmore | Development of an Aberration Corrected Photoelectron Microscope for Surface Studies | 8 |
| Neville Smith | Spin-Polarized Photoemission Studies of Magnetic Surfaces, Interfaces, and Films | 8 |
| Chemical Sciences Division | | 11 |
| John Arnold | Network Silicates With Porphyrin Backbones: Novel Solids and Catalysts | 11 |
| Ali Belkacem | Numerical Treatment of Lepton Pair Production in Relativistic Heavy Ion Collisions Using Parallel Processing | 12 |
| David Chandler Martin Head-Gordon William Miller | Molecular Theory Group | 13 |
| Charles Harris | Magnetic Properties and Electron Localization at Interfaces | 15 |

| Investigator | Project Title | Page Number |
|--|---|-------------|
| Computing Sciences (Information and Computing Sciences Division, National Energy Research Scientific Computing Division, and Departments: Center for Computational Sciences and Engineering, Mathematics) | | 19 |
| Grigory Barenblatt Alexandre Chorin Ole Hald James Sethian | Mathematical and Numerical Algorithms for the Analysis of Cracks, Damage Accumulation, and Fracture in Solids | 19 |
| Phillip Colella Nancy Brown Michael Frenklach | High-Fidelity Simulation of Diesel Combustion | 21 |
| William Johnston Horst Simon | Scientific Computing on Clusters of Multiprocessor Systems (COMPS) | 23 |
| Ron Kimmel Ravi Malladi James Sethian | New Areas for Interface Techniques: Robotic Navigation and Shape Recognition | 25 |
| William Kramer | The Integration of PDSF, HENP Analysis, and the HPSS Data Archive | 25 |
| C. William McCurdy Thomas Rescigno | Electron Collisions With Molecules, Clusters, and Surfaces | 27 |
| Bahram Parvin Ge Cong | Volumetric Description from Multiple Views for 3D Microscopy | 29 |
| Horst Simon Beresford Parlett James Demmel | Sparse Linear Algebra Algorithms for MPPs | 31 |
| Earth Sciences Division | | 33 |
| Ilham Al Mahamid Jennie Hunter-Cevera | Effect of Biosorption on Actinide Migration in the Subsurface | 33 |
| Terrance Leighton Fred Brockman | Molecular and Functional Analysis for Evaluating Microbial Treatment Process Performance | 35 |
| George Moridis | Electromagnetic Methods for Fluid Emplacement and Monitoring in the Subsurface | 37 |
| Satish Myneni | High Resolution Microscopic and Spectroscopic Investigations of Mineral-Adsorbed Humic Substance Influence on Soil Contaminant Behavior | 40 |

| Investigator | Project Title | Page Number |
|---|---|--------------------|
| Karsten Pruess George Brimhall | Reactive Chemical Transport in Geologic Media | 41 |
| Garrison Sposito | Molecular Geochemistry of Clay Mineral Surfaces | 44 |
| William Stringfellow Jennie Hunter-Cevera | Development of Mixed Waste Bioremediation: Biodegradation of Complexing Agent, Ketone, and Heavy Metal Mixtures | 45 |
| Donald Vasco Lane Johnson | Advanced Computing for Geophysical Inverse Problems | 46 |
| Environmental Energy Technologies Division | | 49 |
| Elton Cairns | Direct-Ethanol Fuel Cells | 49 |
| Ronald Cohen | Instruments for the <i>in situ</i> Detection of NO, NO ₂ , and Their Precursors | 49 |
| Michael Frenklach | Mechanism and Modeling of Soot Formation in Hydrocarbon Flames | 50 |
| Mark Levine Lee Schipper Jayant Sathaye Lynn Price Nathan Martin Jonathan Sinton | Energy Efficiency and Demand in Industry: A Global Assessment | 51 |
| Stephen Selkowitz | The Virtual Building Laboratory | 54 |
| Life Sciences Division | | 57 |
| Manjit Dosanjh | Development of Genetically Manipulated Hepatic Cell Lines for the Evaluation of Cytotoxic Effect of Environmental Pollutants by Using Apoptosis as a Molecular Endpoint of Exposure | 57 |
| Robert Glaeser | ALS Protein Microcrystal Diffraction Camera | 59 |
| Joe Gray | Techniques for Discovery of Disease-Related Genes | 60 |
| Teresa Head-Gordon George Oster Daniel Rokhsar | Computational Biology | 62 |
| Paul Kaufman | Analysis of DNA-Damage Sensitivity of Yeast Mutants Lacking Chromatin Assembly Proteins | 65 |
| Terumi Kohwi-Shigematsu Yoshimori Kohwi | Isolation and Characterization of SATB1-Bound Sequences <i>in vivo</i> | 66 |

| Investigator | Project Title | Page Number |
|--|--|--------------------|
| Carolyn Larabell Jon Nagy | A Novel Technique to Follow Consequences of Exogenous Factors, Including Therapeutic Drugs, on Living Human Breast Epithelial Cells in 3D | 68 |
| Ruth Lupu | Development of Novel Biological Targeted Therapies for Breast Cancer | 69 |
| Norman Pace | Survey of Microbial Communities in Chemically Damaged and Control Environments | 70 |
| Maria Pallavicini Ron Jensen | Gene-Specific Biomonitoring to Assess Risk of Developing Environmentally-Induced Leukemia | 70 |
| Materials Sciences Division | | 73 |
| Carolyn Bertozzi | A New Strategy for the Introduction of Biocompatible Adhesive Coatings onto Material Surfaces | 73 |
| Daniel Chemla | Time-Resolved Spectroscopy of Magnetic Insulators | 74 |
| Dung-Hai Lee | Phosphorescent Molecule as a Probe in Near-Field Optical Microscopy and Spectroscopy, and the Electronic Correlation Effects on the Transport Properties of Carbon Nanotubes | 75 |
| Andrew Canning Daryl Chrzan Marvin Cohen Steven Louie John Morris, Jr. | Determining Macroscopic Materials Properties from Microscopic Calculations | 76 |
| Werner Meyer-Ilse John Brown David Attwood | Biological X-Ray Microscopy | 78 |
| John Morris, Jr. John Clarke Kannan Krishnan | SQUID-Based "Magnetic Microscopes" as Sensors for Nondestructive Evaluation | 80 |
| Miquel Salmeron Yuan-Ron Shen | Molecular Scale Imaging and Spectroscopy of Liquid Surfaces: Application to Environmental Studies | 82 |
| Michel Van Hove | MSD Theory and NERSC Computation for ALS Experiments | 84 |
| Shimon Weiss Paul Selvin Deborah Charych | Molecular Rulers for the Study of Synthetic and Biological Macromolecules in Aqueous Conditions | 86 |

| Investigator | Project Title | Page Number |
|---|--|-------------|
| Nuclear Science Division | | |
| Claude Lyneis Zu Qi Xie Clyde Taylor | A Third-Generation ECR Ion Source | 89 |
| Mario Cromaz James Symons Randy MacLeod I-Yang Lee | Distributed Construction and Analysis of Multidimensional Gamma-Ray Coincidence Databases | 90 |
| Jorgen Randrup | Directed Studies in Nuclear Theory | 91 |
| Physics Division | | |
| Saul Perlmutter Bruce Grossan | A Rapid-Response Search for Gamma-Ray Burst Optical Emission | 95 |
| David Nygren Douglas Lowder Martin Moorhead Gilbert Shapiro George Smoot Robert Stokstad | System Design and Initial Electronic Engineering for a Km-Scale Neutrino Astrophysical Observatory | 96 |
| Saul Perlmutter Peter Nugent Gerson Goldhaber Donald Groom Alex Kim | Exploring Scientific-Computational Collaboration: NERSC and the Supernova Cosmology Project | 97 |
| Saul Perlmutter Gerson Goldhaber Donald Groom Stephen Holland Carl Pennypacker R. Stover | Fabrication of Charge-Coupled Devices on a High-Resistivity Substrate for Astronomical Imaging | 99 |
| James Siegrist | Performance Modeling of Pixel and Silicon Strip Detectors for High-Luminosity Experiments | 100 |
| George Smoot Julian Borrill Andrew Jaffe | Cosmic Microwave Background Radiation Data Analysis | 102 |

| Investigator | Project Title | Page Number |
|---|---|--------------------|
| Structural Biology Division | | 103 |
| Stephen Holbrook | Determination of Macromolecular Structure by <i>ab initio</i> Phasing of Crystallographic Diffraction Data | 103 |
| Yeon-Kyun Shin | Structure and Conformational Dynamics Mediating Signal Transduction in Two Classical Membrane Proteins | 105 |
| Cross-Divisional | | 107 |
| Mark Alper Robert Bergman Jonathan Ellman Peter Schultz Heinz Frei | New Chemistry for Pollution Prevention Initiative: Selective Catalyst | 107 |
| Eleanor Blakely Thomas Budinger William Chu | Physics and Biology of Boron Neutron Capture Therapy | 111 |
| Stanley Goldman Tamas Torok | Use of Gene Sequencing, Signature Lipid Biomarker Analysis, and Microbial Physiology Testing—A Polyphasic Approach to Assess and Monitor Microorganisms in Damaged Environments | 113 |
| William Johnston William Greiman Gary Hoo Jason Lee Stewart Loken Brian Tierney Craig Tull Douglas Olson | Large-Scale Computing for Nuclear Physics and High Energy Physics Experiments | 114 |
| Acronyms and Abbreviations | | 117 |

Introduction

The *Ernest Orlando Lawrence Berkeley National Laboratory (Berkeley Lab) Laboratory Directed Research and Development Program FY 1997* report is compiled from annual reports submitted by principal investigators following the close of the fiscal year. This report describes the projects supported and summarizes their accomplishments. It constitutes a part of the Laboratory Directed Research and Development (LDRD) program planning and documentation process that includes an annual planning cycle, projection selection, implementation, and review.

The Berkeley Lab LDRD program is a critical tool for directing the Laboratory's forefront scientific research capabilities toward vital, excellent, and emerging scientific challenges. The program provides the resources for Berkeley Lab scientists to make rapid and significant contributions to critical national science and technology problems. The LDRD program also advances the Laboratory's core competencies, foundations, and scientific capability, and permits exploration of exciting new opportunities. Areas eligible for support include the following:

- Work in forefront areas of science and technology that enrich Laboratory research and development capability;
- Advanced study of new hypotheses, new experiments, and innovative approaches to develop new concepts or knowledge;
- Experiments directed toward proof of principle for initial hypothesis testing or verification; and
- Conception and preliminary technical analysis to explore possible instrumentation, experimental facilities, or new devices.

The LDRD program supports Berkeley Lab's mission in many ways. First, because LDRD funds can be allocated within a relatively short time frame, Berkeley Lab researchers can support the mission of the Department of Energy (DOE) and serve the needs of the nation by quickly responding to forefront scientific problems. Second, LDRD enables the Laboratory to attract and retain highly qualified scientists, and sup-

ports their efforts to carry out world-leading research. In addition, the LDRD program also supports new projects that involve graduate students and postdoctoral fellows, thus contributing to the education mission of the Laboratory.

Berkeley Lab has a formal process for allocating funds for the LDRD program. The process relies on individual scientific investigators and the scientific leadership of the Laboratory to identify opportunities that will contribute to scientific and institutional goals. The process is also designed to maintain compliance with DOE Orders, in particular DOE Order 413.2 dated March 3, 1997. From year to year, the distribution of funds among the scientific program areas will change. This flexibility optimizes the Laboratory's ability to respond to opportunities.

Berkeley Lab LDRD policy and program decisions are the responsibility of the Laboratory Director. The Director has assigned general programmatic oversight responsibility to the Deputy Director for Research. Administration and reporting on the LDRD program is supported by the Directorate's Office for Planning and Communications. LDRD accounting procedures and financial management are consistent with the Laboratory's accounting principles and stipulations under the contract between the University of California and the Department of Energy, with accounting maintained through the Laboratory's Chief Financial Officer.

In FY 1997, Berkeley Lab was authorized by the Department of Energy to establish a funding ceiling for the LDRD program based on 3.7% of the Laboratory's FY 1997 operating and capital equipment budgets. This funding level was provided to develop new scientific ideas and opportunities and allow the Laboratory Director an opportunity to initiate new directions. However, budget constraints limited available resources, so only \$8.7 M was expended for operating and \$0.4 M for capital equipment.

In FY 1997, scientists submitted 156 proposals requesting over \$22 M. Sixty-six projects were funded, with awards ranging from \$9 K to \$423 K.

Accelerator and Fusion Research Division

A Neutron Logging Instrument for the Detection of Water and Chemical Waste

Principal Investigators: Christine Celata, Richard Donahue, K. Leung, Paul Luke, and Peter Zawislanski

Project No.: 96001

Project Description

The purpose of this project was to use LBNL technology to increase by at least an order of magnitude the neutron flux from downhole neutron logging tools, to add to the tools a new state-of-the-art room-temperature semiconductor gamma-ray detector, and to investigate the feasibility of using such an enhanced tool to locate and quantify contaminants in the earth and in other media.

Most of the activity in FY97 was directed to testing the ion source, and designing and testing the acceleration section which would be required in order to propagate the enhanced flux in a commercial tube. It was not possible on the funding provided to incorporate the source into a neutron tube, since the cost of the tube is on the order of \$100K. A small amount of money was used for 3D computer modeling, in order to look at the exciting possibility of 3D localization, which appears to be possible with the enhanced neutron flux available from the LBNL ion source.

Accomplishments

Testing of the rf-driven multicusp ion source, and design and testing of the accelerator section, were

completed. The ion source current (up to 1 A / pulse for a 3-mm aperture, over 90% monatomic) is projected to increase the neutron yield from D-T or D-D tubes by one to three orders of magnitude. More flux is available simply by increasing the aperture diameter. The acceleration section was tested to 100 kV.

Significant advances were made in miniaturizing the rf matching network, enabling it to fit within a 2-inch diameter hole, and in improvements to the rf antenna coating. A novel antenna technology, with promising potential for other rf-driven plasma applications, was developed and tested. This consisted of forming the rf antenna housing using extruded quartz tubing, to relieve electrical and thermal stresses during the high power rf plasma operation. A patent application has been obtained for this technology.

A Ph.D. thesis was published and the degree awarded on the basis of the above and previous year's LDRD work on the ion source and accelerator.

The high current produced by the ion source offers the exciting possibility of having sufficient signal to be able to collimate returning gamma rays, and with deconvolution algorithms to localize detected materials in 3D. With present technology, readings are only taken vs. depth. This past year radiation transport modeling work using the 3D Monte Carlo code MCNP resulted in the preliminary design of a detector / collimator which is predicted to be able to discern 1-mm salt/TCA-filled fractures in granite with a signal-to-noise ratio of about a factor of 10. These fractures may be detected many tens of cm from the source / detector, depending upon source intensity. Angular resolution is as indicated in Fig. 1.

New estimates have also been made for the detection of trace quantities of lead in a sand media. Results indicate that lead may be detected *in situ* in quantities from a few tens of ppm to a few hundred ppm for neutron source intensities from 10^9 n/s to 10^7 n/s, respectively.

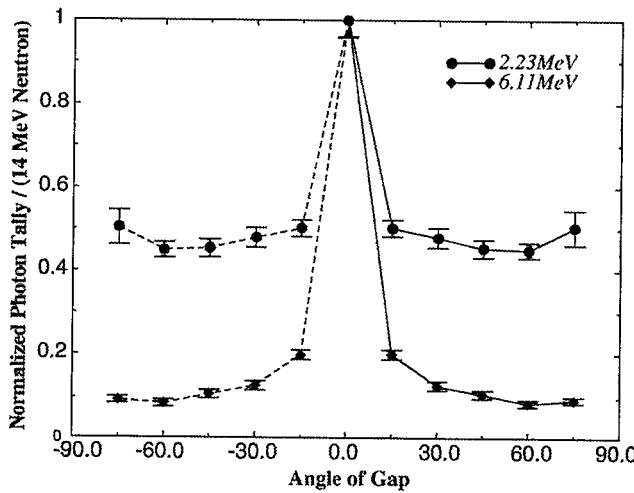


Figure 1. Normalized photon flux detected from a 1-mm salt-water filled fracture. The 2.23 MeV curve is a measure of the flux of 2.23 MeV photons from thermal neutron capture in hydrogen. The 6.11 MeV curve is a measure of the 6.11 MeV photons from thermal neutron capture in chlorine. The angle on the bottom axis refers to the angle of the detector collimator with respect to the fracture.

Publications

L.T. Perkins, C. Celata, Y. Lee, K.N. Leung, D.S. Picard, R. Vilaithong, M.C. Williams, and D. Wutte, "Development of a Compact, RD-Driven, Pulsed Ion Source for Neutron Generation," Proc. of 14th International Conf. on Applications of Accelerators in Research and Industry, Denton, TX, November 6-9, 1996.

C.M. Celata, M. Amman, R. Donahue, E. Greenspan, D. Hua, Y. Karni, K. Leung, P.N. Luke, L.T. Perkins, and Peter T. Zawislanski, "A New Intense Neutron Generator and High-Resolution Detector for Well Logging Applications," poster presented at the 3rd Topical Meeting on Industrial Radiation and Radioisotope Measurements and Applications, October 6-9, 1996, Raleigh, NC.

C.M. Celata, M. Amman, R. Donahue, K. Leung, P.N. Luke, L.T. Perkins, Peter T. Zawislanski, E. Greenspan, D. Hua, and Y. Karni, "A New Intense Neutron Generator and High Resolution Detector for Well Logging Applications," p. 29, Proc. of IEEE Nuclear Science Symposium, Anaheim, CA, November 2-9, 1996.

Luke Perkins, "A Compact Ion Source for Intense Neutron Generation," Ph.D. thesis, Department of Nuclear Engineering, University of California at Berkeley, Berkeley, CA, December, 1997.

C.M. Celata, M. Amman, R. Donahue, D. Hua, K.N. Leung, P.N. Luke, L.T. Perkins, and Peter T. Zawislanski, "A New Intense Neutron Tool for Radiography and Detection of Water and Ground Contaminants," to be published in Proc. of the 1997 Particle Accelerator Conference, Vancouver, B.C., Canada, May 12-16, 1997.

C.M. Celata, Y. Lee, K.N. Leung, D.S. Picard, R. Vilaithong, M.D. Williams, and D. Wutte, "A Compact, Rf-Driven, Pulsed Ion Source for Intense Neutron Generation," to be published in the Proc. of the 1997 Particle Accelerator Conf., Vancouver, B.C., Canada, May 12-16, 1997.

D.D. Hua, R.J. Donahue, C.M. Celata, and E. Greenspan, "Monte Carlo Simulations of Neutron Well-Logging in Granite and Sand to Detect Water and Trichloroethane (TCA)," LBNL-40866, in preparation.

End-to-End Accelerator Modeling in the Presence of Strong, Collective Beam Fields

Principal Investigators: William Fawley and Edward Lee

Project No.: 97001

Project Description

The purpose of this LDRD project was to collect an ensemble of independent, computational simulation tools to examine a variety of physics issues for the simulation of intense particle beams in which collective fields play an important role. A primary focus of this work was directed toward "end-to-end" modeling of a generic heavy-ion accelerator for inertial fusion energy applications. A number of issues (e.g., alignment and mechanical tolerance criteria, emittance growth, multiple beam injector design) must be satisfactorily answered before a major new heavy-ion fusion (HIF) accelerator could be built (at LBNL or anywhere else). The LDRD funded activities in two specific areas: simulation of the "final focus" and reactor transport region of an HIF driver; and simulation of transport through a driver-scale, intra-accelerator focusing lattice to

determine the alignment tolerances needed to limit unwanted transverse emittance growth.

Accomplishments

For the final focus/reactor transport work, we decided to connect two large 3D Particle-in-Cell (PIC) simulation codes, WARP3D and BPIC3D. The former employs an electrostatic field solver and has been in extensive use at LLNL and LBNL to model transport of intense HIF beams in different types of focusing lattices, including a recirculator. We ported WARP3D to the NERSC T3E, which was successful with the exception of being unable to use PVM sockets to control execution from a remote workstation. We also completed BPIC3D's conversion to a "pure" Fortran90 source and began the porting process to the T3E. Significant work was done on perfecting an electromagnetic field boundary algorithm in BPIC3D to subdivide the simulation region into separate regions of different spatial resolution. This type of decomposition is necessary for efficient computation of multiple beam propagation to a target pellet in a single reactor chamber. A simple IO interface based on PDB-library intermediate files permitted BPIC3D to read output particle 6-D phase space information written by WARP3D at a location just before the reactor chamber entrance. BPIC3D then follows the beam to the target, employing a fully relativistic particle mover and full E&M field solver respectively. The two codes examined transport behavior of a beam undergoing longitudinal drift compression via an energy tilt through a HIBALL-II final focus design. Despite the large initial head-to-tail energy variation, we found that approximately 85% of the beam pulse would be deposited upon a 3-mm-radius pellet.

For the intra-accelerator transport simulations, we used the 2D electrostatic code HIBEAM. This code was extensively upgraded to employ numerous Fortran90 features such as dynamic memory allocation, array arithmetic, and modular "privatization" of data. We also wrote a new accelerator lattice generation routine that can parse input files in MAD-style format (originally developed at CERN). Within the context of the LDRD, HIBEAM has been used to study emittance growth of space-charge dominated ion beams in a 100-period lattice of electrostatic quadrupoles. Initial results suggest alignment tolerances of 100-microns or better should be more than sufficient.

Publications

Various aspects of this work were presented at the International Conference on Computational Physics: PC'97 (Santa Cruz, CA; August 1997); the International Symposium on Heavy-Ion Fusion (Heidelberg, Germany; September 1997); and the Plasma Physics Division meeting of the American Physical Society (Pittsburg, PA; November 1997). A paper on the final focus transport simulations is in the early stages of preparation.

W.M. Fawley, J-L. Vay, and D.P. Grote, "End-to-End Modeling of a Heavy-Ion Fusion Accelerator," 1997 International Conference on Computational Physics, *Bull. Amer. Phys. Soc.* **42**, 1583 (1997).

Jean-Luc Vay, "Solution of Elliptic Equations Without Initial Boundary Values," p. 595, Proceedings 11th Conference on the Computation of Electromagnetic Fields, Rio de Janeiro, Brazil, November, 1997.

Jean-Luc Vay, "Transmitted-Information' Boundary Condition for the Wave Equation," p. 7, Proceedings 11th Conference on the Computation of Electromagnetic Fields, Rio de Janeiro, Brazil, November, 1997.

W.M. Fawley, J-L. Vay, D.P. Grote, and W.M. Sharp, "End-to-End Modeling of a Heavy-Ion Fusion Accelerator," *Bull. Amer. Phys. Soc.* **42**, 2022 (1997).

"Superbend"—A 5 T Bending Magnet Design for the ALS

Principal Investigators: Alan Jackson and Clyde Taylor

Project No.: 95002

Project Description

The ALS can be upgraded by replacing some of the gradient bend magnets with superconducting (SC) dipoles, and extra quadrupoles to match the lattice functions. The short 4 T dipoles (at 1.5 GeV) can be ramped to 5.1 T for operation at 1.9 GeV. These magnets would provide bend-magnet synchrotron

radiation with a critical energy of 6 keV. This is much better suited to protein crystallography and other small sample x-ray diffraction and adsorption studies than that currently available at the ALS. This project was to design, build, and test a prototype magnet to verify the concept. The proposed design is unique; it would seem that similar magnets could be developed for other light sources and accelerators.

The C-shaped "cold iron" design has an "internal" pole-piece iron driven to about 5.5 T and a magnetic length of only 24 cm along the beam direction. The magnet (in its cryostat) must be installed around the existing ALS beam line. Since the magnet is very short, end effects are determined by the gap. The final phase of the LDRD was to characterize the magnetic field distribution of this unique magnet.

Accomplishments

After studying several designs during FY95, three coil sets were built during FY96 using round SSC superconductor wire and different construction methods (Figure 1, left). All had excessive training and insufficient operating margin to be practical for use in the ALS.

During FY97, after extensive structural analysis, a fourth coil set, SB 4, was designed and built using

rectangular wire with a 4:1 copper to superconductor ratio and varnish insulation (Figure 1, right). SB 4 was "wet-wound" with filled epoxy, whereas the earlier magnets were vacuum impregnated. Also, the structural support was simplified and improved by eliminating the four-piece "collet" between the winding outer surface and the aluminum ring structure, and also by enlarging the aluminum structure to fill the entire space between the coil outer surface and the 410-mm outer ring diameter. In addition, the coil was assembled with a 0.1-mm gap between the iron pole and the coil inner surface; this gap, which is closed after cooldown, reduces the coil stress due to differential thermal contraction between coil and iron pole.

Each coil set was installed in an iron yoke and tested by increasing the current until a quench occurred. After recooling to 4.2 K with liquid helium, the process was repeated until the maximum current was reached. Figure 2 shows the training quenches for all magnet tests. Quench current is shown normalized to the current required for 1.9 GeV. The final model, SB 4, reached the required current with no training, thus establishing the feasibility of the new approach.

A cryostat is being built in early FY98 to measure field uniformity.

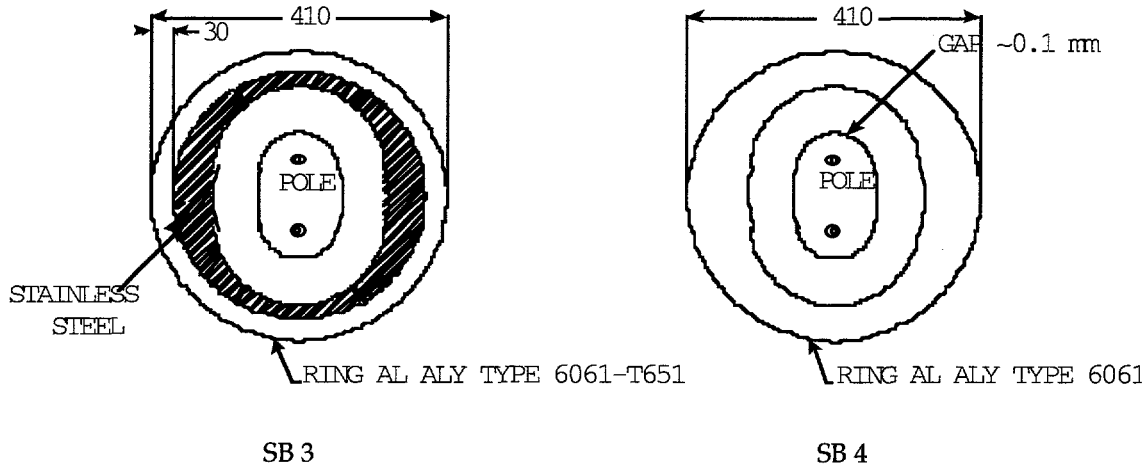


Figure 1. (left): The preliminary design, SB 3, in FY96. (right): The design for SB 4 in FY97.

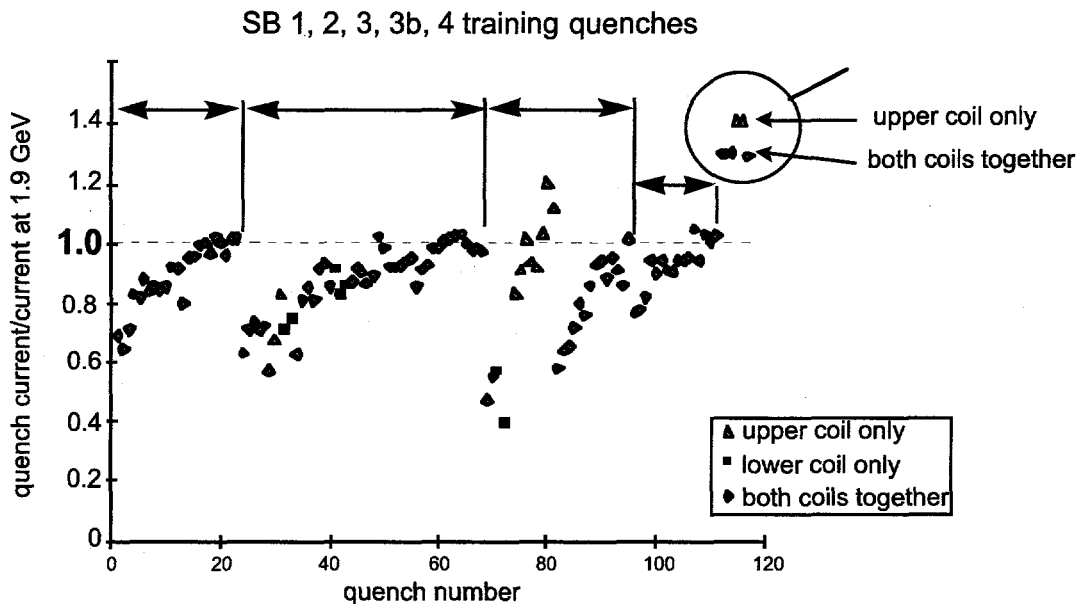


Figure 2. Summary of all test results for the four coil sets.

Publication

C.E. Taylor, A. Jackson, K. Chow, S. Caspi, A. Lidsky, S.T. Wang, and S. Chen, "Superbend—A High Field, Short Bend Magnet for a Synchrotron Light Source," to be submitted to *Nuclear Instruments and Methods*.

plasma channels, and c) to inject femtosecond (fs)-long electron bunches into the channel. Numerical tools and computational codes will be developed and integrated with the experimental program for fast and accurate modeling of the experiments. This work may lead to future compact accelerators using plasma or other advanced accelerator concepts.

Accomplishments

Experiments

During FY97, a terawatt laser system based on chirped pulse amplification has been designed and constructed. The present system is designed to produce a short pulse (50–70 fs) with a peak power of up to 3 TW, with center wavelength around 0.8 μ m and a 100–250 ps-long pulse containing 300–400 mJ at 0.8 μ m. The long pulse will be used to produce 1 cm-long plasma channels by focusing the beam to a line focus with a cylindrical lens. The short pulse will be used to excite the plasma wake. At the present time, all key components of the laser system have been built and are being commissioned. The power amplifier commissioning is to be completed in the next 2 months and is expected to provide up to the designed 3 TW in a short 70-fs pulse.

Initial experiments have begun to study the production of plasma channels. The laser beam was focused into a vacuum chamber filled with nitrogen

Laser-Driven Acceleration of Particles

Principal Investigators: Wim Leemans, Jonathan Wurtele, and Swapan Chattopadhyay

Project No.: 97002

Project Description

This is an experimental and computational study of a particle accelerator based on ultra-high gradient (10's of GeV/m) laser-driven acceleration over long distances (1–10 cm) in plasmas. Experimental techniques will be developed to a) channel ultra-high intensity laser pulses in cm-long, laser-produced plasmas, b) excite, probe, and control longitudinal wakes with multi-GeV accelerating gradients in these

gas or hydrogen gas. A Mach-Zehnder interferometer was built which uses a 70-fs long laser pulse at 400 nm wavelength. Using this interferometer, we have been able to observe the creation of the plasma and subsequent hydrodynamic blow-out, leading to formation of a hollow channel. Parametric studies are underway to determine the optimum laser energy and pulse length for efficient formation of the plasma channel, and the optimum lens configuration for producing long (cm) plasmas in a supersonic gas jet.

We have also developed a single shot frequency resolved optical gating diagnostic which allows optimization and measurement of pulse shape. It will be used in upcoming experiments to study time-resolved wavelength changes during the wake-field driving pulse as it excites the plasma wake.

Theory

As part of an ongoing program of developing fast, efficient numerical tools for designing plasma based accelerators, development is underway of a code for simulating wake-field generation and laser propagation in a plasma channel, where the plasma electrons are modeled as a cold, nonrelativistic fluid. Although fluid codes cannot (fully) account for trapped particles or wave-breaking, as well as other purely kinetic effects, they have the advantage that one has control over the detailed physics involved. Using this model, the response of a nonuniform plasma to a laser pulse, with short duration compared to the plasma period, has been calculated. For non-uniform equilibrium plasma density we observe dissipation of the wake fields and a related fine-scale spatial structure in the electric and magnetic fields.

The imprint of the plasma on the laser pulse evolution in a uniform plasma and a channel has also been studied. From simple one-dimensional scaling laws, laser wavelength reddening and pulse length shortening are qualitatively described.

In collaboration with colleagues from the Naval Research Laboratory, we have also proposed a novel scheme for particle injection into plasma wakes based on a colliding laser pulse scheme. Simulations indicate that the physical mechanism for the particle trapping is a momentum and phase kick caused by the ponderomotive beatwave potential of the two counter-propagating, colliding laser pulses. Particle tracking simulations in 3D further indicate that production of high current electron bunches as short as 1 fs, with a mean energy on the order of 25 MeV, a normalized energy spread of 0.3 %, and a normalized

emittance of 1 mm-mrad are possible, using injection laser pulse intensities on the order of 10^{17} W/cm².

Publications

W.P. Leemans, P. Volfbeyn, K.Z. Guo, S. Chattopadhyay, C.B. Schroeder, B.A. Shadwick, P.B. Lee, J.S. Wurtele, and E. Esarey, "Laser Driven Plasma Based Accelerators, Wakefield Excitation, Channel Guiding, and Laser Triggered Particle Injection," *Phys. Plasmas*, to be published.

E. Esarey, R.F. Hubbard, W.P. Leemans, A. Ting, and P. Sprangle, "Electron Injection Into Plasma Wake Fields by Colliding Laser Pulses," *Phys. Rev. Lett.* **79**, 2682-2685 (1997).

P. Volfbeyn, P.B. Lee, J. Wurtele, W.P. Leemans, and G. Shvets, "Driving Laser Pulse Evolution In A Hollow Channel Laser Wakefield Accelerator," *Phys. Plasmas* **4** (9), 3403-3410 (1997).

Advance Towards the Next Generation of Pixelated Detectors for Protein Crystallography

Principal Investigators: Jacques Millaud, Howard Padmore, Thomas Earnest, and David Nygren

Project No.: 95010

Project Description

To develop fast x-ray area detectors for time-resolved and static crystallography, we have pursued the massively parallel instrumentation of pixel detector arrays. This will lead to a large area detector technology with outstanding rate and dynamic range capability. The system will be capable of handling rates as high as 5×10^2 x rays/s/cm². It will revolutionize time-resolved diffraction studies and significantly improve static crystallography studies currently based on CCD detectors.

The approach is to fabricate separately arrays of PIN diodes (pixels) and the Application Specific Integrated Circuits (ASICs) for read-out. The interconnections between the detector and the ASIC

will use flip chip technology. The resulting modules will be assembled in larger arrays.

Accomplishments

The porting of the design to a more advanced integrated circuit process (0.5 μ m, 3 metals) has been somewhat slower than expected due to some unforeseen design-rule changes by the foundry. However, the latest version of the 16x16 array was delivered and appears to have full functionality. This is the first time that we have demonstrated the combined operation of the high-sensitivity analog front end of the read-out based on the column architecture. Both subsystems have been proven extensively in previous years, however their integration remained to be demonstrated. Threshold levels of 1000 electrons (3.7 KeV) appear to ensure a stable operation of the ASICs. This is very much within the specification of a minimum photon energy of 6.0 KeV. We have worked closely with industry to find a flip-chip assembly process that is compatible with prototyping at the chip level, rather than the wafer level.

Intensive and extensive characterization is being done, and ASICs and detector arrays will then be hybridized. The assembly will undergo full characterization using a rotating anode x-ray source. The data acquisition system has been developed by Professor Xuong and his team at the University of California, San Diego.

A hybridized 8x8 array has been tested as a detector for electron microscopy at Donner Lab and U.C. San Diego. This approach appears promising at energies between 60 KeV and 200 KeV. Two publications have resulted from these tests.

During the period in review, this work was a joint collaboration with a NIH grant at the University of California, San Diego.

Additional support from NIH/UCSD is in place to pursue the design to the level of a 50x50 pixel detector system.

Publications

E. Beuville, C. Cork, T. Earnest, W. Mar, J. Millaud, D. Nygren, H. Padmore, B. Turko, and G. Zizka, "A

2D Smart Pixels Array for Time Resolved Protein Crystallography," *IEEE Trans. on Nucl. Sci.* **43**(3), 1243-7 (1996).

B.T. Turko, E. Beuville, J. Millaud, and H. Yaver, "A/D Processing System for 64-Element Pixel Detector," *IEEE Trans. on Nucl. Sci.* **43**(3), 1623-5 (1996).

E. Beuville, J.F. Beche, C. Cork, V. Douence, T. Earnest, J. Millaud, D. Nygren, H. Padmore, B. Turko, G. Zizka, P. Datte, and N.-H. Xuong, "A 16x16 Pixel Array Prototype for Protein Crystallography," *Nucl. Inst. and Method* **A395**, 429-34 (1997).

N.H. Xuong, P. Datte, E. Beuville, T. Earnest, H. Padmore, J. Millaud, and D. Nygren, "An Extremely Fast Direct Photon Counting Detector for Protein Crystallography," *IUCR*, 1996.

E. Beuville, J.-F. Beche, C. Cork, V. Douence, T. Earnest, J. Millaud, D. Nygren, H. Padmore, B. Turko, G. Zizka, P. Datte, and N.-H. Xuong, "Two-Dimensional Pixel Array Image Sensor for Protein Crystallography," *Proceedings of the SPIE Conference*, Denver, CO, August, 1996.

E. Beuville, J.-F. Beche, C. Cork, V. Douence, T. Earnest, J. Millaud, D. Nygren, H. Padmore, B. Turko, G. Zizka, P. Datte, and N.-H. Xuong, "A Prototype 8x8 Pixel Array X-Ray Detector for Protein Crystallography," *Nucl. Inst. and Method* **A391**, vol. 3 (1997).

G.Y. Fan, P. Datte, E. Beuville, J.-F. Beche, J. Millaud, K.H. Downing, F.T. Burkard, M.H. Ellisman, and N.-H. Xuong, "Event-Driven 2D Detector for Digital Electron Imaging," *Proceedings of the 55th Annual Meeting of the Microscopy Society of America, Digital Imaging in Electron Microscopy*, Cleveland, OH, August 10-14, 1997.

G.Y. Fan, P. Datte, E. Beuville, J.F. Beche, J. Millaud, K.H. Downing, F.T. Burkard, M.H. Ellisman, and N.-H. Xuong, "ASIC Based Event-Driven 2D Digital Electron Counter for TEM Imaging," accepted for publication in *Ultramicroscopy*.

Development of an Aberration Corrected Photoelectron Microscope for Surface Studies

Principal Investigator: Howard Padmore

Project No.: 97003

Project Description

The goal of this project is to develop an aberration balancing scheme for a full-field photoemission microscope. This first year of the project concentrated on developing a full theoretical model of the aberration corrector and its operation in a 30-KV microscope. Photoemission electron microscopy (PEEM) involves illuminating a field, typically 30 μm in diameter, and imaging the emitted photoelectrons. Combined with tunable high brightness synchrotron radiation, this imaging method can be combined with spectroscopy, by recording images at successively higher photon energies through an absorption-edge region. X-ray absorption spectroscopy gives detailed information about chemical state at the surface, and combined with high resolution imaging, it becomes a powerful tool in investigations of surface chemistry. The limitation of the technique is its limited spatial resolution, typically 0.1 μm . This limitation is caused by the combination of the chromaticity of the electron microscope lenses, with the energy spread of the photoemitted electrons. The aim of this project is to overcome this by aberration balancing.

Accomplishments

The key concept for the type of compensation used here was published 3 or 4 years ago by Gertrude Rempfer (University of Portland). It involves the use of an electron mirror to produce equal and opposite aberrations to the sum of those produced by the transmission lenses of the rest of the microscope. Although it is easy to design an electron mirror with the right characteristics, this idea is difficult to implement, as the beam has to pass through a magnet sector to separate the incoming and outgoing beams. We have designed a 90-degree magnetic sector that has the desired double-focusing properties, has flat field planes, and is achromatic. Each arc of the sector, incoming and outgoing, is arranged in a triplet achromat structure. This has been studied using

analytic methods, and real-edge effects have been studied using finite element numerical methods. This study has shown that, combined with a correctly designed mirror, objective, and projector lenses, the microscope will have a resolution of 2 nm. If we can reach this target, this will revolutionize the use of synchrotron radiation spectroscopy in high-resolution surface studies. As part of this work, we have completed the commissioning of a noncorrected high voltage PEEM. The microscope works as predicted and has enabled us to verify the lens-focusing relations for a wide range of conditions. This microscope was designed to accept the new corrector when complete.

Spin-Polarized Photoemission Studies of Magnetic Surfaces, Interfaces, and Films

Principal Investigator: Neville Smith

Project No.: 94027

Project Description

The principal objective of this project, namely, to introduce techniques of spin-polarized photoemission and magnetic circular dichroism at the ALS, has been accomplished. An electron spin analyzer has been installed on the photoemission system of Beamline 9.3.2 and the experimental program has begun. Circularly polarized x rays are being generated on Beamline 7.0 using a quarter-wave retarder of the transmission multilayer type. Preliminary experiments in magnetic circular dichroism in photoemission from Gd have already been performed.

Accomplishments

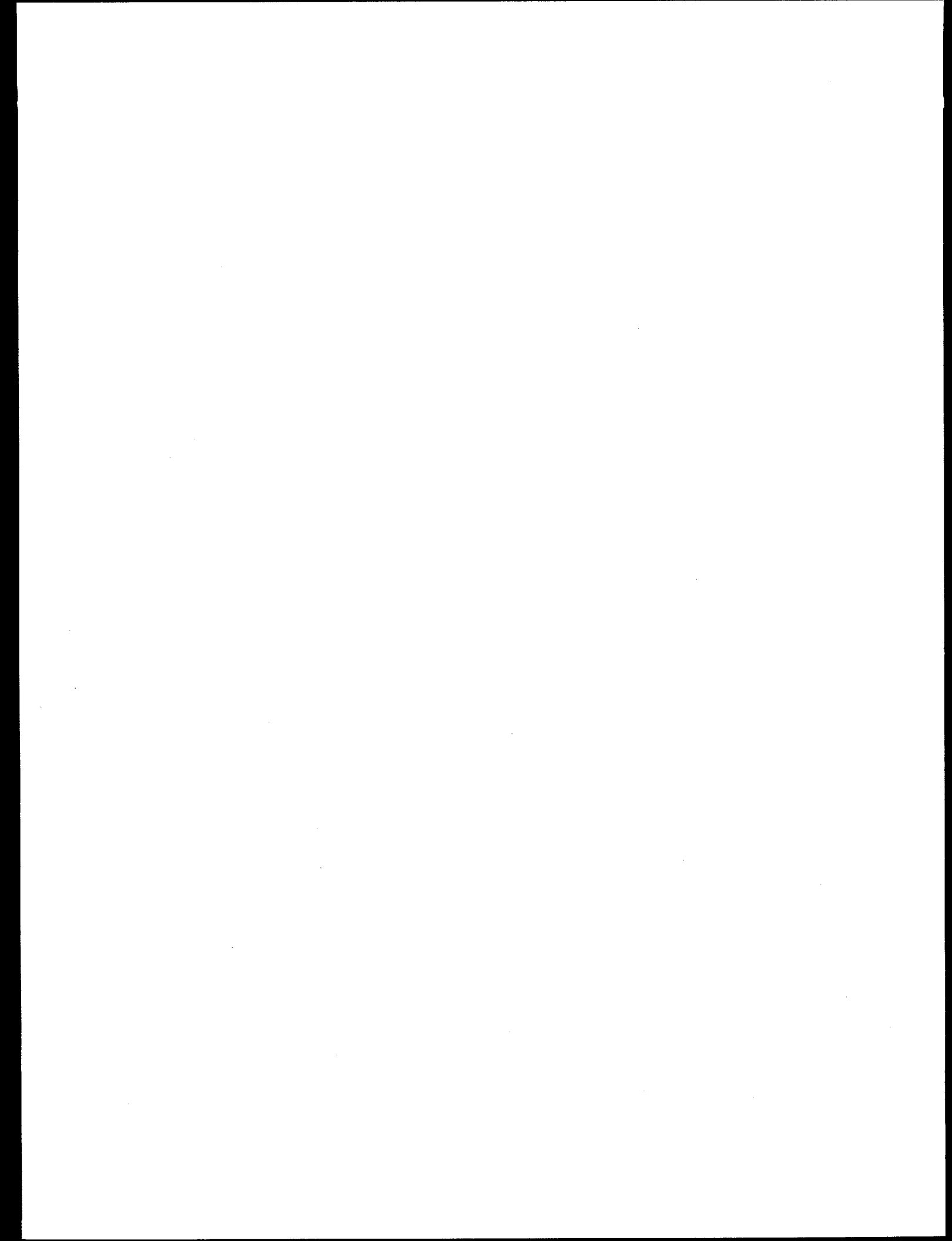
In the final few months of this project (in early FY97), preliminary experiments in magnetic circular dichroism were completed. Linear polarized soft x rays were converted to elliptical polarization at the Fe L₃ line (707 eV) using magnetic circular dichroism (MCD) on transmission through thin Fe films. A linear polarizer measured the transmitted

polarization at different incidence angles and found it to vary as expected from a model for in-plane magnetization, and also to exhibit a weak MCD effect at normal incidence, which was interpreted as originating from perpendicular interface anisotropy. An MCD signal from a downstream Fe film was produced by switching the helicity of x rays transmitted through an upstream circular polarizer. Practical considerations for optimizing the production of circular polarization and synchrotron radiation applications using these circular polarizing filters

were evaluated. Please refer to the FY96 LDRD Annual Report for additional details on techniques and methodology.

Publication

J.B. Kortright, S.-K. Kim, T. Warwick, and N.V. Smith, "Soft X-Ray Circular Polarizer Using Magnetic Circular Dichroism at the Fe L₃ Line," *Appl. Phys. Lett.* **71**(11), 1146 (1997).



Chemical Sciences Division

Network Silicates With Porphyrin Backbones: Novel Solids and Catalysts

Principal Investigator: John Arnold

Project No.: 96003

Project Description

The ability of chemists to control chemical and physical properties on the molecular scale has been the major driving force in synthetic chemistry over the last hundred years. It is only quite recently, however, that attention has been focused on more complex supramolecular systems, where small molecules are employed as templates for the synthesis of complex 2- and 3-dimensional framework structures. We intend to lead this research into a new area of study by fabricating robust arrays incorporating porphyrin backbones, held together by strong siloxane linkages built using sol-gel chemistry. If this approach is successful it will lead to a new class of materials, engineered by molecular chemistry to control structural relationships and pore sizes.

In concert with the idea to build new supramolecular compounds, a second important aspect of this work will apply this chemistry to the preparation of new heterogeneous porphyrin-based catalysts for alkane oxidation and olefin epoxidation.

Over the years, numerous models have been prepared in attempts to mimic enzyme active sites, such as those, for example, in cytochrome P-450. To prevent degradation of the catalytically active site, nature employs protein sheaths to control the local environment. We propose to exert similar control by building frameworks using the chemistry described herein. Since they are based on molecular chemistry, these systems combine the attractive features of both homogeneous catalysts (mainly 'tunability' and control of the catalyst center) with those of solid-

phase heterogeneous catalysts, such as aluminosilicates. This synergism between homogeneous and heterogeneous catalysis may result in the development of a new range of highly selective, environmentally benign catalysts.

In addition to the catalytic potential of these compounds, we envisage a number of other interesting applications, including potential uses as sensors, large-pore molecular sieves, and magnetic and conducting solids.

Accomplishments

Our continuing studies have focused on the synthesis of porphyrin monomers as illustrated in the schemes below. A number of routes are being used to condense these functionalized monomers with reactive metal complexes; one example using a mono-substituted derivative is shown below (Figure 1). The general idea is to first develop one-dimensional model systems to identify the most efficient condensation route, which will then be applied to more complex 2D and 3D structures.

A number of new materials have been prepared and we are currently engaged in studies to determine their structures and catalytic potential. In addition to these advances, work on this project has resulted in the synthesis of a number of novel porphyrins; this is an area of chemistry we hope to develop extensively in the near future.

Our results demonstrate that a high degree of functionality is possible in the network structure building blocks. The ability to control such functionality will become increasingly important as we begin to assemble solid structures, where they will influence factors such as solubility, rates of polymerization, and pore size. We will continue to look for new ways to assemble functionalized porphyrins and for new methods to oligomerize and polymerize these monomers during the course of the project.

Publication

"Metal Complexes of Hydroxyporphyrins," in preparation.

Fig. 1a

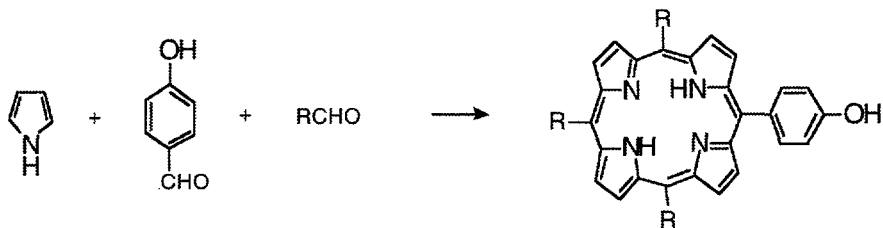


Fig. 1b

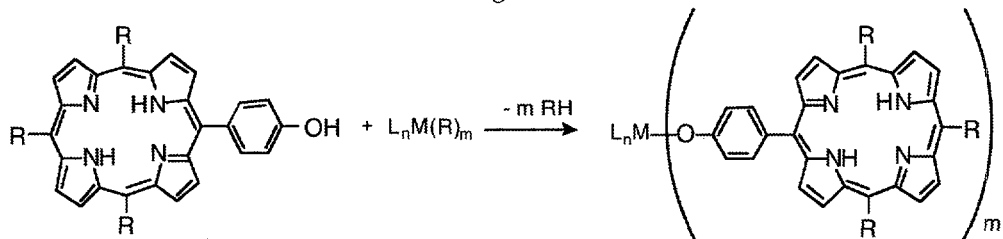


Fig. 1c

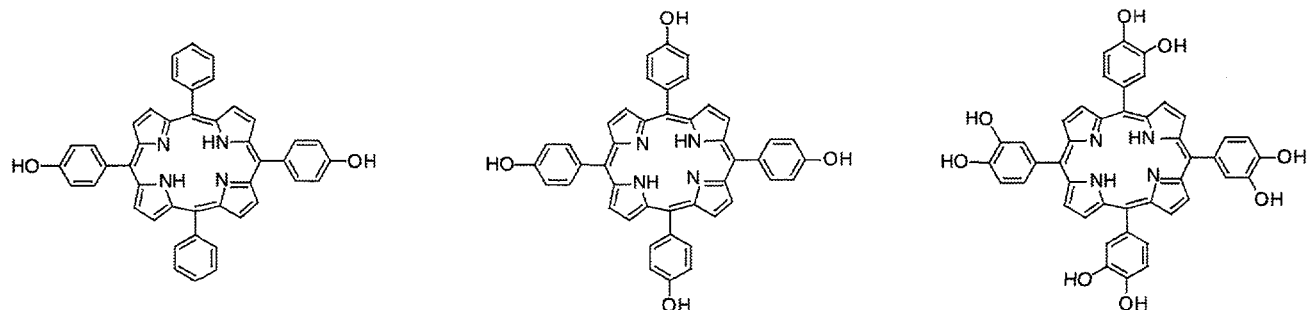


Figure 1. Synthetic scheme for the preparation of hydroxyporphyrins and their metal complexes.

Numerical Treatment of Lepton Pair Production in Relativistic Heavy Ion Collisions Using Parallel Processing

Principal Investigator: Ali Belkacem

Project No.: 97004

Project Description

Electron-positron pair production will play a major role in colliders such as the Relativistic Heavy Ion Collider (RHIC) or the Large Hadron Collider (LHC). For example, a copious number of electron-positron pairs is expected to be produced at each of the

interaction regions at RHIC. More importantly for each central collision, the probability of creating an electron-positron pair is unity. This results in multiple pair production, and the probability of producing a muon pair is also high. Since electrons and muons are expected to be used as probes for the quark-gluon plasma in case it is formed under these collisions, a good understanding and accounting of pair production from the electromagnetic process becomes critical. In addition, a sizable fraction of the electrons from the pairs produced in small impact parameter collisions but without nuclear contact is likely to be created directly bound to the ions, which will change their charge states by one unit. Such ions will end up being lost from the beam and become the main source of luminosity limitations in colliders. The capture from the pair production process is also used at CERN and Fermilab to create antihydrogen atoms.

The purpose of this project is to use the T3E to solve numerically the time-dependent Dirac equation that describes the production of electron-positron pairs in relativistic heavy ion collisions, as well as other atomic processes such as ionization, charge transfer, and excitation. The solution on a grid will give a direct visualization of the pair-creation process as the collisions between the ions evolve in time. Such an approach has enormous advantages in that it provides a great deal of insight through the "animation" of the collision and also provides a powerful nonperturbative treatment for an inherently difficult problem. A great deal of experience in supercomputing and nonrelativistic scattering problems already exists. The success of our project provides a crucial first step for the extension of this expertise to the challenging and uncharted relativistic domain.

Accomplishments

In the collision of two bare ions, there are no "real" electrons present in the initial state. However, since in the Dirac hole theory the negative energy continuum is filled with electrons, we choose a wave packet from these energies as an initial state and follow its evolution in time according to the time-dependent Dirac equation. Pair production takes place when positive energy components start building up in the wave packet. The wave function that contains the information of the collision system will be calculated at each time step and stored. This will allow us to create an animation for visualization of the pair-production process. The final state will give accurate probabilities for pair production.

We implemented successfully the main code to the T3E, enabling us to accumulate valuable experience with PVM and parallel processing in this supercomputing environment. The first version of the computer code scales efficiently up to 32 processor elements (PEs) of the T3E, but the scalability is lost beyond that. Some modifications, in particular those that consist of a parallel implementation of the (although small) sequential part of the code, improved its scalability and portability. In addition, we gained an order of magnitude in computational efficiency by changing the way the tasks are mapped to the processor elements. We found that several of the costly redundancies are removed when we map the integration volume (right hand side of the integro-differential equation) to each PE instead of the more natural approach of mapping variable elements (from the differential part of the equation) to each PE.

The analytical equations for pair production were developed in parallel to the computational implementation. In particular, using a Lorentz transformation, we rewrote the set of equations in the center-of-mass instead of the usual fixed target reference frame. This allowed us to tackle very high collision energies—the corresponding momentum of the ions is smaller in the center-of-mass, and there is a direct relationship between the momentum of the ions and the numerical difficulties and grid size. The new equations are rewritten in such a way that the computer code needs only small modifications to the current version that runs on the T3E.

Molecular Theory Group

Principal Investigators: David Chandler, Martin Head-Gordon, and William Miller

Project No.: 96030

Project Description

The Molecular Theory Group is addressing the principal bottlenecks to extending molecular simulations in three interrelated areas:

- The timescale bottleneck in molecular simulations. Condensed phase chemistry often occurs on timescales that are three to ten orders of magnitude longer than the nanosecond timescale of molecular simulations. Novel ways of following the crucial infrequent events that determine such reactions are required.
- The particle number bottleneck in electronic structure calculations. All widely used electronic structure methods show nonlinear increases in computational cost as molecular size increases. This translates into sublinear improvements in the size of systems which can be simulated for a given improvement in computer power. The development of new linear scaling methods is the most direct attack on this bottleneck.
- The dimensionality bottleneck in quantum reactive scattering. While first principles quantum mechanical calculation of chemical reaction rates is

now a reality for small systems, the complexity of such exact calculations grows exponentially with the number of degrees of freedom. To permit reliable treatment of larger systems, new methods that circumvent this acute dimensionality dependence are needed.

Accomplishments

Significant progress has been made in all three areas. First, we have developed action functionals for directed paths that connect reactants and products via rare crossings of transition states. With the algorithms that we have developed over the past year for sampling these functionals, this is now a practical computational method for obtaining meaningful simulations of reactive processes which occur on timescales far too long for conventional simulations. A range of problems of increasing realism and complexity have been studied, facilitated by use of the NERSC T3E. These include hydrogen bond breaking in liquid water, and the dissociation of NaCl in water.

In the second area, we have addressed several aspects of the particle number bottleneck over the past year, which has resulted in three publications. We have developed improved methods for constructing the effective Hamiltonian in electronic structure theory with effort scaling only linearly with molecule size. This includes exchange interactions and Coulomb interactions for periodic systems. We have also addressed the related problem of converting an effective Hamiltonian into a density matrix in linear scaling effort, via a novel Chebyshev analysis, which is of both formal and practical value.

In the third area, simulation methods based on the direct and correct evaluation of rate constants for chemical reactions have been generalized to approximately include the effect of pressure on a primary chemical reaction of interest. This has been applied to the $O + OH \rightarrow HO_2 \rightarrow O_2 + H$ reaction, which is of central importance in modeling hydrocarbon combustion. Additionally we have made progress in semiclassical initial value representations as a general way of including quantum effects in molecular simulations without the prohibitive cost of a formally exact treatment. Particularly interesting is the generalization we have made that also provides a description of electronically nonadiabatic processes.

Publications

R. Baer and M. Head-Gordon, "Sparsity of the Density Matrix in Kohn-Sham Density Functional Theory and an Assessment of Linear System-Size Scaling Methods," *Phys. Rev. Lett.* **79**, 3962–3965 (1997).

R. Baer and M. Head-Gordon, "Chebyshev Expansion Methods for Electronic Structure Calculations On Large Molecular Systems," *J. Phys. Chem.* **107**, 10003–10013 (1997).

M. Challacombe, C.A. White, and M. Head-Gordon, "Periodic Boundary Conditions and the Fast Multipole Method," *J. Chem. Phys.* **107**, 10131–10140 (1997).

D. Chandler, "Lerici Lecture 3. Finding Transition Pathways: Throwing Ropes Over Rough Mountain Passes, In the Dark," *Il Nuovo Cimento*, in press (1998).

F.S. Csajka and D. Chandler, "Transition Pathways in a Many-Body System: Application to Hydrogen-Bond Breaking in Water," *J. Phys. Chem.*, in press (1998).

C. Dellago, P.G. Bolhuis, F.S. Csajka, and D. Chandler, "Transition Path Sampling and the Calculation of Rate Constants," *J. Chem. Phys.*, in press (1998).

T.C. German and W.H. Miller, "Quantum Mechanical Pressure-Dependent Reaction and Recombination Rates for $OH+O \rightarrow H+O_2, HO_2$," *J. Phys. Chem.* **101**, 6358–6367 (1997).

L.W. Poirier, "Quantum Reactive Scattering for Three-Body Systems via Optimized Preconditioning, as Applied to the $O+HCl$ Reaction," *J. Phys. Chem.*, in press.

E. Schwegler, M. Challacombe, and M. Head-Gordon, "Linear Scaling Computation of the Fock matrix. 2. Rigorous Bounds on Exchange Integrals and Incremental Fock Build," *J. Chem. Phys.* **106**, 9708–9717 (1997).

X. Sun and W.H. Miller, "Semiclassical Initial Value Representation for Rotational Degrees of Freedom: The Tunneling Dynamics of HCl Dimer," submitted to *J. Chem. Phys.*

H. Wang, X. Sun, and W.H. Miller, "Mixed Quantum-Classical Approach for Calculating Thermal Rate Constants," submitted to *Chem. Phys. Lett.*

H. Wang, W.H. Thompson, and W.H. Miller, "Thermal Rate Constant Using Flux-Flux Auto

Correlation Functions: Application to $\text{Cl} + \text{H}_2 \rightarrow \text{HCl} + \text{H}$ Reaction," *J. Phys. Chem.* **107**, 7194–7201 (1997).

Magnetic Properties and Electron Localization at Interfaces

Principal Investigator: Charles Harris

Project No.: 95003

Project Description

Understanding the energy, spatial extent, and dynamics of excited electronic states and their effect on electron transport across interfaces unites our broad-range study of interfacial electronic properties. The combination of recently developed angle-resolved two-photon photoemission (TPPE) with femtosecond (fs) nonlinear optical techniques provides a unique opportunity to study excited-state electrons localized at atomically thin interfaces.

The development of wavelength tunable polymer LEDs and polymer field effect transistors has greatly increased the technological significance of metal-polymer interfaces. The energy, dynamics, and spatial extent of excited electrons at the metal-polymer interface are unique from those of the bulk metal and polymer and play a critical role in determining the function of polymer-based electronic devices. We will address these issues by studying model metal-polymer junctions with hydrocarbon overlayers of various bond order, chain length, branching, and functionalization. By changing the electronic properties of the model polymer which we deposit, we hope to identify general metal-polymer interface electronic properties. Important features which will be analyzed in detail include tunneling dynamics and electron localization.

Self-assembled monolayers (SAMS) often are used to stabilize nanocrystals and have been used as links between nanocrystals in the construction of prototype nanocrystal electronic devices. Despite their common presence in nanocrystal studies, their electron transport properties remain largely unexplored. We have initiated the study of electron

tunneling dynamics at a metal-SAMS interface and intend to study the effect of the organic chain's electronic properties on electron tunneling.

Lastly, angle- and time-resolved TPPE provide an excellent opportunity to study electron relaxation mechanisms and time-scales and the photophysics of two-dimensional systems. This general objective is being pursued in the study of coherent oscillations in electron dynamics and the angular dependence of electron lifetimes. Coherent oscillations result from the quantum mechanical interference of closely spaced energy levels, and provide a means of determining the energy spacings of electronic levels from their dynamics for states that cannot be resolved in the energy spectrum. Angular dependent lifetime studies provide a means of studying the many body dynamics of reduced dimension electronic systems.

Accomplishments

We have studied gas-phase deposited physisorbed overlayers, while making equipment improvements necessary for the future study of low-vapor-pressure semiconducting overlayers. Time-resolved TPPE studies of n-alkane and xenon overlayers on a metal substrate have continued, and new results have been obtained in the study of aromatic overlayers and self-assembled monolayers. We have updated and improved our ultrahigh vacuum (UHV) chamber with the addition of an electron beam doser for the deposition of semiconducting and magnetic materials and have purchased a new LEED/auger spectrometer for characterizing the overlayer deposition process.

Additional studies were done to determine the mechanism by which initially delocalized electrons become spatially localized at metal-alkane interfaces. A small polaron model based on electron transfer theory successfully explains the energy dependence of the delocalized electron lifetimes (Figure 1a). The analysis reveals that both inter- and intramolecular vibrational modes of alkane layers are involved in forming small polarons and their contributions to the lattice relaxation energy have been determined. Oscillatory behavior in the rate originates from nuclear tunneling in the high-frequency intramolecular mode. The non-Arrhenius temperature dependence of the rate is also well reproduced by the model (Figure 1b). These results are essential to the development of a detailed model of electron transport properties at metal-polymer interfaces.

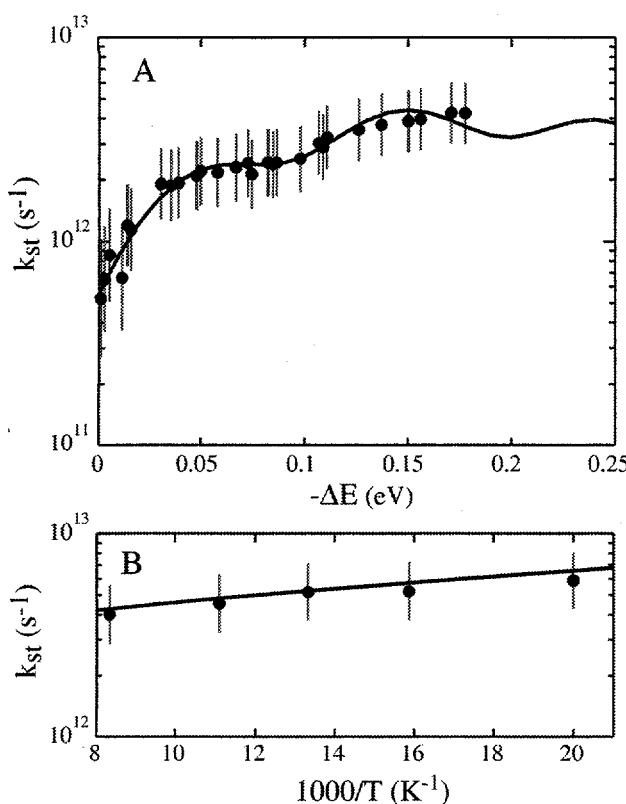


Figure 1. (a) The self-trapping rate of the delocalized state into a small polaron state for bilayer *n*-heptane/Ag(111) as a function of exothermicity. (b) Temperature dependence of the self-trapping rates for $-\Delta E = 0.14$ eV.

Our study of model metal-polymer interfaces now includes aromatic overlayers. The energy, lifetime, and spatial extent of excited interfacial electrons for monolayers of benzene and naphthalene on metal surfaces have been determined. Of particular interest is the study of the attachment of substrate electrons to the molecular overlayer's electron affinity (EA) levels. These orbitals are the precursors to the conduction band in polymeric electronic devices and determine the electron transfer properties of the interface. The 5-fs lifetime of the EA level of a monolayer of benzene strongly suggests that relaxation occurs via resonant tunneling to the substrate conduction band. Additionally, the EA level has a low effective mass parallel to the interface different from the bulk molecular crystal conduction band.

Self-assembled monolayers on a metal surface constitute our first study of a chemisorbed overlayer and the first observation of image states for a chemisorbed molecular overlayer. Our determination

of the image state lifetimes at the methyl sulfide layer begins our study of electron tunneling at SAMS interfaces. By changing the chain length, bond order, branching, and functionalization of the alkyl chain we hope to achieve a detailed understanding of electron transport across SAMS.

Coherent spectroscopy of electrons at surfaces accesses important information on the time evolution of the spatial distribution and phase of electrons in excited image states (Figure 2). The degeneracy of higher image states with the Ag(111) conduction band allows for higher image electron penetration into the bulk which may cause phase relaxation of the coherently excited electrons. The $n=3$ and $n=4$ lifetimes were experimentally determined to be 70 fs and 140 fs, respectively. The lifetimes of higher image states can be predicted from these results and allow the determination of the phase relaxation and spatial distribution as a function of time for higher image states ($n > 4$).

Publications

C.B. Harris, N.-H. Ge, R.L. Lingle, Jr., J.D. McNeill, and C.M. Wong, "Femtosecond Dynamics of Electrons on Surfaces and at Interfaces," *Annual Review of Physical Chemistry* **48**, 711 (1997).

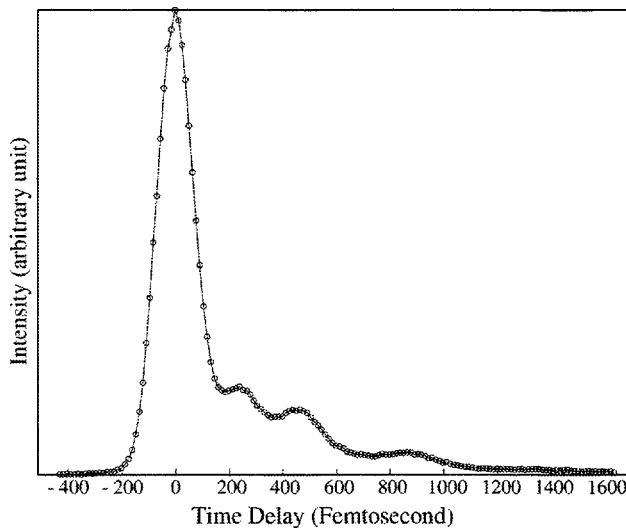
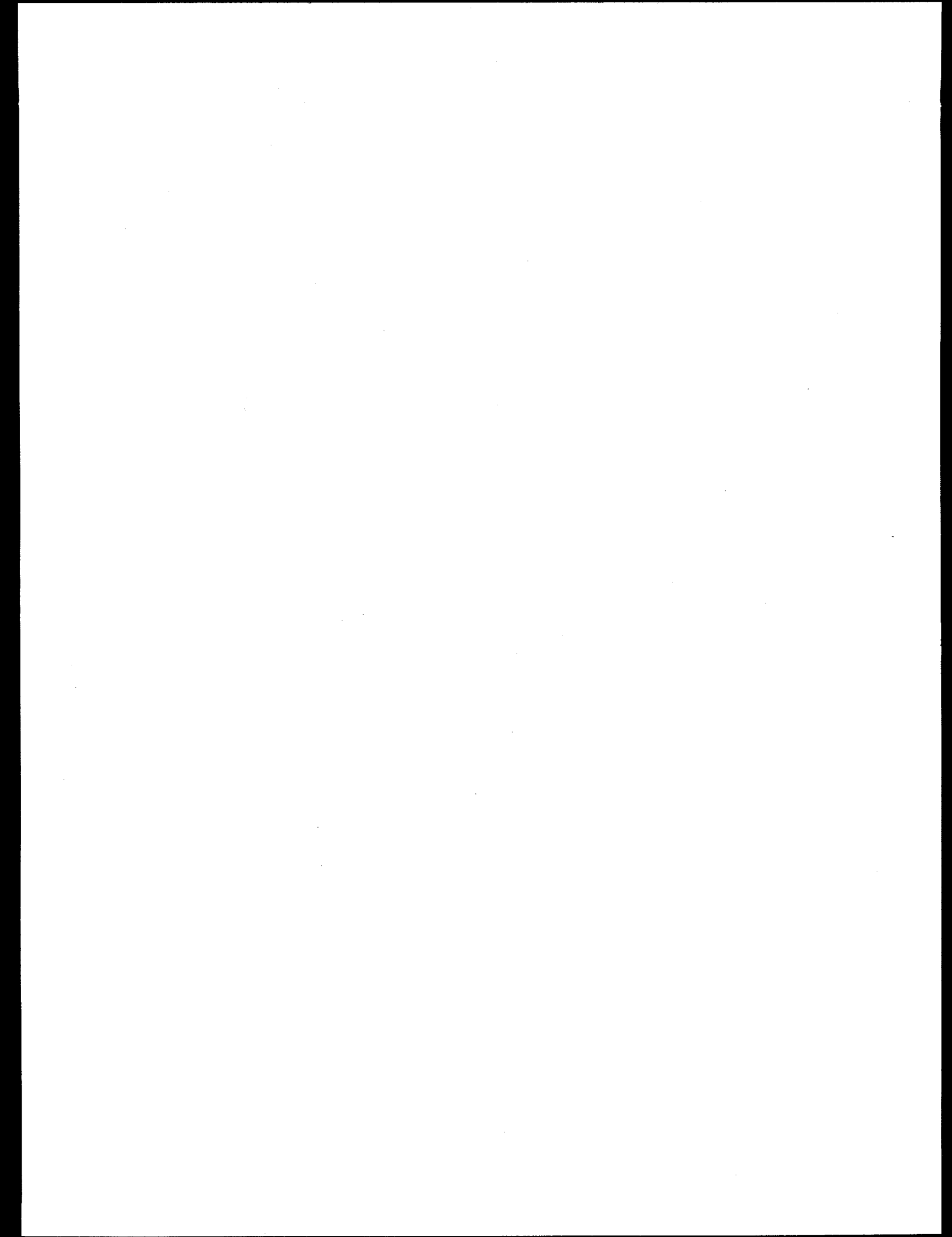


Figure 2. Coherent excitation of $n=4$, 5, and 6 image states. The oscillations are due to interference between these image states. Decay of the oscillations are due to the inherent lifetimes of the image states and possible phase relaxation.

J.D. McNeill, R.L. Lingle, Jr., N.-H. Ge, C.M. Wong, and C.B. Harris, "Dynamics and Spatial Distribution of Electrons in Quantum Wells at Interfaces Determined by Femtosecond Photoemission Spectroscopy," *Physical Review Letters* **79**, 4645 (1997).

N.-H. Ge, C.M. Wong, R.L. Lingle, Jr., J.D. McNeill, K.J. Gaffney, and C.B. Harris, "Femtosecond Dynamics of Electron Localization at Interfaces," *Science* **279**, 202 (1998).



Computing Sciences

(Information and Computing Sciences Division, National Energy Research Scientific Computing Division, and Departments: Center for Computational Sciences and Engineering, Mathematics)

Mathematical and Numerical Algorithms for the Analysis of Cracks, Damage Accumulation, and Fracture in Solids

Principal Investigators: Grigory Barenblatt, Alexandre Chorin, Ole Hald, and James Sethian

Project No.: 97005

Project Description

Forsyth made a remarkable discovery which found important practical applications. Performing a standard fatigue experiment with constant amplitude loading on a slotted plate of aluminum alloy DTD687 used in the aircraft industry, he observed a sequence of alternating smooth and rough strips sharply bounded by curved lines. Fractograms revealed different micromechanisms of fracture in neighboring strips.

An important step in Forsyth's work was processing his experimental data, from which he found that for both sequences of curvilinear boundaries (smooth-rough and rough-smooth transitions) the following relationship holds:

$$\frac{\sqrt{a}}{\ell} = \text{Const.}$$

Here a is the maximum crack depth and ℓ the length of the crack contour. The constant is different for each series.

Forsyth himself understood immediately the value of this result for failure analysis. He wrote "...a change of stress level will change \sqrt{a}/ℓ . By measuring this value at different jumps any changes in the maximum loads experienced in service can be determined. This approach should be a [sic] considerable use in sequencing the failure of a multiple cracked structure."

A qualitative investigation of the Forsyth effect has been performed. The effect was explained by the assumption that the kinetic diagram (averaged over a loading cycle crack velocity $d\ell/dt$ versus critical stress intensity factor N) is represented by a non-single-valued function.

The present work has the following goal: to derive, on the basis of numerical computations of an elastic plate with an extending plane crack bounded by a curvilinear contour, the Forsyth law as an asymptotic relation, and to determine the dependence of the constants $\sqrt{a}/\ell = c_1$ (smooth-rough) and $\sqrt{a}/\ell = c_2$ (rough-smooth) on the dimensionless parameters of the problem.

Accomplishments

The Formulation of the Mathematical Problem

It was found to be appropriate to modify the original mathematical problem by replacing it with a symmetric one (Figure 1). Therefore, the problem is

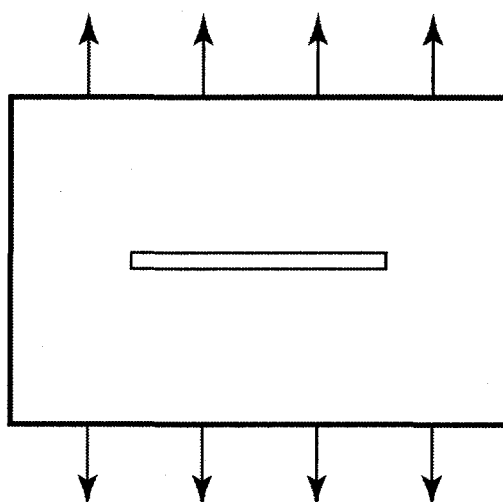


Figure 1. The problem is replaced by a symmetric one, although in reality this scheme is unstable.

solved numerically in an "octavo-region" of the symmetric plate (Figure 2).

The standard equations of the theory of elasticity are solved in the region abcdefgkml having the form of a rectangular parallel-piped. The following standard boundary equations are imposed:

- (1) At abcd $u_1 = 0$, $\sigma_{12} = \sigma_{13} = 0$
- (2) At bcfe $\sigma_{33} = p$, $\sigma_{13} = \sigma_{23} = 0$

Here p is the mean load (the elastic field is averaged over a cycle).

Furthermore,

- (3) At efgk $\sigma_{11} = \sigma_{12} = \sigma_{13} = 0$
- (4) At abek $u_q = 0$, $\sigma_{12} = \sigma_{23} = 0$
- (5) At dcfg $\sigma_{22} = \sigma_{12} = \sigma_{23} = 0$
- (6) At adlm $\sigma_{33} = 0$, $\sigma_{13} = \sigma_{23} = 0$
- (7) At lgkm $u_3 = 0$, $\sigma_{13} = \sigma_{23} = 0$

The nonclassical boundary condition making the problem nonlinear is imposed on the crack contour lm

$$V_n = F(N),$$

where N is the local stress intensity factor, V_n is the local normal velocity of the crack contour advancement, and $F(N)$ is a special nonsingle-valued function.

Block-Scheme of the Computation

The basic difficulty of the problem is the nonsingle-valued relation between the normal velocity of the

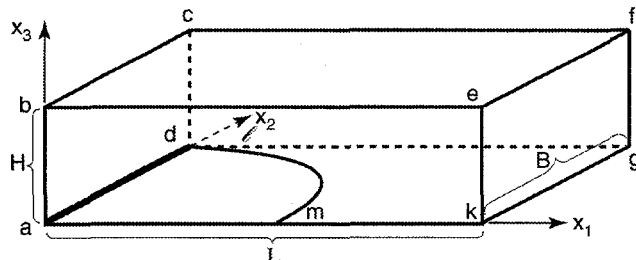


Figure 2. The "octavo-region" where the numerical solution is constructed.

crack contour advancement and the stress-intensity factor. The following block-scheme of computation is proposed. The initial form of the crack contour is prescribed arbitrarily so that for the contour the coordinate of the most advanced point a is less than a_0 , where a_0 is the length of a Griffith crack corresponding to the load p for the fracture toughness (cohesion modulus) K^*

$$a_0 = \frac{2K^*}{\pi^2 p^2}.$$

The next step is the numerical computation of the distribution of the stress intensity factor N along the line lm . There exist several methods for such computations—whether to use them or to invent new ones will be decided in the course of computing. Then, the lower branch of the original kinetic diagram will give the distribution of the normal velocity of the crack extension along the crack contour lm .

The next step is the choice of the time step, δt , and the calculation of the new position of the crack contour by a simple formula, $s_n = V_n \delta t$. After that the distribution of the stress intensity factor N is determined along the new position of the crack contour, and this procedure is repeated up to the step wherein the forward point on the upper critical value of the stress-intensity factor K^* is reached.

The transition to the next stable position of the crack contour is performed in the following way: a line is sought around the previous position of the contour line such that at each point the stress-intensity factor N is equal to the lower critical value K_* . This is the most difficult stage of the computation, and an appropriate numerical procedure should be elaborated during the next stage of present work.

After finding such lines the procedure is repeated again up to the upper critical value of the stress intensity factor at the point m . At each transition the value $\sqrt{a/l}$ is determined, and the calculations are continued up to the stabilization of these values. The numerical tests are going on at the present time.

An application to seek funding to continue this project has been submitted to NSF and also to DOE, as part of the FTP.

High-Fidelity Simulation of Diesel Combustion

Principal Investigators: Phillip Colella, Nancy Brown, and Michael Frenklach

Project No.: 96029

Project Description

The goal of this project is to develop a 3D modeling capability for diesel combustion. Such a capability would fill a critical need for high-fidelity simulations in support of engine design. Our approach is based on the development of high-resolution adaptive algorithms for 3D fluid dynamics in complex geometries, combined with a representation for turbulent combustion based on a partial perfectly-stirred reactor model that can represent complex chemical kinetics appropriate to diesel combustion and mechanisms for the production of soot.

The first major area of the research has focused on the development of suitable extensions to the case of complex boundary geometries arising in diesel engine applications of the high-resolution and adaptive finite difference methodology. This methodology was developed by investigators in Computing Sciences for low Mach number reacting flows. Our approach is based on a Cartesian mesh embedded boundary representation of the boundary geometry, in which complex geometries are represented on a rectangular grid in which the region containing the boundary has been cut away. This approach has the capability of representing highly complex geometries arising in engineering applications, such as diesel engines. This LDRD project has produced three major accomplishments in this area: fundamental discretization issues, robust and efficient discretization for elliptical partial differential equations (PDEs), and software infrastructure for embedded boundary methods.

The second major area of this research has focused upon building a chemical mechanism that includes a robust description of hydrocarbon oxidation and soot formation.

Accomplishments

Fundamental Discretization Issues

We have developed a new general mathematical theory for the design of discretizations for Cartesian grid embedded boundary methods. In this approach, the primary dependent variables are viewed as being at the centers of the rectangular grid cells, while the difference approximations to the differential operators are centered at the centroids of the irregular cell fractions cut out by the embedded cell boundary. This leads to discretizations that are consistent and stable in the formal mathematical sense. This approach has been tested on a variety of problems in classical partial differential equations, including those that make up the components of the standard models for diesel combustion. Such a theoretically sound approach to embedded boundary methods is a fundamental new advance in the field, and promises to have substantial consequences in a variety of applications.

Robust and Efficient Discretizations for Elliptic PDEs

We have applied and extended the theoretical framework described above to develop robust and efficient solvers for discretizations of elliptic PDEs. Our approach is based on multigrid iteration, in which the discretized equations are solved iteratively on a recursively coarsened set of grids. The first key issue is the representation of an embedded boundary grid system as an abstract graph, in which the nodes of the graph are the control volumes in each cell (e.g., due to a thin body intersecting the cell). The second is that the graph can be coarsened in a way that does not require reference to the original surface geometry that generated the graph description on the finest level.

This latter property enormously simplifies the problem of generating the description of the embedded boundary discretization. Using these ideas, we have developed robust multigrid solvers for elliptic PDEs whose CPU and memory usage is comparable to that obtained for the corresponding problems in the absence of geometry.

Software Infrastructure for Embedded Boundary Methods

We have developed an easily used software infrastructure based on the graph-theoretical description given above. In our approach, we

generalize the notion of a rectangular grid index space to the abstract graph of an embedded boundary described above. Arrays are then defined on subsets of the index space, analogous to the definition of ordinary multidimensional arrays indexed by subsets of the rectangular lattice. By treating the index space and its subsets as variables that can be assigned and computed, we enormously simplify the development of these algorithms. We have implemented an initial version of this infrastructure on top of the BoxLib library for rectangular grid calculations, and are implementing a variety of our embedded boundary algorithms using this library.

Chemical Mechanism for Hydrocarbon Oxidation and Soot Formation

In the second major area of the project, we have written an application code that will serve as a sub-grid model of the high-fidelity fluids code. The sub-grid model is that of a perfectly stirred reactor (PSR).

A series of PSR calculations has been performed that allow us to compare numerical predictions for sooting trends in PSRs with those observed in experiments. Isothermal PSR calculations of C_2H_4 /air mixtures were undertaken using a reactor volume of 67 cm^3 for pressures of 0.12, 1.0, and 10 atm. At each pressure, the equivalence ratio was varied from 1.8 to 3.2 by 0.1 and the temperature from 1500 K to 2000 K by 50 K. The residence time was also varied; results are most frequently determined for 0.005 s, the residence times of the PSR experiments.

We considered the following calculated quantities in our analysis: gas-phase concentrations, the values of the soot distribution moments, the average soot particle diameter, total soot surface area, the fractional volume of the soot particles, the nucleation and coagulation rates, the surface growth rates of A4 (pyrene), C_2H_2 , O_2 , and OH , the net gas-phase and surface molar production rates, and the reaction flux changes for A4, C_2H_2 , CO, O_2 , OH, H, and H_2 . We used a detailed chemical kinetics model for soot production that has been tested in laminar flames. The combined hydrocarbon chemistry and soot chemical kinetics model is used without any adjustments. CHEMKIN and PSR codes have been modified considerably to incorporate the method of moments used to describe soot formation. Gas-phase and surface reactions are rigorously coupled in the model. Predicted sooting characteristics are consistent with behavior observed experimentally in premixed laminar flames and well-stirred reactors. Specifically, soot volume fraction exhibited the same

qualitative behavior with equivalence ratio, temperature, and pressure as observed in flames.

Figure 1 is a mesh plot of computed final soot volume fraction (F_v) as a function of equivalence ratio and reactor temperature for C_2H_4 flames reacting at 1.0 atmosphere. The mesh plot curve and the analogous one determined for 10 atm exhibit the well-pronounced bell shape. The bell-shaped temperature dependence is of the same character as that noticed in a number of experiments. The bell shape is explained in terms of the competition between a kinetic driving force at low temperatures and thermodynamic resistance to growth at high temperatures. The maximum in F_v shifts toward higher temperature as the equivalence ratio increases. Although there is a paucity of experimental data on well-stirred reactors, the data of Vaughn suggest the bell-shaped behavior as well. Also, concentration profile shapes were consistent with profile shapes measured in flames. The model also predicts soot threshold values and the relationship of soot volume fraction with temperature and equivalence ratio that has been observed experimentally for well-stirred reactors. Under the conditions of the present investigation, soot production was dominated by nucleation. The temperature dependence of surface reaction rates

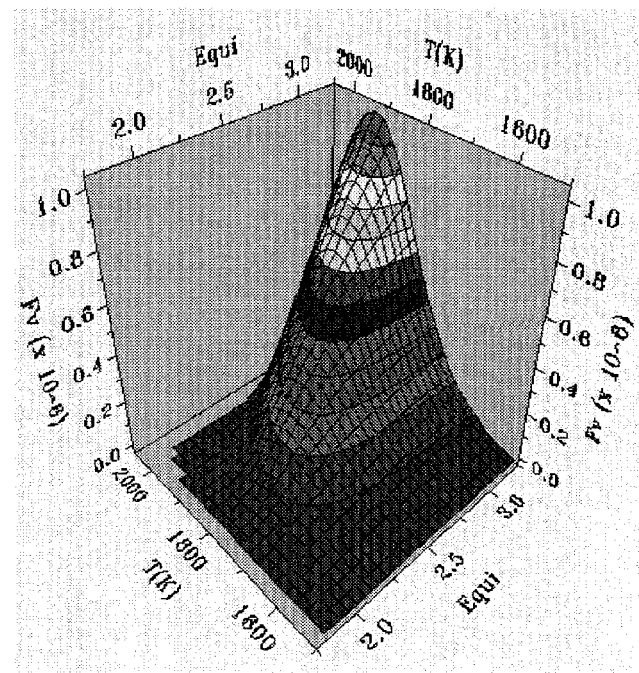


Figure 1. Mesh plot of final soot volume fraction (F_v) as a function of equivalence ratio and temperature (K) for C_2H_4 ethylene mixtures reacting in a PSR at 1 atm for a residence time of 0.005 s.

revealed the importance of the HACA mechanism (H-abstraction-C₂H₂-addition sequence) in surface growth. Under PSR conditions, the extent of the gas-phase and surface chemistry coupling increases with pressure.

Current research includes improving the gas and surface chemistry of the present mechanism using recent experimental and theoretical results.

Mechanism verification will be established by performing calculations in a suite of combustion configurations—PSRs, PSR combined with a plug flow reactor, and laminar flames employing premixed and partially premixed gases—and comparing our calculated results with experiments. We are also adding nitrogen chemistry to the mechanism to enable estimation of oxides of nitrogen. In addition, we are developing a dynamic scheme for mechanism reduction that will be used for modeling combustion in turbulent flow fields.

Publications

M.S. Day, P. Colella, M. Lijewski, C. Rendleman, and D.L. Marcus, "Embedded Boundary Algorithms for Arbitrarily Complex Domains: Adaptive Multigrid Solutions to Poisson's Equation," in preparation.

H. Johansen and P. Colella, "A Cartesian Grid Embedded Boundary Method for Poisson's Equation on Irregular Domains," submitted to *J. Compu. Phys.*

Hans Svend Johansen, "Cartesian Grid Embedded Boundary Methods for Elliptic and Parabolic Partial Differential Equations on Irregular Domains," Ph.D. thesis, Dept. of Mechanical Engineering, University of California, Berkeley, CA, December, 1997.

Nancy J. Brown, Kenneth L. Revzan, and Michael Frenklach, "Detailed Kinetic Modeling of Soot Formation in Ethylene / Air Mixtures Reacting in a Perfectly Stirred Reactor," submitted to the 27th International Symposium on Combustion, University of Colorado, Boulder, August 2-7, 1998.

Scientific Computing on Clusters of Multiprocessor Systems (COMPS)

Principal Investigators: William Johnston and Horst Simon

Project No.: 96037

Project Description

Scientific computing relies increasingly on hardware developed originally for nonscientific applications. The days of expensive special purpose hardware are nearly over, as scientists rely more than ever on commodity and near-commodity equipment. On the low end, scientific computing uses workstations or PCs and to a lesser extent symmetric multiprocessor (SMP) servers, usually with fewer than 10 processors. On the high end, the fastest scientific computers are Massively Parallel Processors (MPPs), which are based on commodity microprocessors and look to the programmer like a tightly integrated collection of single-processor workstations. MPPs use specialized network hardware. Increasingly, high-end computers are being built from commodity hardware, including commodity network hardware. The premise of this LDRD project is that the next important architecture for scientific computing will be clusters of SMP computers (COMPS) connected by commodity networks. SMP clusters, which incorporate aspects of the current high and low end, have the dual advantages of low cost, because of their commodity base, and of scalability and flexibility, because they are distributed.

SMP clusters present a number of challenges that must be addressed by applications and system software. COMPS LDRD research addresses a range of issues that need to be understood before SMP

clusters can be used effectively. It is not clear, for instance, what the programming model should be, as several combinations of message passing, explicit threads, and compiler parallelization are possible. Process scheduling and networking software are more complex and more critical for performance than for traditional MPPs.

The COMPS LDRD is looking simultaneously at system software and application software issues. The application areas—primarily numerical computation but also data-intensive computing and experiment control—serve as drivers for selecting important computing technology areas. System software work includes both evaluation of existing technology, such as the NOW (Network of Workstations) software developed at UC Berkeley, and development of technology where it does not already exist.

Accomplishments

We have put together a small ATM-connected testbed SMP cluster (the "COMPS" cluster), consisting primarily of \$400K of donated equipment from Sun Microsystems. This cluster is our "production" system and has been used as a platform for developing and testing. We have also obtained approximately \$100K of equipment from Intel, as part of the UC Berkeley "Millennium" grant, to establish a testbed cluster based on PC technology. System software development has been moved to this second system.

On the application side, we have established an active collaboration between the Materials Sciences Division and the Computing Sciences Division to examine three related numerical problems. We have made significant progress on the parallel implementation of a Low Energy Electron Diffraction (LEED) Structure Determination code that uses a new approach based on genetic algorithms (GAs). We have demonstrated substantial performance improvements (high parallel efficiency) and have begun to focus on variants of the basic GA that can make better use of SMP cluster nodes. We expect this work to lead to a general purpose parallel GA library.

In other applications of this work, we have explored the suitability of the COMPS cluster for real-time interactive control of experiments. We have also demonstrated the feasibility of using such a cluster as a distributed parallel storage server for data intensive computing.

On the system software side, we have focused on the development of low-latency high-bandwidth networking that will enable tightly coupled parallel

applications to run efficiently on an SMP cluster. Initially, we extended U-Net, a low-latency network interface architecture from Cornell University, and rewrote the device driver for the FreeBSD operating system. The U-Net extensions make it more useful in a production environment as a base for building application libraries such as MPI. We have done a partial implementation of MPI on top of U-Net, obtaining latencies of about 30 microseconds on Fast Ethernet.

Rather than continue with U-Net, we applied the lessons learned there to a U-Net-inspired emerging low-overhead networking standard, VIA (Virtual Interface Architecture), proposed by Intel, Compaq, and Microsoft. We provided feedback on the proposed standard to make sure the needs of high-performance computing were addressed. We also developed one of the first implementations of the proposed standard, demonstrating performance that has drawn attention from Intel and Compaq. The VIA specification has just been finalized, with LBNL listed as a contributor.

We have established an active collaboration with the NOW and Millennium projects at UC Berkeley.

Publications

M.A. Van Hove, R. Doll, S. Sachs, and G. Stone, "Genetic Algorithms and Parallel Computing for Global Optimization, Applied to Complex Surface Structure Determination by Low-Energy Electron Diffraction," International Conference on Computational Physics (<http://aps.org/meet/PC97/>).

M.A. Van Hove, R. Doll, S. Sachs, and G. Stone, "Genetic Algorithms and Parallel Computing for the Global Search in Complex Surface Structure Determination by LEED," 44th National Symposium of the American Vacuum Society (<http://www.vacuum.org/symposium/sessions/author/titles.cfm?personID=7300>).

M.A. Van Hove, "Theory and Computation for Synchrotron Radiation Users," presented at the ALS Workshop on Theory and Computations for Synchrotron Applications (<http://electron.lbl.gov/alsworkshop/>).

B. Pfrommer, P. Bozeman, and W. Saphir, "Implementing the MPICH ADI on an Unreliable Transport Layer," in preparation.

Virtual Interface Architecture specification (<http://www.viarch.org/>).

New Areas for Interface Techniques: Robotic Navigation and Shape Recognition

Principal Investigators: Ron Kimmel, Ravi Malladi, and James Sethian

Project No.: 97006

Project Description

The goal of this project is to extract complex shapes from medical image scans, such as those presented by MR and CAT scans. This extraction typically leads to a mathematical representation of the detected shape, which is then amenable to quantification, including measurement of enclosed volumes, surface areas, corrugations, etc.

The key computational techniques are level set methods and fast marching methods, two numerical techniques invented at LBNL for tracking interfaces that evolve under complex speed laws. These techniques allow propagating interfaces to change topology, merge, and develop, without *ad hoc* nonphysical procedures. The central idea is to synthesize a speed from the image gradient so that the evolving interface stops at the desired boundary.

Our approach to shape recovery is an evolutionary one. In other words, we let the physician specify an initial shape or a set of shapes in the image domain, preferably inside the shape he/she intends to recover. These initial shapes, typically spheres or just a set of mouse clicks, are then made to propagate in the image domain by solving a partial differential equation. Steady state of our solution describes the desired shape.

Accomplishments

For this project, we first extended all of the image processing work to color images, which acts as a preprocessing step. This color anisotropic diffusion scheme allows one to naturally remove background noise and enhance or sharpen color images in such a way that the color channels are naturally linked and connected, leading to robust and efficient schemes. This puts color segmentation in a framework that is consistent with that for gray-scale images, and allows one to extend to a large vector-valued image field. In

addition, the coupling of fast marching methods to level set methods has provided a very efficient framework with which to rapidly compute evolving shapes. Finally, we have developed a series of automatic seeding and editing tools that allow physicians to quickly extract shapes, correct for inaccuracies in the solution, and proceed with minimum intervention.

Publications

R. Malladi and J.A. Sethian, "A Real-Time Algorithm for Medical Shape Recovery," *Proceedings of ICCV '98*, Bombay, India.

R. Malladi and J.A. Sethian, "A Real-Time Algorithm for Medical Shape Visualization and Measurement," submitted for publication, *Computer Aided Geometric Design*, special issue on *Medical Imaging*, January, 1998.

The Integration of PDSF, HENP Analysis, and the HPSS Data Archive

Principal Investigator: William Kramer

Project No.: 97033

Project Description

High Energy and Nuclear Physics (HENP) computing activities for large experiments are geographically distributed as a result of the size of the collaborations and the scale of the manpower effort for software development and data analysis, as well as the hardware resources needed to cover the entire range of computing needs. This proposal will develop and implement an architecture that satisfies these requirements, applies the unique capabilities of NERSC to certain classes of computing needs (simulations, analysis, and data management), and satisfies the global scope of computing for HENP.

Specifically this project will achieve the following:

- develop, demonstrate, and characterize a software-based architecture that supports a high-volume, distributed, data-intensive computing environment to support HENP data handling and analysis, and

- provide a prototype-production HENP computing environment that integrates the Particle Data Storage Facility (PDSF), a high-speed data cache, and archival storage within the NERSC environment.

High Throughput Computational and Storage System Architecture

This project will integrate the computational, high-speed disk cache, and archival storage systems needed to solve the HENP analysis problem. The architecture will be implemented to provide a prototype production HENP analysis environment, and will focus on using the PDSF to provide a prototype production system. The Distributed-Parallel Storage System (DPSS) will be used to provide a high-capacity, high-performance disk cache that is appropriate for the capture and analysis of HENP data. In addition the new NERSC High Performance Storage System (HPSS) will provide the very large capacity archival storage capability.

Workload Characterization

The HENP environment is characterized by the requirement for enormous data-storage, data-communication, and computational resources. The sheer quantity of data and processing required presents significant and unique technological challenges. In order to evaluate potential solutions, it is important that computational workload and data flows are characterized and understood. This characterization will be important both for establishing and evaluating computing systems architectures prior to implementation, and for system design and procurement purposes. Currently, the types of architecture that should be considered span the range from network of workstations (NOW), clusters of symmetric multiprocessors (COMPS), and tightly coupled massively parallel processors (MPPS). Characterizing the workload and data flows will aid in deciding most appropriate and cost-effective architecture, especially as synthetic benchmarks will be developed which will be used in quantitative assessments.

This project will characterize the computational workload of the Solenoidal Tracker at RHIC (STAR) collaboration. A computational profile of the simulation and data analysis will be developed. The details of the profile will include required processor speeds, memory per processor, I/O bandwidth (both aggregate and per processor), the interconnect bandwidth, the storage system bandwidth, etc. This profile will be used to design a test suite of applications that is representative of the STAR computational workload.

Accomplishments

In FY97, this project received initial funding that allowed an early start of the work to accomplish the following:

- develop a portable workload test representative of High Energy and Nuclear Physics computational tasks,
- integrate the DPSS developed at LBNL with the NERSC HPSS, and
- integrate the DPSS with the PDSF at LBNL.

The expected result of this work in FY98 is to enhance the operating environment for the PDSF by providing high-speed disk caching and automatic file migration to archival storage, and to have a test suite of HENP codes to evaluate this and other architectures for HENP applications.

With early funding in FY97, the workload analysis and integration tasks were begun. Specifically, networks were installed and tested to link PDSF with DPSS and HPSS. This sets the stage for further development and testing of DPSS, as well as developing the interfaces between DPSS and HPSS. The additional funding also allowed for a review of HENP programs and codes and the initial planning of the workload analysis task.

The bulk of this work is underway and is on track for integration in the summer of 1998.

Electron Collisions With Molecules, Clusters, and Surfaces

Principal Investigators: C. William McCurdy and Thomas Rescigno

Project No.: 96043

Project Description

Electron collisions, with a variety of different species and in a variety of environments, play a key role in plasma etching and deposition processes, as well as a number of waste remediation processes currently under development at DOE laboratories. Relatively little is known about such collisions, despite the important role they play in surface characterization, plasma-wall interaction, electron-induced desorption, and reorganization of adsorbed particles. Although the past few years have witnessed tremendous progress in the development of sophisticated *ab initio* methods for treating collisions of slow electrons with isolated small molecules, the practical need to study electron collisions with the complex molecules and fragments encountered in real-world plasma processing environments, as well as with molecules in complex environments—e.g., at interfaces, on surfaces, or in clusters—taxes present methods far beyond their current capabilities.

The purpose of this research is to develop theoretical and computational tools for treating electron and photon interactions with targets that are presently beyond the grasp of *ab initio* methods. We want to develop new methods for dealing with heavier molecules, complex molecular clusters and, ultimately, molecules bound to surfaces and interfaces. Moreover, we also want to extend our capabilities to intermediate energies from the ionization threshold to a few hundred eV—a region that presents a formidable challenge for *ab initio* theory.

The approach will build on our unique capabilities, based on the complex Kohn variational method, for calculating cross sections for gas-phase electron scattering (elastic, vibrational excitation, electronic excitation, dissociation, and attachment) and

photoionization processes involving small polyatomic molecules. The formalism will be extended to include pseudopotential methods, complex optical potential interactions, and scattered flux operator techniques.

Accomplishments

The activities covered by this project are characterized by two common themes. The first is a need to develop practical computational methods for treating complex polyatomic targets and molecules found in real-world plasma environments. Such targets typically contain one or more heavy atoms. By incorporating *l*-dependent effective core potentials into our algebraic variational scattering codes to avoid explicitly treating the inner-shell target electrons associated with these heavy atoms, we have been able to increase the complexity of the target gases we can study. We have carried out an extensive study of electron scattering by CF_4 , an important etching gas. Our theoretical study is the first to conclusively establish the presence of a Ramsauer-Townsend minimum in the elastic cross section in the low-energy region below 0.5 eV and also provides differential cross sections in excellent accord with available experimental data. The results are summarized in Figure 1.

We have also initiated a similar investigation on BCl_3 , which is widely used in the plasma etching of silicon, and for which little experimental data presently exist.

The other theme that is addressed in this project is the need for practical schemes to calculate cross sections in energy regions characterized by a dense level of excited states, including ionization continua.

Previously, we had developed a method for rapidly calculating photoionization cross sections over a continuous range of energies without explicitly resolving the variational equations at each desired energy. We have now been able to extend this idea to the calculation of electron-scattering cross sections as well, using analyticity and ideas related to time-independent wave-packet methods. The result is a “continuous energy complex Kohn” method that has a key advantage normally associated with the R-matrix method of allowing easy computation of the scattering amplitude at many energies from a single representation of the Hamiltonian, but that will require no more significant effort to implement than the complex Kohn method currently in use.

Finally, we have continued to make significant progress on developing practical methods to study electron impact ionization. The key feature of the approach we are developing is that it uses flux

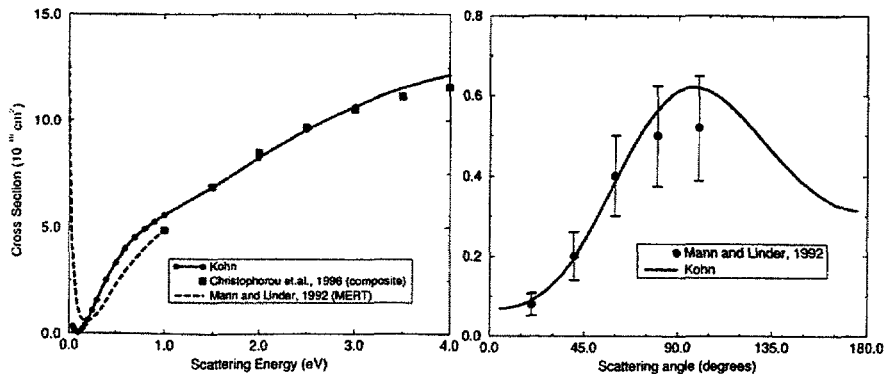


Figure 1. Low-energy e^- - CF_4 scattering cross sections. Left panel: total elastic cross section; solid curve: present results; dashed curve: semi-empirical results using modified effective range theory; solid squares: composite of available experiments. Right panel: differential elastic cross section at 1.0 eV.

operators to extract ionization cross sections from a scattered wave function (see Figure 2) that is constructed without explicit imposition of asymptotic ionization boundary conditions. We have successfully used this method to obtain total ionization cross sections for electron-hydrogen atom scattering in the standard spherical model. We have also shown how the same formalism can be used to obtain differential (energy sharing) ionization cross sections, thereby providing a complete theoretical description of the problem.

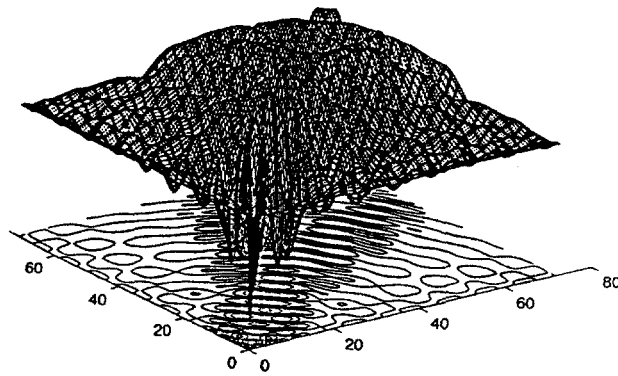


Figure 2. The singlet scattered wave function for e^- - H at 20 eV in the spherical model. Elastic and discrete excitation channels have been projected out.

Publications

T.N. Rescigno, A.E. Orel, and C.W. McCurdy, "Algebraic Variational Approach to Atomic and Molecular Photoionization Cross Sections: Removing the Energy Dependence from the Basis," *Phys. Rev. A* **55**, 342 (1997).
 T.N. Rescigno and A.E. Orel, "Photoionization of Ammonia," *Chem. Phys. Lett.* **269**, 222 (1997).
 T.N. Rescigno, M. Baertschy, D.A. Byrum, and C.W. McCurdy, "Making Complex Scaling Work for Long Range Potentials?" *Phys. Rev. A* **55**, 4253 (1997).
 C.W. McCurdy, T.N. Rescigno, and D.A. Byrum, "An Approach to Electron Impact Ionization That Avoids the Three-Body Coulomb Asymptotic Form," *Phys. Rev. A* **56**, 1958 (1997).
 T.N. Rescigno, A.E. Orel, and C.W. McCurdy, "Low-Energy Electron Scattering by CH_3Cl ," *Phys. Rev. A* **56**, 2855 (1997).
 C.W. McCurdy and T.N. Rescigno, "Calculating Differential Cross Sections for Electron-Impact Ionization Without Explicit Use of the Asymptotic Form," *Phys. Rev. A* **56**, R4369 (1997).
 C.W. McCurdy, T.N. Rescigno, W.A. Isaacs, and D.E. Manolopoulos, "The Calculation of Scattering Amplitudes as Continuous Functions of Energy:

R-matrix Theory Without a Box," submitted to *Phys. Rev. A*.

T.N. Rescigno and C.W. McCurdy, "Improvements to the Standard Complex Kohn Variational Method: Towards the Development of an R-matrix Theory Without a Box," to be published in *Novel Aspects of Electron-Molecule Scattering*, edited by Kurt Becker (World Scientific, 1998).

W.A. Isaacs, T.N. Rescigno, and C.W. McCurdy, "Theoretical Support for a Ramsauer-Townsend Minimum in Low-Energy Electron- CF_4 Scattering," in preparation.

Volumetric Description from Multiple Views for 3D Microscopy

Principal Investigators: Bahram Parvin and Ge Cong

Project No.: 97014

Project Description

Current efforts in automated shape representation for quantitative analysis of microscopic images have been limited to the flat, two-dimensional world because of the short focal lengths of available imaging systems. The natural evolution of this class of scientific investigation is the ability to construct and quantify a 3D volumetric description of an object by processing different perspective views of that object, and to parametrize the 3D description for a) gaining new insights and doing large-scale hypothesis testing, b) quality control, c) efficient storage and query, and d) efficient transmission for collaborative research. The novelty of the proposed research is that it uses existing imaging instruments and a small set of perspective views to infer 3D shape information. Applications of particular interest include 3D shape description for mammary glands (observed at low magnification); nanosize solid and liquid precipitates (observed through electron holography); and droplets deposited on the airways of lungs (observed with scanning electron microscope).

Given the data created by the variety of imaging modalities, the poor image quality, and the artifact present in each modality, we have searched for a framework that can be applied to each scenario. This appears to be a feasible objective for constructing

various computational components. The underlying idea is to construct a rich, high-level representation of each view of the scene. These representations can simplify matching for constructing surfaces and subsequent volumes. Our approach is to apply geometric constraints into low-level image features. In the case of holographic images, the high-level representation shows contours of curvature maxima satisfying closure and convexity constraints. In the case of mammary glands, the high-level representation corresponds to the axis of symmetries that runs through the capillaries and generates a tree structure. In the case of droplets on the lung tissue, the high-level representation corresponds to ellipses where some of the edges correspond to physical edges and others correspond to limb edges. The proposed high-level representation is obtained through an optimization protocol that can operate on curvature features, gradient features, or symmetry features.

This report focuses on shape recovery from holographic microscopy, where object thickness is represented in terms of fringes that correspond to equal thickness contours.

Accomplishments

The problem of shape-from-X has been a central research topic in the computer vision community. These include, but are not limited to, shape from shading, texture, contour, color, etc., with applications to images obtained in controlled environments to natural outdoor scenes that may include more than one view. Here, we introduce a new imaging modality and the corresponding shape recovery method that has not yet been addressed by the computer vision community. This is based on equal thickness contour (ETC), which is obtained through a holographic process. One imaging-source example is holographic electron microscopy of submicron crystal structures. Conventional electron microscopy presents projected images with little or no depth information. In contrast, electron holography, with coherent illumination, provides both magnitude and phase information that can be used to infer object thickness in terms of ETCs from each view of the sample. The holographic images contain interference fringes with spacings, in the best case down to less than an angstrom, where interference is between the transmitted and diffracted beams. The main issue is that this mode of representation is inherently ambiguous since objects with completely different geometry can produce similar ETC. Thus, multiple views of an object are essential for 3D shape recovery.

In practice, however, these images may have low contrast, be noisy, suffer from artifacts, and may contain shading. As a result, it is difficult to compute closed contours from these fringe patterns. Figure 1 shows two views of a real crystal structure that will be used for shape recovery (original images supplied by Ulrich Dahmen of NCEM). There is a small angle of rotation between different views as reflected by the change in the fringe patterns.

Our method for shape recovery consists of five steps, some of which build on existing techniques developed in the computer vision community. The protocol for shape recovery is shown in Figure 2. The dominant features in these images are roof edges corresponding to crease lines. However, it is well known that it is difficult and complex to extract these features directly in the presence of scale-changes and noise. Here, we have adopted a stepwise refinement of images to extract a desirable representation. The first step of the process enhances peaks and valleys of the original data with adaptive smoothing. Next, crease points are extracted and grouped on the basis of collinearity and convexity. It is assumed that grouping does not produce closed contours, and an interactive snake is provided to establish the boundary conditions due to the most inner and outer fringes. The grouping strategy is very conservative to allow closure of small gaps, and at times it successfully provides closed contours. The contour representation, based on lines of second derivatives, provides the basis for obtaining object thickness at each point in the image. We have developed a regularized approach to compute object thickness subject to continuity and smoothness constraints. The final step of our protocol is to integrate object

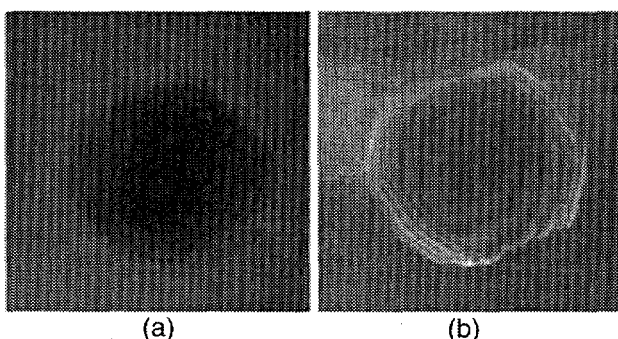


Figure 1. Two views of a cubeoctahedral object with a diameter of 100 nm.

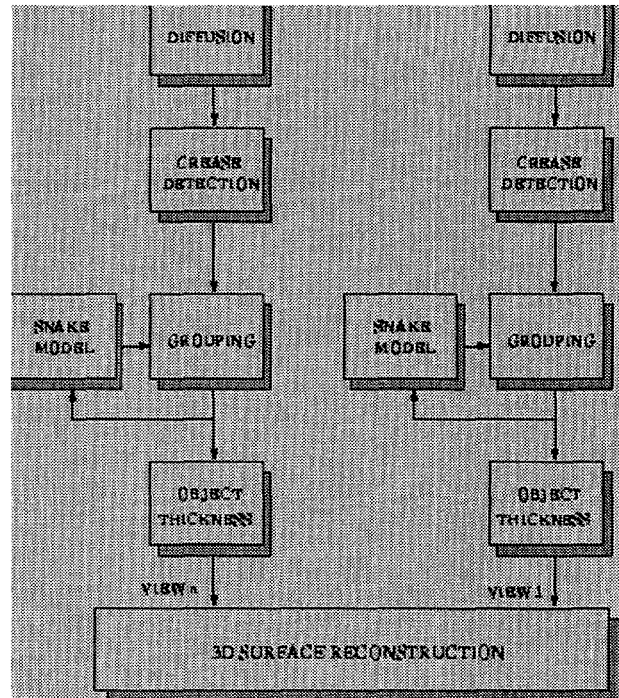


Figure 2. Protocol for recovering 3D shape from holographic images.

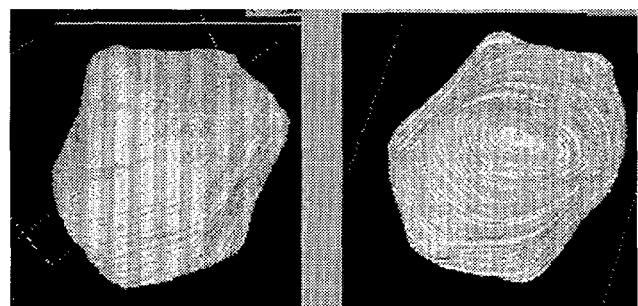


Figure 3. 3D shape recovery from views of the object in Figure 1.

thicknesses obtained from each viewing orientation into a 3D surface representation. The approach is based on a modification of the algebraic reconstruction technique that is essentially a tomographic process. The reconstruction results from our test data sets are shown in Figure 3.

Publication

B. Parvin and G. Cong, "Shape from Equal Thickness Contours," submitted to IEEE Conference on Computer Vision and Pattern Recognition.

Sparse Linear Algebra Algorithms for MPPs

Principal Investigators: Horst Simon, Beresford Parlett (Dept. of Mathematics, UCB), and James Demmel (EECS, UCB)

Project No.: 97026

Project Description

Our goal is to develop a scalable parallel library to solve large sparse symmetric eigenproblems. At present and for the foreseeable future, no general purpose, library-quality solver exists on distributed memory machines. Our research addresses several crucial issues for large-scale parallel machines, such as robustness, scalability, and portability. Although the development of our work is mainly on the T3E, we will use machine-independent software environments, such as Fortran or C with Message Passage Interface (MPI) as message passing. The resulting library will be easily portable to other platforms and the emerging new architectures of the future. We will demonstrate that our new algorithms can enable the efficient solution of such common problems arising from computational chemistry, physics, and material sciences.

A block-shifted and inverted Lanczos algorithm for sparse generalized eigenvalue problems will be implemented. Software components of this algorithm developed elsewhere (Scalapack, UCB, Boeing) will be integrated with newly developed software. Some elements, such as ordering, partitioning, and mapping algorithms, will require new research efforts. This work complements the Scalapack project funded by DOE at UCB. It also complements DOE-funded work in computational chemistry at PNNL.

Accomplishments

We have ported and parallelized the scalar LANSO code by Beresford Parlett. The code runs efficiently on the 512 processor Cray T3E at NERSC, and exhibits very good speed-up. The code is implemented in MPI and portable to other platforms, which has been demonstrated on the COMPS cluster of SMPs. On this cluster we also studied the trade-off between shared memory (threads) and distributed memory (MPI) parallelism.

In the process of comparing our PLANSO code to the PARPACK software from Rice University, we found that PLANSO consistently runs faster than PARPACK. This is due to the inherent higher efficiency of the Lanczos algorithm and to a new algorithmic technique called "thick restart." With "thick restart" the Lanczos algorithm has the same advantage of reduced storage as PARPACK.

In a related algorithmic task, scalable approximate inverse preconditioners based on the SPAI (sparse approximate inverse) approach by Barnard, Grote, and Huckle were investigated for their potential to speed up the Lanczos process. In collaboration with Steve Barnard from NASA Ames Research Center, the SPAI software was ported and tested successfully on the T3E. We believe that this is the first preconditioner that actually can be scaled to 512 processors.

We investigated a number of applications of the Lanczos algorithm:

1) Our algorithmic work demonstrated that the Lanczos algorithm can be applied to image and data compression. It has the same compression properties as the singular value decomposition (SVD), but is considerably more efficient for large matrices. Theoretical properties and error bounds for a Lanczos algorithm compression were derived.

We then applied this algorithm to the problem of large text retrieval in latent semantic indexing (LSI). In our theoretical work we demonstrated the advantages of Lanczos-based LSI, as well as corrected an error in the previously published literature on the topic. In collaboration with the web search engine Inktomi (Hot Bot), we computed the first 5 singular values of a 100,000-terms-by-2,559,430 documents data matrix using our algorithm. To our knowledge this is the first time ever that the SVD of such a large matrix has been computed in the field of text retrieval.

2) A second application of this technology was performed in collaboration with another LDRD project directed by Don Vasco in the Earth Sciences Division. Our algorithms were used to solve inverse problems arising in the study of the Earth's interior structure. The resulting matrices were of order 1.5×10^6 by 2×10^5 .

3) We considered the application of the new Lanczos algorithm in electronic structure calculations in material sciences (Cohen-Louie group at UC Berkeley). In this case the direct application of the Lanczos code proved to be less effective than a conjugate-gradient minimization.

4) We initiated a collaboration with Boeing, where John Lewis and Roger Grimes are working on a related project. Boeing has promised to release to NERSC the sparse symmetric indefinite solver, which will form the core for a shift-and-invert strategy to be developed in the second year.

Other direct participants in this project were John Wu (NERSC); Osni Marques (NERSC); Luis Bernardo (NERSC); Bernd Pfrommer (Dept. of Physics, UCB); and Hongyuan Zha (Pennsylvania State University). Other collaborators were Steve Barnard (MRJ at NASA Ames Research Center); John Lewis (Boeing, Seattle); and Michael Palmer (Inktomi, San Mateo).

Publications

Kesheng Wu and Horst D. Simon, "A Parallel Lanczos Method for Symmetric Generalized Eigenvalue Problems," LBNL Report, in preparation, submitted to *Computing and Visualization in Science*, November, 1997.

Kesheng Wu and Horst D. Simon, "Thick Restart Lanczos Algorithm for Symmetric Eigenvalue Problems," LBNL Report, in preparation.

Bernd G. Pfrommer and Horst D. Simon, "Unconstrained Energy Functionals for Electronic Structure Calculations," LBNL Report, in preparation.

Horst D. Simon and Hongyuan Zha, "On Updating Problems in Latent Semantic Indexing," submitted to *SIAM J. Scientific Computing*.

Horst D. Simon and Hongyuan Zha, "Low Rank Matrix Approximation Using the Lanczos Bidiagonalization Process," LBNL-40767, July, 1997, submitted to *SIAM J. Scientific Computing*.

Stephen T. Barnard, Luis Bernardo, and Horst D. Simon, "An MPI Implementation of the SPAI Preconditioner on the T3E," LBNL-40794, September, 1997, submitted to *Int. J. of Supercomputer Applications*.

Osni Marques and Don Vasco, "Large Scale SVD Computations in Linear Geophysical Inverse Problems," presented at IEEE Supercomputing, San Jose, CA, 1997.

Bernd Pfrommer, Steven Louie, and Horst Simon, "Conjugate Gradient Based Electronic Structure Calculations on the Cray T3E and SCI Power Challenge," Proc. of the 8th SIAM Conference on Parallel Processing, Minneapolis, March, 1997.

Earth Sciences Division

Effect of Biosorption on Actinide Migration in the Subsurface

Principal Investigators: Ilham Al Mahamid and Jennie Hunter-Cevera

Project No.: 97007

Project Description

The presence of actinides in wastes is a major environmental concern due to their long radioactive half-lives, their highly energetic emissions, and their chemical toxicity. Remediation of actinides requires stabilization or removal, as they cannot be degraded like organic contaminants.

This work focuses on the interactions of actinides with microbial soil in the absence and presence of organic chelating agents. Microorganisms can accumulate actinides, leading to either a slower or faster rate of transport depending on the mobility of the microbial population. EDTA is known to be a significant contaminant present with actinide waste. Therefore, we selected EDTA as a chelating agent for plutonium, neptunium, and americium.

The uptake of actinides by several soil microorganisms has been evaluated. The microorganisms that exhibit high uptake capacity will be selected for further studies, which will include soil matrixes. Many factors can influence the uptake of metals by microorganisms, such as ionic radius and electronic bonding properties of the metal ions, concentration of metals and their oxidation state, and the nature of reactive chemical groups and their accessibility to the microbe surfaces. Our goal is to understand the complexing properties of the selected microorganisms in the presence of actinides and determine how these complexing properties will influence actinide migration in the subsurface.

Accomplishments

We investigated the biosorption of actinides on several metabolically inactive microorganisms. Microorganisms were selected for their ability to degrade organic components of mixed wastes or for their environmental relevance. The organisms used for this study consisted of the following: *Gordona bronchialis* RR2 and *Rhodococcus rhodochrous* RR1 (toluene degraders); *Rhodococcus erythropolis* GOMEX2 and *Pseudomonas stutzeri* P-16 (PAH degraders); *Mycobacterium parafortuitum* ATCC19686 and *Micrococcus luteus* (common gram-positive); *Pseudomonas aeruginosa* NRRL B-4452 (heavy metal uptake strain), *Pseudomonas aeruginosa* CV1 (phenol degrader from refinery); and *Pseudomonas fluorescens* and *Acinetobacter* sp. (common gram-negative).

We examined the sorption of Pu(III) and Am(III) by the microorganisms mentioned above. We obtained very high sorption for several of the microorganisms tested. Figure 1 shows the sorption of Am(III) on these microorganisms; series 2 represents the duplicate for the Series 1. We selected 5 microorganisms from the above study and tested them for the Pu(IV)-EDTA and Am(III)-EDTA systems. The results showed that the sorption of actinide-EDTA complexes is significantly lower than the sorption of the actinide ions.

We tested the sorption of Np(V) on two microorganisms: *Pseudomonas aeruginosa* NRRL B-4452 and *Mycobacterium parafortuitum* ATCC19686. At microbial mass of about 3 mg/ml, the sorption on *Pseudomonas aeruginosa* reached 45% of the initial Np concentration, while the sorption on *Mycobacterium parafortuitum* did not exceed 12%. Figure 2 shows the sorption of Np(V) on *Pseudomonas aeruginosa* as a function of microbial mass; series 2 represents the duplicate for the Series 1. R is the sorption ratio and is defined as:

$$R\% = \frac{C_0 - C_f}{C_0} \times 100$$

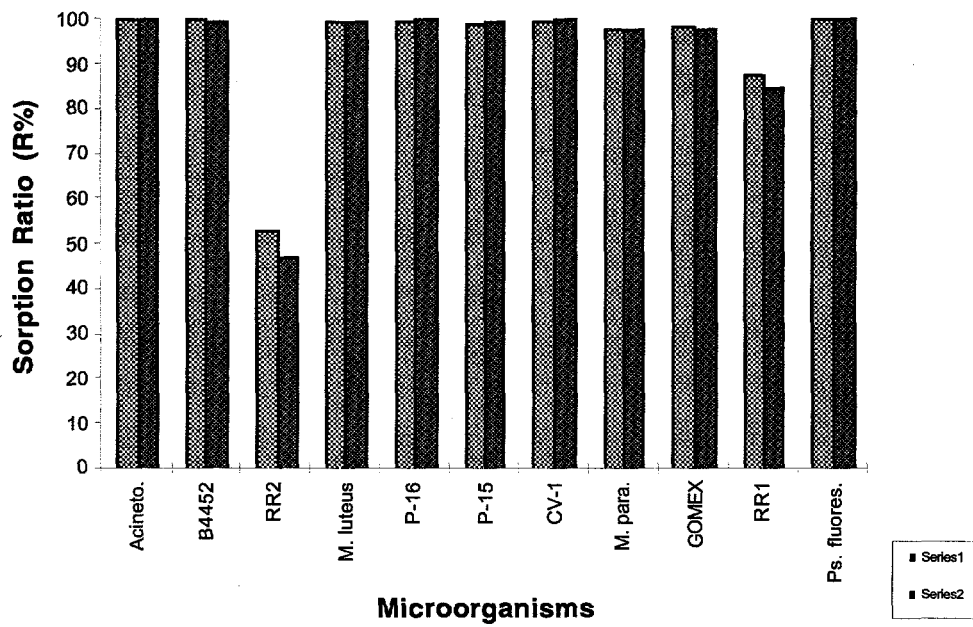


Figure 1. Sorption of Am(III) on soil microorganisms initial concentration: $[Am(III)] = 1.62 \times 10^{-8} M$.

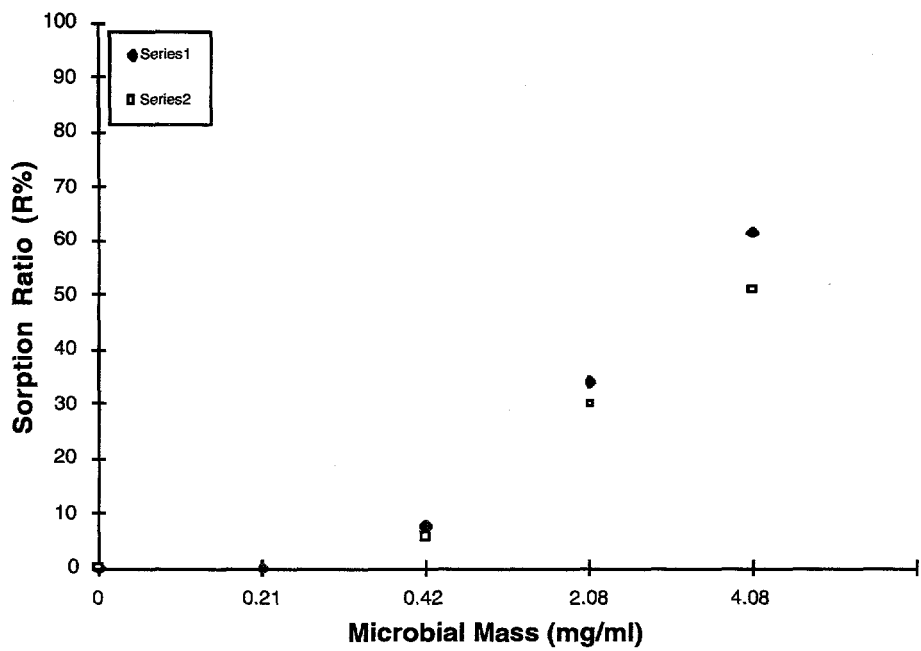


Figure 2. Sorption of Np(V) on Pseudomonas aeruginosa initial concentration: $[NP(V)] = 5.3 \times 10^{-5} M$.

where,

C_0 = actinide initial concentration (M)

C_f = actinide final concentration (M).

Publications

The research results were presented at the Sixth International Conference on the Chemistry and Migration Behavior of Actinides and Fission Products in the Geosphere, MIGRATION '97.

I. Al Mahamid, N. Hakem, W.T. Stringfellow, and J. Hunter-Cevera, "Effect of Actinide Biosorption on Actinide Migration in the Subsurface," Sendai, Japan, October 26-31, 1997, LBNL-40940.

Molecular and Functional Analysis for Evaluating Microbial Treatment Process Performance

Principal Investigators: Terrance Leighton and Fred Brockman (PNNL)

Project No.: 97034

Project Description

Microbial processes are widely used to destroy and detoxify organic and inorganic contaminants in groundwater pump-and-treat systems, petroleum refining, and other industrial wastewaters. However, these systems often experience process upsets and poor efficiency due to changes in the composition of the wastewater and/or changes in the structure/function of the microbial community. Currently, only rudimentary efforts have been made to understand what is happening, at a microbial community-structure level, during periods of poor system performance. Thus, engineers have a poor understanding of the specific microorganisms responsible for optimal system performance and how the treatment process could be enhanced. This project will develop and use a genosensor microarray to identify and characterize the types of microorganisms in petroleum refinery wastewater during efficient and inefficient periods of operation. This information will provide an enabling technology for informed operational decisions. It will also improve management of the treatment process and minimize the environmental impacts of wastewaters.

Accomplishments

This project focused on gaining an understanding of the planktonic microbiological community of an EXXON activated sludge wastewater process (BIOX), using culturing methods and community-level physiological profiling. An initial survey of the BIOX planktonic community diversity, as assessed by the Biolog microbial identification system, made 14 Biolog identifications.

Additional BIOX samples were collected and analyzed by both Biolog and 16S rDNA methods to assess the correlation between these two technologies for microbial identification. The Biolog method has the advantages of high sample throughput, speed, and lower cost. The 16S rDNA method is more time consuming and costly, but has the advantage of directly determining the phylogenetic position of environmental isolates. The Biolog classification data for a suite of EXXON BIOX isolates are presented in Table 1.

Table 1.

| Strain | Biolog ID | Similarity |
|---------|---|------------|
| Ex3b-30 | <i>Klebsiella pneumoniae</i> ss <i>pneumoniae</i> | 0.842 |
| Ex2a-30 | <i>Klebsiella pneumoniae</i> ss <i>ozaenae</i> | 0.846 |
| Ex3c-30 | <i>Bacillus subtilis</i> var <i>globigii</i> | 0.822 |
| Ex4-30 | <i>Aeromonas veroni</i> | 0.845 |
| Ex3a-30 | <i>Klebsiella pneumoniae</i> ss <i>pneumoniae</i> | 0.905 |
| Ex1-30 | <i>Pseudomonas pseudoalcaligenes</i> | 0.901 |
| Ex5a-30 | <i>Bacillus pasteurii</i> | 0.869 |
| Ex5b-30 | <i>Xanthomonas maltophilia</i> | 0.984 |
| Ex1-37 | <i>Pseudomonas pseudoalcaligenes</i> | 0.877 |
| Ex2a-37 | <i>Bacillus subtilis</i> var <i>globigii</i> | 0.78 |
| Ex5a-37 | <i>Vibrio metschnikovii</i> | 0.544 |
| Ex4-37 | <i>Bacillus mycoides</i> | 0.503 |
| Ex2b-37 | <i>Xanthomonas maltophilia</i> | 0.856 |
| Ex3b-37 | <i>Yersinia enterocolitica</i> | 0.783 |

The corresponding 16S rDNA BIOX isolate classification data are presented in Table 2. Microbial classification by 16S rDNA sequencing is generally regarded as the "gold standard" method for taxonomically positioning an unknown isolate. However, both the 16S rDNA (10,000 organisms) and Biolog (1400 organisms) databases may not contain genera or species that are significant populations in industrial wastewater treatment systems. Similarity coefficients to database hits are difficult to rigorously interpret, although all of the values obtained would be expected to be accurate to at least the genus level. It would appear that the Biolog database is substantially more deficient in environmental isolates than the 16S rDNA database. These results suggest that a custom Biolog database, based on 16S rDNA strain assignments, will have to be constructed to accurately and rapidly classify wastewater treatment systems isolates.

The readily accessible BIOX planktonic microbial community has been the initial focus of the LBNL Community Level Physiological Profile (CLPP) treatment system monitoring program. This project has two goals: the development of monitoring tools to assess microbial community adaptation and adjustment to variations in treatment system

operating parameters; and the use of CLPP as a high-throughput screening system to engineer the microbial community metabolically for optimal toxic metal bioremediation. CLPP has proven to be a very sensitive and incisive tool for assessing the integrity and functionality of the EXXON treatment system microbial community. CLPP has been used to track a treatment system upset that was caused by an alteration in the food-to-mass ratio of the wastewater feed stream. This perturbation resulted in significant negative impacts on treatment system nitrification and settling parameters. These data validate the utility of CLPP for stability/recovery analysis of activated sludge petroleum refinery treatment systems. They also demonstrate that there is a defined recovery path and the potential of this technology for treatment process monitoring and control. Based on these promising findings, EXXON is establishing an on-site Biolog monitoring capability at their Baton Rouge, LA, refinery. EXXON, LBNL, and UC Berkeley personnel are collaborating in the development, demonstration, and validation of CLPP for the assessment and control of activated sludge microbial treatment processes. CLPP data analysis and process control software for the petroleum industry is being developed. CLPP stability/recovery analysis of typical process upsets will create an expert system that can predict the occurrence and nature of treatment system failures before the integrity of the microbial community is violated. The long-term goal of the project is to disseminate this technology to the forty worldwide EXXON plants that use activated sludge wastewater treatment systems.

Table 2.

| Strain | 16S rRNA ID (27f, 519r primer) | Similarity |
|---------|--------------------------------------|------------|
| Ex3b-30 | <i>Escherichia coli</i> | 0.845 |
| Ex2a-30 | <i>Escherichia coli</i> | 0.845 |
| Ex3c-30 | <i>Bacillus subtilis</i> | 1.00 |
| Ex4-30 | <i>Aeromonas veroni</i> | 0.982 |
| Ex3a-30 | <i>Escherichia coli</i> | 0.928 |
| Ex1-30 | <i>Azospirillum</i> | 0.928 |
| Ex5a-30 | <i>Bacillus cereus</i> | 0.972 |
| Ex5b-30 | <i>Symbiont Melanocetus johnsoni</i> | 0.644 |
| Ex1-37 | <i>Azospirillum</i> | 0.952 |
| Ex2a-37 | <i>Bacillus subtilis</i> | 1.00 |
| Ex5a-37 | <i>Aeromonas veroni</i> | 0.946 |
| Ex4-37 | <i>Bacillus cereus</i> | 0.989 |
| Ex2b-37 | <i>Pseudomonas putida</i> | 1.00 |
| Ex3b-37 | <i>Escherichia coli</i> | 0.845 |

We have determined that the planktonic microbial community represents greater than 10% of the total BIOX biomass. The majority of the BIOX biomass is contained in an attached microbial community that is associated with treatment system activated carbon granules.

A companion project was carried out by PNNL to assess the materials, architecture, and operating principles of genosensor microarrays being developed by various microelectronic companies engaged in biotechnology research and development. PNNL has initiated an effort to better understand the attached microbial community in the BIOX biomass and to determine what portions of the community the microarray should target most strongly.

In contrast to most published studies on analysis of community 16S rDNA, 70% of the types in the BIOX sample (39 of 56) had a similarity to sequences in databases of greater than 90%. However, only two

genera (*Azospirillum* and *Pseudomonas*) were identified in both the planktonic cultural approach (LBNL) and the direct extraction attached community approach (PNNL), highlighting the differences in planktonic and attached microbial community diversity.

Publications

S.H. Shafikhani and T. Leighton, "Signal Transduction and Transcriptional Control of *spoIIJ* and *spoOP* Genes in *Bacillus subtilis*," 9th International Conference on Bacilli, Lausanne, Switzerland, July 15-19, 1997.

P. Longchamp, M. Adamkiewicz, B.B. Buchanan, and T. Leighton, "Proteins Synthesized During Selenite Reduction by *Bacillus subtilis*," 9th International Conference on Bacilli, Lausanne, Switzerland, July 15-19, 1997.

T. Leighton, P. Longchamp, S. Shafikhani, G. Montanez, C. Garbisu, M. Adamkewicz, D. Carlson, and B.B. Buchanan, "Developmental and Molecular Genetic Regulation of Selenite Detoxification in *Bacillus subtilis*," Plenary Lecture-7th International Conference on the Chemistry of Selenium and Tellurium, Vaals, Netherlands, July 20-25, 1997.

T. Leighton, "Bioremediation Education Science and Technology Program," Society for Industrial Microbiology Annual Meeting, Reno, NV, August 3-7, 1997.

G.E. Montanez, P. Longchamp, and T. Leighton, "Molecular Analysis of the Thioredoxin System in *Bacillus subtilis*," Society for Industrial Microbiology Annual Meeting, Reno, NV, August 3-7, 1997.

D. Sauri, M. Velazquez, F. Rivera, E. Resto, D. Caro, D. Cacho, and Y. Bernier, "Bioremediation of Toxic Metals Using the Soil Bacterium, *Bacillus subtilis*," Society for Industrial Microbiology Annual Meeting, Reno, NV, August 3-7, 1997.

M. Ratliff, T. Leighton, T. Pham, B. Martinez, R. Perez, M. Ruiz, and D. Sauri, "Bioremediation Potential of Microorganisms Isolated From EXXON and Grassland Water Samples," Society for Industrial Microbiology Annual Meeting, Reno, NV, August 3-7, 1997.

T. Leighton, P. Longchamp, S. Shafikhani, G. Montanez, C. Garbisu, M. Adamkewicz, D. Carlson, and B.B. Buchanan, "Physiological and Molecular Genetic Regulation of Selenite Detoxification in *Bacillus subtilis*," Emerging Technologies in Hazardous Waste Management, 9th American Chemical Society, Pittsburgh, PA, September 15-17, 1997.

Electromagnetic Methods for Fluid Emplacement and Monitoring in the Subsurface

Principal Investigator: George Moridis

Project No.: 97008

Ferrofluids are stable colloidal suspensions of magnetic particles in various carrier liquids with very high saturation magnetizations (100-2,600 Gauss). The solid, magnetic, single-domain particles have an average diameter of 3-15 nm, and are covered with a molecular layer of a dispersant. Thermal agitation (Brownian motion) keeps the particles suspended, while the dispersant coating prevents agglomeration of the particles. Ferrofluids are superparamagnetic and move as a homogeneous single-phase fluid under the influence of a magnetic field, with no separate consideration for the magnetic particles and the carrier liquid. This attribute is responsible for the unique property of ferrofluids, i.e., that they can be manipulated in virtually any fashion, defying gravitational or viscous forces in response to external magnetic fields.

Project Description

The objectives of the proposed research are to investigate the potential of ferrofluids (stable suspensions of colloidal ferromagnetic particles in a carrier liquid)

- to accurately and effectively guide reactants (for *in-situ* treatment) or barrier liquids (low-viscosity permeation grouts) to contaminated target zones in the subsurface using electromagnetic forces, and
- using geophysical methods, to trace the movement and position of liquids injected in the subsurface.

Ferrofluids for Guiding Liquids in the Subsurface

Ferrofluid for Guiding liquids (FGs) have low viscosities (<5 cp, allowing easy injection into the subsurface), small particle size (3.5-15 nm, minimizing potential filtration problems), and a very high saturation magnetization (100-2,600 Gauss). The ability of FGs to be guided precisely to specific areas in response to an external field has potentially important applications in the environmental

restoration of the subsurface. We propose to use FGs to enhance the efficiency of *in-situ* treatment and waste containment through 1) accurate guidance and delivery of reagent liquids to the desired subsurface contamination targets, and / or 2) effective sweeping of the contaminated zone as FGs move from the application point to an attracting magnet / collection point. FGs can be manufactured with the appropriate carrier liquids, reactants (e.g., oxidants) for *in-situ* treatment and barrier liquids.

Current delivery and emplacement practices for *in-situ* remediation or containment consist entirely of injection, and suffer from the adverse effect of heterogeneity, which may cause the treatment effort to be short-circuited by preferential flow through highly permeable zones. Magnetic fields are easier to manipulate than pressure fields, are unaffected by the significant heterogeneity of the soil hydraulic properties, and are significantly less effected by heterogeneity in the soil magnetic properties. Emplacement of liquids (for *in-situ* treatment or containment) in response to a magnetic field is thus expected to be more accurate and effective by allowing liquids to be focused and guided to the desired locations in the subsurface and more effectively sweeping the targeted treatment zone.

Ferrofluids for Tracing and Detection of Liquids

Ferrofluid for Tracing liquids (FTs) have strong electromagnetic signature. Because of this signature, FTs are used commercially for magnetic pattern recognition in magnetic tapes, hard and floppy disks, and crystalline and amorphous alloys. The high saturation magnetization in the FGs provides a signature sufficiently strong for magnetic detection methods at low loading volumes (i.e., 1–5%). We propose to exploit this property to develop a method for monitoring of liquid movement and position during injection using electromagnetic methods. FTs can also provide a significant detection and verification tool in containment technologies, where they can be injected with the barrier liquids. This provides a strong signature and allows determination of the barrier geometry, continuity, and integrity. FTs can also be used to identify high-permeability pathways, and thus allow the design of more effective remediation systems.

Accomplishments

Preliminary Theoretical Analysis

FG Studies. Starting from first principles, the equation of FG flow in porous media was derived. This equation is analogous to the conventional Darcy equation, from which it differs by the inclusion of magnetic and magnetostrictive forces. The appropriate multi-phase and / or solute transport equations governing the flow of subsurface liquids in the presence of FGs were identified, as well as relationships affecting the rheology of FGs. The corresponding equations of induction and magnetic field (Maxwell equations) were determined, and the appropriate modifications were made. Analytical solutions were developed for an FG moving in an FG-saturated medium in response to a magnetic field. Practical FG applications involve the solution of coupled, strongly nonlinear equations of flow and magnetic field which are tractable only through numerical simulation. Using the TOUGH2 general simulator of flow and transport through porous media, the new module EOF7M, describing the behavior and flow of ferrofluids in the presence of a magnetic field, was developed and tested. The EOS7M module accounts for the effects of the magnetic field on the ferrofluid, as well as the coupled effects of water-miscibility on the ferrofluid properties and its flow and transport characteristics.

FT Studies. We demonstrated the feasibility of using conventional magnetometry for detecting subsurface zones of injected FTs used to trace liquids injected for remediation or barrier formation. The geometrical shapes considered to date are a sphere and a flat thin square plate. Spheres with FT concentrations of 5% and 1% were shown to be easily detectable at depths of 12 m and 7 m, respectively. Two-cm thick plates with 5% and 1% FT concentrations were detectable at depths of 10 m and 6 m, respectively. The foundations of a new detection method, based on the superparamagnetic properties of FTs, were developed. The superparamagnetism of FTs manifests itself as energy absorption at very low fields. The notion of a complex magnetic susceptibility was introduced; the real component defines the ferromagnetic behavior, while the imaginary component determines its energy absorption

properties. Sinusoidal (AC magnetization) and step excitations can be used in conjunction to determine FTs in the subsurface.

Scoping and Laboratory Studies

Scoping Studies. FGs were shown to move under the influence of fields as low as 15 Gauss. Scoping calculations were made to calculate the distance over which FGs could be moved. Using permanent magnets, the maximum effective distance for $d = 12\text{-cm}$ dipole was calculated as 125 cm. Using superconducting magnets, an effective distance of 218 cm was calculated for a coil distance $D = 5\text{ cm}$. Depending on the magnetic field configuration, the maximum distance for moving FGs increases linearly with d or the square root of D .

FG Laboratory Studies. We studied the movement of an FG of relatively low saturation magnetization (200 Gauss) in response to weak magnetic fields from permanent (NdFeB with $B_r = 11,000$ Gauss) magnets and electromagnets. Permanent magnets were shown to be far more effective in these small-scale experiments. A column of ferrofluid was induced to move upward (against gravity) as a cohesive unit over a distance of 12 cm. Ferrofluid drops with a volume of 1.3 mL were attracted to a NdFeB magnet located 14 cm away (confirming the calculated distance). FG was injected into a wet sand and was directed by an applied field from a NdFeB magnet 12 cm away (Figure 1). Upon reaching the magnet, the ferrofluid began to pool and form a semicircular symmetric structure. Excavation through the sand tray revealed that the ferrofluid traveled evenly throughout the depth of the sand. Ferrofluid was mixed with colloidal silica, a gelling barrier liquid. The ferrofluid did not have any adverse effect on the gellation of CS, and FG concentrations of 20 and 30% allowed movement in response to a magnetic field generated by a NdFeB magnet located 6 cm away.

Publications

S. Borglin and G.J. Moridis, "Experimental Investigations of Magnetically-Driven Flow of Ferrofluids Through Porous Media," LBNL-40126, Lawrence Berkeley National Laboratory, March, 1997.

K. Das, A. Becker, and G.J. Moridis, "Magnetic Detection of Ferrofluid Injection Zones," LBNL-40127,

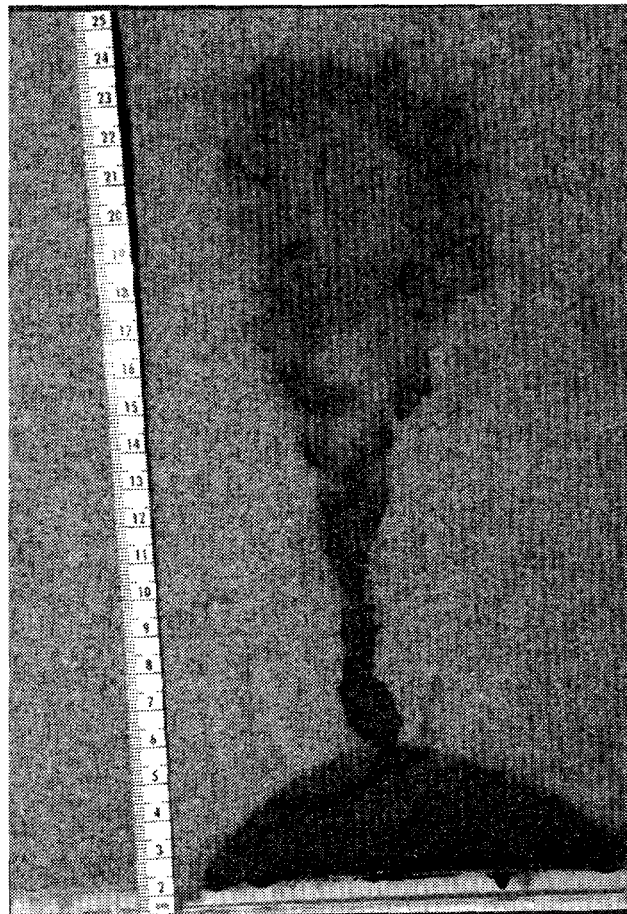


Figure 1. After flowing through sand under the influence of a magnetic field, ferrofluid accumulates symmetrically next to the magnet.

Lawrence Berkeley National Laboratory, Berkeley, CA, March, 1997.

G.J. Moridis and C. Oldenburg, "Ferrofluid Flow in Porous Media," LBNL-40167, Lawrence Berkeley National Laboratory, Berkeley, CA, September, 1997.

G.J. Moridis, C. Oldenburg, S. Borglin, A. Becker, and K. Das, "Theoretical and Experimental Investigations in the Use of Ferrofluids to Guide and Detect Liquids in the Subsurface," LBNL-41069, Lawrence Berkeley National Laboratory, Berkeley, CA, November, 1997.

C. Oldenburg and G.J. Moridis, "On Modeling Flow and Transport of Magnetic Fluids in Porous Media," LBNL-40146, Lawrence Berkeley National Laboratory, Berkeley, CA, March, 1997.

High Resolution Microscopic and Spectroscopic Investigations of Mineral-Adsorbed Humic Substance Influence on Soil Contaminant Behavior

Principal Investigator: Satish Myneni

Project No.: 97009

Project Description

Humic substances are common in natural earth materials and constitute molecules with wide ranges of sizes and reactive functional groups. These substances are derived from the degradation of plant and animal tissue and exist in soils or natural waters as mineral surface coatings, soluble ions, and colloids. They play a key role in geological processes such as mineral weathering, soil formation, colloid stability, plant nutrient availability, and pollutant solubility and transport. While these natural organic molecules contain C-, N-, P-, and S-functional groups, their molecular behavior is altered by the properties of the mineral substrate (structure, bonding to selected functional groups) and solution (ionic strength, pH, complexing ions). At present, different spectroscopic techniques such as luminescence, NMR, and IR have been applied by researchers to characterize their behavior. However, all of these studies are limited by their sensitivity toward differentiating various functional groups in dilute samples. We propose to investigate the functional group chemistry and the macromolecular structure of natural organic molecules and their influence on contaminant sorption with the help of soft x-ray absorption techniques.

The specific research objectives were:

- Examine the *in-situ* macromolecular structure of humic substances as modified by pH, ionic strength, humic substance concentration, and mineral substrate composition and structure.
- Evaluate the C-, N-, P-, and S- functional group chemistry of natural organic molecules, and
- Examine the metal-, and organic-organic interactions (complexation) in water and on mineral surfaces.

In this research we proposed to use x-ray microscopy (XM) and atomic force microscopy (AFM) to examine the *in-situ* macromolecular structure of fluvial and soil humic substances. While the XM allows imaging at a resolution better than 50 nm and permits probing of the internal structures of soil and aquatic humic substances, AFM also allows higher resolution imaging on flat, soil-mineral surfaces. In addition, transmission-NEXAFS spectra of the same samples can be collected from different locations in the organic molecule using a scanning transmission x-ray microscope at the ALS (resolution ~ 100 nm). For the functional group chemistry evaluation of humic substances at dilute concentrations, we designed special instrumentation, called Soft-X-Ray Endstation for Environmental Research (SXEER), that will allow the examination of dilute aqueous solutions of organic compounds, and the L-and higher edges of heavier elements at atmospheric pressures. Using these tools we propose to evaluate the humic substance macromolecular structure, functional group chemistry, and reactivity simultaneously.

Accomplishments

This study focused on the design and fabrication of SXEER, examination of the macromolecular structures of humic substances and soil organic matter using XM, and preliminary investigation of the functional group chemistry of humic substances.

Soft-X-Ray Endstation for Environmental Research (SXEER).

This movable endstation has been designed to examine the K-edges of organic compounds and the L- and other edges of heavier elements of environmental importance in dilute aqueous solutions and at atmospheric pressure (or at conditions of higher pressures than conventional UHV). SXEER can be attached to any existing vacuum beamline at the Advanced Light Source (ALS). The high brightness of the ALS beams allows the use of extremely thin windows to separate the UHV part of the beamline and the sample chamber at atmospheric pressures. The estimated photon flux in the endstation is comparable to that available inside a vacuum beamline, and the windows absorb only 25–40% of the total flux. SXEER contains ion pumps and several valves through which x-rays enter the sample chamber, which is maintained at ambient conditions.

Macromolecular Structures of Humic Substances

Using the changes in the macroscopic solution parameters, such as viscosity and vapor pressure osmometry, researchers have predicted that humic substances coil at low pHs and high ionic strengths, and form linear strands at high pHs and low ionic strengths. However, no direct proof of their behavior in aqueous solution is currently available. The vacuum conditions of the electron microscopes prevented their examination in solutions. Although the recent AFM studies on humics offered more information on adsorbed humics on mica surfaces, these studies are limited to extremely flat substrate surfaces. Using XM, our *in-situ* experiments on soil and fluvial humic substances indicated that different types of structural conformations are possible under the same solution conditions, and the predominant factor controlling their behavior is the concentration of humic substances.

Functional Group Chemistry of Humic Substances

Preliminary investigations of the functional group chemistry of humic substances have been conducted at the Advanced Light Source and Stanford Synchrotron Light Source. These results suggest that several different C-, N-, P-, and S-containing groups can be identified using x-ray absorption techniques. The spectral resolution at each of these element x-ray absorption edges is sufficient enough to distinguish all the primary functional groups of humic substances. Although NMR has higher sensitivity in distinguishing several different chemical moieties, the soft XAS methods we are developing at the ALS are ideal for probing dilute (mM) samples without sacrificing spectral resolution. In addition, the soil samples can be examined directly without being subjected to any special chemical treatment or extraction procedures. We have also examined the metal complexation reactions for the fluvial humic substances, and the spectral resolution is sufficient to identify the functional groups participating in complexation reactions. In the future we wish to explore humic substance reactions with the metal/hydrophobic organic contaminant and mineral surface.

The principal investigator would like to thank the following for their participation and for providing research facilities: Drs. Zahid Hussain, Neal Hartman, Adrian Garcia, and Anthony Warwick of the Advanced Light Source; Werner Meyer-Ilse and John Brown of the Center for X-ray Optics; and Gustavo Martinez of the Agricultural Experiment Station,

University of Puerto Rico. Special acknowledgment is also extended to Dr. Tetsu Tokunaga and Dr. Sally M. Benson for support and encouragement.

Publications

S.C.B. Myneni, J.T. Brown, W. Meyer-Ilse, G.A. Martinez, A. Garcia, and A. Warwick, "Molecular Conformation and Functional Group Chemistry of Humic Substances Using Soft X-Ray Synchrotron Radiation," abstract for the American Geophysical Union National Meeting, San Francisco, CA, 1997.

S.C.B. Myneni, J.T. Brown, G.A. Martinez, and W. Meyer-Ilse, "Molecular Conformation of Humic Substances in Water and Soils," to be submitted to *Nature*.

Reactive Chemical Transport in Geologic Media

Principal Investigators: Karsten Pruess and George Brimhall

Project No.: 96031

Project Description

The purpose of this project is to develop a detailed three-dimensional simulation of the geologic evolution of an actual ore deposit through reactive porous media flow, subject to unique geologic constraints. The site chosen for the analysis is the El Salvador mine, which is located in the Atacama desert of northern Chile. El Salvador is operated by CODELCO, whose data base of ore grades, derived from 11,000 drill holes, is available to the project.

The site-specific modeling effort will determine the interplay between paleoclimatic change, hydrogeologic conditions, erosion and uplift, and the mobilization and enrichment of massive amounts of copper-bearing minerals in response to spatially and temporally varying redox conditions. TOUGH2 (refer to URL <http://ccs.lbl.gov/TOUGH2/>), Berkeley Lab's existing general-purpose, multiphase,

multicomponent simulator, will be applied to model the evolution of hydrogeologic conditions over geologic time. The simulator will also be enhanced to describe the transport of multiple chemical species subject to kinetic and equilibrium-controlled reactions, and will be ported to advanced massively-parallel computing platforms. Data from laboratory leach column experiments will be used to determine reaction kinetics, and to test the ability of the simulator to adequately describe reactive chemical transport processes. Existing speciation and reaction path models will be implemented and utilized in the analysis.

Results from the project are expected to aid in future exploration efforts for porphyry copper deposits, and in the management of acid mine waters, leach dumps, mine tailings, and waste disposal facilities. The reactive chemical transport capabilities will also be useful for assessing and remediating environmental contamination at DOE and industrial sites.

Accomplishments

The CODELCO data base has been implemented on a Silicon Graphics workstation. Kriging techniques incorporated in the commercial VULCAN mining engineering software were used to develop two- and three-dimensional visualizations (refer to URL http://vis.lbl.gov/site_info/gallery.html) of the distribution of ore grades. Mass balance calculations were performed to analyze the relationship between the present-day ore body and the distribution of protore from which it originated. This analysis demonstrated the crucial role of faults in the development of a laterally-offset "exotic" ore body (so-called because it occurs several kilometers away from its original source of copper in the primary ore deposit).

Our TOUGH2 flow and transport simulator was ported to Cray supercomputers at NERSC. Development of two-dimensional vertical section models of the hydrogeology at El Salvador has been completed. Figure 1a shows an east-west cross section of the different hydrogeologic units in this heterogeneous flow system that was developed with the VULCAN software. For simulation purposes this section was discretized into approximately 11,600 rectangular grid blocks. Figure 1b shows simulated water saturations at steady state for an applied net infiltration of 20 cm/yr, which is believed to be a realistic value during the transition from pluvial to semiarid conditions at approximately 15 Ma. The

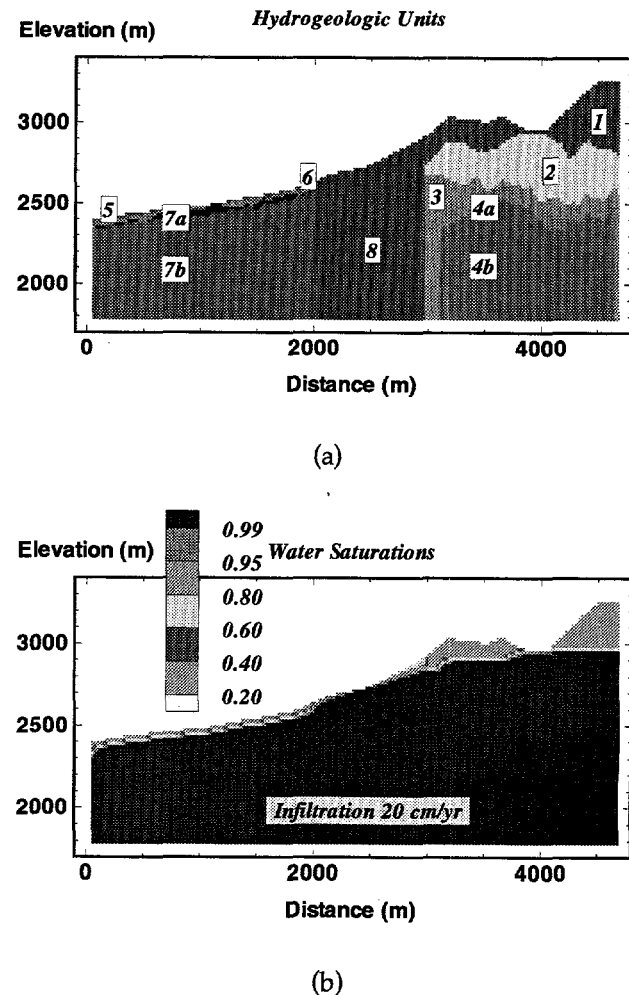


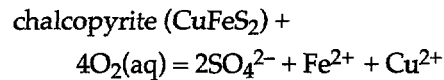
Figure 1. East-west cross section through El Salvador. (a) hydrogeologic zonation based on ore grade data (1 - leached cap, 2 - enrichment blanket, 3 - protore, 4 - protore with precipitated sulfate, 5 - gravels, 6 - weathered andesite, 7a - exotic ore body, 7b and 8 - fresh andesite); (b) simulated water saturations at steady state for a net infiltration of 20 cm/yr.

water table is seen to intersect the land surface near 2,500 m distance, which is consistent with the inferred location of paleo-springs in this region. An inverse version of TOUGH2 known as ITOUGH2 (refer to URL <http://ccs.lbl.gov/ITOUGH2/>) was implemented on the massively-parallel T3E machine. Using data parallelism required minimum changes to the code. The data were found to distribute well between processors, the required communication is modest, and problems scaled nicely with the number of processors.

We have focused the geochemical work in this project on application of the EQ3/6 speciation and reaction path code which represents the most comprehensive and rigorous capability presently available for modeling the chemical behavior of complex mineral assemblages. Earlier modeling of supergene enrichment of porphyry copper deposits addressed one-dimensional reactive flow in a coarsely-discretized medium with five chemically distinct subdomains. Here we have begun to refine this test case using EQ3/6 with TOUGH2 to further clarify how economic ore deposits evolve from an interplay between water table fluctuations, variable redox conditions, and mobilization and reprecipitation of copper. We are in the process of validating the first results of the new codes by comparison with the results from the earlier published study in which theoretically-predicted mineral assemblages generally were found to be in excellent agreement with those observed in natural systems.

A mathematical model for reactive multispecies transport in multiphase flow conditions was developed which serves as blueprint for our evolving fully-coupled process simulation code. This is being implemented through coupling of TOUGH2 with EQ3/6. A first coupling was achieved using the sequential iteration approach, which can cope with any number of gaseous, aqueous, and mineral species. A number of aqueous speciation and reaction path calculations were performed to evaluate subsets of the supergene enrichment process that produced the El Salvador ore body. As an example we present a simulation of chalcopyrite (CuFeS_2) oxidation under variably-saturated conditions in a fractured-porous medium. A 2D vertical section in an idealized system geometry was simulated (Figure 2a). Water containing dissolved oxygen at a partial pressure of 0.2 bar infiltrates at the top of the vertical fracture

zone at a rate of 1 cm/day. The initial mineral assemblage in fracture zones and matrix rock includes chalcopyrite, quartz, alunite, and kaolinite. Chalcopyrite is oxidized and dissolved by aqueous phase oxygen according to the following reaction:



At the same time, alunite and quartz also dissolve while kaolinite precipitates. As aqueous-phase oxygen is depleted through reaction with chalcopyrite, additional oxygen dissolves from the gas phase. This in turn is replenished by diffusive transport from the atmosphere at the land surface boundary. Maximum dissolved copper concentrations occur near the fracture zones (Figure 2b), which indicates the important role of gaseous oxygen in this reaction. Spatial profiles along the vertical fracture at different times show the rapid downward migration of a broad reaction front (Figure 2c).

Publications

F. Gérard, T. Xu, G. Brimhall, and K. Pruess, "Modeling Reactive Chemical Transport Problems with the Codes EQ3/6 and TRANQUI," Lawrence Berkeley National Laboratory Report LBNL-40505, July, 1997.

K. Pruess, "Incorporating Chemistry and Kinetics into Field-Scale Numerical Models," Lawrence Berkeley National Laboratory Report LBNL-40862, September, 1997.

T. Xu, F. Gérard, K. Pruess, and G. Brimhall, "Modeling Nonisothermal Multiphase Multispecies Reactive Chemical Transport in Geologic Media," Lawrence Berkeley National Laboratory Report LBNL-40504, July, 1997.

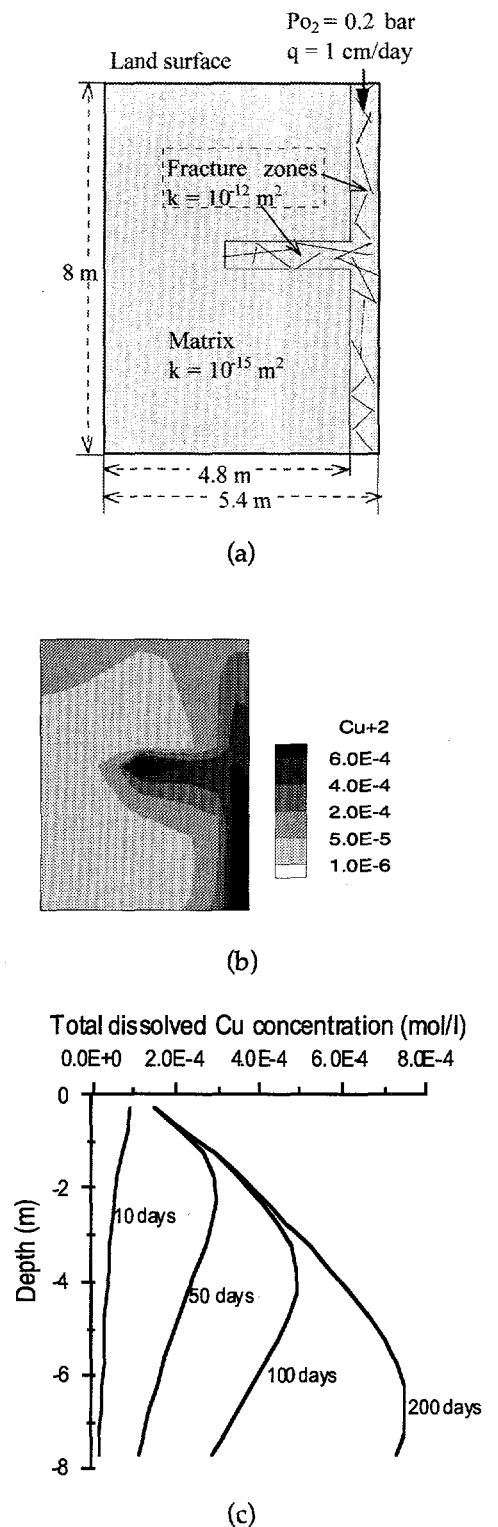


Figure 2. Simulation model of chalcopyrite dissolution under variably-saturated conditions. (a) model setup; (b) dissolved copper concentrations after 200 days; (c) temporal evolution of dissolved copper concentrations in the vertical fracture zone.

Molecular Geochemistry of Clay Mineral Surfaces

Principal Investigator: Garrison Sposito

Project No.: 96032

Project Description

This project involves basic research towards an accurate model of molecular structure at the surface of hydrated 2:1 layer-type clay minerals (smectites). These minerals are of great importance in petroleum production, nuclear waste containment, and contaminant attenuation. The objective to be addressed is concurrent Monte Carlo and molecular dynamics simulations of interfacial molecular structure on smectite minerals adsorbing water and cations (counterions). The results obtained should provide a significantly improved quantitative understanding of clay-clay, clay-water, and cation-clay interactions that will be used to test and, if necessary, improve existing experimental data as well as the potential function models used in our Monte Carlo CMC and molecular dynamics (MD) simulations of hydrated 2:1 clays.

Computational algorithms for the MC/MD simulations, based on the codes MONTE and MOLDY, have been developed by our collaborators, Dr. N.T. Skipper and Dr. K. Refson. The codes are fully optimized and running well on the Cray J90. Recently, Dr. Refson has produced a fully-parallel version of the code MOLDY, which we hope to compile and run on the Cray T3E at NERSC.

Accomplishments

Monte Carlo and molecular dynamics simulations were performed to elucidate interlayer structure in hydrated Li-smectites (hectorite, beidellite, or montmorillonite with interlayer Li^+ counterions) at low water content ($H_2O/Li = 3$). Previous spectroscopic studies of these stable clay mineral hydrates have led to interlayer structural models based on a postulated inner-sphere surface complex comprising Li^+ bound directly to the smectite surface while surmounted by exactly three solvating water molecules that execute hindered rotational motions. Our simulation results, based on tested water-water, Li^+ -water, water-clay mineral, and Li^+ -clay mineral

potential functions, showed that in fact the nature of the interlayer Li^+ solvation complexes depends critically on the location of negative charge sites within the smectite layers. Inner-sphere surface complexes were observed to form exclusively on Li-beidellite (tetrahedral charge sites); outer-sphere surface complexes formed exclusively on Li-hectorite (octahedral charge sites); and both types of surface complex formed on Li-montmorillonite, which also contains both types of charge site. The Li^+ solvation number in these clay hydrates can vary from two to four. Rotational motions of the water molecules solvating Li^+ occurred (on a picosecond time scale) only if inner-sphere surface complexes had formed, again strongly contradicting the spectroscopic models.

Our MC/MD simulations of interlayer molecular configurations in $\text{Li}(\text{H}_2\text{O})_3$ -smectites thus indicate clearly that the inner-sphere trihydrate surface complex, proposed originally for $\text{Li}(\text{H}_2\text{O})_3$ -hectorite and extended to other 2:1 clay minerals on the basis of spectroscopic data, was an oversimplification in several respects. Firstly, both inner-sphere and outer-sphere surface complexes are possible, depending on the type of surface charge site, and Li^+ solvation number can vary from two to four. Secondly, rotational motions of these surface complexes are restricted to those of the water protons around C_2 axes, (at least over 200 ps time scale) and even these rotations are absent when outer-sphere surface complexes of Li^+ occur exclusively in the interlayer region (hectorite). Water molecules in $\text{Li}(\text{H}_2\text{O})_3$ -hectorite that are not in surface complexes with Li^+ do show C_2 -rotation, however.

Our simulation results for $\text{Li}(\text{H}_2\text{O})_3$ -hectorite, a system which has been studied extensively by spectroscopy, are in general agreement with the interpretation of both IR and NMR spectral data insofar as the average orientation of water molecules is concerned, but differ sharply with the interpretation of these latter spectral data, as well as with QNS spectral data, in respect to rotational motions. On the other hand, the Li^+ oscillations that were inferred as the cause of isotropicity in high-incident energy QNS spectra are also predicted by our MD simulations. There is not agreement between our simulations and the spectroscopic models with regard to Li^+ solvation number or the type of surface complex formed. These major differences should be resolved by constructing new spectroscopic models guided by the results in this project and comparing them with extant or new spectral data.

Publications

F.-R.C. Chang, N.T. Skipper, and G. Sposito, "Monte Carlo and Molecular Dynamics Simulations of Interfacial Structure in Li-Montmorillonite Hydrates," *Langmuir* **13**, 2074-2082 (1997).

F.-R.C. Chang, N.T. Skipper, and G. Sposito, "Monte Carlo and Molecular Dynamics Simulations of Electrical Double Layer Structure in Potassium-Montmorillonite Hydrates," *Langmuir*, in press (1998).

F.-R.C. Chang, N.T. Skipper, K. Refson, J.A. Greathouse, and G. Sposito, "Interlayer Molecular Structure and Dynamics in Li-, Na-, and K-Montmorillonite-Water Systems," In *Kinetics and Mechanisms of Reactions at the Mineral/Water Interface* (eds. D.L. Sparks and T. Grundl). American Chemical Society Symposium Series, in press (1998).

J. Greathouse and G. Sposito, "Monte Carlo and Molecular Dynamics Studies of Interlayer Structure in $\text{Li}(\text{H}_2\text{O})_3$ -Smectites," submitted to *J. Phys. Chem. B*.

Development of Mixed Waste Bioremediation: Biodegradation of Complexing Agent, Ketone, and Heavy Metal Mixtures

Principal Investigators: William Stringfellow and Jennie Hunter-Cevera

Project No.: 97010

Project Description

The presence of complexing agents and ketones in mixed wastes directly and indirectly influences the migration of toxic metals and radionuclides from land disposal sites at DOE facilities. The objective of this research is to gain fundamental information concerning the fate of mixed wastes in biologically active environments. In this research, it is hypothesized that biodegradation of organic components in mixed wastes will influence the biogeochemistry and mobility of co-contaminant actinides and metals. Results from this project will be used in support for larger, longer-term research projects examining the bioremediation of mixed wastes containing both heavy metals and actinides.

The approach taken will be to apply classic methods of microbial ecology and physiology to elucidate fundamental information needed for modeling the biogeochemistry and environmental fate of mixed wastes. The physiology and kinetics of EDTA-metal complex and ketone degradation will be examined in both mixed and pure cultures. Environmental samples containing EDTA-metal complexes and ketones will be enriched for degrading organisms and strains of bacteria will be isolated for study. Once isolated, the physiology of the organisms and their degradative capabilities will be investigated. Strains isolated as part of this study will be examined for their ability to influence the mobility of plutonium and other actinides.

Accomplishments

The first year of study focused on the isolation and characterization of microorganisms capable of degrading methyl isobutyl ketone (MIBK) and methyl ethyl ketone (MEK). Twenty-one strains of bacteria and seven strains of yeast capable of ketone degradation were isolated from ketone-contaminated environments. This is the first report of yeast degrading the mixed waste components MIBK and MEK. Nineteen strains were identified as known organisms, and three strains are believed to be novel strains not previously characterized. The yeast strains have not yet been fully characterized for identification.

It was determined that a stable mixed culture containing both yeast and bacteria could be maintained in specially designed batch reactors that provide the ketones as vapors rather than liquids. The kinetics of MEK and MIBK degradation by these mixed cultures are compared to the degradation observed with pure cultures. The kinetics observed in the mixed culture appear to be influenced by population shifts in the reactor and are not adequately described by the dominance of any one culture.

Cultures isolated for their ability to degrade organic components of mixed wastes were supplied to Dr. Ilham Al Mahamid for studies examining their ability to adsorb actinides. Her results demonstrated the actinide-binding properties of these organisms. Our combined results suggest that the release of mixed wastes into biologically active environments will result in extensive blooms of ketone-degrading organisms and the rapid depletion of oxygen. The impacts of these blooms on the environmental fate of actinides released with mixed wastes have not been previously studied, suggesting that the models

currently used for determining the environmental risk associated with such releases may not be valid.

Advanced Computing for Geophysical Inverse Problems

Principal Investigators: Donald Vasco and Lane Johnson

Project No.: 96033

Project Description

The advent of plate tectonics has brought about an increased interest in the lateral variations of Earth's material properties. The three-dimensional distribution of density, temperature, and the compressional (P) and shear (S) velocities within Earth have a direct relationship to its dynamics. Therefore, fundamental issues related to convection within our planet, such as earthquake generation, resource distribution (petroleum and minerals), and environmental issues, may be answered by studies of the aspherical Earth structure. Over the last few years a collaborative effort between the Center for Computational Seismology at LBNL and U. C. Berkeley's Department of Geology and Geophysics has concentrated on determining the 3D structure of Earth. For example, recently we estimated the 3D distribution of P and S velocities in Earth's mantle.

In this project we are using several million seismic travel times and massively parallel computing to produce the first 3D image of the structure of the entire planet (crust, mantle, outer core, and inner core). In addition, we simultaneously estimate the topography of the internal boundaries of the Earth, such as the core-mantle boundary. In particular, we imaged the outer core, the region in which Earth's magnetic field is generated. Recent 3D numerical models of convection in the core have generated renewed interest in this region. Our results indicate intriguing coherent structure in the lowermost region of the outer core which may be related to the convection process. This structure has never been imaged before and the facilities at NERSC are allowing us to obtain a rigorous inversion of the seismic data.

The second half of this project involves the use of observations routinely gathered by petroleum engineers to infer the permeability and porosity distribution in a reservoir. Elucidating the 3D porosity and permeability structure of oil and gas reservoirs is a primary problem for the petroleum industry. Unfortunately, there are very few data which can be used to estimate porosity and permeability variations. One form of data recorded in almost all oil fields is the water-to-oil ratio of the fluid pumped from the wells. It is this ratio that determines if the well is economical and should be maintained or shut down. However, the relationship between water-cut and the porosity and permeability structure of a reservoir is highly nonlinear. Furthermore, to date no one has been able to analyze such information or relate it to 3D reservoir structure. Recently, we have developed an efficient algorithm for the inversion of such production data for reservoir. The use of the T3E is essential in this work and has enable us to produce the first inversion of oil-field production data for reservoir structure.

Accomplishments

We have completed work on our first 3D image of the structure of the entire planet. The results are described in the *Journal of Geophysical Research* (in press). An additional paper, submitted to *Science*, examines intriguing structure in Earth's fluid outer core, which is symmetric about the equator (Figure 1). We are in the process of writing up the results of Lanczos recursion approach, which is a significant

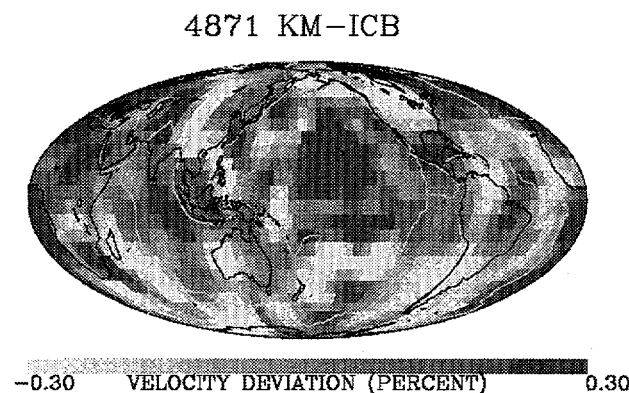


Figure 1. Map of the seismic velocity variations at the bottom of Earth's outer core. Lighter tones signify slower velocities and darker tones regions of faster seismic velocity.

improvement on conventional imaging methods because it enables us to calculate the spatial resolution of Earth structure as well as its uncertainty. The Lanczos algorithm has been implemented on the T3E at NERSC. Current work involves a much more detailed inversion which makes the problem four times larger but allows us to estimate fine-scale 3D Earth structure. Also, we are incorporating seismic waveform data in our inversion to better determine deep Earth structure.

Production data from the North Robertson oil field in the Permian Basin of west Texas have been used to infer the permeability variations in a 5-layer model of the reservoir. A Parallel Virtual Machine (PVM) code has been ported over to the T3E and used to construct the image of the reservoir (Figure 2). Recently we have discovered a new approach to the inversion of hydrologic data, which promises to be orders of magnitude more efficient than current methods. This technique was used to image an aquifer using densely sampled tracer data. We are now applying the technique to the inversion of production data at the North Robertson oil field.

Work continues on the application of Lie group techniques to transform nonlinear inverse problems to linear inverse problems. The method we have developed is described in a recently published paper.

Also, we are exploring techniques developed in commutative algebra and algebraic geometry which could prove extremely useful for solving nonlinear inverse problems. These methods may prove computationally intensive, and parallel computation will be very helpful.

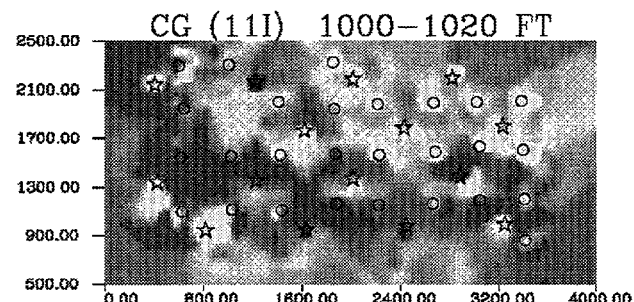


Figure 2. Permeability variations in the uppermost 20 ft. of the North Robertson field, Permian Basin, west Texas. Dark colors denote high permeability regions, and lighter tones correspond to low permeability areas. Injection wells are denoted by stars and production wells by circles.

Publications

D.W. Vasco, "Groups, Algebras and the Nonlinearity of Geophysical Inverse Problems," *Geophys. J. Int.* **131**, 9 (1997).

D.W. Vasco., J.E. Peterson, and E.L. Majer, "Resolving Seismic Anisotropy: Sparse Matrix Methods for Geophysical Inverse Problems," *Geophysics*, in press (1997).

D.W. Vasco, A. Datta-Gupta, and J.C.S. Long, "Integrating Field Production History in Stochastic Reservoir Characterization," *SPE Form. Eval.*, in press (1997).

D.W. Vasco and L.R. Johnson, "Whole Earth Structure Estimated from Seismic Arrival Times," *J. Geophys. Res.*, in press (1997).

D.W. Vasco, "Regularization and Trade-Off Associated with Nonlinear Geophysical Inverse Problems," submitted to *Inverse Problems* (1997).

D.W. Vasco and L.R. Johnson, "The Seismological Signature of Core Dynamics?" submitted to *Science* (1997).

D.W. Vasco and A. Datta-Gupta, "Asymptotic Solutions for Solute Transport: A Formalism for Tracer Tomography," submitted to *Water Resources Research* (1997).

Environmental Energy Technologies Division

Direct-Ethanol Fuel Cells

Principal Investigator: Elton Cairns

Project No.: 97011

Project Description

The goal of this R&D project is to improve the performance of direct-ethanol fuel cells to meet or approach the performance requirements of electric vehicles. This exploratory effort will focus the testing and analysis of direct-ethanol fuel cells utilizing advanced Pt-containing electrocatalysts, polymer electrolytes, and alkaline Cs_2CO_3 -based electrolytes for the direct electrochemical oxidation of ethanol.

The first phase of the project is the construction of the equipment necessary for the operation of laboratory cells at elevated temperatures up to 200° C, and elevated pressures up to several atmospheres. This equipment must include provision for accurate flow control, humidification of fuel and air streams, and the analysis of products. In addition, facilities and equipment for the preparation of electrodes and membrane-electrode assemblies are necessary.

Accomplishments

The first phase of this project has been the design and construction of improved cell components, and the design and construction of a cell chamber for operation at elevated temperatures (up to 200° C) and pressures (up to several atmospheres). These permit a thorough investigation of reaction rates over a significant range of operating conditions. The new cell components have been fabricated and tested for leak-tightness. The cell chamber has been designed and constructed. Testing of the chamber at several temperatures and pressures is under way. Software for controlling the experiments and gathering performance and material balance data has been written and is being tested. Electrode and cell fabrication techniques have been established for the PEM version of the cell, and good progress has been made on the design and fabrication of electrodes for use with the aqueous Cs_2CO_3 electrolyte. Preliminary

cell performance on hydrogen fuel is as it should be. Following completion of the temperature and pressure testing of the cell chamber, experiments will commence on the performance of ethanol in the cells with selected electrocatalysts over a range of operating conditions.

Instruments for the in situ Detection of NO , NO_2 , and Their Precursors

Principle Investigator: Ronald Cohen

Project No.: 96006

Project Description

This project was aimed at improving our understanding of the chemical mechanisms that control the abundance of nitrogen oxide radicals, NO_x (where NO_x is defined as $\text{NO} + \text{NO}_2$), in the troposphere. The importance of NO_x in tropospheric chemistry is well known—the NO_2 radical is believed to be the rate-limiting species in tropospheric oxidant production on a global scale. NO_x emissions from industrial combustion are thought to be responsible for the manifold increase in global tropospheric ozone that has occurred during the last 100 years, and NO_x emissions are a primary cause of regional photochemical smog. However, the factors that control the distribution of NO_x in the remote atmosphere remain poorly understood for several reasons. It is difficult to accurately and precisely measure NO_2 at ambient concentrations, because the technology to measure the concentrations of many precursors to NO_2 with the combination of sensitivity, specificity, and the spatial and temporal resolution needed to thoroughly test the chemical mechanisms does not yet exist. In addition, our understanding of the atmospheric photochemistry of NO_x and its precursors is limited. Substantial uncertainty also surrounds descriptions of the magnitudes and locations of the primary sources and sinks of NO_x : lightning, industrial emissions, biomass burning, fertilizers and microbial activity, and transport from the stratosphere.

We are developing new techniques for measuring the concentration and fluxes of NO_2 and its more labile atmospheric reservoirs, N_2O_5 , and the organic nitrates in the free troposphere. The goals are to develop lightweight, portable, autonomous experiments to enhance existing capabilities for observations of these species. We have begun by demonstrating in the laboratory that laser-induced fluorescence detection of NO_2 is more sensitive, specific, and free from interferences than existing instrumentation. We are now going on to package the experiment as a fully robotic, highly reliable instrument. This new technology will be used to make sensitive (parts per trillion), accurate, and precise observations from aircraft platforms in the remote atmosphere, and from ground-based platforms in urban and forested environs. The experiments to detect nitrates are using a combination of laser-induced fluorescence (LIF) and temperature-programmed thermal dissociation for detection of those compounds that thermally dissociate to yield an NO_2 fragment.

Accomplishments

We have completed assembly of two laser systems designed for detection of NO_2 . Each system has a sensitivity of 5 ppt/10 s at a signal-to-noise ratio equal to 2. We are using these systems to 1) extend capabilities for detection to sensitivities of 5 ppt/10 s; 2) test new techniques for rapid detection of organic nitrates such as peroxyacetic nitric anhydride (PAN); and 3) explore the kinetics of nitrogen oxides on atmospheric aerosol.

To enhance the sensitivity we have demonstrated new photon-counting capabilities using large area (8x8 mm) silicon photon-counting detectors. We have shown that these detectors increase the efficiency of detection of NO_2 by a factor of 3, that they can be operated reliably with quantum efficiency (30%) higher than that of competing PMTs (17%), and that there are clear benefits of the large area for our application. We have also shown that time-gated detection can be optimized to decrease the noise in the experiment by a factor of 10. We are presently completing the integration of these new techniques into an automated instrument that will be used for detection of NO_x and have demonstrated a detection threshold of 7 ppt/10 s with an instrument that is fully automated and weighs less than 150 pounds. Simultaneously we have begun to test the package by making observations of NO_2 out the door of our laboratory.

Our kinetics and organic nitrate experiments are just beginning. We have synthesized PAN and have built a versatile aerosol generator capable of producing 50- to 1000-nm particles composed of carbon, iron, silicates, and other refractory materials.

Mechanism and Modeling of Soot Formation in Hydrocarbon Flames

Principal Investigator: Michael Frenklach

Project No.: 96007

Project Description

Soot formation is one of the key environmental problems associated with the operation of practical combustion devices. The goal of this project is to develop reliable models of soot formation that can be used in numerical simulation and optimization of combustion devices. The specific goals include reaching a fundamental understanding and modeling of gas-surface processes; development of a model for fractal growth of soot particles; and modeling approaches to turbulence-chemistry interactions.

The project is of a theoretical/computational and experimental nature and is focused on the development and testing of chemical and physical models of soot particle formation and growth. The research will involve theoretical exploration of reaction mechanisms via quantum chemistry, chemical kinetics, numerical simulation of flames, aerosol dynamics, and Monte Carlo and molecular dynamic simulations, and will include shock-tube experiments.

Accomplishments

During the second year of the project, progress has been made in the following areas:

Testing and Calibration of Revised Soot Formation Model

A revised model of soot formation has been tested on a series of laminar premixed flames. Preliminary

results indicate that the new detailed model is capable of correctly predicting soot volume fractions and soot particle sizes reported for all of these flames. A single steric coefficient was found to fit all the flame conditions.

Stochastic Modeling of Soot Particle Aggregation

Soot aggregation with simultaneous surface growth was modeled using a dynamic Monte-Carlo method. Simulations were performed in the environment of a 10-bar laminar premixed flame. The physical model begins with a single solid particle (a collector particle) immersed in an inexhaustible ensemble of solid primary particles and gaseous surface growth species. Primary particles are modeled by perfect spheres with a monodispersed distribution. The Monte Carlo algorithm begins in the particle inception zone and constructs soot particles via ensemble-averaged collisions between small spheres and deposition of gaseous species on the sphere surfaces. Aggregation with simultaneous surface growth was analyzed using two different scenarios. Scenario one increases radii of units in the primary particle ensemble at the same rate as the collector particle. Scenario two keeps primary particles a constant size for the duration of the simulation.

The results demonstrate that aggregation of spherical particles in the presence of surface growth can lead to a spheroidal shape. Computationally, as the simulations show, there are two factors that affect the level of collector particle sphericity. The first factor is a sufficiently fast surface growth rate. In the absence of surface growth, we would not observe the smoothing effect necessary to construct spheroidal collector particles. However, if the geometry is to become spheroidal, the finite surface growth rate established by the gaseous flame environment must be capable of burying primary particles stuck to the collector surface. If they are too large, even the flame's maximum surface growth rate may not be able to bury them quickly enough. Thus, the second factor is the size of colliding primary particles. Smaller particles are more easily covered. Therefore, an ensemble replete with small primary particles is optimal for generating spheroidal collector particles.

The simulations show that particle aggregation is not separated in time from particle nucleation, as often presumed. Instead, aggregation begins with the onset of nucleation. At this point collisions ensue between the collector and small polycyclic aromatic hydrocarbon (PAH) clusters. The collisions deform the incoming PAH clusters, which lose their

individual characteristics. This contributes further to an overall spheroidal shape. Coupled with the two factors discussed above, we conclude that the spheroidal shape of particles is attributed to rapid surface growth, intense particle nucleation, and rearrangement of the internal structure of colliding PAH clusters.

Publications

P. Mitchell and M. Frenklach, "Numerical Study of Soot Particle Aggregation with Simultaneous Surface Growth," Spring Technical Meeting of the Western States Section of the Combustion Institute, Sandia National Laboratories, Paper No. 35, Livermore, CA, April 14-15, 1997.

P. Mitchell and M. Frenklach, "Monte Carlo Simulation of Soot Aggregation with Simultaneous Surface Growth—Why Primary Particles Appear Spherical," submitted to the 27th International Symposium in Combustion, University of Colorado, Boulder, August 2-7, 1998.

Energy Efficiency and Demand in Industry: A Global Assessment

Principal Investigators: Mark Levine, Lee Schipper, Jayant Sathaye, Lynn Price, Nathan Martin, and Jonathan Sinton

Project No.: 97012

Project Description

The purpose of the project has been to develop tools and data to significantly improve the analysis of the role of energy efficiency in reducing greenhouse-gas emissions and contribute to national and regional economic development objectives. This project will provide an in-depth assessment of energy use in the industrial sector of national, regional, and global energy systems. Energy and CO₂ impacts of energy efficiency technologies and practices will be assessed for the most energy-intensive and energy-consuming industries. A major goal of the project is to create a new activity at LBNL involving energy efficiency in industry.

Our approach has focused on analyzing the drivers of energy demand in major energy-using industrial subsectors, with an initial focus on iron and steel, cement, and pulp and paper production. This will be accomplished by the establishment of, and our collaboration with, an international set of expert working groups to provide data, perform analysis, build analytical tools, and develop scenarios. The major activities involve a continuation of collecting higher quality disaggregated subsectoral data, analyzing technologies that can influence industrial energy use at the subsectoral level for various countries; building a network of collaborators so that the data gathering and analysis at this level of detail can continue in the future; and establishing and applying techniques to use the information we are gathering to project global energy demand for industry (as a function of economic conditions, demographic variables, technology choice, and policy).

The specific outcomes which we identified earlier in the project are still feasible and on-track with our project planning. These include:

- Completion of a major global assessment of energy efficiency in industry, with a focus on iron and steel, cement, and pulp and paper.
- Establishment of an international network of collaborators on industrial energy efficiency, including governmental representatives, academic researchers and analysts, and technical staff of the major energy-consuming industries in many nations.

An additional result of undertaking this work is that, given the increasing visibility and importance of understanding the potential to reduce industrial energy demand as a means of mitigating greenhouse-gas emissions, LBNL is now placing itself in a key position to become a center for international analysis in this area. Both the U.S. Department of Energy and the U.S. Environmental Protection agency are becoming increasingly interested in this work.

Accomplishments

Data Collection and Analysis

We are completing the first phase of data collection which focuses on the collection of key structural data (output, energy, economic data) to understand the drivers of industrial energy demand. A user-friendly database is now being designed which will allow easy access of the data by LBNL researchers and inter-

national network staff to undertake in-depth analysis. The database covers 6 industrial subsectors (iron and steel, aluminum, building materials, chemicals, pulp and paper, petroleum refining) and over 15 countries, with data coverage levels varying by sector and country. Database development is continuing.

In addition to the database, a small industrial library has been established that allows for easy access to some of the most key and up-to-date industrial energy-demand information. This library has been electronically catalogued, allowing for rapid access to specific information. Library development is continuing.

We expect to complete our primary analytical report after the database is further developed, but we have completed several preliminary analyses using existing data. One small study we conducted which focused on understanding current trends in industrial energy demand in China found that energy requirements to produce a unit of raw material are still 20–40% higher than those in industrialized countries.

In the area of scenario development and tool building, LBNL is taking a leading role in developing methodology and parameters for energy-demand scenarios based on detailed data collected through this project. It is expected that such scenarios will be used by the Intergovernmental Panel on Climate Change, as well as by regional and national policymakers, to assess policies and measures intended to reduce energy use and greenhouse-gas emissions. In addition, LBNL is developing and applying a number of analytic tools, such as decomposition analyses, best practice and international comparisons, and energy conservation supply curves, to better understand energy-demand trends in the industrial sector. We recently completed a simplified energy-demand scenario for steel energy demand in the Asia Pacific Economic Cooperation countries. LBNL analysis found that significant expected increases in steel demand will lead to an increase of energy demand of 1.0% per year in these countries between 1990 and 2010, but that structural factors (especially the increase in the use of secondary steel) will allow for greater steel output and a 20% reduction of overall energy requirements per metric ton of steel.

Institutional Linkages and Support

We have continued to make progress in expanding our international contacts with various institutions interested in collaborating on the project, and a

summary listing of these contacts is provided in Table 1.

Publications

E. Worrell, L. Price, N. Martin, J. Farla, and R. Schaeffer, "Energy Intensity in the Iron and Steel Industry: A Comparison of Physical and Economic Indicators," *Energy Policy*, 25 (7-9) (1997).

L. Price, E. Worrell, N. Martin, J. Farla, and R. Schaeffer, "Energy Efficiency in the United States Iron and Steel Industry: An International Perspective," *Proceedings of the American Council for an Energy-Efficient Economy, Summer Study on Energy Efficiency in Industry*, June, 1997.

L. Price, "Industrial Energy End-Use Demand Analysis," *Proceedings of the Asia Pacific Research Centre*

Workshop on Methodologies and Data for Energy Demand/Supply Outlook, March 17-19, 1997.

E. Worrell, L. Price, N. Martin, J. Farla, and R. Schaeffer, "International Energy Efficiency Comparisons and Policy Implications in the Iron and Steel Industry," *Proceedings of the European Council for an Energy-Efficient Economy, Summer Study*, July, 1997.

M.D. Levine, L. Price, J. Sinton, "Reducing Growth in Global Energy Use and Greenhouse Gas Emissions: A Regional and Sectoral Analysis of Energy Efficiency Opportunities," *Proceedings of the World Energy Council Asia-Pacific Forum*, April 22-24, 1997.

M.D. Levine and L. Price, "The Role of Energy Efficiency in Reducing Growth in Global Energy Use and Greenhouse Gas Emissions: A Regional and Sectoral Analysis," *Proceedings of the ABARE Outlook '97 Conference*, February 4-6, 1997.

Table 1.

| Institution | Country | Institution | Country |
|---|---------------|---|----------------------------|
| The Department of Science, Technology, and Society, Utrecht University | Netherlands | Fraunhofer Gesellschaft (ISI) | Germany |
| Federal University of Rio de Janeiro | Brazil | Institute of Science and Technology, Lund University; Goran Bryntse | Sweden |
| University of Coimbra | Portugal | Canadian Industry Energy End-Use Data and Analysis Center | Canada |
| Gtowny Urzad Statystyczny | Poland | Asia Pacific Energy Research Centre | Japan |
| Australia Bureau of Agricultural and Resource Economics | Australia | Tata Energy Research Institution | India |
| Inha University; Korea Energy and Economics Institute | Korea | Energy Research Institute (SPC); Beijing Energy Efficiency Center | People's Republic of China |
| Comision Nacional para el Ahorro de Energia (CONAE); Universidad Nacional Autonoma de Mexico (UNAM) | Mexico | Universidad Austral | Chile |
| Intergovernmental Panel on Climate Change | International | International Energy Agency | International |
| World Energy Efficiency Association | International | European Commission | Europe |
| U.S. Dept. of Energy; U.S. Environmental Protection Agency | United States | | |

The Virtual Building Laboratory

Principal Investigator: Stephen Selkowitz

Project No.: 97013

Project Description

Buildings account for about 35% of all energy used in the U.S. and about 60% of all electricity, with associated environmental impacts. Potential savings through energy efficiency are large, approximately 50% of current consumption, or \$100 billion per year. Improved technology (e.g., energy-conserving windows and electronic ballasts) has captured only a small part of this potential; to fully capture it will also require innovative, sophisticated, and complex approaches to building design and the provision of building services. Yet the building industry resists innovation, because the costs and risks of design failure are large. Researchers estimate that one third of U.S. buildings suffer from sick-building syndrome, which can occur throughout a building's life, undermining worker productivity and increasing health-care costs. Serious design flaws in specific buildings can necessitate costly retrofits shortly after construction. These costs—if they are incurred—dwarf any potential energy-efficiency savings. This project is aimed at the creation of a "virtual building laboratory" in which one can develop, test, and optimize energy-efficient design solutions. The goal is the rapid and reliable prediction of design success, in terms of maximum energy savings as well as occupant comfort, health, and productivity, without recourse to prohibitively expensive full-scale prototyping.

In the initial phases the work is naturally divided into two areas: 1) visual, e.g., luminous environment, visual comfort, and performance, and 2) nonvisual, e.g., heat transfer, moisture migration, air flow, pollutant concentrations, and thermal comfort. The computational tools necessary for prediction in the two areas are quite different. In the former, one needs photometrically accurate visual/spatial 3D rendering, while in the latter one needs to model the physics of building flows in those areas where current building simulation models are inadequate: computational fluid dynamics (CFD) and the detailed treatment of

radiation. The Environmental Energy Technologies Division (EETD) has extensive expertise in both areas. In addition to a 20-year lead role in constructing building thermal simulation models, e.g., DOE-2 and multi-zone airflow models, the EETD has developed *Radiance*, currently the only rendering system able to compute accurately all significant light interactions in geometrically complex environments. Ultimately, however, these two areas must be combined because of the strong linkage between visual appearance, thermal comfort, air quality, and energy efficiency inherent in the design process.

Accomplishments

In the visual simulation task the objective is to create a lighting simulation and display system that provides a real-time "walk-through" of a virtual building space, utilizing stereoscopic visual display to convey complex visual quality and spatial information. The key problem is real-time computational speed: the observer can change the viewing direction very rapidly by eye or head motion and somewhat more slowly by moving around. In order to prevent motion sickness, a stable new view must be presented within about 0.2 s of such a motion. We developed and began implementing a scheme in which parallel renderings by *Radiance* on the T3E are used to construct an intermediate spatial model (ISM) that can be rapidly displayed using a virtual reality display device (Figure 1). One area of implementation is the production of realistic-visibility rendering on the VR display (Figure 2).

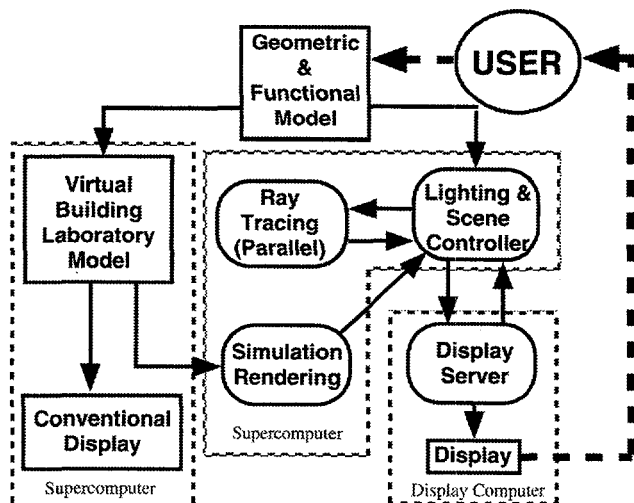


Figure 1. Interlinkages of physical simulation model, interactive lighting and scene display, and the user.

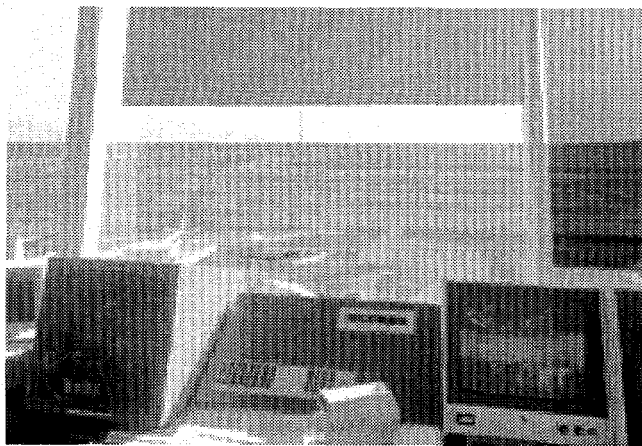


Figure 2. Visual realism makes it necessary to represent the large range of intensities to which the eye is sensitive on a medium with a much smaller dynamic range, as illustrated by this photo produced by a Radiance simulation of the San Francisco Airport control tower. At the outset of this project it was necessary to use two photos to capture the full visibility range of this scene.

In the nonvisual simulation task the immediate problem was how to best combine existing developments in CFD with building simulation modeling. A brute-force, 3D CFD simulation of a large building in sufficient detail is still well beyond existing supercomputer computational capability, so the key question was how to model a selected portion of the building in conjunction with a building simulation model, and how large that portion could be. Several aspects of the problem distinguish it from the usual aerospace or forced-ventilation calculation: 1) thermally-induced buoyancy is a significant—possibly the sole—driver of the flows; 2) simulation of the thermal boundary layer is important; 3) radiation

(e.g., sunlight in an atrium) may be a significant thermal source; 4) geometries of varying—but usually high—complexity are of interest; and 5) high problem throughput (in the final code) will be important. Aspects 1 and 2 imply that the problem will be considerably more stiff than the normal CFD application. We surveyed a number of commercial and public-domain CFD codes that would meet these requirements, formulated an initial approach to the problem in terms of an overset grid methodology, and as a starting point obtained and tested a research code with some of the desired properties. Initial results from the code are shown in Figure 3.

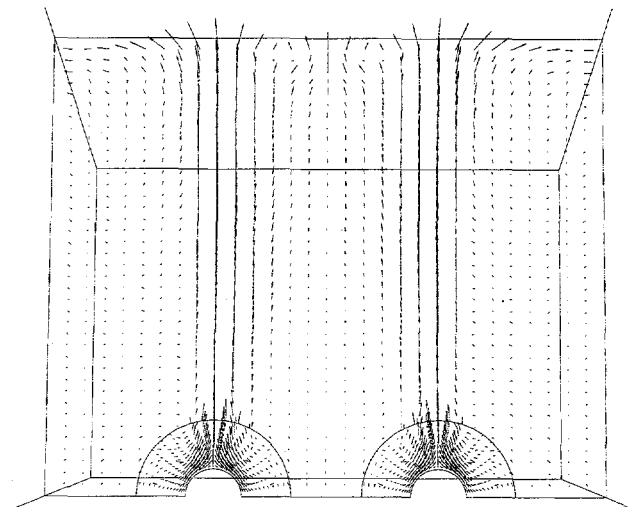
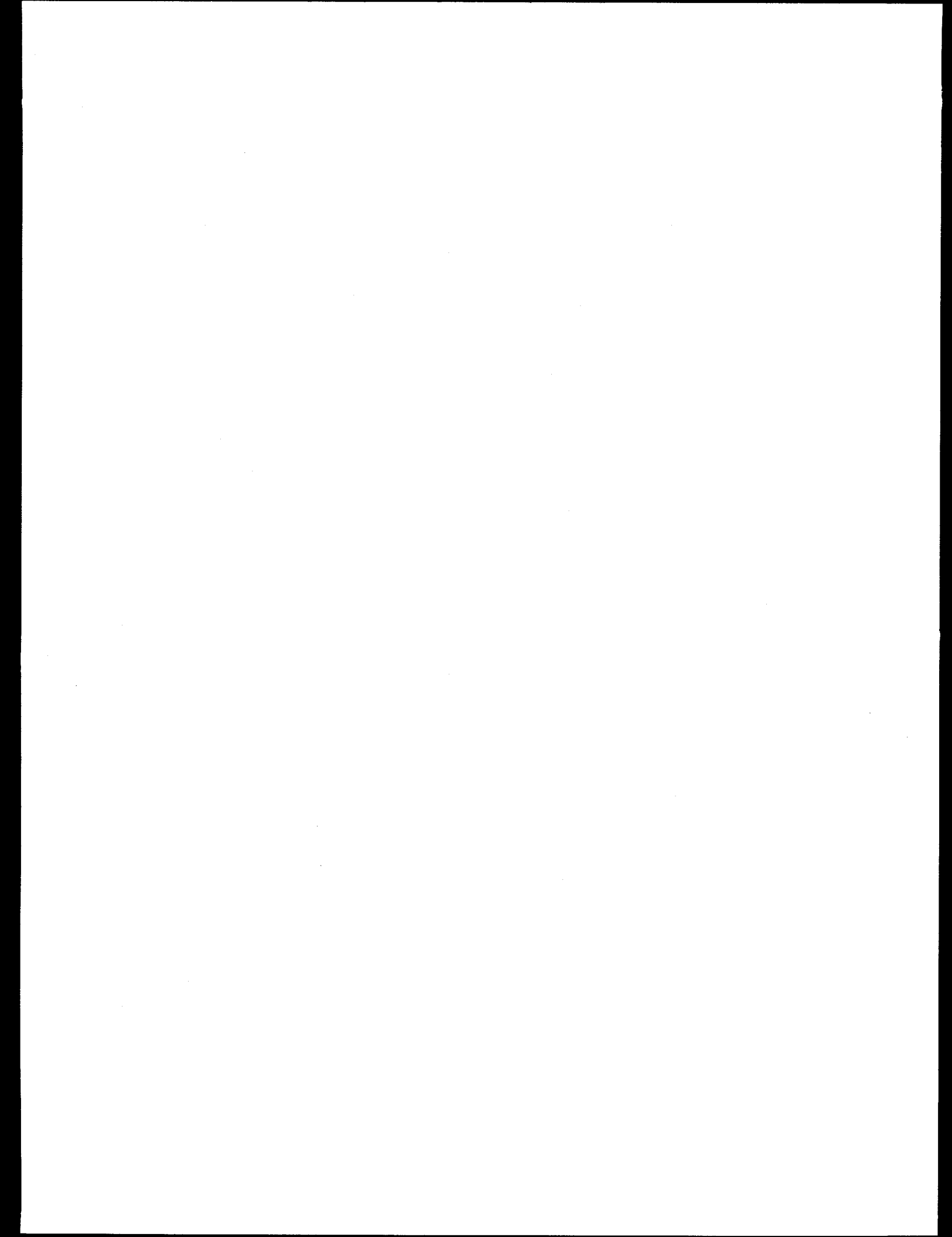


Figure 3. Buoyancy-driven laminar thermal plumes from hot spheres on the floor of an atrium-shaped 3D enclosure, an initial test of the research code. The figure shows a planar slice through the enclosure. The hot spheres are a convenient shape for a relocatable test object, and are not intended to represent any specific architectural feature.



Life Sciences Division

Development of Genetically Manipulated Hepatic Cell Lines for the Evaluation of Cytotoxic Effect of Environmental Pollutants by Using Apoptosis as a Molecular Endpoint of Exposure

Principal Investigator: Manjit Dosanjh

Project No.: 97015

Project Description

Information on genetic toxicology related to human health risk assessment has gained increasing importance, particularly in the aspects that pertain to the molecular mechanisms of toxicity, since they allow understanding of the basic mechanisms and effects of specific chemicals present in complex mixtures. In ecotoxicology, however, little has been done to analyze the molecular mechanisms of genotoxic effects observed in ecosystems or to fingerprint the effects of specific environmental pollutants. The main reason for this is the serious limitations encountered with the classical approach when measuring the amount of the chemicals present, either in the organisms or in the environment, and in relating that amount to adverse effects, through animal experimentation. In addition to the problem of the toxicity of complex mixtures and in extrapolating from laboratory to field conditions as well as of the marked differences in interspecies sensitivity, there are also difficulties in knowing how much of the material is actually bioavailable. Hepatocytes have been proposed as an ideal model for *in vitro* studies for testing exposure to environmental pollutants, since many of the compounds are metabolized in the liver by the cytochrome P-450 enzyme system.

Apoptosis (programmed cell death) is an ideal biomarker for environmental exposure since it can provide information on exposure at low doses that do not result in disease symptoms and it allows exposure

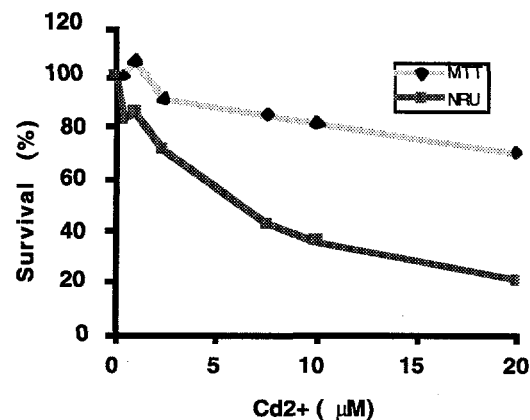
assessment long before a chronic disease, such as cancer, develops. At the same time it can provide insight into the mechanism by which a toxicant interacts with a specific intracellular target and gives rise to the disease. Identifying and measuring the molecular mechanisms of toxicity are important goals in hazard assessment. Interference with the molecular mechanisms of apoptosis would promote survival of cells under conditions that normally lead to their death. The rate of apoptosis can be altered by altering the genetic make-up of cells, since there are several genes which are known to induce apoptosis (e.g., c-myc, p53, c-fos), while others suppress this process (e.g., bcl-2). Manipulations of such genes can be used to modify the apoptotic tendency of specific cells.

The goal of the present study is to assess the role of apoptosis in a human hepatic cell line (HepG2) used for genotoxicity and cytotoxicity testing of environmental pollutants. This will be useful in deciding whether the detection of apoptosis should form a part of an integrated approach to the assessment of chemical toxicity.

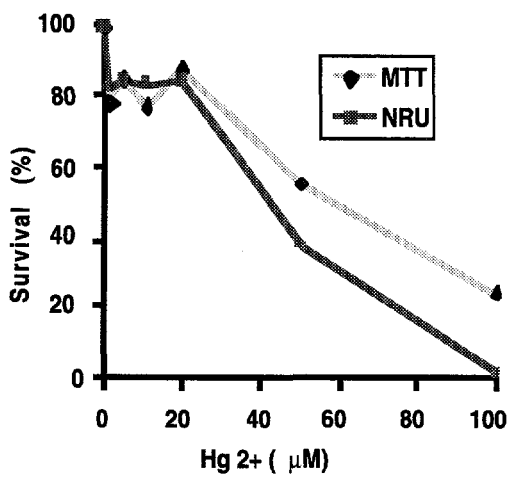
Accomplishments

During the first period funded by this grant, the basic parameters of the human HepG2 cell line were established. This included the establishment of the MTT, NRU, and LDH release cytotoxicity assays. These are standard assays used for determining cytotoxicity and LC50 values (the concentration at which 50% of the cells die) of chemicals. We are using benzo(a)pyrene [B(a)P] as a model polycyclic aromatic hydrocarbon and cadmium and mercury chloride as examples of heavy metals commonly found as pollutants. Typical results obtained for these compounds are shown in Figure 1.

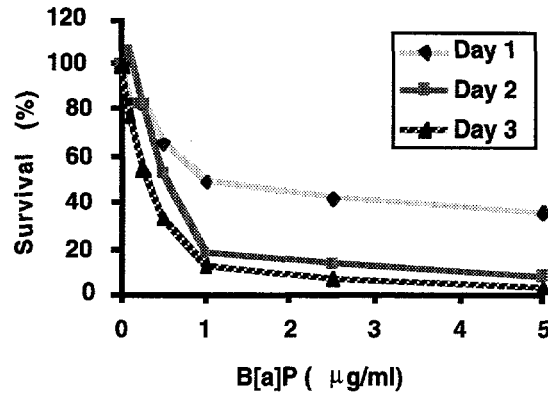
Prior to genetically manipulating the cell line in order to alter its rate of apoptosis, it first had to be determined that the HepG2 cell line indeed undergoes apoptosis. The DNA from HepG2 cells after treatment with cadmium and mercury chloride was shown to result in laddering/fragmentation typical of apoptosis by both gel electrophoresis and ELISA assays (Figure 2).



(a)

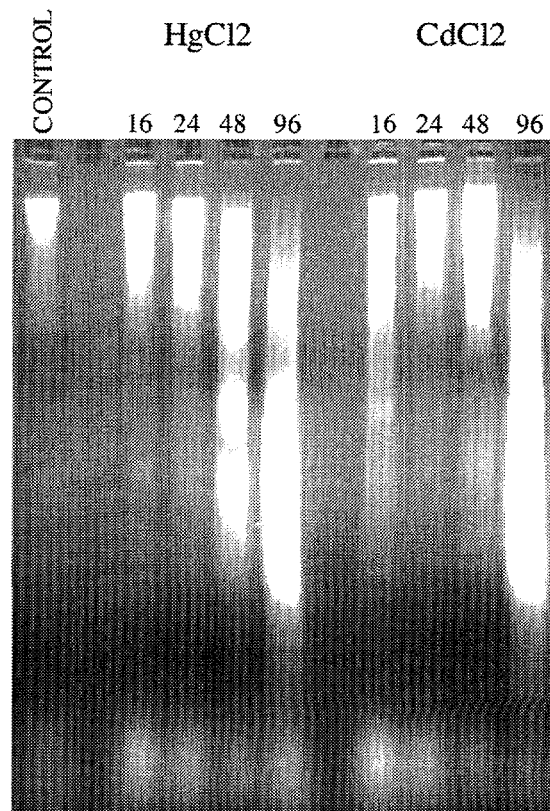


(b)

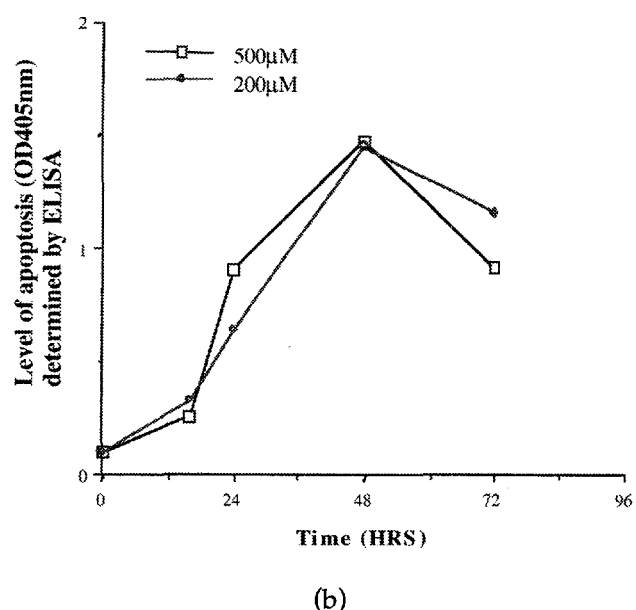


(c)

Figure 1. (a) Shows the effect of increasing concentration of $CdCl_2$ on HepG2 cell survival using MTT and NRU assays. (b) Shows the effect of increasing concentration of $HgCl_2$ on HepG2 cell survival using MTT and NRU cytotoxicity assays. (c) Shows the effect of both dose and time of exposures of $B(a)P$ on HepG2.



(a)



(b)

Figure 2. (a) DNA fragmentation assay as a function of time (h) after exposure to $CdCl_2$ (5 μM) or $HgCl_2$ (20 μM). (b) Kinetics of apoptosis after treatment as measured by ELISA.

In the second period of the grant, the role of apoptosis was measured by developing genetically manipulated hepatic cell lines which have an altered rate of apoptosis. This was carried out by introducing vectors containing bcl-2—a gene which suppresses the rate of apoptosis—and the control plasmid into the HepG2 cells. HepG2 cell lines, which differed only in their expression of bcl-2, were established by screening positively transfected cell lines by northern and western analyses. These cell lines are currently being used to evaluate the effects of B(a)P and heavy metals (cadmium and mercury chloride) in *in vitro* assay by using ELISA and DNA laddering for apoptosis, MTT for cytotoxicity, RT-PCR for cytochrome P-450 (cyp1A1), and western analyses for expression of p53, p21, Rb, and bcl-2 protein.

Publication

C. Cherbonnel-Lasserre and M.K. Dosanjh,
"Suppression of Apoptosis by Overexpression of bcl-2 or bcl-xL Promotes Survival and Mutagenesis After Damage," *Biochimie* **79**, 613 (1997).

ALS Protein Microcrystal Diffraction Camera

Principal Investigator: Robert Glaeser

Project No.: 97035

Project Description

The objective of this project is to conduct research into modifications and enhancements of the protein crystallography equipment on Beamline 5.02 at the Advanced Light Source (ALS). These instrumental upgrades will make it possible to collect x-ray diffraction data from protein microcrystals. LDRD funds were allocated late in 1997 for preliminary efforts. The overall plan is to develop instrumentation and research protocols that will make it easy to collect data from protein microcrystals; to collect a full data set from one or more proteins; and, on the basis of these initial results, generate one or more research

proposal(s) for expanded operation of protein crystallography facilities at the ALS.

Accomplishments

Two major steps in the research plan were completed in FY97: a design decision was made for the optical system to be used in aligning the microcrystal and the x-ray beam, and a recently published protocol for crystallization of membrane proteins was put into routine operation in our own laboratory.

Alignment of protein crystals as small as 30 μm on edge requires high quality optics, which must have a resolution that is much better than the crystal size. After a review of different options, a decision was made to purchase the Questar long-working-distance microscope. This instrument has a resolution of 3 μm at a working distance of 6 inches. The long working distance is needed in order to prevent the microscope lens from interfering with moving parts on the sample goniometer, the cold N₂ stream, and other elements of the instrumental hardware. This microscope was ordered and a mechanical design was decided upon for supporting the microscope in an appropriate position.

The new protocol for crystallizing membrane proteins is based upon a bicontinuous, infinitely periodic gel of lipid bilayers and water. Landau and Rosenbusch first reported the crystallization of the membrane protein, bacteriorhodopsin (bR), in December, 1996, and a high resolution refinement of the bR structure was reported in September, 1997. We have repeated the protocol for crystallization of bR in this system, and we have begun to investigate the use of a wide variety of alternative techniques for mounting such crystals. Parameters to be optimized include 1) mounting with minimal amounts of surrounding material, so as to minimize the background scattering; 2) mounting with minimal amounts of mechanical disturbance of the protein crystal, especially considering the high viscosity of the gel; and, ideally, 3) mounting several microcrystals, well separated from one another, in order to facilitate moving rapidly from one to another without the need to mount a separate stub for each crystal. We have also contacted a number of laboratories to establish collaborators and a user group that would benefit from crystallization of membrane proteins by this new approach.

Techniques for Discovery of Disease-Related Genes

Principal Investigator: Joe Gray

Project No.: 96014

Project Description

The purpose of this project is to contribute to basic genomic knowledge and technologies developed in the Human Genome Center and the Resource for Molecular Cytogenetics, apply this knowledge to analysis of the genetic basis of cancer and other diseases, and support the development of technologies needed for these studies. This will be carried out in collaboration with projects in the Life Sciences Division, the UCSF Cancer Center, and other Bay Area institutions.

Accomplishments

Contig Assembly

Techniques for assembly of physical maps have been developed during assembly of a 1.5 Mb BAC and P1 based physical map spanning a region of recurrent amplification in tumors of the breast, ovary, colon, and head and neck. The physical map has been annotated with regard to all Sequence Tag Sites (STSs, public

and new), Expressed Sequence Tags (ESTs), trapped exons, direct selected cDNAs, and genes. Five genes and one pseudogene have been identified. These are the kruppel-related zinc finger genes ZABC2 and ZABC1; PIC1L, a homolog of PIC1; the previously cloned gene CYP-24; AIBC1; and the cyclophilin-related pseudogene, CRP. All of these genes have been assessed for expression in breast cancer cell lines and normal human tissue, and only ZABC2, ZABC1, and AIBC1 were found to be expressed. The locations of the genes are shown in Figure 1.

Fiber FISH, one of the techniques used for map assembly, appears increasingly useful for large-scale physical map assembly. New this year is a technique to map cloned sequences onto DNA fibers isolated from interphase nuclei. This should speed fiber mapping by allowing many mapping substrates to be prepared at one time and used as needed for map assembly. This approach has now been proposed for development as a routine physical map assembly tool for use by the Joint Genome Institute.

DNA Sequencing

This project has continued to work with the LBNL Genome Center to increase the efficiency of directed genomic sequencing. As a prototype effort, genomic sequence has been obtained for ~650 kb of the cloned 20q13.2 amplicon (see map). Sequence has been assembled into contigs of 101 kb, 80 kb, 70 kb, 76 kb, 49 kb, 44 kb, and 42 kb, all ordered and oriented on

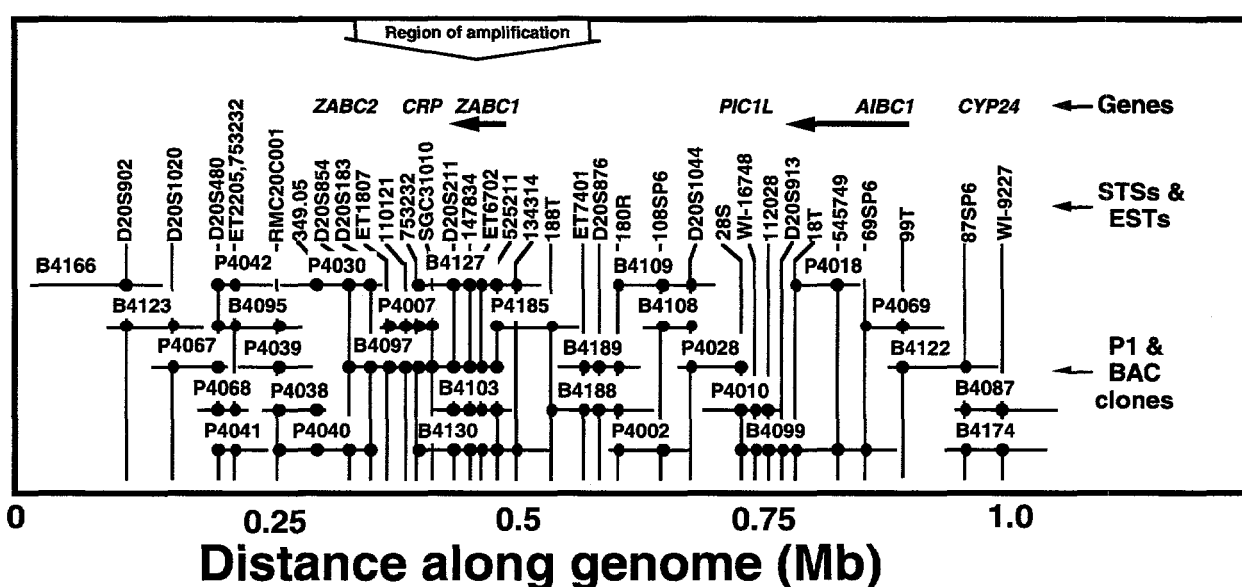


Figure 1. Physical map of the 1.5 Mb region of chromosome 20q13.2.

the physical map. The analysis of this sequence has been automated to include searches for predicted exons, gene peptides, ESTs, and repetitive elements using Genotator. In addition, all sequence is analyzed for repetitive elements, CpG islands, exons, and gene models using XGRAIL. Finally, the sequence is masked for repeats and searched against all public databases on a regular basis. To manage these data and make it available to collaborators, a secure web site has been developed where all data may be viewed via an ACEDB database that includes physical maps, sequence, and graphical views of sequence analysis performed using Genotator, XGRAIL, and SORFIND. Current efforts are directed toward the comprehensive biological annotation of this sequence. This annotation will include all genes (experimentally determined and modeled), all ESTs, all repetitive elements (including novel repeats) with plots distribution and density, all STSs, all significant homologies, all XGRAIL, Genotator, and SORFIND data and all problem areas.

Gene Identification and Functional Analysis

Prototype studies of gene function have focused on genes in the 1.5 Mb region of chromosome 20q13.2 described above. Two novel genes were discovered in this region that may play a role in breast cancer, ZABC1 and AIBC1. The complete sequence of the human gene ZABC1 and its mouse homolog have been obtained. Computational analysis of the full-length gene revealed 8 putative DNA-binding zinc fingers, a separate proline-rich region which may be a transcription activation domain, and mRNA destabilization motifs in the 3'-UTR. ZABC1 was shown to be amplified and overexpressed in human breast tumors. It was determined to be a nuclear protein by transfection with a GFP construct. The intact gene was cloned into a retrovirus to investigate its oncogenic potential in cultured cells. Expression arrays are now being used to identify genes whose expression is altered in normal mammary cells and cultured tumors cell lines upon infection with the ZABC1-retrovirus construct. Finally, antibodies have been developed against ZABC1 that appear to be specific and suggest that ZABC1 protein level increases with amplification. The second gene, AIBC1, is amplified and overexpressed in breast tumors. AIBC1 has been cloned into a retrovirus for phenotypic studies. GFP data suggest that AIBC1 encodes a cytoplasmic protein. Comparative mouse-human studies are underway.

Analysis of gene function through construction of transgenic mice is just beginning. Our approach is to create transgenic mice carrying BAC clones spanning regions of genetic abnormality and/or cloned genes from these regions in order to assess the function of genes encoded in the BAC. Our long-term plan is to cross the BAC transgenic mice with other transgenic mice known to develop tumors in order to determine the influence of the 20q genes on the rate of tumor progression. Our first transgenic mice will carry a BAC clone centered on the region at 20q13.2 that is amplified in breast cancer.

Publications

C. Collins, J. M. Rommens, D. Kowbel, T. Godfrey, M. Tanner, S. H., D. Polikoff, G. Nonet, J. Cochran, K. Myambo, K. E. Jay, J. Froula, T. Cloutier, W.-L. Kuo, P. Yaswen, S. Dairkee, J. Giovanola, G. B. Hutchinson, J. Isola, O.-P. Kallioniemi, M. Palazzolo, C. Martin, C. Ericsson, D. Pinkel, D. Albertson, W.-B. Li, and J. W. Gray, "Positional Cloning of ZABC1 and AIBC1: Genes Amplified at 20q13.2 and Overexpressed in Breast Carcinoma," submitted to *Proc. Natl. Acad. Sci. (USA)*.

M. Schoenberg-Fejzo, W.-L. Kuo, C. Collins, D. Pinkel, and J. Gray, "Molecular Cytogenetic Analysis of Consistent Abnormalities at 8q12-q22 in Breast Cancer Localizes a Novel Oncogene to YAC 928F9," *Genes, Chromosomes and Cancer*, in press.

L. Shayesteh, Y. Lu, W.-L. Kuo, C. Collins, D. Pinkel, G.B. Mills, and J.W. Gray, "PIK3CA is Implicated as an Oncogene in Ovarian Cancer," submitted to *Nature Genetics*.

D. Pinkel, R. Segraves, D. Sudar, S. Clark, I. Poole, D. Kowbel, C. Collins, W.-L., Kuo, C. Chen, Y. Zhai, S. Dairkee, B.-M. Ljung, J.W. Gray, and D.G. Albertson, "Quantitative High Resolution Analysis of DNA Copy Number Variation in Breast Cancer Using Comparative Genomic Hybridization to DNA Microarrays," submitted to *Nature Genetics*.

J.-F. Cheng and H.-U.G. Weier, "Approaches to High Resolution Physical Mapping of the Human Genome," Biotechnology International, C.F. Fox and T.H. Conner, eds., Universal Medical Press, San Francisco, 149-157 (1997).

T. Duell, M. Wang, J. Wu, U.-J. Kim, and H.-U.G. Weier, "High Resolution Physical Map of the Immunoglobulin Lambda Variant Gene Cluster

Assembled by Quantitative DNA Fiber Mapping." *Genomics* 45, pp. 479-486 (1997).

T. Duell, L.B. Nielsen, A. Jones, S.G. Young, and H.-U.G. Weier, "Construction of Two Near-Kilobase Resolution Restriction Maps of the 5' Regulatory Region of the Human Apolipoprotein B Gene by Quantitative DNA Fiber Mapping (QDFM)," *Cytogenet. Cell. Genet.*, in press.

Computational Biology

Principal Investigators: Teresa Head-Gordon, George Oster, and Daniel Rokhsar

Project No.: 96038

Project Description

The Computational Biology group as part of the Life Sciences Division is tackling biological computation at the molecular, cellular, and developmental levels. Our goals are the prediction of molecular protein structure from amino acid sequence (Teresa Head-Gordon), the simulation of cellular mechanics (George Oster), and further understanding of the connections between output cells and the brain (Daniel Rokhsar). These projects have strong interactions with a mature experimental area, share a need for high performance computing to realize the following scientific goals, and are areas of computational biology that address postgenomic research.

The first project is to predict protein structure from amino acid sequence. A recognized difficulty in protein structure prediction is that a chemically realistic approximation to the conformational behavior of proteins results in an exponentially large number of protein conformations that must be searched in order to find the global (i.e., native structure) minimum. Our computational framework for protein structure prediction is the Antlion conformational search strategy that smoothes a theoretical protein energy surface to retain only the region near the desired (global) minimum. The smoothing operation involves the design of mathematical functions that are manifestations of neural network predictions of secondary structure. The Head-Gordon group has developed neural network algorithms that provide for our source of

predictions of protein secondary structure. These mathematical functions are designed to ensure that a one-to-one mapping between the desired minimum on the complex energy surface and that of the simplified surface is maintained, otherwise the method may ultimately converge to a higher energy minimum. In collaboration with computer science researchers at the University of Colorado, we are developing a joint global optimization approach, based on sampling, perturbation, and smoothing, that has been quite successful working directly on the potential energy surfaces of small homopolymers. The collaboration will entail the development of new techniques in the global optimization algorithm that incorporate secondary predictions and supersecondary features effectively and focus on tertiary structure determination for real proteins.

The second project is the simulation of stochastic trajectories of model motor proteins to generate force/velocity curves or as input into Fokker-Planck equations to provide model distributions consistent with the experimental statistics. There has been a revival of interest in the class of "motor" proteins that convert chemical energy into mechanical forces to perform useful work in the cell. Again, advances in experimental instrumentation now make it possible to measure protein ensemble statistics, or even individual motor protein displacement or velocity as a function of imposed force at the molecular scale. It is now possible to make realistic models of molecular mechanochemical processes that can be related directly to experimentally observable, and controllable, parameters. These advances in experimental technology have initiated a renaissance in theoretical efforts to readdress the central question concerning the operation of protein machines: how do they work? More precisely, how is chemical energy transduced into directed mechanical forces that drive so many cellular events?

Third, in the construction of a functioning visual system, precise connections must be formed between output cells of the retina and the parts of the brain that will process this information. To study the processes involved in establishing these connections, we will carry out large-scale simulations (millions of elements) of cellular automata whose behavior models the various cell types found in the early retina. The goal will be a quantitative analysis of temporal and spatial structures that are generated by this automata, which can be compared directly to waves and domains visualized by calcium imaging in the developing retina. In a second project, simplified lattice and off-lattice models for protein-folding

thermodynamics and kinetics were used to study both the phase diagram for heteropolymers and the nature of their folding pathways. These calculations have shown explicitly that 1) the molten globule is a distinct third phase of proteins, analogous to the liquid phase of ordinary materials, and 2) the folding pathway of model proteins is not described by a "folding funnel," but rather by a series of one or more first-order phase transitions characterized by a rate-limiting nucleation step.

Accomplishments

The primary accomplishment for the first project is the design and implementation of our global optimization algorithm, which was developed on the Cray T3E at NERSC, and is currently searching for global structures of five targets ranging in size between 70 and 154 amino acids. One paper is in preparation for the global optimization research. For improved energy surfaces we have published two papers in the area of hydration around amino acid side chains.

Global Optimization Algorithmic Design:

- (1) Make prediction of protein class
Is it helix, sheet, helix/sheet, helix+sheet?
If helix \rightarrow TARGET
- (2) Make neural network prediction of 2° structure
helix, sheet, coil for each amino acid
- (3) Optimize on following energy surface:

$$V_{\text{Total}} = V_{MM} + V_{\phi\psi} + V_{HB}, \text{ where}$$

$$V_{\phi\psi} = k_{\phi} [1 - \cos(\phi - \phi_0)] + k_{\psi} [1 - \cos(\psi - \psi_0)];$$

$$V_{HB} = q_i q_j / r_{i,j}$$

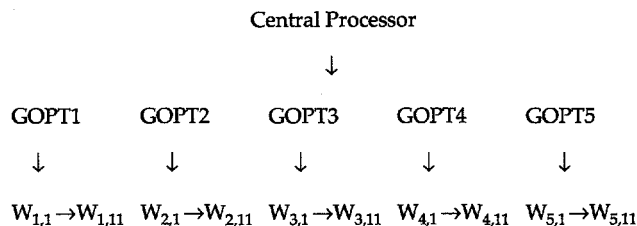
where the parameters for $V_{\phi\psi}$ and V_{HB} are defined by the neural network output for all residues predicted to be helix.

- (4) Using optimized structure from (3), use stochastic/perturbation to find global optimum in sub-space, where the subspace is defined as the coil regions predicted by the neural network.

Global Optimization Algorithm Implementation on the Cray T3E. The complexity of the protein structure prediction problem requires high-performance computing. We conservatively estimate that the number of operations for one run of the stochastic perturbation method with an empirical potential is

$$(10^2 N^2 \text{ Flops/EF}) \times (10^2 N^2 \times 10^4 N) \text{ EF}$$

where N is the number of atoms and EF represents an energy and force evaluation. Based on the current generation Cray T3E platform, we are using both 64 and 128 processors, although any number of processors can be used by our algorithm. We have ported our algorithm to the Cray T3E. The parallel algorithm is designed as follows.



The central processor assigns starting coordinates to the GOPTs processor, and the GOPTs divide up subspace into 11 regions per worker (W_{ij}) for the global search in the defined subspace. The Workers then return a list of minimizers to the GOPTs, and the GOPTs rank the 10 best local minimizers from each worker. The GOPTs in turn send their best 10 minimizers to the central processor, and the central processor determines the five of lowest energy. The algorithm passes these new five starting structures to begin the global optimization phase all over again.

Hydration around Amino Acid Side Chains. A technician is doing x-ray scattering experiments on single amino acids in water, in collaboration with Robert Glaeser at UC Berkeley. We have completed preliminary work to extract potentials of mean force for these amino acids. Jon Sorenson, a UC Berkeley chemistry graduate student doing his thesis work with Dr. Head-Gordon, will aid the theoretical and computational effort to reproduce the scattering curves and to understand the underlying thermodynamic consequences of the scattering profiles.

For our second project, studies were begun and completed of three molecular motors: the bacterial flagellar motor, the Fo motor in ATP synthase, and RNA polymerase. The publications resulting from these studies are listed below. Each project involved a close collaboration with experimental laboratories that supplied us with the latest data that we used to calibrate and validate the models. The models consisted of constructing equations representing the mechanical and chemical dynamics of the protein. The general modeling framework consisted of constructing a set of nonlinear Langevin and Fokker-Planck differential equations describing the

mechanical motions. These equations were coupled to a Markov chain describing the chemical transitions. The resulting set of equations included stochastic as well as electrostatic and elastic forces. The results of these numerical simulations are contained in the preprints which can be downloaded from the web. For the ATP synthase model we have also constructed an MPEG movie to illustrate the principle of operation. The models were constructed and the simulations carried out, principally by Hongyun Wang, who was supported by a NERSC postdoctoral fellowship.

In the third area, during the past year two principal activities were supported. Both of these activities made extensive use of the Cray T3E at NERSC. In the first activity, a computational model for the developing retina was constructed and its behavior studied by both simulation and analytical methods. The model is based on the known anatomy of the immature retina, and includes a representation of a hidden layer of cells (starburst amacrices) whose behavior has not been measured directly. Our model implicates these cells in the retinal waves observed in the developing retina of mammals. In recently published work, we present an extensive statistical analysis of the spatio-temporal patterns observed in the developing retina, and construct a novel two-layer model that accurately describes these patterns. The model makes nontrivial predictions for future experiments and demonstrates that the starburst amacrine cells are an essential element in the local circuitry that generates retinal waves.

In the second activity, the folding pathways of simplified models of protein folding dynamics were studied and used to formulate a "neoclassical" model for folding, in which the folding process is viewed as a sequence of cooperative phase transitions between metastable phases. The nature of the transition state for these transitions is analyzed, and it is argued that the transitions proceed by a nucleation mechanism. The thermodynamic properties of lattice and off-lattice models for proteins were studied. We find that the rigidity of the lattice model, which mimics the rigidity generated by side-chain packing, gives rise to a phase diagram with a distinct molten globule phase separated from the unfolded and native phases by first-order phase transitions. By contrast, the off-lattice model we study lacks side-chain packing, and there is no free energy barrier between the molten globule and the native states. The nature of the free

energy barriers are analyzed by direct calculation of polymer and mixing entropy contributions.

Publications

A. Pertsemidis, A.M. Saxena, A.K. Soper, T. Head-Gordon, and R.M. Glaeser, "Direct, Structural Evidence for Modified Solvent Structure Within the Hydration Shell of a Hydrophobic Amino Acid," *Proc. Natl. Acad. Sci.* **93**, 10769-10774 (1996).

T. Head-Gordon, J.M. Sorenson, A. Pertsemidis, and R.M. Glaeser, "Differences in Hydration Structure Near Hydrophobic and Hydrophilic Amino Acid Side Chains," *Biophys. J.* **73**, 2106-2115 (1997).

R.C. Yu, I. Dubchak, and T. Head-Gordon, "Improved Neural Networks for Protein Secondary Structure Prediction Without Use of Sequence or Structural Homologies," *J. Comp. Biol.*, in preparation.

S. Chang, T. Head-Gordon, R.M. Glaeser, and K. Downing, "Chemical Bonding Effects in the Determination of Protein Structures by Electron Crystallography," submitted to *Acta. Cryst.* (1997).

S. Crivelli and T. Head-Gordon, "Structure Prediction of Five Helical Proteins Using Global Optimization Techniques and Potential of Mean Force Descriptions of Hydration," in preparation.

T. Elston and G. Oster, "Protein Turbines I: The Bacterial Flagellar Motor," *Biophys. J.* 703-721 (1997).

T. Elston, H. Wang, and G. Oster, "Energy Transduction in ATP Synthase," *Nature*, in press.

H. Wang, T. Elston, A. Mogilner, and G. Oster, "Force Generation in RNA Polymerase," *Biophys. J.*, in press.

M. Feller, D. Butts, H. Aaron, D. Rokhsar, and C. Shatz, "Dynamic Processes Shape Spatiotemporal Properties of Retinal Waves," *Neuron* **19**, 293-306 (1997).

V. Pande, A. Grosberg, T. Tanaka, and D. Rokhsar, "Pathways for Protein Folding: Is a "New View" Needed?" *Current Opinion in Structural Biology*, in press.

V. Pande and D. Rokhsar, "Is the Molten Globule a Third Phase of Proteins?" *Proc. Natl. Acad. Sci.*, in press.

V.S. Pande and D.S. Rokhsar, "Transition States and Intermediates in a Lattice Model for Protein Folding," in preparation.

Analysis of DNA-Damage Sensitivity of Yeast Mutants Lacking Chromatin Assembly Proteins

Principal Investigator: Paul Kaufman
Project No: 96039

Project Description

This project focuses on the protein complex termed Chromatin Assembly Factor-I (CAF-I). CAF-I is an evolutionarily conserved factor that assembles nucleosomes in a manner linked to DNA replication *in vitro*. This project studies the relationship between CAF-I activity and radiation sensitivity in the yeast *Saccharomyces cerevisiae*, which can be studied genetically as well as biochemically.

Many advances in cancer research depend on understanding how eukaryotic chromosomes are assembled and protected from damage. Earlier work showed that human CAF-I will assemble nucleosomes on DNA templates that undergo nucleotide excision repair. Therefore, the initial phase of this project has tested the role of CAF-I in DNA damage sensitivity *in vivo*.

Accomplishments

We first demonstrated that cell extracts from the budding yeast *Saccharomyces cerevisiae* contained a biochemical activity that would perform DNA replication-linked nucleosome assembly, as had been previously observed in humans, *Drosophila*, and *Xenopus*. Detection of this activity allowed for the biochemical purification of the yeast factor.

We have identified the genes encoding each of the three yeast CAF-I subunits by amino acid sequence analysis of purified protein. Two of these genes are termed *CAC1* and *CAC2* (for Chromatin Assembly Complex), respectively. The third gene was previously termed *MSI1*. Identification of these genes

demonstrated that each is homologous to its human counterpart, and allowed for construction of yeast strains lacking individual or multiple CAF-I subunits.

We have established that CAF-I plays a role in protecting the genome from certain types of DNA damage. Specifically, we quantitatively assessed the degree of sensitivity to different DNA-damaging agents using cells lacking each of the CAF-I subunits. Ultraviolet light (forming thymine dimers and other photoproducts) and x-ray irradiation (causing double-strand breaks) were tested. Interestingly, mutations in all CAF-I subunits result in increased sensitivity to ultraviolet radiation, but not x rays. These data suggest that nucleosome assembly by CAF-I is activated by some, but not all, forms of DNA damage.

In order to determine which repair process involves CAF-I *in vivo*, we used double and triple mutants involving *cac1*Δ and deletions of yeast repair genes to show that the *CAC1* gene falls into the *RAD6* epistasis group with respect to its UV-repair defect. Double mutants involving *cac1*Δ and either *rad6*Δ or *rad18*Δ were no more UV-sensitive than the corresponding *rad*Δ mutants alone. In contrast, double mutants involving *cac1*Δ and the excision repair mutants *rad1*Δ or *rad14*Δ showed increased UV sensitivity, as did double mutants involving *cac1*Δ and deletions of members of the *RAD51* recombinational repair group. These and other findings suggest that CAF-I facilitates post-replicative DNA repair mediated by the *RAD6* pathway.

Publications

P.D. Kaufman, R. Kobayashi, and B. Stillman, "Ultraviolet Radiation-Sensitivity and Reduction of Telomeric Silencing in *Saccharomyces cerevisiae* Cells Lacking Chromatin Assembly Factor-I," *Genes Dev.* **11**, 345 (1997).

A. Verreault, P.D. Kaufman, R. Kobayashi, and B. Stillman, "Nucleosomal DNA Regulates the Core-histone-binding Subunit of the Human Hat1 Acetyltransferase," *Current Biology* **8**, 96–108 (1998).

J.C. Game and P.D. Kaufman, "Saccharomyces cerevisiae Chromatin Assembly Factor-I Plays a Role in Repair of Ultraviolet Radiation Damage Mediated by the *RAD6* Epistasis Group," submitted for publication.

Isolation and Characterization of SATB1-Bound Sequences in vivo

Principal Investigators: Terumi Kohwi-Shigematsu and Yoshimori Kohwi

Project No.: 97016

This was a joint project in FY97 and will be two separate projects in FY98. Consequently, two project reports follow.

Project Description: Isolation and Characterization of SATB1-Bound Sequences *in vivo*; Kohwi-Shigematsu

The higher order structure of eukaryotic chromosomes consists of independent loop domains, which are separated from each other by the attachment of specialized genomic sequences (matrix attachment region or MARs) onto the nuclear matrix (reviewed in Nelson et al., 1986; Gasser and Laemmli, 1987). Such loop domain structures are not only important for compacting genomic DNA, but presumably they also play a role in regulating DNA function, including replication, recombination, and transcription. In fact, much evidence has been accumulated to show that active replication and transcription processes are undertaken at the site of the nuclear matrix, suggesting that MARs could be important targets for regulation of DNA function. MARs have been identified to date on the basis of their *in vitro* binding to the nuclear matrix. Therefore, an important question still remains as to what type of genomic sequences actually anchor genomic DNA onto the nuclear matrix *in vivo*. Once such a series of loop attachment sequences is analyzed, one could then address what makes these sequences attach to the nuclear matrix and the consequent biological roles. Such information will promote understanding of the three-dimensional utility of linear genomic sequences.

We previously cloned a T cell factor, SATB1, which is a cell-type specific MAR-binding protein predominantly expressed in thymocytes. SATB1 binds specifically to a particular region (a base unpairing region or BUR) typically found in MARs. BURs (which typically span 100–300 bp) have a very

high propensity to unwind and they represent key structural elements of MARs. SATB1 and anti-SATB1 antibody can be used to isolate BUR sequences that bind to SATB1 *in vivo* to examine their biological function.

Accomplishments

We have devised a method to clone genomic sequences that bind to SATB1 *in vivo*. Using this method, we isolated a set of genomic sequences from Jurkat cells and thymocytes, and demonstrated that a MAR-binding protein binds to BURs *in vivo* at the bases of chromatin loops. These experiments unambiguously demonstrated for the first time that a specific set of genomic DNA sequences is anchored onto the nuclear matrix and bound *in vivo* to a cell-type specific MAR-binding protein. Another important finding has been that anchoring of specific genomic sequences is cell-type dependent: a genomic sequence that binds to SATB1 is anchored onto the nuclear matrix in Jurkat cells, but not in breast cancer SKBR-3 cells. This demonstrates that the three-dimensional organization of chromatin is cell-type specific.

We have established SATB1 knockout mice and found that multiple genes are dysregulated in the absence of SATB1, and SATB1 knockout mice suffer from arrested T cell development. These results indicate that BUR sites are important targets for developmental regulation.

In addition to cloning SATB1-binding sequences *in vivo* from Jurkat cells and thymocytes, we have also established a quick method to clone any BUR sites from P1 and YAC clone. Such a quick method for identification of BUR sites is potentially very useful as an annotation of genomic sequences. Unless it is pointed out, scientists cannot easily detect such sequences. We will continue to examine BUR sequences cloned by using SATB1 as a tool with respect to their potential role in DNA replication and cleavage sites for apoptosis to dismantle chromatin in response to a death signal.

Publication

I. deBelle, S. Cai, and T. Kohwi-Shigematsu, "The Genomic Sequences Bound to SATB1 *in vivo* are Tightly Associated with the Nuclear Matrix at the Base of the Chromatin Loops," *J. Cell Biol.*, in press (1997).

Project Description: Studies of the Expression of Trinucleotide Repeat Sequence Binding Proteins (TRIPs) in the Brain; Kohwi

The discovery of a new class of mutations, the expansion of trinucleotide repeats, in the genes responsible for several genetic disorders inspired us to search for the mechanisms of the mutation in humans. These mutations include the trinucleotide-repeat expansion of (CGG)_n in the mutant gene responsible for the inherited mental retardation disorder fragile X syndrome; (CAG)_n in the gene responsible for myotonic dystrophy (Dystrophia Myotonica, DM, an autosomal dominant neuromuscular disease); the androgen receptor gene of X-linked spinal and bulbar muscular atrophy, a rare motor neuron disorder (SBMA or Kennedy's disease); the gene responsible for Huntington's disease; and the genes responsible for spinocerebellar ataxia type1 (SCA1), hereditary dentatorubral-pallidolysian atrophy, and Machado-Joseph disease. In many of these conditions, severity and / or age of onset of the disease is determined by the number of repeating units. Although the expansion of trinucleotide repeats has been associated with genetic disorders, it is not known how trinucleotide repeats expand or how this expansion causes disease.

Huntington's disease (HD) is an autosomal dominant genetic disorder, estimated to affect approximately 1 in 10,000 individuals. It is characterized by progressive neurodegeneration resulting in involuntary movements, and cognitive decline and dementia as a result of neuronal cell death, particularly in the nucleus caudate and Putamen of the basal ganglia. Dentatorubral-pallidolysian atrophy (DRPLA) is an autosomal dominant neurodegenerative disorder characterized by a varying combination of progressive myoclonus, epilepsy, ataxia, choreoathetosis, and dementia. It is particularly prevalent in Japan.

Recent work in transgenic mice production and analysis indicates that the expression of the toxicity by polyglutamine in expanded trinucleotide repeat genes may be sufficient to generate a mouse model of such diseases. Especially, HD model mice provide an intriguing mouse model in which the introduced-HD genes are ubiquitously expressed and the features of the movement disorder and the complex HD phenotype are reproduced, although the specific neuronal cell death in HD mice is not apparent.

The neuron-selectivity of the cell death by triplet disease gene products may suggest the involvement of other factors in the brain. To understand the

mechanism of neurodegenerative diseases resulting from trinucleotide repeat sequence expansion, we searched for other factors to interact with trinucleotide repeat sequences. Previously, we detected and purified two proteins responsible for single-stranded (ss)-(CAG)_n repeat binding activity in mouse brain. The (CAG)_n-repeat sequence binding proteins bind a specific subset of single stranded-trinucleotide repeat sequences, including ss(CGG)_n repeats. We named these two proteins TRIP-1 and TRIP-2 (where TRIP represents trinucleotide repeat-binding protein).

We hypothesized that TRIP expression is correlated with cognitive ability in neurogenetic disorders and age-dependent dementia. In this LDRD grant, we proposed to find whether there is altered expression of TRIPs in the brain with neurodegenerative diseases, including Huntington's disease.

Accomplishments

Recently, we isolated the cDNAs encoding TRIP-1 and TRIP-2. The transcripts of TRIP-1 and TRIP-2 were detected by Northern blot analysis and showed that they were brain specific. The level of RNA expression of TRIP-1 and TRIP-2 in postnatal mouse brain at different time points after birth revealed that the TRIP-1 and TRIP-2 mRNAs at day 1 were virtually absent but they increased postnatally in parallel day by day and reached a plateau level within 2-3 weeks of age. We investigated the cellular localization of TRIP expression in mouse brain section by *in situ* hybridization. The data clearly demonstrated that the TRIP-1 and TRIP-2 mRNAs were localized predominantly in neurons.

To elucidate the biological function of TRIPs in neuron, we investigated the subcellular localization of TRIPs and the effect of TRIP expression on neurite outgrowth in PC12 cells. In tissue cultured PC12 cells in the presence of nerve growth factor (NGF), these cells extend long branch-characteristics of sympathetic neurons. The endogenous TRIP-1 level is very low in PC12 cells detected by RNA hybridization. To detect TRIP protein in cell, FLAG-fused TRIP-1 expression vector was constructed and the protein was detected by anti-FLAG antibody. When FLAG-fused TRIP-1 was expressed in PC12 cells, the cells were induced to differentiate, and neurite outgrowth was triggered without NGF. The immunostaining of the PC12 cells with anti-FLAG antibody showed that TRIP-1 proteins were not only detected in the cell bodies (cytoplasm surrounding nuclei), but also were distributed along the newly

formed neuronal fibers as well as in the leading edges of growth cone-like structures. On the other hand, those cells that were unsuccessfully transfected did not show any neurite outgrowth. These data indicate that TRIP-1 expression enhances neurite outgrowth and is important for neuronal fiber elongation in the growth cone. We also demonstrated that TRIPs actually bind native mRNA *in vitro*. These data suggest that TRIPs play an important role in the neuron to elongate neurite outgrowth. Elongation of neurites occurs exclusively at their growth cones, which are the actively growing tips of all branches of axons and dendrites. Messenger RNA localization in neuron fiber and growth cone may be important to allow for timely regulation of protein synthesis in response to local stimuli especially at a considerable distance from the nucleus. The enhancement of neurite outgrowth by TRIP expression and the existence of TRIPs in growth cone may indicate a contribution of TRIP in stability, transport, and localization of mRNA in neuron.

A correlation between TRIP expression and hereditary neurodegenerative diseases has yet to be established.

Publication

H. Yano-Yanagisawa, B.-E. Wang, I. Ahmad, J. Zhang, T. Abo, J. Nakayama, and Y. Kohwi, "Trinucleotide Repeat Sequence Binding Proteins (TRIPs) are RNA-Binding Proteins in Neuron and Enhance Neurite Outgrowth," in preparation.

A Novel Technique to Follow Consequences of Exogenous Factors, Including Therapeutic Drugs, on Living Human Breast Epithelial Cells in 3D

Principal Investigators: Carolyn Larabell and Jon Nagy

Project No.: 97017

Project Description

An understanding of how agents differentially affect normal tissues as opposed to cancer cells is essential

for the development of rational treatments for these cancers. Most studies of breast cancer have utilized monolayer cultures of cells. Unfortunately, these studies do not accurately reflect the 3D organization of breast tissue in the body. A number of excellent model systems in which to study the early events that accompany the progression of normal to malignant cell types in three-dimensional cultures are now being utilized. These models present technical difficulties with microscopical analyses required to understand the structure-function relationships of normal versus malignant cells using immunolabeling techniques. In addition, these cell clusters are too large for traditional microscopical analyses of living cells. The purpose of this project was to 1) develop a 3D culture system containing extracellular matrix components thick enough to yield typical cell growth and, at the same time, permit immunocytochemical labeling and imaging of intact cultures; and 2) develop the methodology to label components in living cells using dyes that do not affect cell viability but permit monitoring of living cells in response to addition of exogenous factors.

Accomplishments

We utilized human mammary epithelial cell lines, obtained from Dr. Mina Bissell's laboratory, that range from normal to premalignant to cancerous. We have determined the culture requirements of these cell lines that generate the characteristic growth patterns in Matrigel yet permit imaging in the light microscope. We have also established the labeling protocol required for whole-mount immunocytochemical analyses of cell surface and cytoplasmic proteins. This approach provides 3D views of cell-cell and cell-ECM (extracellular matrix) interactions that are extremely difficult (and often impossible) to obtain from sectioned material. This work was accomplished in collaboration with Dr. Sophie Lelievre, a postdoctoral fellow in Dr. Mina Bissell's laboratory.

We then developed the methodology to examine these 3D cell clusters, in the living state, using confocal microscopy. We utilize modified Petri dishes in which a portion of the bottom of the dish has been replaced with a glass coverslip. This facilitates imaging the cells using an inverted microscope without opening the dish and risking contamination of the cultures. We have labeled cells with vital dyes and monitored the cell clusters over time. We are now in a position to monitor the growth of these cell lines and their responses to the addition of exogenous

factors. We can also transfect the cell lines with gfp-constructs to specific proteins and monitor the redistribution of these proteins in response to the addition of exogenous agents.

Development of Novel Biological Targeted Therapies for Breast Cancer

Principal Investigator: Ruth Lupu

Project No.: 97018

Project Description

The overall aim of the current study is to design novel targeted therapies for breast cancer. In order to achieve our aim, we will define the functional sites of the *erbB*-receptors, both to define their role in cellular transformation and to identify the sites that contribute to receptor dimerization. In order to define functional sites at the *erbB*-2 extracellular domain, we have developed a set of *erbB*-2 deletion mutants. As part of the current proposal, the mutants will be used to examine their contribution in receptor activation and dimerization.

We will take advantage of our previously characterized peptido-mimetic, corresponding to the predicted ligand interaction domain of the *erbB*-2 receptor extracellular domain. This peptide appears to interfere with HRG induction of receptor tyrosine phosphorylation. We will use the known peptide sequence to develop peptide libraries containing all the possible sequences. Molecular diversity libraries represent a powerful new way to generate millions of assayable structures using only a minimum of preparative chemical steps. Solid-phase synthetic techniques are used to prepare combinatorial peptide libraries on small resin beads, each having a unique sequence. The bead library can be passed through a biological assay whereby certain members can be identified as active and removed from the mass. Micro sequencing of the bead or beads will then yield the active peptide analog(s). Studies *in vitro* and

in vivo will then be performed to define the potential capacity of the peptides as therapeutic tools.

Specifically we will 1) determine the functional site of the *erbB*-2 receptor by transfecting the *erbB*-2 mutants into breast cancer cells; 2) determine the ability of other related peptides to induce growth inhibition in culture and *in vivo*; 3) identify other putative antagonists using a peptide library; and 4) generate HRG mutants (D-HRG) that will lack the predicted binding sites.

To determine the functional domains of *erbB*-2, specific deletion mutants will be transfected into breast cells. Transfected cells will be biochemically and biologically characterized *in vitro* and *in vivo*. To identify specific antagonists, we will generate a peptide library using the related sequences to the known peptide. The library will be incubated with cancer cells. Positive peptides will be isolated, sequenced, and re-synthesized. Identified peptides will be tested *in vitro* and *in vivo*. To determine if the RL2 congeners interfere with receptor function and growth *in vitro* and *in vivo*, synthetic peptides will be tested on the growth of cells in culture and in nude mice. To develop recombinant HRG mutants that lack the predicted high- or low-affinity binding sites, we have shown using HRG neutralizing antibodies that HRG exerts two binding sites. Mutated recombinant HRG will be generated and characterized both biochemically and biologically.

Accomplishments

During the first year of funding, two major tasks were accomplished. We generated a large and specific range of related *erbB*-2 blocking peptides derived from the original peptide sequence and a number of specific *erbB*-2 deletion mutants at the predicted critical/functional sites. We predict that a better understanding of the mechanism of action of these molecules will enable us to design novel biological therapies. Collectively, these experiments will provide a better molecular framework for understanding ligand-receptor and receptor-receptor interaction. The results of this proposal may provide specific tools for the development of *erbB*-2 targeted therapies based on its interaction with its activator or co-receptors.

Survey of Microbial Communities in Chemically Damaged and Control Environments

Principal Investigator: Norman Pace

Project No.: 97019

Project Description

The purpose of this project was to correlate the spatial and temporal distribution of microorganisms with xenobiotic contaminants in chemically damaged and control environments. This program continues the development of molecular methods for the analysis of the nature of environmental microorganisms without the requirement for cultivation. Analyses include ribosomal RNA (rRNA) gene cloning and sequencing to identify organisms phylogenetically.

Hybridization probe technology based on the sequences will be developed as a rapid and economical way to map organism-distribution onto chemical contaminant-distribution. Environmental samples for analysis have been chosen in consort with LBNL scientists engaged in parallel studies of physiology and cultivation (Dr. T. Torok et al.).

Initially two sites (Alameda Naval Air Base, CA, and Wurtsmith Air Force Base, MI) with paired 'control' samples from uncontaminated sites, have been selected for analysis.

Accomplishments

Hydrocarbon-contaminated and uncontaminated core samples from two sites have been collected: one from the Alameda shipyard and the second from Wurtsmith Air Force Base. The chemical properties of the latter site already had been determined, and collaboration was established with the Center for Microbial Ecology for corroboration of results.

Chemical properties of the Alameda site remain to be determined (LBNL). Following microscopic examination, microbial analysis of the Wurtsmith core was begun. DNA samples were prepared from three nominally distinct chemical habitats: iron-reducing, sulfate-reducing, and methanogenic. The DNAs were used with polymerase chain reaction to obtain rRNA genes present in the environment. Several hundred sequences have been analyzed by restriction fragment

length polymorphism or by sequence analysis. Results are informative in regard to the nature of the site examined and to broader aspects of microbial ecology.

This study has so far resulted in the discovery of two novel bacterial divisions, and contributed significantly to a growing number of other major environmental taxa that have no cultivated representatives. The sequences will provide for further analyses by serving as the basis for hybridization probes to obtain further information on the novel organisms. The results highlight some dominant organisms which were not suspected in these environments, providing the basis with which to seek funding to study such organisms. The results are the first direct analysis of such environments using the molecular techniques and identify an unexpected suite of organisms of potential significance to the environment.

Publication

M. Dojka, P. Hugenholtz, S. Haack, and N.R. Pace, "Microbial Diversity in Different Redox Zones of a Hydrocarbon-Contaminated Aquifer," *Appl. Environ. Microbiol.*, in preparation.

Gene-Specific Biomonitoring to Assess Risk of Developing Environmentally-Induced Leukemia

Principal Investigators: Maria Pallavicini and Ron Jensen

Project No.: 97020

Project Description

An increased incidence of hematologic malignancies (e.g., leukemia) is a potential health risk associated with human exposure to chemicals found in contaminated ground water, toxic sites, and atmospheric microenvironments. The goal of our project is to increase understanding of the genetic and functional alterations that occur in hemopoietic cells

exposed to environmental contaminants. Specifically, we will determine whether loss of sequence from a region of the genome with genes that regulate hematopoiesis is an early event after genotoxin exposure. We anticipate that these data will facilitate 1) development of a gene-specific biomonitoring assay to identify agents and complex mixtures with potential leukemogenic ability; and 2) investigation of the mechanisms underlying leukemic predisposition and progression.

Nonrandom loss or rearrangement of sequence from human chromosome 5 occurs in approximately 20-50% of secondary leukemias (including those developing after chemotherapy and/or exposure to mutagenic agents found in solvents and pesticides). We hypothesize that loss of function of genes on chromosome 5 represents an early event in leukemogenesis. Specifically, we postulate that exposure of hematopoietic stem cells (hsc) to environmental genotoxins with leukemogenic potential induces preferential loss of function of genes on human chromosome 5. A consequence of loss of function of genes on chromosome 5 is selective cell proliferation resulting in clonal expansion of aberrant cells that lack genes critical for regulation of hematopoiesis. The aims of our project are to:

- Determine whether radiation- or benzene-induced leukemias in mice show recurrent loss of sequence from murine chromosome 11 A5-B1 and 13 A2-B2 (syntenous with sequence on human 5q31);
- Apply and develop molecular approaches to assess gene deletion and loss of gene expression from a critical genomic region which, when deleted in "knockout" mice, predisposes to clonal hematopoiesis. We predict that mice carrying one copy of the "critical region" will show increased susceptibility to the genotoxic effects of radiation and benzene which will be reflected in a higher frequency of genetically aberrant stem cells and an increased rate of leukemogenesis.

Accomplishments

First, we generated myeloid leukemias in SJL mice that are genetically susceptible to radiation-induced

leukemogenesis. These leukemias will be evaluated for loss of sequence from regions of the mouse genome syntenous to human 5q31.

Second, five mouse strains with varying genetic predisposition to development of malignancy have been obtained, bred, and exposed to genotoxins. Primer pairs for microsatellites in the critical chromosomal region have been identified and evaluated for heterozygous allelic resolution.

Third, we developed methodologies to measure allelic imbalance in stem cells and leukemias. A method has been developed to quantify the number of copies of specific regions of the genome using real time fluorescence polymerase chain reaction (PCR) analysis. This technique uses a newly developed instrument that can measure fluorescence intensities at particular wavelengths from all wells in a 96-well plate during PCR cycling. To perform allele enumeration, PCR primer pairs which encompass CA-repeat microsatellites are placed into PCR wells along with a specific fluorescently labeled CA-repeat probe and a target DNA. During each cycle of PCR, the action of Taq enzyme on the fluorescent probe releases a fluorescent reporter and increases the intensity of fluorescence relative to the amount of target DNA present. This generates a set of fluorescence versus cycle number plots that can be used to determine the frequency of alleles in each well.

This analysis was applied to DNA samples extracted from knockout mice to test the applicability of the measurement. DNA was extracted from normal mice and mice with a 1 Mb knockout (K.O.) in chromosome 11, which were obtained from the laboratory of Dr. E. Rubin. PCR primer pairs were obtained which mapped to the knockout region, to regions immediately adjacent to the knockout, and to regions on other chromosomes. These were simultaneously amplified in the fluorescence-based real-time PCR instrument, and the relative number of allele copies at each locus was measured. The results of this measurement (Figure 1) show that amplification of a locus mapped to the knockout region (D11MIT23) reflects half the number of alleles as the other loci adjacent to the knockout region. Since the mice being tested were heterozygous K.O. /++, this result fits with expected allelic

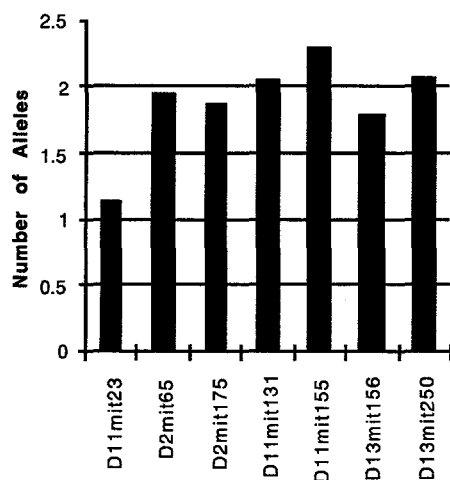


Figure 1. Allelic enumeration for seven loci in knockout mice. Real-time fluorescence PCR analysis was used to determine the allelic frequency in heterozygous 129/K.O. mice relative to the frequency in homozygous 129/129 mice. Since the normal 129/129 mice are diploid at all loci, the number of alleles at each locus in the 129/K.O. is normalized to this frequency.

frequencies of disomy for all adjacent loci and monosomy for the locus in the knockout region.

There are at least three advantages to using this system for measuring loss of alleles as a measure of genetic abnormalities in tumor samples. Firstly, it is a rapid measurement, even as compared with fluorescence gel electrophoretic allelic imbalance measurements, since a PCR reaction is all that is necessary to perform the procedure. Secondly, the measurement is performed on 96 wells simultaneously. At present we perform triplicate measures on each sample, resulting in the ability to perform allelic enumeration on 32 samples simultaneously. With more experience, we expect that duplicate measurements will provide sufficient precision, allowing 48 samples per run. This would result in the capability to perform this measurement on about 200 sample loci per day. Finally, the most important advantage to this technique is that it can be performed on homozygous loci, since it does not use differences in allelic size to distinguish between alleles. This will allow allelic imbalance measurements to be performed routinely on homozygous strains of mice, with no crossbreeding necessary.

Materials Sciences Division

A New Strategy for the Introduction of Biocompatible Adhesive Coatings onto Material Surfaces

Principal Investigator: Carolyn Bertozzi

Project No.: 97021

Project Description

There is an urgent need in the materials and biotechnology industries for new biocompatible materials. Many currently available materials, such as metals, ceramics, and organic polymers, have favorable bulk properties but are chemically incompatible with living tissue. The chemical composition of the material surface is very different from the bioenvironment, precluding the formation of an adhesive layer at the biological / material interface. This problem could be solved if the material surface were made to more closely resemble the biological tissue.

During the last year, our research has been developing a revolutionary new technology for coating materials with a biocompatible surface that mimics the bioenvironment. Our strategy for controlling material surface biocompatibility is to coat the material with a new surface that perfectly mimics the bioenvironment. The unique feature of our approach is that we use living cells to construct the biomimetic coating. The challenge is to develop a method for attaching a uniform layer of cells to a material surface in a chemically defined fashion, without damaging the cells' physiology. We have developed two new technologies to meet this challenge. First, we coat material substrates with a monolayer of reactive organic functional groups using the technique of organic self-assembly. Second, we decorate cells with a complementary reactive functional group via biosynthetic engineering of cell surface oligosaccharides. The two functional groups are designed to be mutually reactive under physiological conditions and will covalently ligate to form a uniform layer of cells on the material surface.

Once the material is coated with cells, its surface will mimic the bioenvironment. This breakthrough technology has the potential to expand the utility of metals, polymers, and ceramics in biotechnology and medicine.

Accomplishments

There are two critical technical elements in this novel material coating strategy: 1) the metabolic incorporation of chemically reactive functional groups onto cell surfaces, and 2) the introduction of organic monolayers with complementary reactivity onto materials. We have made rapid progress on both of these fronts during the last year.

A major accomplishment is the development of a powerful new method for installing an unnatural reactive functional group, the ketone, onto cell surfaces by simply feeding the cells a synthetic sugar molecule. The cells ingest the synthetic sugar and convert it to a cell surface-bound oligosaccharide, delivering ketone groups to the cell surface. The choice of the ketone as a reactive group was based on two important considerations. First, the ketone is chemically unique among the functional groups normally present on a cell surface. Second, the ketone can be selectively coupled with hydrazide groups under biologically compatible conditions, affording the corresponding hydrazones. This enables the selective attachment of ketone-coated cells to hydrazide-coated material surfaces, and the concomitant formation of a biocompatible coating on the material as depicted in Figure 1.

Our accomplishments at the forefront of material surface modification are twofold. We have focused on inorganic materials such as glasses and ceramics, and on organic polymers such as polyhydroxyethylmethacrylate (PHEMA) hydrogels. The latter are the most commonly used organic polymers in the biomedical materials industry and the former are important substrates for adhesion-dependent bioreactors. First, we have developed a self-assembled monolayer approach for coating silicon oxide surfaces with hydrazide groups, which react selectively with ketones and will therefore support the adhesion of ketone-coated cells. Second, we have prepared PHEMA-based polymers containing various percentages of hydrazide groups. We are currently investigating the physiological

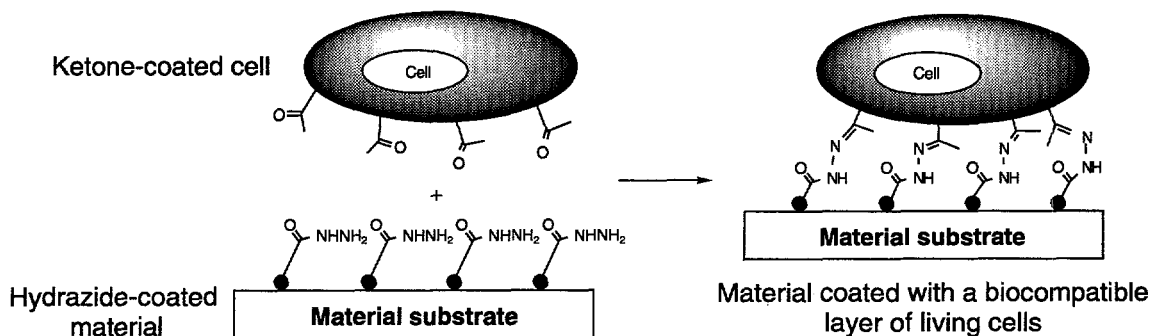


Figure 1. Introduction of a biocompatible coating of cells onto a material surface. The material is first modified with an organic monolayer containing a hydrazide group. A layer of cells metabolically decorated with complementary ketone groups is then covalently attached to the surface. The new surface resembles biological tissue and is fully biocompatible.

consequences of ketone-hydrazide bonding between cells and materials.

Publications

L.K. Mahal, K.J. Yarema, and C.R. Bertozzi, "Engineering Chemical Reactivity on Cell Surfaces Through Oligosaccharide Biosynthesis," *Science* **276**, 1125-1128 (1997).

L.K. Mahal and C.R. Bertozzi, "Engineered Cell Surfaces: Fertile Ground for Molecular Landscaping," *Chemistry & Biology* **4**, 415-422 (1997).

now appropriate and compelling. This research is highly relevant to our understanding of high temperature superconductors, which are magnetic insulators in their undoped state.

Accomplishments

To study the charge and spin dynamics of strongly correlated electron systems, we have developed several specialized tools for our laboratory. For metallic systems and other exploratory studies, we have built a low-temperature pump-probe set-up, which has both a small magnetic field and polarization-sensitive optics available for time-resolved magneto-optic studies. We are currently studying the thermal relaxation dynamics of itinerant ferromagnets with this system, in particular SrRuO_3 and $\text{Ni}_x\text{Cu}_{1-x}$ alloys. SrRuO_3 is an undoped, metallic perovskite ferromagnet which is of technical interest as a metallic contact for ferroelectric and superconducting oxides. We have identified the $\text{O}(2p) \rightarrow \text{Ru}(4d, E_F)$ optical excitation in the conventional thermoreflectance signal, which may be used to monitor the electron temperature in ultrafast studies. Our work on $\text{Ni}_x\text{Cu}_{1-x}$ alloys, provided by Z. Qiu's group in Berkeley, complements recent work on ultrafast spin dynamics in pure nickel metal, as it allows us to continuously change the Curie point by changing copper concentration.

Our study of the magnetic excitons in Cr_2O_3 is under way. We have acquired the first high quality epitaxial films of Cr_2O_3 made by Professor Beasley's group at Stanford, and have completed the conventional photoluminescence and linear absorption measurements necessary to embark on time-resolved studies. The group at Stanford has expressed interest in our optical characterization as an additional tool for

Time-Resolved Spectroscopy of Magnetic Insulators

Principal Investigator: Daniel Chemla

Project No.: 97022

Project Description

The objective of this research is to study the nonlinear optical response of magnetic insulators and related materials, using femtosecond (fs) pulsed laser spectroscopy. Previously, researchers have successfully employed pulsed laser techniques to clarify the physics of charge dynamics and Coulomb correlation in semiconductors, as well as quasiparticle-lattice relaxation in metals. The application of these tools to the charge and spin dynamics of strongly correlated electron systems is

assessing the quality of their oxide film growth. We have begun a study of the Mott-Hubbard gap excitations at 3 eV of Cr_2O_3 , following similar studies on conventional semiconductors. The Urbach tail of magnetic insulators may have a significant component which is due to states with a strong magnetic polaron character, of the type originally discovered by Brinkman and Rice in the early 1970s. These magnetic polaron states are widely viewed as essential to the physics of high- T_c superconductivity, but their study has been limited in recent years to layered cuprous oxides. This study, while relevant to high- T_c superconductivity, is considerably more general in scope, and takes advantage of the high quality material currently available from Stanford. For this work, we have also constructed a regeneratative amplifier capable of microjoule pulses with less than 100-fs duration. This system may be used to generate a pulsed, broadband continuum, enabling us to probe the wide energy range necessary for these studies.

To expand our ability to study coherent optical effects under a wider variety of experimental conditions than DFWM permits, we have developed a Fourier transform spectral interferometry (FTSI) setup, which allows us to measure the phase of the light field produced by the sample. In order to get started in using this technique, we have applied it to study linear transmission in bulk GaAs. This material is the most studied III-V semiconductor, and therefore is a good choice to learn how to use a new approach. For the case of this simple experiment, the amplitude of the measured electrical field is related to the absorption and the phase related to the refractive index. Using this procedure, we studied the behavior of the absorption and phase for both Lorentzian exciton lines and Fano resonances, as a function of temperature and magnetic field. The experimental set up is now ready for application to less well-studied magnetic insulators and related materials, in particular the magnetic excitons of Cr_2O_3 .

Publication

M.V. Marquezini, P. Kner, S. Bar-Ad, J. Tignon, and D.S. Chemla, "Density-Dependence of the Spectral Dielectric Function Across a Fano Resonance," accepted for publication in *Brief Reports, Phys. Rev. B.*

Phosphorescent Molecule as a Probe in Near-Field Optical Microscopy and Spectroscopy, and the Electronic Correlation Effects on the Transport Properties of Carbon Nanotubes

Principal Investigator: Dung-Hai Lee

Project No.: 97036

Project Description

This project investigates the effects of local environment on the optical properties of molecules or nanosystems. In particular, we propose to use the fact that spin-flipping excitations of a substrate enhance the phosphorescence of C_{60} as a local probe of the excitations. If successful, this probe will reveal spin excitations of a surface at the molecular scale and will undoubtedly become the most effective probe of local spin dynamics. Also being investigated are the effects of electron-electron correlation on the properties of carbon nanotubes. In particular, renormalization group calculations are being performed to treat the electron-electron correlation and compare the results with the prediction of band theory.

Accomplishments

When a C_{60} molecule is pressed to a substrate, we find that the spin flipping interaction between the electrons in C_{60} and those in the substrate fundamentally alter the optical properties of the fullerene molecule. In particular, an original, dark phosphorescence line is created. This effect can be used to design a local probe of the magnetic properties of the substrate.

We have completed the renormalization group treatment of the correlation effects in carbon nanotubes. The results suggest that electron-electron correlation can qualitatively change the behavior away from the prediction of the band theory. For example, we find that for undoped carbon nanotubes,

the ground state is an antiferromagnetic insulator instead of being a metal, as predicted by the band theory. Moreover, upon doping we find that electron-electron correlation can cause superconductivity.

Publications

D-H Lee, "Neutral Fermions at $\nu = 1/2$," preprint.

Y. Krotov, D.-H. Lee, E. Burstein, and I.A. Yurchenko, "Induced Molecular Phosphorescence as a Local Probe of Spin Spectral Function," preprint.

D.-H. Lee, Y. Krotov, J. Gan, and S.A. Kivelson, "Composite Fermion Hall Conductance at $\nu = 1/2$," *Phys. Rev. B* 55, 15552 (1997).

Y. Krotov, D.-H. Lee, and S.G. Louie, "Low Energy Properties of the (n,n) Carbon Nanotubes," *Phys. Rev. Lett.* 78, 4245 (1997).

Y. Krotov, D.-H. Lee, and A. Balatsky, "Superconductivity in Metallic Stripes," *Phys. Rev. B*, in press.

advanced computational facilities under development at LBNL. The *ab initio* component involves electronic structure calculations similar to those the investigators performed in the past, but rephrased to exploit new computational methods that take advantage of parallel processing. Using only the atomic numbers and masses of constituent atoms, it is now possible to compute electronic, vibrational, structural, and thermodynamic properties of, and dynamic processes in, materials. These fundamental calculations are used to develop scaling formulae to determine the macroscopic properties of complex materials and define in-out parameters for property simulations. Systems under investigation include fullerene base solids, semiconductor clusters, and hard materials.

Accomplishments

In a search for superconductivity in stable fullerenes other than C_{60} , we have investigated the possibility of phonon-induced superconductivity in doped solid C_{36} . Conventional BCS superconductivity relies on a fine interplay between electron-phonon coupling and electron density of states. Thus, one expects a higher transition temperature T_c in solids which contain the smallest possible stable fullerene, because the larger curvature is expected to enhance electron-phonon coupling. C_{36} is an excellent candidate for such a new superconductor. Among the various possible structural candidates, our local density functional (LDA) calculations show that the D_{6h} symmetry C_{36} fullerene has the largest binding energy. We performed LDA calculations of different solid phases and determined their electronic density of states (DOS) and relative stability. We find that the C_{36} electron-phonon coupling is nearly 50% larger than that of C_{60} , and given the favorable density of states (depending on which mode is coupled), we predict significantly larger T_c values than those of the C_{60} solid. In addition, we show that both endohedral and substitutional doping may be used to provide a possible enhancement of both the electron-phonon coupling and the DOS near the Fermi level, which can lead to a further enhancement of T_c .

For semiconductor clusters, we have investigated the electronic and structural properties of Si clusters in the tetrahedral (i.e., bulk) symmetry. Using a recently developed real-space method based on the *ab initio* pseudopotential density functional approach, we were able to evaluate the optical gap of a series of hydrogen-capped Si clusters containing up to 800 atoms. Previously *ab initio* calculations can treat

Determining Macroscopic Materials Properties from Microscopic Calculations

Principal Investigators: Andrew Canning, Daryl Chrzan, Marvin Cohen, Steven Louie, and John Morris, Jr.

Project No.: 96041

Project Description

The goal of this research is to exploit advances in computer hardware and computational techniques, advances in the fundamental theory of bonding in solids, and advances in the theory of plastic deformation to construct new predictive models of the properties of real materials.

The project is a collaborative program to compute the macroscopic properties of materials *ab initio*, by combining modern methods in theoretical solid state physics and materials science, and exploiting the

clusters up to, at most, approximately 100 atoms. In particular, the optical gap of these systems is determined by three size-dependent effects: quantization of the single-particle energy levels due to the nanometer dimension of the cluster, change in the so-called self-energy of the electron due to changes in the many-electron interactions, and change in the electron-hole Coulomb attraction. We include all three effects and find that both the changes in self-energy correction and electron-hole attraction are very large for small clusters, but they are of opposite sign. Our calculated results yield excellent agreement between theory and experiment with no adjustable parameters.

We have also developed and implemented a Wannier function method for calculating nanocrystal electronic structure. This scheme diagonalizes the nanocrystal Hamiltonian in a basis of localized Wannier states, which are particularly suitable given the similarity between the interior of a large nanocrystal and the bulk crystal. We have applied this method to computations of the energy of the lowest excitation and of the electronic density of states of nanocrystals of semiconductors such as InAs.

We have executed a systematic program of *ab initio* LDA, pseudopotential calculations of metals, carbides, and nitrides with the goal of understanding hardness and predicting new hard materials. In particular, we have computed electronic and structural properties of Ti, TiC, TiN, V, VC, VN, Cr, CrC, CrN, Mo, MoC, MoN, W, WC, WN, Re, ReC, ReN, Os, OsC, and OsN. These calculations include full structural relaxation, total energies, equation of states, and angular resolved density of states. We have found patterns relating the bulk modulus of each structure to the properties of the constituent atoms. We have also investigated the effects of adsorbates on the mechanical properties of surfaces, e.g., boron and nitrogen atoms on the diamond surface.

We have continued to examine the theoretical and experimental underpinnings to the relationship between atomistic level material properties and the macroscopic engineering concept of "hardness." We have clearly documented that while indentation hardness does scale closely with bulk or shear moduli for a given class and structure of material, the scaling factor can vary by several orders of magnitude as bonding type shifts from metallic to ionic to covalent. Preliminary use of a simple model of the Peierls stress, the stress required to move a dislocation one atomic Burgers vector, appears to reconcile some of the differences between classes of materials.

Our investigation of the transition metal carbides and nitrides revealed two features of the variation of hardness with composition, which initially were curious. First, although transition metal nitrides uniformly have significantly higher elastic bulk moduli than the corresponding metal carbides, the carbides in all cases have higher indentation hardnesses. In addition, intermediate compositions of ternary carbonitride systems all have higher hardnesses than the corresponding binary compounds. Although the hardness of ternary systems can be partially explained by solid solution hardening, we have shown that changes in bonding character are also important. The difference in hardness between carbides and nitrides can be explained by examining shear modulus instead of bulk modulus. We have also discovered an anomaly in the experimentally reported Poisson's ratio of ZrN. Since it is significantly lower (0.19) than the Poisson's ratios of other measured transition metal nitrides (0.25, 0.26, and 0.28), we suspected experimental error. Recent *ab initio* calculations of the elastic constants of ZrN by Jhi and Ihm predict a much more consistent value of 0.27.

In addition to *ab initio* calculations, we have begun to explore hardness using two approximate techniques. First, we have initiated a massively parallel, $O(N)$ tight-binding-based study of dislocation cores in diamond. The intent is to use this technique to calculate, at the atomic scale, the Peierls stress of a dislocation in diamond. Second, we have completed development of a kinetic Monte Carlo simulation of dislocation dynamics. The kinetic Monte Carlo calculations provide an important link between atomic scale calculations and larger scale, dislocation-based studies. In particular, the simulations provide a means to explore the dynamics of dislocation motion, and the means to develop a suitable continuum description of dislocation motion. The simulations indicate that for the hard materials studied here, the dynamics are best described as diffusive. Work is underway to determine which parameters govern the coefficients entering the diffusive description of flow, and how the equation of motion can be related to the bulk mechanical properties of the materials in question. Once these aspects of the dynamics are understood, we intend to use the atomic scale calculations to determine the relevant parameters, e.g., the Peierls potential, that serve as input for the kinetic Monte Carlo simulations.

As for code performance, we have ported our LDA/ plane-wave/ pseudopotential code to the T3E.

The existing parallel version for the SGI PowerChallenge served as a starting point. At the heart of it is a 3d Fast Fourier Transform (FFT), which we hand-coded using calls to library 1d FFTs, and MPI to communicate between different processors. Some changes to the PowerChallenge version were necessary to hide the higher memory latencies on the T3E. In the end, the achieved performance and scaling was very good. For some large systems, a performance as high as 80 GFLOPs on 512 nodes of the T3E has been achieved.

Publications

S. Ogut, J.R. Chelikowsky, and S.G. Louie, "Ab Initio Self-Energy Corrections and Optical Gaps in Si Quantum Dots," *Phys. Rev. Lett.* **79**, 1770 (1997).

A. Mizel and M.L. Cohen, "Electronic Energy Levels in Semiconductor Nanocrystals: A Wannier Function Approach," *Phys. Rev. B* **56**, 6737 (1997).

A. Mizel and M.L. Cohen, "Electronic Transitions in InAs Nanocrystal using Wannier Function Method," *Solid State Comm.* **104**, 401 (1997).

J.C. Grossman, M. Cote, S.G. Louie, and M.L. Cohen, "Electronic and Structural Properties of Molecular C₃₆," *Chem. Phys. Lett.*, in press.

S. Han, J. Ihm, S.G. Louie, and M.L. Cohen, "Enhancement of Surface Hardness: Boron on Diamond (111)," *Phys. Rev. Lett.*, in press.

C.R. Krenn, J.W. Morris Jr., S.-H. Jhi and J. Ihm, "Relationships between Atomistic Bonding and Intrinsic Macroscopic Hardness," in *Hard Coatings Based on Borides, Carbides & Nitrides: Synthesis, Characterization & Applications*, (Y.-W. Chung, R.W.J. Chia, and A. Kumar, eds.), Warrendale, PA: TMS, 1998.

J.C. Grossman, M. Cote, S.G. Louie and M.L. Cohen, "Electronic and Structural Properties of Molecular C₃₆," *Bull. Am. Phys. Soc.* **42**, 270 (1997).

M. Cote, J.C. Grossman, and M.L. Cohen, "Electronic Structure Calculations of Solid C₃₆," *Bull. Am. Phys. Soc.* **42**, 270 (1997).

S. Ogut, J.R. Chelikowsky, and S.G. Louie, "Quasiparticle Gaps and Self-Energy Corrections in Si Quantum Dots," *Bull. Am. Phys. Soc.* **42**, 573 (1997).

A. Mizel and M.L. Cohen, "Size and Shape of Semiconductor Nanocrystals: A Wannier Function Approach," *Bull. Am. Phys. Soc.* **42**, 182 (1997).

K. Lin and D.C. Chrzan, "Kinetic Monte Carlo Simulation of Dislocation Dynamics," *Bull. Am. Phys. Soc.* **42**, 743 (1997).

Biological X-Ray Microscopy

Principal Investigators: Werner Meyer-Ilse, John Brown, and David Attwood

Project No.: 95023

Project Description

The Center for X-ray Optics built a soft x-ray transmission microscope (XM-1) at the Advanced Light Source. The goal of this LDRD project is to establish x-ray microscopy as a valuable tool in biology by providing the operational support to apply the microscope to biological applications.

Accomplishments

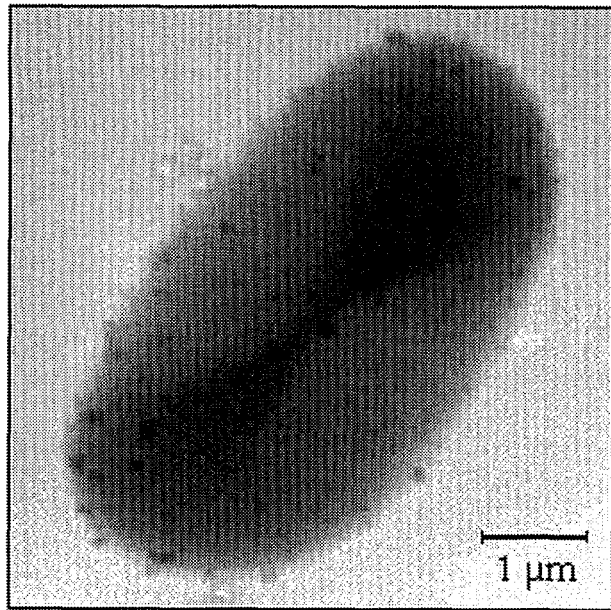
In summary, our x-ray microscopy projects continue to solve biological problems with this technique. Most recently, we developed specific labeling techniques for x-ray microscopy. Using labeling, we've begun to learn more about specific questions related to the functioning of cell nuclei. In addition to these new and exciting results, we gained new insights into malaria, nuclear matrix structure, secretion, alga, and bacterial spores.

Specific labeling uses antibody probes to place markers at specific places within the sample. In visible light microscopy, these markers are fluorescent molecules. For electron microscopy, the probes are decorated with small colloidal gold particles. These gold particles can be enlarged to a specific size by growing silver around them. We used this technique together with C. Magowan, Life Sciences Division, to establish relationships between surface proteins of malaria infected red blood cells and proteins on melanoma cells. Figure 1a shows a red blood cell labeled for the surface protein Glycophorin-C.

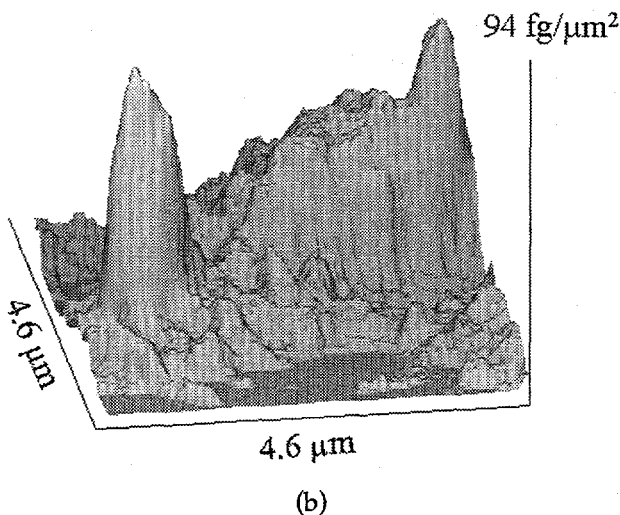
X-ray absorption is very specific and can therefore be used to produce elemental maps. We produced the first maps of iron in malaria-infected red blood cells.

Iron is an element of the hemoglobin molecule, which is used as a food source for the parasite. With images as shown in Figure 1b we've begun using this method to study the digestive process of the parasite, hoping to develop ways to interfere with this process.

Together with C. Larabell and S. LeliÈvre we developed techniques to place labels for x-ray microscopy inside cells. The big advantage of x-ray techniques is high spatial resolution combined with



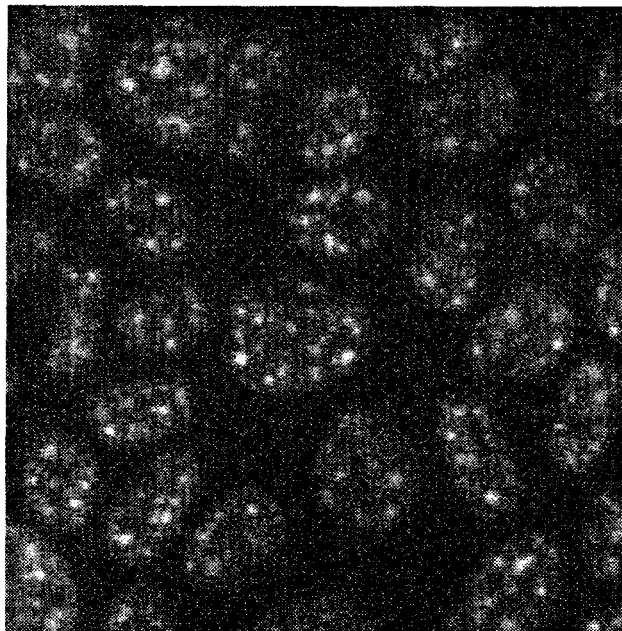
(a)



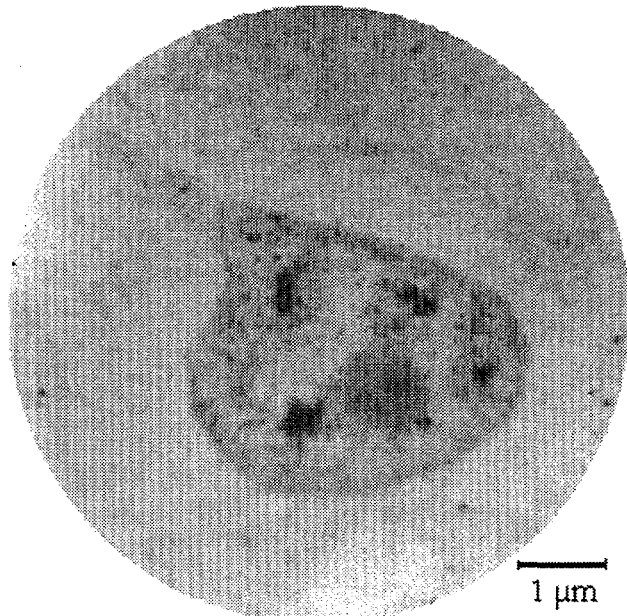
(b)

Figure 1. (a) Human red blood cell with the surface protein Glycophorin C labeled with Au-antibody label, Ag enhanced. (b) Iron concentration in a malaria parasite measured by dichromatic x-ray analysis at high spatial resolution.

the ability to penetrate whole hydrated cell nuclei. We used this technique to locate splicing factor (a protein important for gene expression) inside intact hydrated nuclei (Figure 2). Through the use of x-rays we 1) can



(a)



(b)

Figure 2. Hydrated mammary epithelial cell nuclei, labeled with FluoroNanogoldÆ for splicing factor. (a) Shows the visible light fluorescence (FITC) image, taken with a 60×, 1.4NA objective in a confocal microscope. (b) For the x-ray images, the gold beads at the FluoroNanogoldÆ were enhanced with silver.

see the distribution of the protein in relationship to other nuclear organelles, 2) have an enhanced spatial resolution as compared to visible light microscopy, and 3) retain the sample in a hydrated condition. The thickness of the nuclei prevents electron microscopy.

We established, through the work funded by this LDRD, x-ray microscopy as a unique and valuable tool for biology, and a much wider community than before now realizes this.

Publications

W. Meyer-Ilse, H. Medecki, J.T. Brown, J. Heck, E. Anderson, C. Magowan, A. Stead, T. Ford, R. Balhorn, C. Petersen, and D.T. Attwood, "X-ray Microscopy in Berkeley," in *X-ray Microscopy and Spectromicroscopy* (J. Thieme, G. Schmahl, E. Umbach, D. Rudolph, eds.), Springer Heidelberg, in press (1997).

C. Magowan, J.T. Brown, J. Liang, J. Heck, R.L. Koppel, M. Narla, and W. Meyer-Ilse, "Intracellular Structures of Normal and Aberrant *Plasmodium falciparum* Malaria Parasites Imaged by Soft X-ray Microscopy," *Proc. Natl. Acad. Sci.* **94**, 6222 (1997).

J.T. Brown, C. Magowan, R. Balhorn, J. Heck, T. Ford, A. Stead, and W. Meyer-Ilse, "Biological Applications of XM-1," in *X-ray Microscopy and Spectromicroscopy* (J. Thieme, G. Schmahl, E. Umbach, D. Rudolph, eds.), Springer Heidelberg, in press (1997).

R. Balhorn, et al., "Application of X-ray Microscopy to the Analysis of Sperm Chromatin," in *X-ray Microscopy and Spectromicroscopy* (J. Thieme, G. Schmahl, E. Umbach, D. Rudolph, eds.), Springer Heidelberg, in press (1997).

J. Heck, W. Meyer-Ilse, J. T. Brown, E. Anderson, H. Medecki, and D. Attwood, "Resolution of XM-1," in *X-ray Microscopy and Spectromicroscopy* (J. Thieme, G. Schmahl, E. Umbach, D. Rudolph, eds.), Springer Heidelberg, in press (1997).

A.D. Stead, P.A.F. Anastasi, J.T. Brown, T. Majima, W. Meyer-Ilse, D. Neely, A.M. Page, S. Rondot, H. Shimizu, T. Tomie, E. Wolfrum, and T.W. Ford, "If Carbon Discrimination Is More Important to Biologists than Resolution Will Soft X-Ray Microscopy Become a Useful Biological Technique?" in *X-ray Microscopy and Spectromicroscopy* (J. Thieme, G. Schmahl, E. Umbach, D. Rudolph, eds.), Springer Heidelberg, in press (1997).

A.D. Stead, J.T. Brown, J. Judge, W. Meyer-Ilse, D. Neely, A.M. Page, E. Wolfrum, and T.W. Ford, "Use of Soft X-Rays to Image Hydrated and Dehydrated Bacterial Spores Using Either Contact Microscopy or Direct Imaging," in *X-ray Microscopy and Spectromicroscopy* (J. Thieme, G. Schmahl, E. Umbach, D. Rudolph, eds.), Springer Heidelberg, in press (1997).

T.W. Ford, A.M. Page, W. Meyer-Ilse, and A.D. Stead, "A Comparative Study of the Ultrastructure of Living Cells of the Green Alga *Chlamydomonas* Using Both Soft X-Ray Contact and Direct Imaging Systems and an Evaluation of Possible Radiation Damage," in *X-ray Microscopy and Spectromicroscopy* (J. Thieme, G. Schmahl, E. Umbach, D. Rudolph, eds.), Springer Heidelberg, in press (1997).

SQUID-Based "Magnetic Microscopes" as Sensors for Nondestructive Evaluation

Principal Investigators: John Morris, Jr., John Clarke, and Kannan Krishnan

Project No.: 97023

Project Description

There is a broad and increasingly recognized need for nondestructive evaluation (NDE) techniques capable of determining the remaining useful life of a variety of structural materials, such as turbine blades, airplane wings, nuclear reactors, bridges, and oil rigs. To address this need, this project is aimed at measuring the magnetization of materials subjected to thermal or mechanical stress and at characterizing the same materials by optical and electron microscopy. The magnetic properties of the materials are imaged by means of a high-transition temperature (T_c) Superconducting QUantum Interference Device (SQUID) that is brought to within 0.2 mm of the sample. The magnetic field of the sample is mapped as it is rastered over the SQUID. To characterize the underlying microstructure responsible for the magnetic behavior, a magnetic etching technique is used to image the domain walls at the surface, and Lorentz imaging is used to evaluate the microstructure with high spatial resolution. The Lorentz imaging is

performed in a specially adapted transmission electron microscope (TEM) at the National Center for Electron Microscopy.

Accomplishments

A new scanning SQUID microscope has been designed and constructed. This microscope has a large scanning area, approximately 50×50 mm, and is capable of carrying out *in situ* measurements of the effects of mechanical stress or thermal aging on the remanent magnetization of magnetic steels. A miniature tensile stage applies *in situ* stress by variable strain to the sample while its remanent magnetization is measured by the scanning SQUID. The apparatus is surrounded by a large mu-metal shield to exclude external magnetic field fluctuations. The stepper motors driving the scanning stage are controlled by a personal computer, which also acquires and displays the magnetic field data as a function of the position of the sample. As an example of a preliminary study, a sample of 1040 steel (Fe-0.4wt.%C) was heat treated in a manner that produced a gradient in both the metallurgical phase and the microstructure. The phase ranged from a ferrite-pearlite mixture at one end of the sample to a martensitic phase at the other. Figure 1 shows the magnetization near the surface of the sample. The sample was first magnetized in a magnetic field of 50 mT and the remanent magnetization was measured

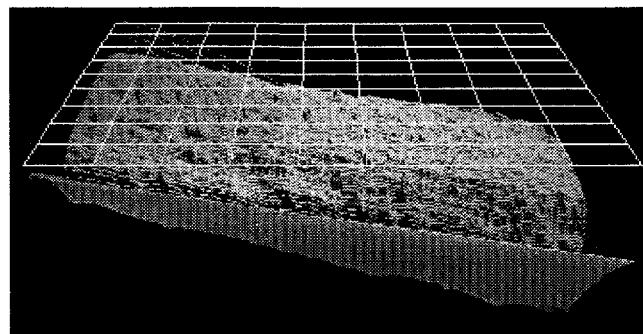


Figure 1. Scanning SQUID image of the remanent magnetization of a heat-treated sample of 1040 steel. The grid defines zero magnetization, and in false color ranges from red (left) at zero magnetization to blue at maximum (right). The large peak at the near edge, and the hidden one at the far edge, are due to geometrical effects. The increase in (negative) magnetization from left to right in the image shows the effects of the different microstructures introduced by the thermal gradient.

by scanning the sample over the SQUID. The grid defines zero magnetization, and the false color scale ranges from red at zero magnetization to blue at maximum. The large peak at the near edge, and the hidden one at the far edge, are due to geometrical effects. The increase in (negative) magnetization from left to right in the image shows the effects of the different microstructures introduced by the thermal gradient. Other studies showing pronounced variations in the magnetization include samples which were deformed by rolling and samples of the same material subjected to a range of uniform temperatures. These results confirm that the scanning SQUID microscope can image variations in magnetization produced by thermal and mechanical stress.

Effective development and use of magnetic characterization of the metallurgical and deformational states of ferromagnetic materials require an examination and understanding of the pertinent structures at the grain-size scale, as well as the more local scale afforded by techniques such as Lorentz microscopy. The externally measured magnetic fields are a function of the magnetic domain structures in the material. The configuration of the magnetic domains and thus the external fields are sensitive to the interaction of the domain walls with microstructural defects such as dislocations and second phases, as well as the local crystallographic orientation and local stresses. A study of these interactions requires techniques that allow imaging of the domains or domain walls. We have developed expertise in the application of a magnetic etching technique to the range of ferromagnetic materials in which we are currently interested. This technique is a variant of the Bitter technique and utilizes a colloidal suspension of magnetic particles to decorate domain walls on a polished specimen. Since the domain walls represent areas with high external magnetic flux, the 50-100 Å-diameter suspended particles are attracted to the domain walls. We have examined various carbon steels as well as a Fe-Al-Si damping steel using this technique. Figure 2(a) is a micrograph of a small region of the 1040 steel sample, whose remanent magnetization is shown in Figure 1, that had been heated into its austenite range and then cooled to form a ferrite + perlite microstructure. It was subsequently polished and magnetically etched. The final lamellae regions at the lower left and the upper right represent the perlite colonies, while the coarser structures are the surface domain structure within the ferrite phase.

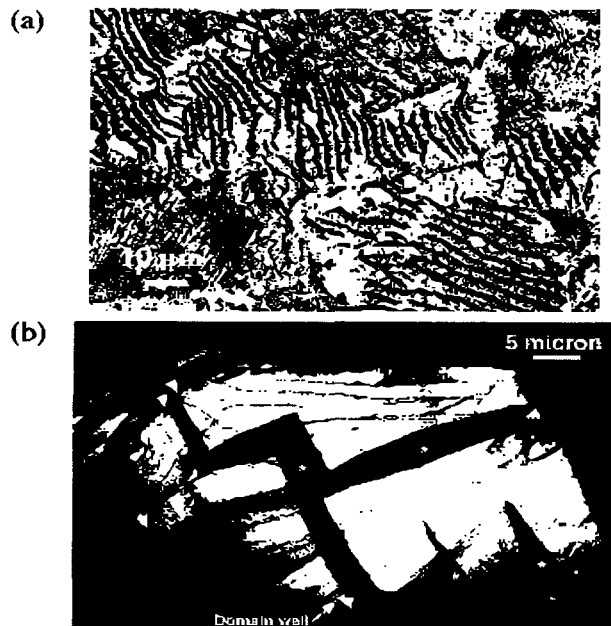


Figure 2. (a) Micrograph of a small region of the 1040 steel sample, whose remanent magnetization is shown in Figure 1, that had been heated into its austenite range and then cooled to form a ferrite + pearlite microstructure. It was subsequently polished and magnetically etched. The fine lamellae regions at the lower left and the upper right represent the pearlite colonies, while the coarser structures are the surface domain structure within the ferrite phase. (b) A Foucault image of a ferrite region in a 1040 sample. The domain walls are indicated by arrows. The domains labeled by an asterisk have no in-plane magnetization component along the direction investigated.

The third characterization technique is Lorentz imaging, a form of transmission electron microscopy which allows one to study the detailed structure of magnetic samples at high spatial resolution. Such information can be combined with microstructural information obtained from conventional TEM. Several new developments, greatly improving the spatial magnetic resolution, have been implemented on a Philips CM200 electron microscope. The use of a highly coherent field emission source enables one to obtain information on the domain wall width. Individual adjustments of the lens currents by means of software allow one to create various kinds of magnetic contrast in the sample under investigation. The relatively low level of magnification is compensated by a post-column image filter which magnifies 20 times. Since the images are captured digitally, they can be further magnified electronically. Furthermore, dynamical *in situ* magnetization studies

are possible. The combination of field emission source, lens editing software, and image filter with digital-image-capturing capabilities create a state-of-the-art instrument for static and dynamical magnetic observations. The 1040 steel samples which have undergone different heat treatments show a magnetic microstructure that is clearly different. As an example, Figure 2(b) shows the domain walls that are evidently along crystallographic directions. Other topics under investigation include domain wall pinning at small inclusions in martensite and the behavior of domain walls at the ferrite/cementite interface.

These preliminary measurements indicate that the remanent magnetization of steels depends strongly on their thermal and mechanical treatment, and that the microstructure responsible for the magnetization can be characterized on the surface by a magnetic etching technique and at high resolution by Lorentz imaging. Ongoing work is aimed at a systematic investigation of a wide range of samples using these three complementary microscope techniques.

Molecular Scale Imaging and Spectroscopy of Liquid Surfaces: Application to Environmental Studies

Principal Investigators: Miquel Salmeron and Yuan-Ron Shen

Project No.: 97024

Project Description

In this project, we performed several sets of experiments to determine the atomic- and molecular-scale structure of thin liquid surfaces and interfaces using the newly developed Scanning Polarization Force Microscopy (SPFM) and Sum Frequency Generation (SFG) techniques. We developed new spectroscopic aspects of the SPFM, in particular the frequency response of the polarization force that allowed us to determine for the first time ionic mobility on wet surfaces.

Accomplishments

The following is a list of highlights and results obtained during this LDRD development period.

Technical Aspects

On the experimental side, the SPFM was extended from its previous use in the static, dc-polarization mode of operation to a high frequency ac-mode. This allows us to determine the dielectric response and to map the liquid films surfaces at various frequencies with simultaneous nanometer spatial resolution. Up to the mechanical resonance of the cantilevers (~20 KHz) the ac-response of the lever motion to the applied ac-voltage was followed by simple use of a lock-in amplifier. We operated also in the time domain by measuring the response of the polarization force to applied square waves of voltage. Results obtained in these low-frequency modes are described below. At frequencies above 20 KHz, we measured the average dc-response of the lever, which is also determined by the dielectric response at the applied frequency. We proved the concept by successfully imaging gold films up to 400 MHz.

A new environmental chamber was built to allow SFG experiments to be carried out in samples exposed to high pressure of various vapors, in order to study the structure of condensed films in equilibrium with the gas phase.

Scientific Results

Using the low-frequency spectroscopic method, SPFM was used to determine the mobility of different ionic species (H, K, Mg, and Ca) on mica surfaces. These ions were introduced by exchange of the native K with the other ions by immersion of the mica in appropriate ionic solutions. The idea is to simulate the ion exchange processes occurring in soil rocks and in airborne particles during contact with waste and toxic solutions. Ionic mobility was determined as a function of degree of hydration, at different humidity levels in the environment. The results proved that indeed SPFM is an excellent and unique method for determination of the transport properties of surface ions and of their nanoscale spatial distribution. These results are either submitted or being prepared for publication.

Using the same concepts, the low-frequency spectroscopic capability of SPFM was applied to the study of the deliquescence (dissolution in the presence of water vapor) of alkali halides, the role of steps, and the cationic and anionic solvation and mobility. These results are important in relation to problems of atmospheric pollution, acid rain, and ozone depletion that are in part due to halide species

liberated from salt aerosols when acids and water condense on their surfaces. Again, papers containing these results are in preparation for publication.

Finally, the first studies of nanoparticles and films of ice growing on mica have been initiated. The first results show in a rather spectacular way that liquid water droplets and ice coexist at temperatures down to -30°C. These results were presented for the first time at the American Vacuum Society Meeting in San Jose, CA, October 20-24, 1997.

SFG experiments on the condensation (monolayer thickness) of water on mica have been performed and are still in progress. The first results appear to confirm a previous proposal by the authors, that the first layers of water are ordered in an ice-like structure. When completed these results will also be published.

Overall, the SPFM/SFG project can be considered to be very successful. On the spectroscopic side, we plan to move into the rf (both MHz and GHz) regime by using amplitude modulation of the bias voltage, so that the lever can oscillate at the lower frequency (down conversion). We will explore the use of a microwave cavity with the AFM tip acting as an antenna, following the method of Xiao-Dong Xiang at LBNL. We will also continue to apply SFG in the environmental chamber built for studies of liquid films on surfaces, particularly in connection with environmental sciences.

Publications

Lei Xu and M. Salmeron, "The Mobility of Different Surface Ions on Mica as a Function of Relative Humidity," submitted to *J. Chem. Phys.*

Lei Xu, H. Bluhm, and M. Salmeron, "The Effects of Surface Ions on the Friction and Adhesion Properties of Mica," submitted to *Langmuir*.

M. Luna, F. Rieutord, N.A. Melman, Q. Dai, and M. Salmeron, "Mobility of Surface Ions and Deliquescence of Alkali Halides in Humid Environments in the Nanoscale Level," submitted to *J. Phys. Chem.*

Lei Xu, H. Bluhm, and M. Salmeron, "An AFM Study of the Tribological Properties of NaCl(100) Surfaces Under Moist Air," submitted to *Surf. Sci.*

P. Miranda, Lei Xu, M. Salmeron, and Y.R. Shen, in preparation.

MSD Theory and NERSC Computation for ALS Experiments

Principal Investigator: Michel Van Hove

Project No.: 96042

Project Description

This project supports theoretical and computational efforts by experimental users of LBNL's Advanced Light Source (ALS). The ALS exploits sophisticated state-of-the-art facilities to produce a rapidly increasing amount of experimental data that require advanced numerical treatment and simulation to yield scientifically useful results. Thereby, important information can be obtained about the atomic-scale structural, electronic, magnetic, chemical, corrosive, tribological and biological properties of surfaces and interfaces of materials with technological relevance. Examples include electronic nanostructures, magnetic storage materials, chemical catalysts and sensors, corrosion protection, hard coatings, and biological membranes. To enable the timely interpretation of these data, NERSC brings massively-parallel computing methods and capabilities to bear on the theory being developed for this purpose in LBNL's Materials Sciences Division (MSD). This enables experimentalists to plan and simulate future experiments, to rapidly evaluate and fine-tune ongoing experiments, and to fully analyze and refine finished experiments.

This project develops and applies powerful theoretical and computational methods to deal with the complex electron multiple-scattering processes that underlie experimental techniques like photoelectron diffraction and holography, x-ray absorption spectroscopies, and spectromicroscopies, which are used by many research groups at the ALS. Collaboration between NERSC and MSD staff leads to new approaches to maximize computational efficiency. Close interaction with ALS users enables the most effective application of these methods to extract technologically relevant information about a wide variety of materials. As a result, computational methods are implemented that utilize NERSC capabilities to tackle problems of unprecedented scale and to open up the field to research on new classes of materials. Further

extensions of the existing methods and new techniques are introduced in response to the needs and requests of ALS users.

Accomplishments

New Photoelectron Diffraction Code Implemented

A new code, the Multiple Scattering in Cluster Diffraction (MSCD) package, has been developed using the novel Backward Summing Method within the Rehr-Albers approximation, which reduces the computation time an order of magnitude in real simulations compared to prior codes. By applying object-oriented programming, the new code provides a much better user interface (particularly important for convenient use by experimentalists), general data formats, and fully functional subsidiary utilities. These unique features save the user a great deal of time in data preparation and management.

The sequential version of the code has been implemented on supercomputers (under UNIX) and Sun workstations (UNIX), as well as on PC and Macintosh desktop computers. Comprehensive test calculations agree well with more exact (but much slower) calculations. Extensive comparisons of code performance on the Cray T3E and on COMPS parallel architectures have been conducted under MPI.

Our new code is currently being generalized to take into account circular dichroism (effects obtained by contrasting measurements performed with right- vs left-circular polarized light from the ALS), and spin effects such as magnetism (including magnetic circular dichroism), and relativistic spin flip. These are capabilities that are in growing demand with ALS users.

Code Ported to Cray T3E

With the opening up of NERSC's Cray T3E to scientific use, our MSCD photoelectron diffraction code has been parallelized under MPI (facilitated by its object oriented C++ programming) and ported to the T3E. See URL <http://electron.lbl.gov/mscdpack/index.html> for graphical representations of the results.

Other Activities

This project allowed the acquisition of two powerful Sun Ultra 2 workstations for code development. Also, Dr. Yufeng Chen, co-author of an earlier version of the photoelectron diffraction code, joined the project

in December 1996. He thereby provided a running start for the project, and brought close familiarity with the physical and computational requirements of the project, with actual experiments and with experimental needs at the ALS, as well as with parallel computing methods.

These NERSC-run work groups, novel for us, have already defined clear avenues of progress on computational methodologies for the project. In particular, the Fast Fourier Transform approach will be enhanced by P. Tang to permit new and efficient methods for holographic reconstruction of 3D atomic maps of surfaces and interfaces, a most valuable method to obtain structural and magnetic detail about materials. Work with J. Carter continues to explore issues of parallelism. In a related project, our codes are being ported by S. Sachs and G. Stone to a Cluster of Multi-Processor Systems (COMPS) to test the optimum utilization of the advanced architecture of a Network of Workstations (NOW), starting with the application of genetic algorithms. Several active collaborations are extending the capabilities of the underlying theoretical methods: Prof. C.S. Fadley (LBNL and UC-Davis), Mr. J. Menchero (LBNL and UC-Berkeley), Prof. J.J. Rehr (Univ. of Washington-Seattle), Prof. W. Schattke (Univ. of Kiel), Dr. A. Chassé (LBNL and Univ. of Halle), Drs. F.J. Garcia de Abajo and J. Osma (LBNL and Univ. of San Sebastian).

A number of interactions with experimental users of the ALS have also started. Thus, pre-experiment feasibility studies have been performed for the Ross group to explore the optimum conditions for studying substitutional adsorption systems with photoelectron diffraction at the ALS. Related quantum chemical calculations to obtain molecular orbital information and core-level shifts for molecules adsorbed on metal surfaces have also been undertaken, in consultation with the group of C.W. McCurdy. The MSCD code development benefited from extensive prior collaborations with the Fadley group and application to various photoemission data measured at the ALS in his group. Collaborations with the Shirley group (in which the Backward Summing Method was initiated) also benefited from the application of our newer codes to the interpretation of other ALS photoemission data. Similar interactions have begun with the ALS group of Tonner, Kevan, Rotenberg and Denlinger, who have produced a considerable amount of experimental data that await interpretation.

Publications

F.J. García de Abajo, Y. Chen, M.A. Van Hove, and C.S. Fadley, "New Accurate Convergent Representation of Multiple Scattering in Photoelectron Diffraction, Including Magnetic and Relativistic Effects," in preparation.

Y. Chen and M.A. Van Hove, "MSCD Package User Guide: Simulation of Photoelectron Diffraction Using Rehr-Albers Separable Representation," in preparation.

Y. Chen, H.S. Wu, D.A. Shirley, C.S. Fadley, and M.A. Van Hove, "Fast Calculation of Photoelectron Diffraction Using Curved-Wave Multiple Scattering Theory," in preparation.

Y. Chen, F.J. Garcia de Abajo, A. Chassé, R.X. Ynzunza, A.P. Kaduwela, M.A. Van Hove, and C.S. Fadley, "Convergence and Reliability of the Rehr-Albers Formalism in Multiple Scattering Calculations of Photoelectron Diffraction," in preparation.

Y. Chen, J. Carter, S. Sachs, G. Stone, and M.A. Van Hove, "Parallelization of Multiple Scattering Calculations of Photoelectron Diffraction," in preparation.

P. Tang, M.A. Van Hove, and Y. Chen, "Fast Fourier Transform and Parallelization of the Reconstruction of 3-Dimensional Atomic Images from Photoelectron Diffraction Holograms," in preparation.

Y. Chen, G. Zhuang, P.N. Ross, M.A. Van Hove, and C.S. Fadley, "Equivalent-Core Approximation of Core-Level Relaxation Energy in Photoelectron Spectroscopy," in preparation.

R.X. Ynzunza, E.D. Tober, F.J. Palomares, Z. Wang, H. Daimon, Z. Hussain, Y. Chen, C.S. Fadley, and M.A. Van Hove, "Full-Solid-Angle Photoelectron Diffraction from Bulk and Surface Atoms of Clean W(110): A Test of Theoretical Methodologies," in preparation.

R.X. Ynzunza, H. Daimon, F.J. Palomares, E.D. Tober, Z. Wang, Y. Chen, C.S. Fadley, and M.A. Van Hove, "Structural Analysis of O-Covered W(110) Surfaces by Low-Energy Photoelectron Diffraction," in preparation.

V. Zhuang, Y. Chen, P.N. Ross, and M.A. Van Hove, "Structural Determination of the Substitutional Alloy Li/Al Surface Using Angle Resolved Photoelectron Diffraction," in preparation.

P.M. Len, J.D. Denlinger, E. Rotenberg, B.P. Tonner, S.D. Kevan, M.A. Van Hove, and C.S. Fadley, "Holographic Atomic Images from Surface and Bulk W(110) Photoelectron Diffraction Data," in preparation.

J. Morais, R. Deneke, R.X. Ynzunza, J. Liesegang, C.S. Fadley, J. Menchero, Y. Chen, and M.A. Van Hove, "Interpretation of Angle- and Temperature-Dependent Magnetic Circular Dichroism in Photoelectron Diffraction from Gd(0001)," in preparation.

R. Deneke, J. Morais, C. Wetzel, J. Liesegang, E.E. Haller, C.S. Fadley, Y. Chen, and M.A. Van Hove, "Modeling of Photoelectron Diffraction from Hexagonal GaN(0001) Thin Films," in preparation.

(conformations) of macromolecules. We also demonstrated the ability to measure orientations and orientation changes of macromolecules with very high accuracy. The spectroscopic signature of the fluorescent light coming from two different color labels, which are attached to two sites on the macromolecule, is a sensitive measure for dynamic conformations. Distance changes between two sites on the macromolecule are measured via single-pair fluorescence resonance energy transfer (spFRET), and orientation changes are measured by detecting changes in the dipole orientation of a rigidly attached probe or changes in the degree of rotational diffusion of a tethered probe via single molecule fluorescence polarization anisotropy (smFPA). These techniques may prove to be important for measuring the dynamics of chemical and biochemical reactions on a single-molecule level. They also provide tools for testing semiclassical and quantum mechanical theories of light-matter interaction.

Molecular Rulers for the Study of Synthetic and Biological Macromolecules in Aqueous Conditions

Principal Investigators: Shimon Weiss, Paul Selvin, and Deborah Charych

Project No.: 97025

Project Description

The advances in room temperature single molecule detection (SMD) and single molecule spectroscopy (SMS) by laser-induced fluorescence provide new tools for the study of individual synthetic and biological macromolecules under physiological conditions. Two properties of a single fluorescent probe attached to a macromolecule can be exploited to provide local structural information. The first is the very high sensitivity of the fluorophore to its immediate local environment, including the sensitivity to the presence of other nearby fluorophores and quenchers. The second is its unique absorption and emission transition dipoles, which can be interrogated by polarized excitation light and/or by analyzing the emission polarization. Recently, we have developed "molecular rulers" which use SMD/SMS to measure nanometer distances and distance changes

Accomplishments

The photostability of fluorescent dyes in physiological conditions is a crucial element for successful SMD/SMS measurements. We studied photobleaching lifetimes for a large number of individual molecules in oxygenated/deoxygenated deionized water, in various buffered solutions, and in solutions containing radicals scavengers. These studies helped us find optimal fluorophores and solution conditions for protein dynamics studies.

After establishing fluorophore immobilization on glass-water interface, it was possible to study the polarization response of single fluorophores rapidly rotating in liquid. Comparison with a simple model calculation allowed us to obtain information on the hindered motion as well as on the rotational diffusion in the presence of specific molecular interactions. We also observed rotational jumps between surface-bound and unbound states and showed that they are photoactivated.

These initial studies provided us with tools that are currently being used for various protein dynamics experiments. As an example, Figure 1a shows millisecond resolution fluorescence spFRET time-traces of the donor (tetramethylrhodamine, TMR, in black) and acceptor (CY5, in gray) emissions of a dually-labeled single endonuclease S⁺Nase enzyme. The protein is immobilized on a glass surface in a physiological environment. The anti-correlation

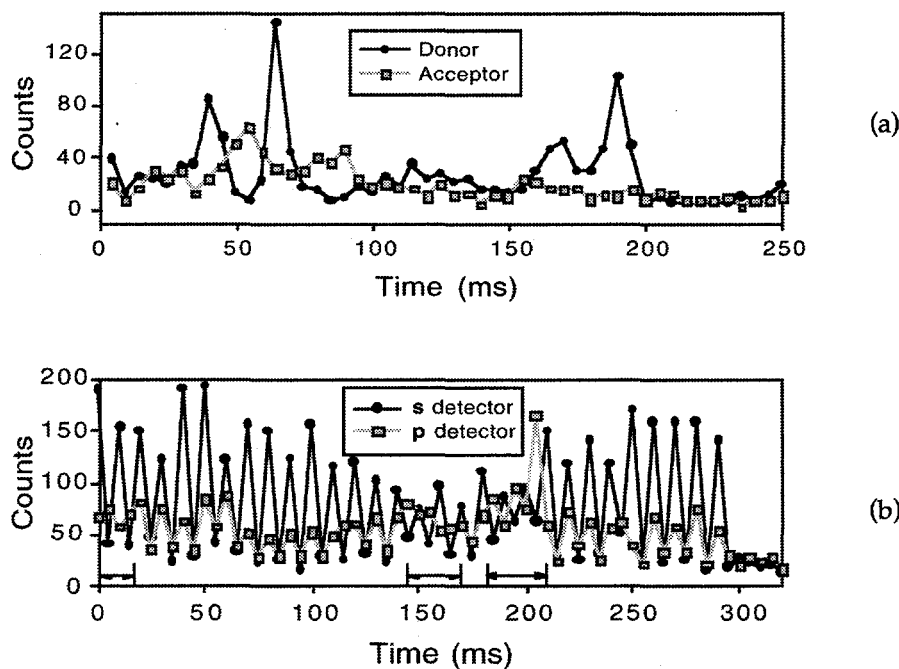


Figure 1. (a) spFRET on SNase. (b) smFPA on ras.

behavior of the two time traces (from 35 ms to 100 ms) is evidence for fluorescence resonance energy transfer. The changes in energy transfer efficiency are the result of either changes in the dipole orientation of the fluorophores or changes in distance.

Figure 1b shows a single-molecule fluorescence polarization anisotropy measurement done on a singly-labeled ras, a G-protein. The two time traces represent the s (in black) and p (in gray) components of the polarized emission as a function of time. The molecule is excited with a linear polarized light with successively alternated orthogonal polarizations. In this scheme the two time traces are correlated for a fixed fluorophore and anti-correlated for a rapidly rotating fluorophore (marked by arrows at the bottom of the graph). The data indicate switching behavior between fixed and rotating fluorophore, most probably due to changes in steric interactions, and demonstrate the ability of a single molecule to characterize the fluorophore's degree of freedom of motion.

We also studied synthetic macromolecules in solutions. The polarization response and rotational dynamics of individual, polymerized PDA liposomes were studied using a confocal optical microscope. Because of the intrinsic ordering of PDA, light absorption and emission are highly polarized. We measured the degree of polarized response and utilized it to directly map the time trajectory of 3D rotational diffusion of individual liposomes. Fluorescence polarization anisotropy measurements of freely diffusing liposomes are shown in Figure 2. Each time a liposome enters the laser excitation volume, the emitted photons are analyzed along the orthogonal s (in black) and p (in gray) emission polarizations. The intensity fluctuations and the anti-correlation behavior between the two time traces are evidence for rotational diffusion. The rotational diffusion time scale, as evident from the intensity fluctuations, is faster in pure water (Figure 2a) and dramatically slowed down when the liposomes are placed in a viscous (60% sucrose) solution (Figure 2b).

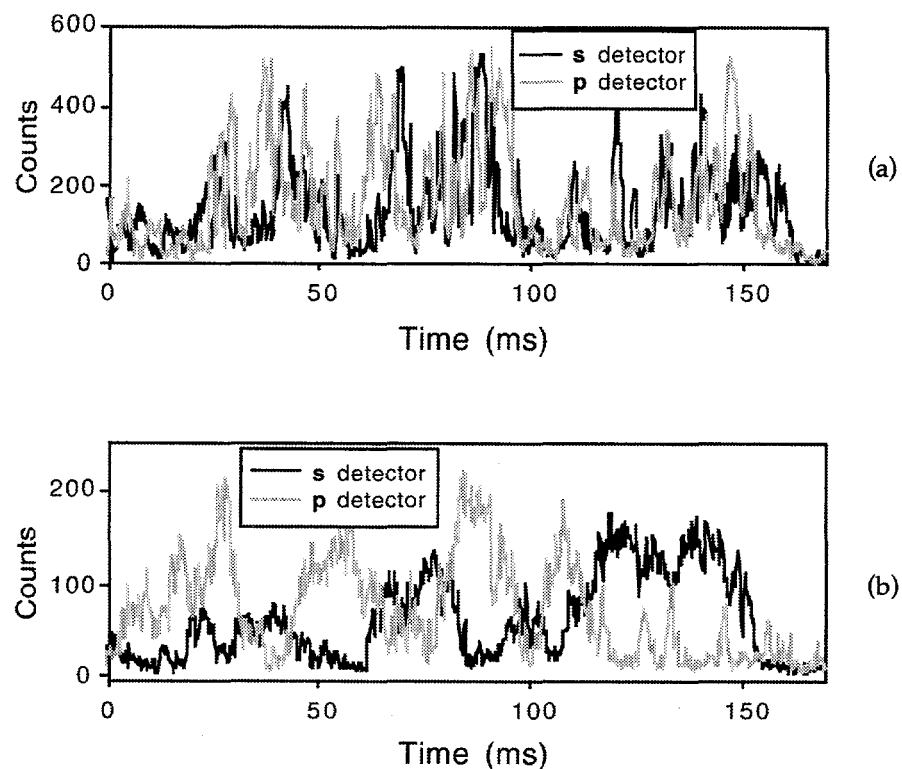


Figure 2. (a) Liposome in water. (b) Liposome in 60% sucrose.

Publications

T. Ha, J. Glass, T.H. Enderle, D.S. Chemla, and S. Weiss, "Hindered Rotational Diffusion and Rotational Jumps of Single Molecules," *Phys. Rev. Lett.*, in press.

T. Ha, D. Charych, Y. Liang, J. Glass, D.S. Chemla, and S. Weiss, "Rotational Dynamics of Single Anisotropic Liposomes," in preparation.

T. Ha, Y. Liang, J. Glass, D.S. Chemla, and S. Weiss, "Fluorescence Polarization Anisotropy of Single Molecules," in preparation.

Nuclear Science Division

A Third-Generation ECR Ion Source

Principle Investigators: Claude Lyneis, Zu Qi Xie, and Clyde Taylor

Project No.: 96022

Project Description

The purpose of this project was to demonstrate the technical feasibility of building a superconducting magnet structure capable of producing sufficiently strong magnetic fields to provide a basis for the construction of a new third-generation electron cyclotron resonance (ECR) ion source. The development of a third-generation ECR source at Berkeley Lab would provide both new scientific opportunities in nuclear science research at the 88-inch cyclotron and would advance ECR source technology. Application of ECR source technology to

heavy-ion accelerators has already provided significant performance gains. This approach continues to be a highly effective way to improve heavy-ion accelerators such as those funded by DOE for the study of nuclear science.

In FY96, a prototype superconducting coil system consisting of a sextupole coil and three solenoid coils was constructed. In FY97 this project focused on installing the prototype magnet in an existing test dewar, cooling the structure to liquid-helium temperature, and determining the magnet structure's performance. Performance was assessed by its maximum magnetic field characteristics, the interaction between the solenoid and sextupole coils, quench behavior of the superconducting magnets, and the adequacy of the mechanical clamping of the coils.

Accomplishments

The tests on the prototype superconducting magnet structure showed that the high magnetic fields required for the third-generation ECR ion source can be achieved. The prototype coil assembly, consisting of the sextupole and three solenoid coils, along with the quench protection circuitry was mounted on a vertical fixture so that it could be tested in a 20-inch i.d. helium dewar. The coils were powered by four 250-amp 1-volt power supplies which were manually controlled. After training, the sextupole magnet reached 105% of its design current with the solenoids off. With the solenoids operating at approximately 70% of their full design field, the sextupole coils operated at 95% of the design value, which corresponds to a sextupole field strength at the plasma wall of more than 2.1 T.

Two sets of tests were made with the prototype superconducting magnet structure. Initially, each solenoid coil and the sextupole was individually trained to determine its inherent performance, and then the magnets were tested in a combined mode. The training results are summarized in Table 1. After more than 40 quenches, the sextupole trained up to 152 amps, which is 104% of its design current. This corresponds to a maximum radial field at $r=80$ mm (approximate inner radius of the magnet warm bore) of 2.7 T and at $r = 75$ mm (design radius for the plasma wall) of 2.38 T. Solenoid 1 (at the injection end) went to 64 amps, or 71% of its design field, in a relatively small number of quenches but did not train

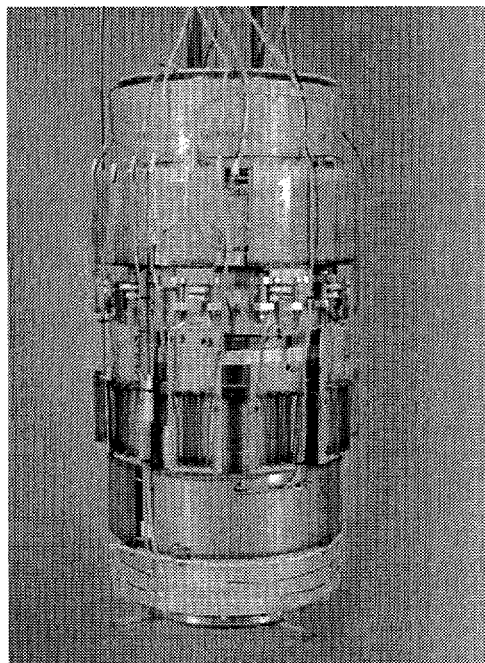


Figure 1. Prototype superconducting magnet structure with quench protection circuits on a vertical test stand prior to testing at liquid helium temperatures.

Table 1. Summary of tests done on the superconducting prototype coil system.

| | Sextupole | Solenoid 1 | Solenoid 2 | Solenoid 3 |
|--------------------|-----------|------------|------------|------------|
| Design current (A) | 146 | 89.6 | 82.5 | 59.8 |
| Individual tests | | | | |
| Max. current (A) | 152 | 64 | 85 | 87 |
| Percent of design | 104% | 71% | 103% | 145% |
| Combined tests | | | | |
| Current (A) | 139 | 50 | 66 | 42 |
| Percent of design | 95% | 56% | 80% | 70% |

to higher fields. Solenoid 2 (at the extraction end) trained to 85 amps, which was 103% of design current, and solenoid 3 (at the mid plane) trained to 87 amps, 145% of its design value. Following the individual tests, the combined tests with all coils powered provided data on the interaction of the solenoid field on the sextupole, which was a major technical issue. In these tests, solenoids 1 and 2 were set to 50 and 66 amps, respectively, which produces peak mirror fields at injection and extraction of about 2.3 T. Solenoid 3 was set to 42 amps, which is roughly 70% of the design value and corresponds to the average percentage of the design values used for solenoids 1 and 2. With the solenoids in operation, the sextupole initially quenched at 60 amps, but then trained up to 139 amps, which is 95% of its design value. This corresponds to a sextupole field strength at the radius of the plasma wall of 2.16 T.

Analysis of the tests and measurements made of the thermal contraction of a sample of the sextupole coil indicates that increased clamping force on the race track sextupole coils is needed to better constrain the coil and reduce the quenching at high field. Some redesign of the solenoid coil will also be done to reduce the stress carried by the epoxy-superconducting wire composite. The knowledge gained in these tests provided an excellent basis for design and fabrication of the third-generation magnet, as an Accelerator Improvement Project is now underway.

Publications

C.M. Lyneis, Z.Q. Xie, and C.E. Taylor, "Design of the 3rd Generation ECR Ion Source," Proceedings of the 13th International Workshop on ECR Ion Sources, Texas A&M University, College Station, Feb. 26-26, p. 115, and LBNL-40154.

C.M. Lyneis, Z.Q. Xie, and C.E. Taylor, "Development of the Third-Generation ECR Ion Source," to be published in *Rev. Sci. Instrum.* 69(2) 1998, and LBNL-40864.

Distributed Construction and Analysis of Multidimensional Gamma-Ray Coincidence Databases

Principal Investigators: Mario Cromaz, James Symons, Randy MacLeod, and I-Yang Lee

Project No.: 97027

Project Description

The aim of this project is to develop software that allows analysis of high-fold gamma-ray coincidence data acquired using new detector arrays such as Gammasphere. This new generation of gamma-ray spectrometers is able to record large samples of four- and higher-dimensional coincidences for which signal-to-noise ratios are greatly enhanced. Unfortunately, analysis programs available to physicists working in this field are restricted to two- or threefold coincidences. These cannot be extended to higher dimensions in a straightforward manner because of fundamental limitations in the algorithms and storage techniques used.

Our approach to this problem can be divided into two parts. Our first goal is to develop techniques that allow storage and retrieval of very large numbers of events. Our second goal is to develop analysis

techniques that can locate correlations in these data. These correlations can then be used to investigate novel aspects of nuclear structure.

Accomplishments

One aspect of the project is to develop an efficient database for the storage and retrieval of the large multidimensional datasets required for the analysis of experiments using modern gamma-ray spectrometers such as Gammasphere. The code DSPEC (distributed spectrum), written at the University of Pennsylvania, was evaluated as a basis for this database. Due to problems with the stability of this program and difficulty in extending this code to meet our requirements, we decided to implement our own database which has now been prototyped. This latter database employs an adaptive, hierarchical, indexing scheme, which allows queries of the type required in traditional spectroscopic analysis and cluster-finding programs to be executed very quickly. Tests on the prototype were very promising and a production version of this code is being implemented.

We have also begun to develop software to analyze the high-fold events. A program to search for clusters in five- and higher-dimension data has been written and tested. This has proven to be a challenge, due to the size of the data samples and because the clusters are immersed in a background that can vary in density by orders of magnitude within a single data set. In our algorithm, cluster candidates are identified using a minimum spanning tree method in which the scale factor is adjusted dynamically to match the local background density. These candidates are then examined to ensure that they represent statistically significant deviations from the background. We have also written programs to make one-dimensional projections from data of arbitrary fold and to search for superdeformed bands using grid search techniques.

This approach to data analysis will require considerable computing resources. We have begun to work with the NERSC staff to move these codes to the NERSC facility.

Directed Studies in Nuclear Theory

Principal Investigator: Jorgen Randrup

Project No.: 97028

Project Description

Berkeley Lab has played a significant design and construction role in three major new nuclear science projects: Gammasphere, Sudbury Neutrino Observatory (SNO), and the Solenoidal Tracker at the Relativistic Heavy-Ion Collider (STAR, RHIC). Gammasphere, which started scientific operation in 1995, studies the detailed structure of nuclei, particularly under very high angular momentum states. SNO is to begin operation in early 1998 to study the three flavors of neutrinos from extra-terrestrial sources such as the sun. RHIC, to be operational in 1999, will study very high-energy plasma states, e.g., a quark-gluon plasma, similar to the conditions of the early universe. All three of these experiments have, or will generate, significantly greater volume of experimental results than prior detectors in their respective scientific fields.

The purpose for this LDRD project was to examine some of the numerous theoretical questions and issues that have been or might be raised in these experiments. Such theoretical studies would be of great value in the analysis and / or predictions on the new or soon-to-be available experimental results, as well as anticipate additional studies that could be usefully conducted with these experiments and their new capabilities.

Accomplishments

The LDRD project supported studies associated with all three projects by visitors, members of the appropriate experimental groups, and members of the Nuclear Theory Group in the Nuclear Science Division at Berkeley Lab.

Five studies were conducted examining the physics now accessible by Gammasphere.

- Comparison between theoretical moments of inertia and experimental data showed substantial deviations from rigid body moments of inertia for some nuclei. This variation of the moments of inertia is remarkably similar to the variation of shell energy through shell, a manifestation of the shell structure of quantum levels.
- Extending the previous study, the dependence of moments of inertia on spin interval and with odd mass nuclei was added to the calculations, showing a new correlation between the binding energies and the deviations of the moments of inertia. The existence of induced currents at high angular momentum and the onset of the Jacobi instability in rapidly rotating nuclei were also considered.
- A detailed comparison was made of theoretical calculations to the surprising discovery of "identical" rotational bands in different nuclei with the same transition energies. The calculations were able to reproduce the overall variation and the overall spread in the moments of inertia $J^{(2)}$, but were not (yet) able to predict which bands were likely to be most similar or reproduce the near perfect 1 unit "alignment" seen in a few examples.
- A small number of observations have suggested that superdeformed states decay to normally deformed states at 5 MeV, which have chaotic properties. A model for "chaos assisted tunneling and ionization" was examined, which demonstrated that decays can be enhanced through such a mechanism and that preliminary calculations show the excitation energy is quite close to the measured excitation energy.
- For superdeformed nuclei, the case of decay-out transitions from superdeformed bands was studied to gain insight into the mechanism for barrier penetration from superdeformed bands to normally deformed states, establishing that data for different lower noise-level cut-off in different energy regions should be combined, and the statistical consistency between regions be checked. For understanding fluctuations of rotational spectra, the mathematics of three-versus-two dimensional fluctuations was worked out and Compton subtractions estimated in order to be able to subtract the effects of unwanted impurities in the spectrum. The effect of a spurious vibration, the Goldstone mode, was also addressed for

calculations on the self energy of single-particle states.

Five studies were conducted in anticipation of the experimental data from SNO and the questions these data might address.

- Techniques were studied to analyze SNO data in a model-independent way, i.e., without necessarily assuming the MSW effect or the standard solar model.
- A detailed estimate was made of the expected number of photons to be observed due to neutral currents oxygen excitation for a supernova event in the center of our galaxy, in particular due to potential muon and tau neutrinos. The signals should also enable an upper limit for the mass of these two heavy flavor neutrinos.
- Studies in applicable fundamental symmetries, particularly in weak interactions, examined a strangeness transition form factor in the chiral quark model, calculations of the meson exchange current contributions to the nuclear anapole moment, and two-photon exchange dispersion correction in electron scattering.
- Remaining cross-section uncertainties of SNO were examined, including those relevant for neutrinos of higher energies, nuclear structure uncertainties effecting calibrations, and potential understanding of details in supernova explosion mechanism.
- Studies were conducted relating experiments on solar neutrinos, atmospheric neutrinos, and accelerator- and reactor-based oscillation experiments.

An additional six studies anticipate that the physics realm will be made accessible by the STAR detector at RHIC.

- Issues in the thermo- and fluid dynamics of relativistic heavy ion reactions were examined. For example, at higher energies the flow measurement will not be trivial, and a change of the flow structure will appear as a new flow component above the side splash and squeeze out. Chiral fluctuations and "over-simplification" in freeze-out descriptions also need further understanding.
- Space-time asymmetry in ultrarelativistic heavy-ion collisions was studied for determining the relative shift in emission time of unlike particles, e.g., pions and kaons. Long-time delays are possible in the formation of a quark-gluon plasma.

- Anisotropic flows are possible at STAR, and specific problems studied include reaction plane resolution, nonidentical two-particle correlations method, and multidimensional analysis of proton-proton correlations.
- In the area of semiclassical transport theory, effective Lagrangians are presently the only possibilities for studying the expansion of a quark-gluon plasma. Specifically, the expansion using the Nambu-Jona-Lasinio model is the most promising in the data analysis and data interpretations, while questions remain whether hydrodynamical calculations are sufficiently realistic or more microscopic, and therefore more approximative approaches are necessary.
- Efforts were made toward developing a model of treating soft and hard processes in nuclear collisions in a coherent fashion. These included testing the final state parton cascade compared to electron-positron annihilation through solving an Altarelli-Parisi equation with a final step of

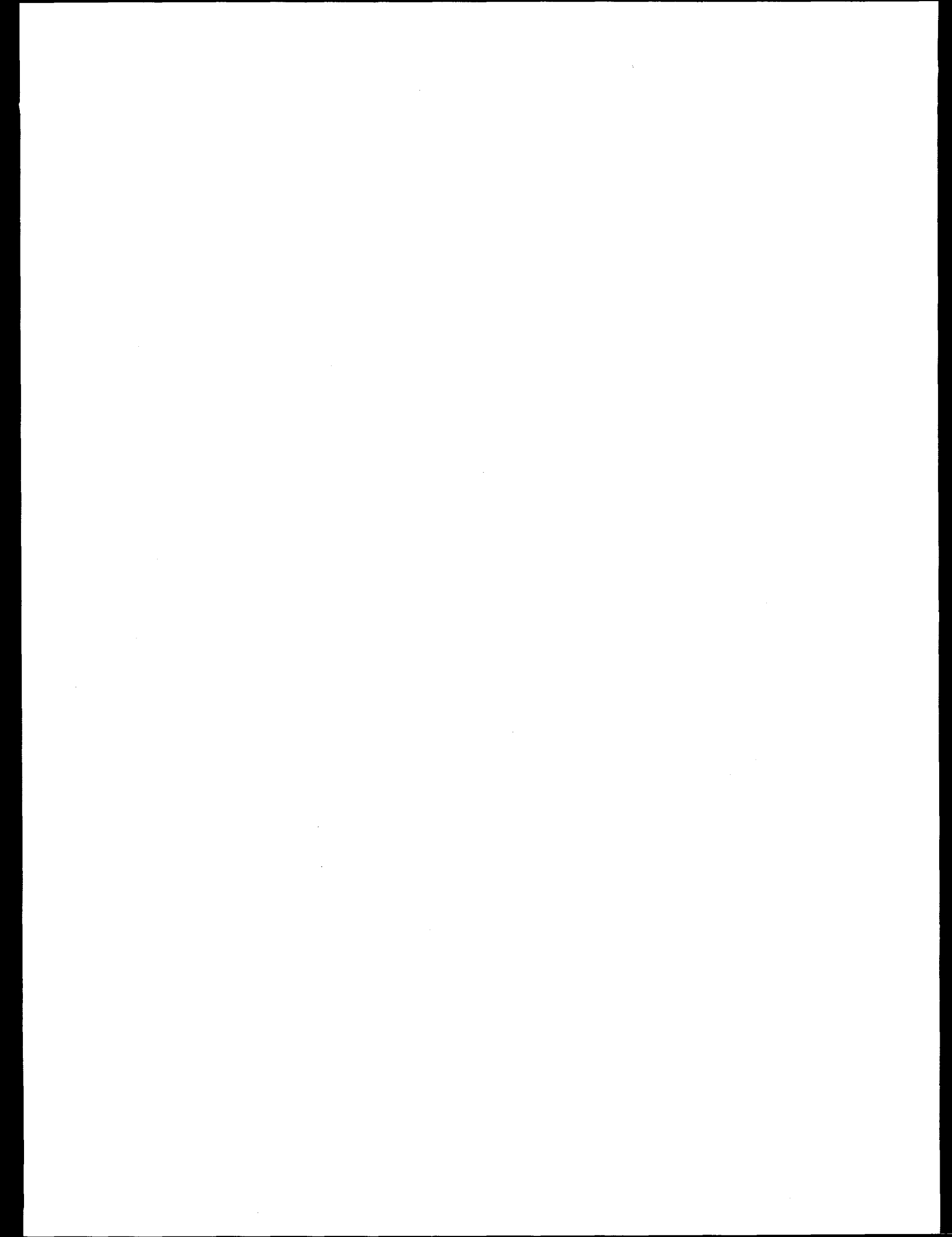
hadronization, and studying electron-proton scattering also solving an Altarelli-Parisi equation, but with a space-like cascade.

- Improvements of applicable computer codes were accomplished by improving the baryon stopping physics in the HIJING Monte Carlo generator used for simulation studies with the STAR detector, and adding a parton cascade after-burner to the HIJING code to study signatures of collective dynamics to measured by STAR.

Publications

R. Lednický, S. Panitkin, and N. Xu, "Search for Delays Between Unlike Particle Emissions in Relativistic Heavy-ion Collisions," to be submitted to PRL.

S. Voloshin, S. Panitkin, and N. Xu, "Relative Space-Time Asymmetries in Pion and Proton Production in Noncentral Nucleus-Nucleus Collisions at High Energies," submitted to PRL, September, 1997.



Physics Division

A Rapid-Response Search for Gamma-Ray Burst Optical Emission

Principal Investigators: Saul Perlmutter and Bruce Grossan

Project No.: 97037

Project Description:

For more than 25 years, both the type of object that produces gamma-ray bursts (GRBs), and the physics of producing these bursts have remained a mystery. Recently GRB optical emission was measured for the first time, occurring from ~10 h to ~days after gamma-ray emission, but the bursting object remains unidentified. This project will measure GRB optical emission sooner after GRBs than previous projects, and with a much higher event rate, yielding more lead time and more opportunities for follow-up spectroscopic studies. Such a program would be likely to lead to the identification of the burst source and the physics of the bursts.

We use the Automated Patrol Telescope (APT) in New South Wales, Australia, triggered by the Gamma-Ray Observatory (GRO) spacecraft instruments, to image GRB position error regions beginning ~ 30 s after GRB triggers. Observations continue for up to 4 days to sample various emission time scales. The search is dormant between triggers, and so uses only a few percent of the total telescope time. The APT was selected because it has one of the only fields of view (5 degrees square) large enough to cover the GRO error region with a digital (CCD) imager. The feasibility of the project has already been demonstrated in a brief pilot search: GRB fields 1997 3/26b and 3/29 were imaged by the APT beginning < 90 seconds after trigger. Starting in mid-1998 we

expect to be measuring 5-10 optical counterparts to GRBs discovered by our project each year.

Accomplishments

During the initial LDRD support in late FY97, we analyzed existing data, prepared publications, and did calculations and design work for the next phase of our project. An important observation occurred, requiring us to recalculate our event rate. We receive most of our GRB alerts from the GRO satellite, and so our rate of detection of these GRBs is directly dependent on the rate and position accuracy of the GRO alerts. During the LDRD period, the details of a new kind of alert, the GRO/LOCBURST, became available. We recalculated our event rate in a more sophisticated manner than before, and presented the results (along with a full description of our system) at the 4th Huntsville GRB Symposium. Additional work on the design and specification of our proposed upgraded camera was done in consultation with our vendors, in order to obtain a camera at reasonable cost.

In order to show that we can identify optical transients (OTs) from gamma-ray bursts, we need to show that OTs unrelated to gamma-ray bursts are rare. We have multiple images of large areas of the sky from the Supernova Cosmology project. Analysis of images of one square degree of sky has shown that no transients were found that could be consistent with observed GRB optical counterparts, to a flux of > 24th mag in the R band. Analysis of additional data covering two degrees of sky is still continuing, awaiting final image calibration. The result will be by far the most sensitive large-area search for such transients. In the next phase of our project, funded by NSF and NASA, we will begin a slow ramp-up of the percentage of available time the search is operating, working toward the full automation of the system required to achieve 100% operation time.

Publication

B. Grossan, S. Perlmutter, and M.A. Ashley, A Search for Optical Counterparts to Gamma-Ray Bursts with the Automated Patrol Telescope, Proceedings of 4th Huntsville Gamma-Ray Burst Symposium, September 15-20, 1997 (C. Meegan, R. Preece, and T. Koshut, editors). New York: AIP, in preparation.

System Design and Initial Electronic Engineering for a Km-Scale Neutrino Astrophysical Observatory

Principal Investigators: David Nygren, Douglas Lowder, Martin Moorhead, Gilbert Shapiro, George Smoot, and Robert Stokstad

Project No.: 96026

Project Description

Ultra-high energy neutrinos from astrophysical sources may provide unique information about the most energetic events/processes in the universe. The nature of active galactic nuclei, the search for WIMPs, neutrino oscillations, and the detection of supernovae and gamma-ray bursters are among the varied scientific goals. It may well be that major unanticipated discoveries await, since only ultra-high energy neutrinos can traverse cosmological distances without degradation in energy or direction. The exploration of this new frontier of science has begun with the advent of the detectors AMANDA at the south pole and BAIKAL in Siberia. However, neither of these detector designs can be expanded efficiently to km-scale systems. Key Berkeley Lab technologies for the development and realization of km-scale detector systems are detector systems design (Physics), full custom application-specific integrated circuit (ASIC) design (Engineering), and massively parallel processing data capabilities (NERSC).

The general approach is the deployment of several thousand photomultiplier tubes (PMT) in an optimized 3D array to detect neutrino interactions in

water by the Cerenkov radiation emitted by the products of these interactions. Precise timing measurements combined with the knowledge of the PMT locations permits the reconstruction of muon trajectories or electromagnetic showers. Ultra-high energy muons radiate considerable energy, resulting in complex event signatures. Waveform information from the PMTs is regarded as essential to extract fully the information about these events, as well as to be prepared for unexpected phenomena. The Analog Transient Waveform Recorder (ATWR), a novel and powerful ASIC developed by Stuart Kleinfelder, provides the central element of our system design, the digital optical module (DOM).

Accomplishments

Two DOMs Deployed in Ice at South Pole

Two prototype digital optical modules based on the Berkeley Lab design using the ATWR were constructed at the Jet Propulsion Laboratory and successfully deployed at the South Pole in the AMANDA project. Waveforms from muons were returned from the deep ice (1.6-km depth) for the first time ever. This is a great success, and data are being analyzed. These DOMs, however, lack the time-stamping capability needed for fully autonomous operation.

New ATWR—the Analog Transient Waveform Digitizer (ATWD)

Stuart Kleinfelder has designed an advanced version of the ATWR which contains an internal, highly parallel 10-bit ADC. All samples of a captured waveform are digitized simultaneously, in approximately 10 microseconds. This is approximately 100 times faster than for the previous ATWR. One ATWD can process the expected trigger rate with negligible deadtime. The first silicon device demonstrated that the 10-bit signal-to-noise appears possible, but also revealed minor problems. A second fabrication pass is planned for December, 1997. The new ATWD provides the equivalent of a one-GHz FADC for just milliwatts of power. This is an impressive achievement; a possible commercial application is a hand-held oscilloscope.

Simulations

Progress in this area was achieved. The Monte Carlo is now at the state where the impact of optical properties of a medium (scattering and absorption) can be simulated rather realistically.

System Architecture

Considerable progress has been achieved in this area. One critical aspect of our decentralized architecture concept is local time-stamping of events, with infrequent calibration of the local clock. The anticipated stability of the local oscillator was shown not only to be realizable, but a particular device from Toyocom was shown by G. Przybylski to be more stable than necessary by approximately three orders of magnitude—for a price of \$25! Specifically, our test setup measured typical drifts of 6×10^{-11} over an interval of 10 s. This result eliminates stability of local clocks from the list of system issues.

The system architecture of the DOM for ice and water environments has been defined and interface issues partly evaluated. A very considerable simplification has emerged from this: no local data multiplexing/power distribution module would be needed for either ice or water. Instead, a hard-wired, simple party-line protocol appears to be feasible, available in the form of a well-tested commercial family of "Lonworks" products from Motorola.

A new multibeam optical beacon was designed and constructed. These should be about 30 times brighter than the previous design, which employed a plastic diffusing ball. Twelve will be deployed within AMANDA-II this winter.

Publications

"Progress Toward a Km-Scale Neutrino Detector in the Deep Ocean," LBNL-41083, which includes a description of the Berkeley Lab system design and DOM results, was presented at an international workshop and will be published in the proceedings.

Paper describing the two DOMs that have been deployed, in preparation.

Paper describing the ATWR/ATWD ASICs, in preparation.

Exploring Scientific-Computational Collaboration: NERSC and the Supernova Cosmology Project

Principal Investigators: Saul Perlmutter, Peter Nugent, Gerson Goldhaber, Donald Groom, and Alex Kim

Project No.: 96044

Project Description

Using astrophysics techniques developed in the Supernova Cosmology Group, in the next few years we will be measuring the fundamental parameters of cosmology. This project already requires unusual computational environments and capabilities. The future, larger amount of data will need innovations for near-real-time computation, fast access to large data sets, and tools for scientific visualization, networking and "collaboratory" environments—all of which are research interests of NERSC. As a first step in a collaboration, we are using T3E calculations to interpret our supernova spectra. We have also begun studies of image processing with supercomputers.

The key to successful cosmological measurements is to attack the statistical error and the systematic errors. To improve the statistical error, it is necessary to move to significantly larger data sets in order to study larger samples of supernovae at greater distances. We are now scaling up our supernovae search, using larger wide-field cameras and multi-telescope coordination to produce data sets that are 5 to 20 times larger, and thus beyond our current computational resources. We also aim to reduce the systematic errors associated with the minor variation in intrinsic brightness among Type Ia supernovae (SNe Ia) by calibrating on features of the supernovae spectrum. This spectral work involves supercomputer simulations of supernovae atmospheres to produce "synthetic spectra." This theoretical and phenomenological research will make it possible to prepare simulated spectra to understand the distant supernova spectra and thus calibrate the supernova's brightness.

Accomplishments

Spectrum Synthesis on the T3E

During our most recent supernovae search this winter, we were able to find 17 supernovae using the Big Throughput Camera at CTIO. Spectra for all of these were obtained at the Keck telescope, including SN 1997ek at the astonishing redshift of $z = 0.86$. This makes it the most distant spectroscopically confirmed supernova. Interpretation of such a large, highly redshifted data set of spectra (where one is working mostly in the rest frame UV) is best performed through spectrum synthesis, since comparison to nearby supernovae at the appropriate wavelengths is often impossible. In addition, such data reduction tasks as k -corrections (placing the highly redshifted photometry on the same scale as nearby photometry through spectra) are best performed on a parallel supercomputer, since they involve the processing and analysis of several hundred nearby spectra, each of which needs to be properly flux calibrated, redshifted, and have its colors determined at every redshift we have discovered in a supernova. As part of this LDRD, three major projects involving spectrum synthesis are currently in progress to interpret the approximately 40 high-redshift supernovae spectra obtained so far at the Keck telescope. The methods involved and the present status of each is outlined below.

The first involves classification and age determination via the spectra. On the basis of Peter Nugent's work, we have now confirmed and calibrated the relationship between the spectral ratios and luminosity using approximately 20 recently obtained nearby supernovae spectra in the Hubble flow. In addition, A. Riess and colleagues have shown how the age of SNe Ia can be determined from a single spectrum with surprising accuracy. These investigators have combined these methods to determine the peak luminosity of a Type Ia supernova (SN Ia) from a single spectrum found anywhere from two weeks before to two weeks after maximum light. These results will be used as a check of our light-curve-based determination of the peak luminosity for our high-redshift supernovae. Spectrum synthesis will be used to get at the reason behind these relationships in an effort to give them a more solid theoretical footing and allow interpolation between dates for which comparison spectra are available.

The second challenge for the spectrum synthesis of SNe Ia is to get at any possible evolutionary effects in our high-redshift supernovae. Our highest redshift

supernovae—SNe 1996c1, 1997ap, 1997ek, 1997en, and 1997ez (all with $z > 0.75$)—exploded when the universe was approximately one half to two thirds of its present age. The environment of the progenitors for these supernovae could be considerably different than the ones in which our nearby (calibrating) set of supernovae were formed. Current calculations running on NERSC's T3E and the IBM SP2 at the University of Oklahoma are pursuing the effects of metallicity in the progenitor system, mixing during the explosion, and how both of these effect the resultant spectra. More than half of these calculations have been completed, and we hope to be writing up this work within the month.

Finally, we are working on a method to determine the reddening due to interstellar dust (in either our own or the host galaxy) for a SN Ia. It has been observed that at 35 days after peak brightness almost all SNe Ia have the same color and that the excess color is solely due to interstellar reddening. It is our aim, through spectrum synthesis, to test this hypothesis by examining the colors of a grid of models with a variety of initial conditions, chief among these being luminosity.

We currently have a static model atmosphere code running very well in parallel on the T3E with wallclock times, which compare favorably to the IBM SP2's. Current progress on getting the full spectrum synthesis code PHOENIX 9.0 to run on a T3E (by users Nugent at NERSC and Baron and Hauschildt at SDSC and NERSC) is going well. More than 90% of this code is now able to run in parallel on the T3E, and, with a little more work on determining the best way to handle multiple, large files in parallel, we should have everything running smoothly. We have also used the LDRD-purchased Sparc Ultra II to perform several preliminary spectrum synthesis runs in preparation for a larger grid of models to be run on the T3E.

NERSC—Supernovae Cosmology Project Cooperative Efforts

As part of this NERSC-Astrophysics LDRD, we have been working closely with the NERSC staff in our efforts to utilize the T3E for both spectrum synthesis and a future project aimed at using a massively parallel computer for image reduction. Richard Gerber has been quite helpful in getting the spectrum synthesis code up and running on the T3E. He has attended some of our group meetings and has given us insight into various compiler options and possible hang-ups our code would present to the T3E.

Peter Tang has been working with us in our effort to explore new methods in image reduction and to implement these on a massively parallel machine like the T3E. So far he has created several of the fundamental building blocks for this analysis, including the development of a set of matlab tools to perform image deblurring and denoising. Currently, he is working on selecting a suitable optimization algorithm and, after completion, its migration to the T3E.

Publications

S. Perlmutter, et al., "Discovery of a Supernova Explosion at Half the Age of the Universe," *Nature* 391, 51 (1998).

P. Nugent, E. Baron, P.H. Hauschildt, and D. Branch, "Synthetic Spectra of Hydrodynamic Models of Type Ia Supernovae," *Ap. J.* 485, 812 (1997).

A. Riess, P. Nugent, A. Filippenko, R. Kirshner, and S. Perlmutter, "Snapshot Distances to Type Ia Supernovae All in 'One' Night's Work," submitted to *Ap. J.*, 1997.

P. Nugent, et al., "Spectroscopic Correlations Among Type Ia Supernovae," *Ap. J.*, 1998, in preparation.

P. Nugent, et al., "Metallicity Effects in the Spectra of Type Ia Supernovae," *Ap. J.*, 1998, in preparation.

Fabrication of Charge-Coupled Devices on a High-Resistivity Substrate for Astronomical Imaging

Principal Investigators: Saul Perlmutter, Gerson Goldhaber, Donald Groom, Stephen Holland, Carl Pennypacker, and R. Stover

Project No.: 97029

Project Description

Techniques developed at LBNL for central tracking applications in particle detectors are being applied to the design of CCDs for astronomical imaging. These will overcome present performance limitations, as

well as price and availability limitations. Having now demonstrated imaging and high quantum efficiency with small test devices, the most important goal during the first year of this LDRD was fabrication of a scientifically useful 2048×2048 pixel astronomical imaging device scaled up from the current prototype design. If the new technology is to have its expected impact, it is crucial that it be developed with all due speed.

In the course of detector R&D for the SSC, a LBNL Physics Division Group developed a silicon device process that provided the first demonstration of monolithic integration of high-quality detector diodes with high-density, low-noise electronic circuitry that is also compatible with conventional IC processes. The key is a highly efficient gettering process that actively removes detrimental impurities from the active volume. Present test structures have extended this method in two ways. On one side of a wafer, a fairly conventional CCD structure is fabricated. On the "back" side of the wafer is a window that also serves as an electrode during totally depleted operation. Imaging has now been demonstrated with small (200×200 pixel) test CCDs of this dramatically new design, and windows with superior properties have been produced. It remains to thoroughly characterize these structures and to make a full-sized CCD.

Accomplishments

A small prototype CCD was fabricated in the LBNL Microsystems Laboratory, with the first devices completed in spring 1996. The 200×200 , $(15 \mu\text{m})^2$ CCD utilized fabrication technology developed at LBNL. The devices were tested in collaboration with our colleagues at the University of California's Lick Observatory.

As part of this LDRD, several milestones were achieved. Back-side illumination with high quantum efficiency was demonstrated in lab tests and at Lick Observatory. A unique feature of this CCD is high quantum efficiency in the near infrared due to the $300\text{-}\mu\text{m}$ thick photosensitive volume, and this capability was demonstrated by imaging of the Orion Nebula at the Lick Observatory's 3-m telescope. Stars obscured at shorter wavelengths (visible red) by interstellar dust and gas were visible at $1 \mu\text{m}$ wavelength. In addition, the CCD has high quantum efficiency in the blue (60% at 400 nm) without the need for thinning.

A concern for back-illumination operation of this CCD is possible loss of spatial resolution. The concern is signal charge spreading due to diffusion while the photogenerated charges drift from the back side, where short-wavelength light is absorbed, to the CCD potential wells located 300 μm away. This was experimentally characterized at the Lick Observatory CCD laboratory. The experiment consisted of imaging short-wavelength light through a pinhole mask placed directly on the CCD. The charge spreading was measured as a function of bias voltage, and the results agree well with theoretical models developed for both the case of a fully depleted CCD, as well as for the case when field free regions exist in the CCD.

With these results the next step is the development of larger area CCDs for scientific cameras. However, the fabrication equipment in the LBNL Microsystems Laboratory limited the size of the device that could be fabricated to approximately 1.5 cm \times 1.5 cm. Efforts by the LBNL Microsystems personnel resulted in the procurement, via donation from Intel, of a high performance lithography tool capable of exposing an entire 4-inch diameter wafer. This equipment was delivered and installed to OEM specifications during summer, 1997. A mask set containing 2048 \times 2048 CCDs was designed and will be used for the first fabrication run of large-area CCDs.

Publications

S.E. Holland, et al., "Development of Back-Illuminated, Fully-Depleted CCD Image Sensors for Use in Astronomy and Astrophysics," IEEE Workshop on Charge-Coupled Devices and Advanced Image Sensors, Bruges, Belgium, 1997.

R.J. Stover, et al., "Characterization of a Fully-Depleted CCD on High-Resistivity Silicon," Solid State Sensor Arrays: Development and Applications, Proceedings of SPIE, pp. 183–188, 1997.

S.E. Holland, et al., "A 200 \times 200 CCD Image Sensor Fabricated on High-Resistivity Silicon," IEDM Technical Digest, pp. 911–914, 1996.

Performance Modeling of Pixel and Silicon Strip Detectors for High-Luminosity Experiments

Principal Investigator: James Siegrist

Project No.: 97030

Project Description

Charged particle tracking in high-luminosity experiments such as ATLAS depends heavily on measurements using pixel and silicon strip detector devices. The U.S. ATLAS groups have been developing such detectors for use at high-rate hadron colliders, but many of the components still need research and development to provide a tracker designed to run for many years at a luminosity of $10^{34} \text{ cm}^{-2}\text{s}^{-1}$. Survival at the high luminosities projected necessitates the use of pixels at radii below 30 cm. Strips must be placed at larger radii, and must survive larger fluences than those foreseen for the silicon trackers designed for the SSC.

This project will concentrate on some outstanding technical questions relating to silicon tracker development, both in the pixel system and the silicon strip system. Not yet resolved, under the constraints noted above, are the chip testing specification and a prototype test system, simulation of signal development in radiation-damaged devices, or the mechanical characterization of the thermal behavior of these devices. Systematic work to characterize viability and performance of rad-hard circuits up to the 50 mRad level will be performed. Devices will be characterized, analyzed, and modeled before and after irradiation at the Berkeley Lab 88-inch cyclotron and with cobalt sources.

Accomplishments

A system for module assembly and characterization was purchased just before the close of the fiscal year. Fabrication of the system will continue into next year. Modules assembled using this new system will undergo both electrical and mechanical characterization, including thermal behavior and electronic noise performance.

Students supported by the LDRD worked on signal simulation programs for the silicon detector. Figure 1 shows a plot of the weighting field computed for one strip of a 5-strip array. This computation is an essential step in the eventual complete modeling of

the signal development in silicon. Our new code supports full 3D electric field calculation for use in both strip and pixel geometries. The effect of the magnetic field on motion of the charge carriers in the silicon has been included. The new code supports a quasi-particle calculation of the drift, diffusion, and self-interactions of the electron and hole charge clouds. A proper description of the energy deposition from charged particles exists but has not yet been incorporated in the code. We are currently investigating the code performance for x rays both in the ATLAS group, and in Nygren's x-ray imaging group.

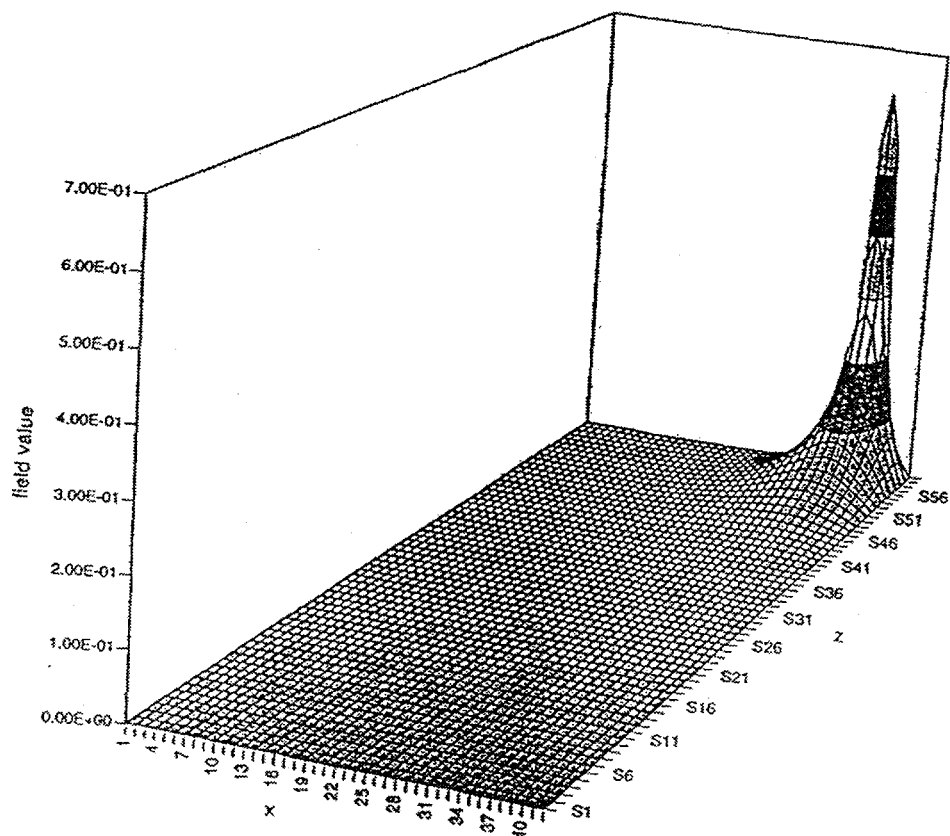


Figure 1. Weighting field: 40x40x60 (100 iterations). Strip: 5/5, Y: y extent/2.

Cosmic Microwave Background Radiation Data Analysis

Principal Investigator: George Smoot

Co-Investigators: Julian Borrill and Andrew Jaffe

Project No.: 97038

Project Description

This project is to develop the novel computational techniques necessary to extract fundamental cosmological parameters from forthcoming Cosmic Microwave Background (CMB) datasets.

The CMB provides a picture of the universe as it was a mere 100,000 years after the Big Bang. As the earliest possible photon image available to us it is our most powerful discriminant between different cosmological models. The unprecedented detail of CMB datasets obtained in the next 10 years will allow us to determine the fundamental cosmological parameters, in many cases currently known to no better than a factor of 2, to the 1% level.

Central to our task is being able to locate and describe the maximum of the likelihood function of the cosmological parameters given the data, in this case an N -pixel map generated by any one of the forthcoming CMB observations. At present, N is at most a few thousand, but this will increase to tens and hundreds of thousands with the MAXIMA and BOOMERANG balloon flights, and to an order of millions with the MAP and PLANCK satellite missions. Our present approach scales as N -squared in size and N -cubed in time, so a supercomputer like the T3E is essential to our work. However, even this will be unable to handle the largest datasets; we must therefore develop alternative algorithms with either better scaling properties, or ones that repeatedly

analyze only a subset of the overall dataset at any time.

Accomplishments

Our project received initial funding late in FY97. The first action was to hire a postdoctoral fellow effective September 1, 1997, and to begin work on implementing algorithms. Since then we have completed the development of two generations of the quadratic estimator formalism for performing a rapid search of the parameter space for the maximum of the likelihood function, and have implemented them on the T3E both in serial and in parallel (using the LAPACK and ScaLAPACK libraries respectively). We are currently working to demonstrate the ability of the parallel code to analyze at least the first generation MAXIMA/BOOMERANG data. To this end we are now developing simulated datasets, comprising the signal from a known underlying theory and a model of the instrument noise and sky foregrounds associated with each experiment.

At the same time, we had a successful flight of the BOOMERANG balloon-borne instrument and the early portion of data processing has begun. We anticipate that it will result in a map with an order of ten thousand pixels or more.

We have also posted a WWW page summarizing our progress at the following URL:
<http://cfpa.berkeley.edu/group/cmbanalysis/reports/nersc2.html>

Publications

J.R. Bond, A.H. Jaffe, and L. Knox, "Estimating the Power Spectrum of the Cosmic Microwave Background," to be published in *Phys. Rev. D*.

G. Smoot, "The Cosmic Microwave Background Anisotropy Experiments," in *The Cosmic Microwave Background*, Kluwer Academic: Netherlands, 1997.

J. Borrill, "Power Spectrum Estimates for Large Data Sets," in preparation.

Structural Biology Division

Determination of Macromolecular Structure by *ab initio* Phasing of Crystallographic Diffraction Data

Principal Investigator: Stephen Holbrook

Project No.: 96046

Project Description

A major roadblock to x-ray crystallographic structure determination is that the phases of the scattered x rays are unknown. A great deal of effort is expended in determining approximations to these phases by various procedures such as multiple isomorphous replacement (MIR), multiwavelength anomalous diffraction (MAD), and molecular replacement (MR). In some cases, none of these approaches is successful and the structure cannot be determined.

Our goal is to solve the phase problem of x-ray crystallography by applying a simple but computationally intensive method to determine a minimum set of x-ray diffraction data with phases sufficiently accurate to produce electron-density maps showing a clear molecular boundary. These initial maps will then be improved by iterative map modification methods and phase extension to produce an interpretable map from which a structural model may be traced.

The initial phases used in tracing an electron-density map or defining a molecular boundary may have a root mean square difference of up to 60–70° from the phases of the final, refined model. Starting with MIR- or MR-determined initial phases, it has been shown that solvent flattening, histogram matching, and map averaging are very successful in improving these phases and producing an interpretable map from one which is totally uninterpretable. The key to performing these phase improvements is to obtain an initial map in which the solvent and protein regions can be approximately defined.

Since highly accurate initial phases are not critical, we propose to randomly assign the phases to a subset of

reflections (the most intense) that dominate the generation of an electron-density map. As modern supercomputers become more and more powerful, the time required to compute initial Fourier maps from all possible phase combinations of limited reflection sets will become shorter and shorter. If we can effectively select potential maps on which to perform statistical phase improvement, direct phase determination for macromolecular crystallography can be accomplished.

We previously demonstrated that the molecular envelope defined by a small number of correctly phased low-resolution reflections is very similar to the correct molecular envelope calculated from a well-refined, high-resolution structure. The remaining problem is identification of the correctly phased electron-density map or cluster of maps among the incorrect ones.

Accomplishments

As stated above, we have established that random or combinatorial, *ab initio* phasing is computationally feasible by demonstrating that electron density maps, which are highly correlated to the "correct" map, can be calculated with only 12 out of the total 20,000 diffraction intensities and that some incorrect phases do not significantly degrade the map. These findings are summarized in Tables 1 and 2.

Four results were achieved in this project. First, Fourier maps generated by 12 strong reflections with correct phases have a strong correlation (70% in centric case, 49% acentric) to the 2 Å correct map generated by 20,000 reflections (Table 1, #3).

Second, rounding up of the correct phases from the 12-reflection map to the closest of 0, 90, 180, and 270° does not reduce the correlation by much (Table 1, #4). Twelve reflections with four possible phases each results in ca. 4,000,000 possible phase sets or electron-density maps. We can handle this amount of calculation with modern workstations and supercomputers.

Third, averaging maps with both correct and incorrect phases does not reduce the correlation by much. For example, point-by-point averaging of maps generated by 12 strong reflections with 0, 1, 2, 4, and 6 wrong

Table 1. Mask (envelope) correlation, noncentric case. The correlation of a mask generated by less than 1/1,000 of reflections (3,4) yielded good correlation to the high resolution map.

| Resolution of map | | Number of reflections | Mask correlation w.r.t. 2 Å mask |
|-------------------|--|------------------------|-------------------------------------|
| #1 | 2 Å | 20,000 all reflections | 1.0 |
| #2 | 10 Å | 120 all reflections | 0.7 |
| #3 | 10 Å | 12 most intense | 0.5 |
| #4 | 10 Å, phases of 0, 90, 180, 270° only | 12 | 0.5 |

Table 2. Effect of map averaging. (*phases are rounded to closest 0, 90, 180, or 270°).

| # | # of reflections | selection of phases | # of wrong phases | Correlation w.r.t. #1 | Averaging method | Averaged Correlation w.r.t. #1 |
|---|------------------|---------------------|-------------------|-----------------------|------------------|--------------------------------|
| 1 | 120 | correct | 0 | 1 | | |
| 2 | 12 | rounding* | 0 | 0.76 | | |
| 3 | 12 | rounding* | 1 | 0.42 | #2+3 | 0.66 |
| 4 | 12 | rounding* | 2 | 0.69 | #2+3+4 | 0.70 |
| 5 | 12 | rounding* | 4 | 0.70 | #2+3+4+5 | 0.73 |
| 6 | 12 | rounding* | 6 | 0.19 | #2+3+4+5+6 | 0.73 |

phases gave an average map with a correlation coefficient better than 70% to the 10 Å map generated by over 100 reflections with correct phases.

These results show that a correct Fourier map can be reasonably well represented by a few strong reflections, and a correct map can tolerate significant phase errors by averaging process. This is encouraging since a combinatorial screening of 12 reflections with four possible phases each is now computationally achievable.

We have also shown that phase sets that produce electron-density maps with high correlation to the correct map can be identified by a map-clustering method as described below.

The final result is in studies of map clustering. Maps with phases of 0, 90, 180, or 270° generated by Monte Carlo or grid-sampling methods can be clustered according to the correlation among them. Similar maps are averaged to bring out their common

features. We have observed an interesting result concerning the number of maps in the clusters. Usually, there is one or a few clusters containing many more maps than the others. In our limited experience, these clusters generally correspond to the ones with higher correlation to the correct map among all clusters. We are currently investigating the basis of this result. One assumption is that a correct map can tolerate more phase error, so its correlation cluster forms a larger volume in phase space. Once phase space is equally sampled, either randomly or systematically, the 'correct cluster' contains the greatest number of maps. See Figures 1 and 2 (next page).

Publication

L.-W. Hung, S.-H. Kim, and S.R. Holbrook, "Low Resolution Electron-Density Map Clustering in *ab initio* Phasing of Macromolecular Diffraction Data," in preparation.

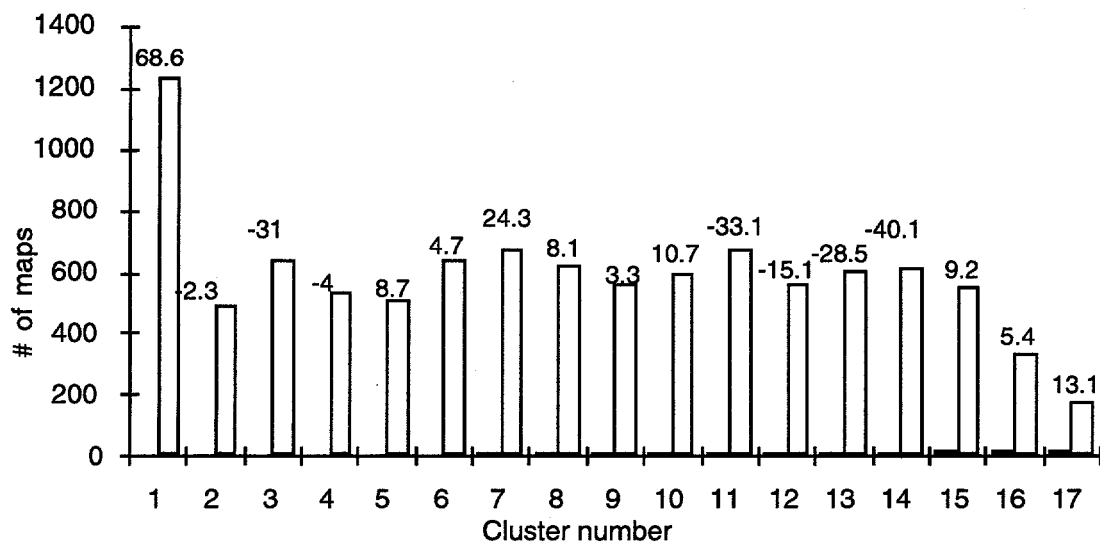


Figure 1. A typical distribution of cluster analysis of 10,000 maps with phases generated by Monte Carlo simulation. The number on top of each bar is the correlation coefficient of that cluster to the correct 10 Å map.

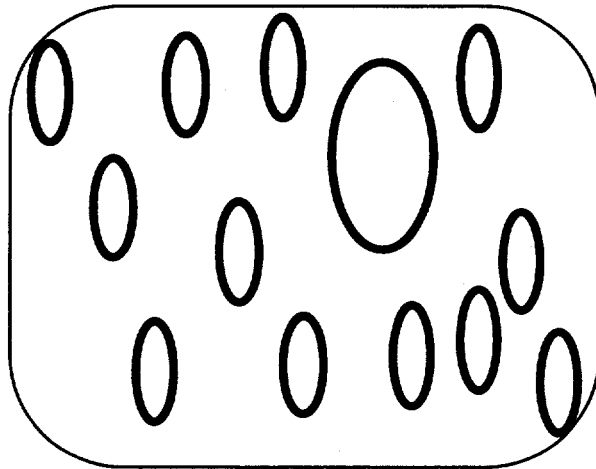


Figure 2. Schematic diagram showing 'phase space.' Dots indicate the phase sets sampled in phase space. Each sampled phase set is used to generate a Fourier map corresponding to the calculated electron density distribution in real space based on the selected reflections. Ovals indicate 'clusters' in which all maps are correlated better than a given threshold. If a certain type of 'electron-density' distribution tolerates greater phase errors, the corresponding 'cluster size' should be bigger in phase space. As a result, the number of maps in that particular cluster is greater than the others provided that the phase space is homogeneously sampled.

Structure and Conformational Dynamics Mediating Signal Transduction in Two Classical Membrane Proteins

Principal Investigator: Yeon-Kyun Shin

Project No: 97031

Project Description

Little is known about the conformational dynamics of membrane proteins, and this hinders our understanding of their roles in many essential physiological processes such as transmembrane signaling and energy transduction. This project will elucidate the structures and rearrangements of two paradigmatic signaling proteins: the 7-helical receptor bacteriorhodopsin and the voltage-gated Shaker K⁺ channel. Through a unique combination of techniques that have high structural and dynamic resolution, we are in a position to obtain important new structural information about the dynamics of these proteins at the atomic scale.

The key to the approach of this proposal lies in the combination of methods that provide structural and kinetic information about the rearrangements of membrane proteins that have long been refractory even to static high resolution structural studies. This involves tagging proteins at specific sites with probes that can "instantly" report conformation, and it requires that the functional state of the protein be known, or, when possible, that it be directly monitored at the same time as the physical measurement of conformation is determined. The general strategy is to place one or two nitroxide spin labels (for electron paramagnetic resonance, EPR), or fluorophores (for fluorescence), at selected sites in a protein by site-specifically replacing native residues with cysteines that provide sites for the specific and directed attachment of thiol probes. Mapping of protein structure and the determination of rearrangements are made by measuring either changes of environment or position of a label at a single site on the protein, or by measuring the physical distance between pairs of sites. By monitoring protein structure with EPR and / or fluorescence, we obtain a report of conformation at a rate that is orders of magnitude faster than the rate of the structural rearrangements that the proteins undergo, thus permitting these movements to be followed in real-time, with a high kinetic resolution. The continuous nature of the physical measurements provides unique information about the structure and life-time of transition states that could not be obtained from conventional structural methods. In terms of protein dynamics-function relationships, this information is essential for the interpretation of the static pictures of these proteins that emerge from crystallographic methods.

Accomplishments

Potassium Channel

We have employed fluorescence resonance energy transfer (FRET) as a spectroscopic ruler to measure distances between pairs of sites scattered throughout the outer surface of the Shaker K⁺ channel protein. Energy transfer between donor fluorescein and acceptor rhodamine was quantified by indirectly measuring donor lifetime. By combining voltage clamp fluorimetry with FRET, we have succeeded in

measuring activation gating movements that change the efficiency of energy transfer. These measurements indicate that the transmembrane movements of the charged S4 segment that activate the channel in response to changes in membrane voltage are accompanied by S4 rearrangement parallel to the plane of the membrane. This new dimension of S4 movement may explain how voltage-driven movement of S4s in each of the four identical subunits can open the ion conduction pathway of the pore. Our results also provide the first illumination of the packing arrangement, and gating rearrangements, of the channel's other transmembrane segments.

Bacteriorhodopsin

Active translocation of ions across membranes requires that the ion-binding site inside the pump has alternate access to each of the membrane surfaces. Proton translocation by bacteriorhodopsin (bR), the light-driven proton pump in *Halobacterium salinarium*, involves a change in the accessibility of the centrally located retinal Schiff base to the opposite membrane surfaces. This key event in bR's photocycle ensures that proton-release occurs on the extracellular side and proton uptake on the cytoplasmic side. To study the role of protein conformational changes in this reprotonation switch, spin labels were attached to pairs of engineered cysteines in the cytoplasmic interhelical loops of bR. Light-induced changes in the distance between a spin label on the EF interhelical loop and a label on either the AB or the CD interhelical loop were observed, and the changes were monitored following photoactivation with time-resolved EPR. Both distances increase transiently by about 5 angstroms during the photocycle. This transient opening occurs between proton release and uptake, and may be the conformational switch that changes the accessibility of the retinal Schiff base to the cytoplasmic surface after proton release on the extracellular side.

Publication

T.E. Thorgeirsson, W. Xiao, L.S. Brown, R. Needleman, J.K. Lanyi, and Y.-K. Shin. "Transient Channel-Opening in Bacteriorhodopsin: an EPR Study," *J. Mol. Biol.* 273, 951-957 (1997).

Cross-Divisional

New Chemistry for Pollution Prevention Initiative: Selective Catalyst

Principal Investigators: Mark Alper, Robert Bergman, Jonathan Ellman, Peter Schultz, and Heinz Frei

Project No.: 96027

Project Description

A major issue in the development of environmentally benign synthetic processes is the lack of selectivity, which results in disposal problems of unwanted byproducts, energy-intensive separations, and inefficient use of starting materials. The development of selective catalysts that promote only the desired reaction and products is therefore of great importance. The use of catalysts also allows the introduction of different reaction conditions, which can be less energy-demanding and may decrease the dependence on toxic or wasteful solvents and reactants.

The focus of this research is the exploration of three approaches to selective catalysis, which are listed below. A fourth project, "Selective Conversion of Hydrocarbons," which was supported by this program last year, was funded by DOE this year.

- A combinatorial approach to catalyst discovery and optimization, with the expectation that this will improve dramatically the time-consuming and costly trial-and-error process currently practiced.
- New "light-assisted" routes for the selective chlorination and nitration of small hydrocarbons, especially benzenes, to commercially important products. Current methods for the synthesis of these compounds produce very large amounts of environmentally harmful waste.
- Catalytic processes for the removal of the atmospheric gases NO and CO₂.

Accomplishments

Combinatorial Approach to Catalysis

The discovery of new catalysts and the optimization of existing catalysts can have a large impact on energy use, the environment, and industrial competitiveness. Examples include catalysts for desulfurization, partial hydrocarbon oxidation, and the production of bulk and fine chemicals. Unfortunately, a detailed understanding of catalyst structure, its influence on transition state energy, and the nature of the interaction between catalyst and support are not well understood. These difficulties have led to a trial-and-error approach to catalyst discovery and optimization. We hope to impact this process by the application of combinatorial approaches—the ability to cost effectively design, execute, and analyze tens of thousands of experiments in parallel versus one at a time. This approach does not change the scientific method, only the efficiency and time effectiveness with which it is carried out. Specifically, we applied this approach to the development of catalysts for bulk chemical production—late metal metallocene catalysts for olefin polymerization.

For example, the immune system generates 10¹² antibody molecules simultaneously and then screens them to identify those few that specifically recognize and bind a foreign pathogen. Recently it has been shown that a similar approach can be applied to material. Methodology has been developed for 1) the parallel synthesis of solid state materials, 2) the processing of these materials, and 3) the detection of specific electronic, magnetic, or optical properties. This pollution prevention project was based on applying this "combinatorial" approach to the discovery of new catalytic systems.

The program involves the development of 1) methods for the synthesis of combinatorial libraries of novel late transition metal olefin polymerization catalysts (homogeneous and supported) based on our existing theoretical and empirical understanding, and 2) methods for evaluating both the properties of the catalysts as well as the polymers produced. The generation of catalysts that can catalyze the efficient polymerization of ethylene and propylene feedstocks

with a variety of functionalized olefins, while controlling polymer composition, microstructure, molecular weight, and molecular weight distribution, would lead to a whole new generation of polymers with tremendous impact on industries generating and utilizing polymers. In addition, this technology may be applicable to many other problems in catalysis.

To date our efforts have focused on the development of a general synthetic approach to the "Brookhart" family of olefin polymerization catalysts shown in Figure 1. The catalysts copolymerize olefins that contain heteroatom substituents and produce long-chain polyolefins.

A highly efficient solution route has been developed that allows us to generate bisimines with control over the substituents on the carbon and nitrogen atoms of the bisimine skeleton. We have adapted this method to the solid phase synthesis of Brookhart ligands where R is the hydrogen. A small library of ligands has been synthesized. A variety of ligands that are half Brookhart (ortho-substituted amiline imino) and half an heterologous chelating group may be synthesized by simple variation of the procedure described above. Such hybrid ligands include Brookhart-salen ligands, Brookhart-phosphine ligands, Brookhart-phosphine ether ligands, Brookhart-amine ligands, and Brookhart-phenol ligands. The project focused on the solid-phase methodology for synthesizing the Brookhart-phosphine and Brookhart-amine ligands. Conditions

have also been established for metallating the ligands and assaying the MAO-dependent polymerization of propylene and ethylene. Libraries are assayed for their ability to catalyze the polymerization of propylene in the presence of heteroatom-containing olefins (methylacrylate, acryonitrile, etc.) and under a range of solvent conditions, including water.

Light-Assisted Functionalization of Small Hydrocarbons

We have recently discovered highly selective oxidation of abundant alkanes, alkenes, and alkyl benzenes to industrial intermediates and organic building blocks by gaseous oxygen in zeolites under visible light. These reactions are mediated by the high electrostatic field inside the cages and channels of alkali or alkaline earth-exchanged zeolite X, Y, or L. Based on this result, we proposed to explore new routes for the selective chlorination and nitration of small hydrocarbons, especially benzenes, to commercially important products. Current methods for the synthesis of these compounds produce very large amounts of environmentally harmful waste.

Our approach is based on the very strong polarizing effect of high electrostatic fields inside cation-exchanged zeolites on molecular chlorine or nitrogen dioxide. Loading of the gaseous reactant with the hydrocarbon into the zeolite may lead to a spontaneous or light-activated reaction at or around room temperature. Such mild reaction conditions

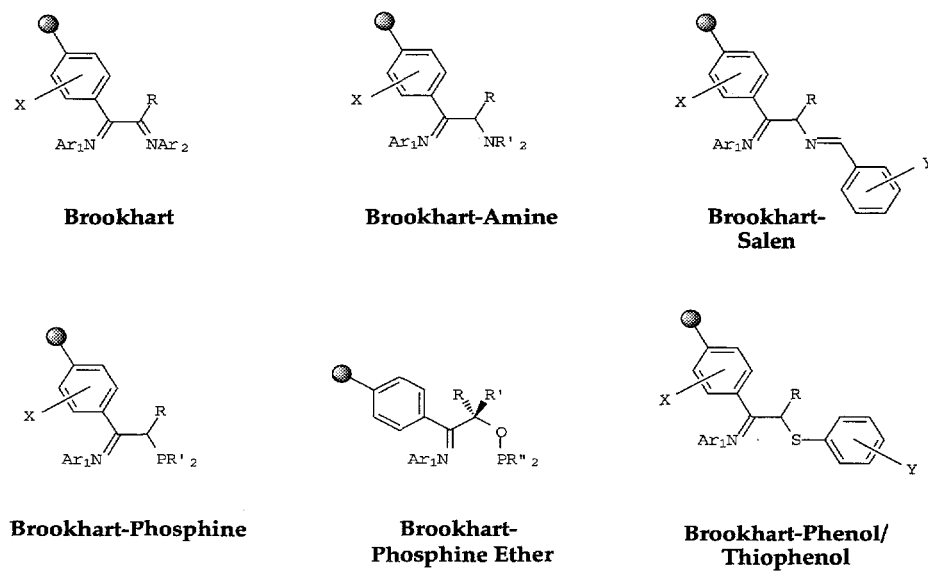


Figure 1.

coupled with the diffusional and steric constraints of the microporous solid may result in substantial improvement of the product selectivity over existing methods. More importantly, use of environmentally undesirable reagents such as large amounts of strong acid may be avoided.

We have established a new route for the selective conversion of benzene to 1,4-dichlorobenzene or to 1,2,4-trichlorobenzene using molecular chlorine (Figure 2). Partially chlorinated benzenes play a key role as agrochemicals (insecticides, herbicides) and in the manufacture of polymers such as high-performance thermoplastics. Substantial improvement of the selectivity of partial benzene chlorination over existing commercial processes is urgent for two reasons: unwanted chlorinated products are harmful to the environment, and the amount of starting materials—benzene and chlorine—has to be minimized in order to reduce the processing volume of these hazardous reactants.

Our method uses zeolite NaZSM-5 as the reaction medium and a combination of low temperature and visible light energy for accomplishing selective benzene chlorination. We found that 1,4-dichlorobenzene is produced spontaneously at a fast rate when loading benzene and chlorine gas into the dehydrated, solvent-free zeolite at -100°C . No by-products are observed. The reaction was monitored *in situ* by FT-infrared spectroscopy, and chlorobenzene was observed as reaction intermediate. After selective conversion of over 80% of the benzene, irradiation of the zeolite matrix with visible light (450–520 nm) resulted in further chlorination of the dichlorobenzene products to 1,2,4-trichlorobenzene. No other chlorobenzene isomer was observed even at conversion of 70% of the 1,4-dichlorobenzene starting material. In existing processes for the manufacture of these products, benzene chlorination has to be kept at low conversion in order to minimize the formation of unwanted chlorinated by-products. This requires energy-consuming separation and recycling processes that are obviated by the new concept demonstrated in this work.

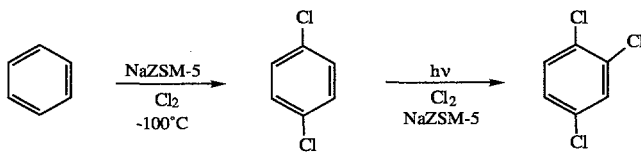


Figure 2.

We have exploited this extremely mild approach to selective functionalization of arenes for partial nitration of benzene and toluene. Mononitration of these hydrocarbons yields important intermediates for the manufacture of dyes, agrochemicals, and pharmaceuticals. When exposing zeolite NaZSM-5 loaded with benzene or toluene to nitrogen dioxide gas at room temperature, spontaneous nitration of the arene occurred in the absence of any added catalyst or solvent. Exclusive products were nitrobenzene and *p*-nitrotoluene, respectively. Monitoring by *in situ* infrared spectroscopy did not reveal any by-product, even at conversion of greater than 80% of the hydrocarbon, which is unprecedented. The mechanism involves formation of nitronium ion under the influence of the strong electrostatic fields inside the solvent-free zeolite, followed by electrophilic attack of this intermediate on the benzene. All existing methods for partial nitration require the use of large amounts of strong acid, disposal of which constitutes severe harm to the environment. The new route to nitrobenzene and *p*-nitrotoluene explored here completely avoids acids and opens up an environmentally friendly alternative to existing processes that is urgently needed.

Catalytic Conversion of CO₂ and NO

The need to deal with CO₂ and NO released into the atmosphere is well documented.

As shown in Figure 3, the binuclear zirconium-iridium complex 1 was found to react with hydrogen to give the dihydride complex 2. This material reacts with carbon dioxide to give product 3, in which insertion of CO₂ into one of the metal-hydrogen bonds has occurred. Treatment of this complex with organolithium reagents, such as phenyllithium, cleaves the inserted HCO₂ group from the complex, resulting in the formation of benzene, lithium formate, and regeneration of the initial starting complex 1. Although it has not been realized yet, the regeneration of complex 1 in the final step of the sequence indicates that this system holds promise for catalytic reduction of CO₂ to formate.

In initial experiments focused on synthesizing metal complexes capable of converting harmful nitrogen oxides to the natural atmospheric gases N₂ and O₂, we have found an organometallic complex that reacts with nitric oxide (NO) at an extremely rapid rate, even at -110°C . The reactive starting material is

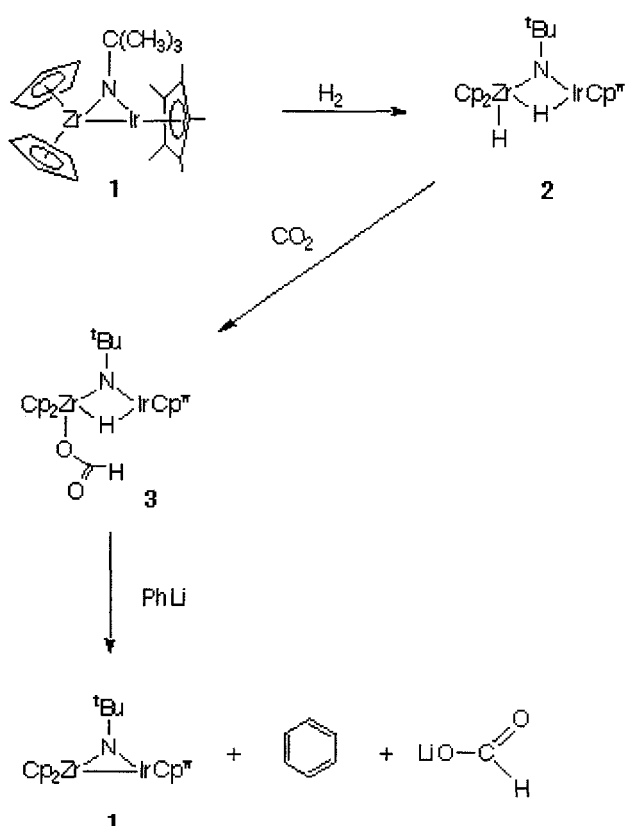


Figure 3.

$\text{Cp}_2\text{Zr}(\text{PMe}_3)_2$, illustrated as compound 4 in Figure 4. This complex reacts with excess nitric oxide to give N_2 and oxozirconocene cluster complex 5. In controlled experiments, we have found that the first phase of this reaction involves reaction of 4 with two moles of NO ,

leading to N_2O and the oxozirconocene cluster. N_2O is then reduced to N_2 by reaction with another mole of 4 in a subsequent step. Evidence that these reactions proceed via the intermediate monomeric $\text{Cp}_2\text{Zr}=\text{O}$ (6) was obtained by trapping experiments, where it was found that when Me_3SiCl was added to the reaction medium, trapped product 7 was formed in place of 5. When Cp_2ZrMe_2 was used, the monomeric oxo complex was trapped, which yields bridging oxo complex 8.

Publications

- I. Shin, P. Harbury, and P.G. Schultz, "The Combinatorial Synthesis of Polymerization Catalysts," in preparation.
- S.J. Kirkby and H. Frei, "Chlorination of Benzene to 1,4-Dichlorobenzene and 1,2,4-Trichlorobenzene in Zeolite NaZSM-5 Under Visible Light," to be submitted to *J. Phys. Chem.*
- S.J. Kirkby and H. Frei, "Selective Nitration of Benzene and Toluene in Zeolite NaZSM-5," to be submitted to *J. Phys. Chem.*
- K.P. McNeill and R.G. Bergman, "Development of a Catalytic System for the Conversion of Nitrous Oxide to Dinitrogen," LBNL-70744.
- T.A. Hanna and R.G. Bergman, "Reaction of Heterocumulenes with an Unsymmetrical Metal-Metal Bond. Addition of CO_2 Analogues Across a Zr-Ir Bond and Stoichiometric Reduction of CO_2 to Formate," LBNL-41070.

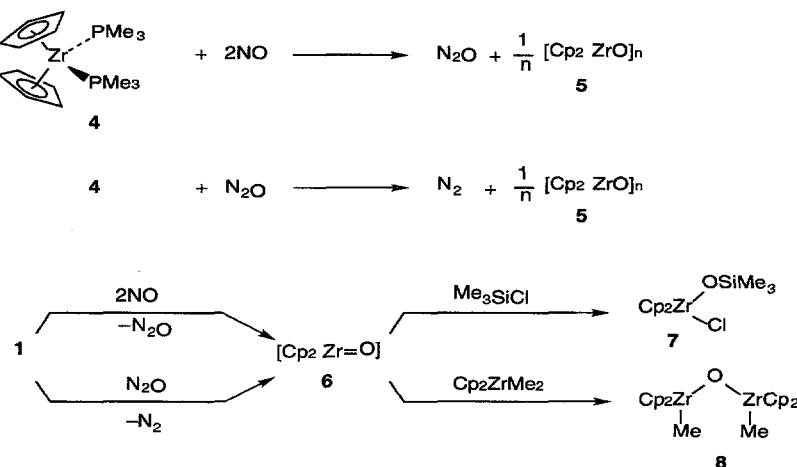


Figure 4.

Physics and Biology of Boron Neutron Capture Therapy

Principal Investigators: Eleanor Blakely, Thomas Budinger, and William Chu

Project No.: 96002

Project Description

Glioblastoma multiforme is a cancer of the brain, known for the manner in which the cancer cells extend their tendrils into surrounding healthy brain tissue. The disease is virtually inoperable, resistant to conventional radiation therapies, and always fatal, usually within six months of onset. Each year, glioblastoma multiforme kills approximately 15,000 people in the United States.

Boron Neutron Capture Therapy (BNCT) is a potential treatment procedure. BNCT uses neutron absorption in a boron nucleus to create a localized radiation that would, hopefully, be highly selective in killing the cancer cells wherever they are located in the brain.

Research into BNCT supported by this LDRD is represented by three subprojects.

Subproject 1: Influence of Micro-environmental Factors on the Uptake and Cytotoxicity of BOPP

E. Blakely (Project Leader), D. Callahan, and T. Forte, LSD; D. Deen, J. Fike, S. Kahl, J. Tibbitts, and T. Phillips, UCSF

This portion of the LDRD proposed to acquire scientific data on pharmacokinetics and toxicity of boron compounds in cells. Small and large mammals were needed to help fulfill the necessary requirements for an Investigational New Drug (IND) application for Phase I clinical trials of specific boron compounds in preparation for BNCT. In addition, work was initiated this year to investigate the lipoprotein receptor status of human glioblastoma cells. The project was conducted in Berkeley Lab and UCSF laboratories.

Accomplishments

The focus of our work during FY97 has been tumor biology of human glioma cells, including an *in vitro* screening of the low density lipoprotein (LDL) receptor status of biopsy material from the UCSF Brain Tumor Tissue Bank, and investigations of the effects of the boronated protoporphyrin (BOPP) on human endothelial cells and on the tissue distribution and systemic/organ toxicity of BOPP administered to Fischer 344 rats bearing 9L intracerebral tumors.

Specific studies included LDL receptors on glioblastoma cells (T. Forte, E. Blakely); effects of BOPP on human endothelial cells *in vitro* (J. Tibbitts, S. Kahl); and *in vivo* evaluation of BOPP in glioma models (D. Deen, J. Fike, S. Kahl, and E. Blakely).

In extending our toxicity testing of a BOPP during the past year, we have revealed some toxicities at high drug concentrations that may limit its potential application to boron neutron capture therapy and the level of preferential boron uptake by tumor cells. Our previous BOPP toxicity investigations in dogs (not bearing tumor) did not demonstrate any remarkable BOPP toxicity at 35 mg/kg. The rodent model (laden with an intracerebral tumor) did indicate preferential boron uptake into tumor versus normal brain at 35 mg/kg. However, the level of boron in the brain tumors is less than generally considered optimal for therapy, and the tumor-to-blood ratio is suboptimal. Separate studies with human umbilical cord endothelial cells indicate these cells lining the blood vessels may be specific targets of sensitivity to BOPP. Finally, the work on the tumor biology of glioma cells has uncovered a significant glioma receptor that may prove useful in the design of new BNCT compounds. These and other studies still ongoing have contributed to an IND application for BOPP which will be submitted in the first few months of 1998. The drug has been approved for use at lower drug levels with photodynamic therapy (PDT) of human brain tumors at the Royal Melbourne Hospital in Melbourne, Australia.

Subproject 2: Noninvasive Determination of Biodistribution of BNCT Compounds

T. Budinger (Project Leader), H. VanBrocklin, C. Lange, S. Taylor, K. Brennan, and J. Nagy, Center for Functional Imaging, LSD

The overall objectives of our work are to 1) develop the methodology for the radiolabeling of boronated

BNCT compounds with positron-emitting isotopes; 2) develop a noninvasive method to determine the spatial and temporal distribution of boron complexes in tumors and other tissues and to monitor blood clearance; 3) develop new and unique compounds to increase boron deposition in tumors; 4) assist in the selection of the appropriate compounds for boron neutron capture therapy in collaboration with other laboratories; and 5) to utilize PET to develop clinical strategies to maximize the boron uptake in the individual patient.

Accomplishments

We have continued our development of radiochemistry techniques for the radiolabeling of boronated compounds, specifically with ^{67}Cu and ^{64}Cu . We have continued our studies with ^{64}Cu -BOPP, utilizing a rabbit model that has diet-induced levels of blood lipoproteins and atherosclerosis development that mimic adult humans. Imaging and autoradiographic studies indicate that BOPP is taken up into the endothelial layer of the arteries. This indicates a potential hazard in the use of BOPP and other porphyrin-based BNCT compounds, arising from neutron-boron-induced damage to the brain blood vessels during neutron therapy.

We have also continued our work on the production of new BNCT compounds, including boronated residualizing disaccharides and spermine analogs. We have prepared synthetic polyamines, which are derivatives of polyamines that were originally developed as anti-tumor agents, that target tumor DNA but show relatively low cytotoxicity. These will be conjugated with boron complexes in a collaborative effort with Professor F. Hawthorne of UCLA. These conjugated products have been designed so that they can be radiolabeled by numerous radioisotopes, including ^{125}I , ^{64}Cu , ^{67}Cu , ^{76}Br , and ^{18}F .

Subproject 3: Measurement of Low-Energy Neutron Production

W. Chu (Project Leader) and B. Ludewigt from LSD; K.-N. Leung from AFRD; G. Wozniak, L. Phair, L. Moretto, and L. Beaulieu from NSD; and Nicola Colonna from INFN-Bari, Italy

We are developing an electrostatic quadrupole (ESQ) accelerator and a lithium target. The neutron production will be through the $^7\text{Li}(\text{p},\text{n})$ reaction at proton energies ~ 2.3 MeV. The ESQ accelerator will produce 2.5 MeV protons at 20 mA time-averaged

current, and a Li target will be able to remove a heat-load of 50 kW to keep the target temperature below the Li melting point (179°C). Based on our recent R&D work, we are confident that we will be able to deliver an ESQ-based clinical facility. The main goal of this study was to determine if there is an alternative reaction that would result in a simpler and less expensive accelerator and target system while satisfying all of the requirements for BNCT.

Accomplishments

We have conducted experiments at the 88-inch cyclotron (in July and August, 1997), in which neutron energy spectra were measured through time-of-flight method. The results are summarized below.

- $^9\text{Be}(\text{d},\text{n})^{10}\text{B}$ reaction, for thick and thin targets, at $E_d = 1.5$ MeV, produces abundant neutrons of energy around 400 keV, but higher-energy contamination (to > 4 MeV) is at the 30–40% level, which depends on the target thickness and somewhat on E_d as well. It is unlikely that the high-energy contaminant ever falls below an acceptable level for BNCT.
- $^{12}\text{C}(\text{d},\text{n})^{13}\text{N}$, thick target, $E_d = 0.9, 1.1, 1.3, 1.5$ MeV: There are no higher-energy contaminants produced, but the yield may be too low ($\sim 1/20$ of that of the $^7\text{Li}(\text{p},\text{n})$ reaction) to be a viable alternative.
- $^{13}\text{C}(\text{d},\text{n})^{14}\text{N}$, thin target, $E_d = 0.9, 1.1, 1.3, 1.5$ MeV: Total yield at 1.3 MeV for a thick target is estimated to be $\sim 1.62 \times 10^8$ neutrons/ $\mu\text{Coulomb}$. (Compare it with $^7\text{Li}(\text{p},\text{n})$ reaction with $E_p = 2.4$ MeV and thick target, which yields 8×10^8 neutrons/ μC , with no high-energy neutrons.) Contamination neutron energy is low (~ 1.2 MeV), which may be readily moderated.

Complete simulations of the moderation process and a dose distribution analysis in patient body have been performed for these reactions. The analyses show that we will need 1,100 and 277 mA of deuteron beams for $^{12}\text{C}(\text{d},\text{n})$ and $^{13}\text{C}(\text{d},\text{n})$ reactions, respectively, to approach the neutron flux produced by 20 mA of proton beams in $^7\text{Li}(\text{p},\text{n})$ reaction. We are continuing this investigation at the 88-inch cyclotron, supported by the FY98 LDRD.

Publications

T. Ozawa, J. Afzal, B.J. Wyrick, L.J. Hu, K.R. Lamborn, A.W. Bollen, W. F. Bauer, J.R. Fike, T.L. Phillips, E.A. Blakely, S.B. Kahl, and D.F. Deen, "In vivo Evaluation

of a Boronated Porphyrin in Malignant Glioma Models," to be presented at the Annual Meeting of the American Association of Cancer Research, New Orleans, LA, March 28–April 1, 1998.

D. Callahan *et al.*, "Boronated Protoporphyrin (BOPP) Localizes in Lysosomes of the Human Glioma Cell Line SF-767 With Uptake Modulated by Lipoprotein Levels," in preparation.

D. Deen *et al.*, "BOPP: Cytotoxicity and Pharmacokinetics in a Human Glioma Cell Model," in preparation.

D. Deen *et al.*, "BOPP: Cytotoxicity and Biodistribution in Rodent Tumor models," in preparation.

S. Kahl *et al.*, "Pharmacokinetics and Toxicology of BOPP in the Normal Canine," in preparation.

S.E. Taylor, J.P. O'Neil, S. Kahl, and T.F. Budinger, "Preparation of a ⁶⁴Cu-Labeled Boronated Porphyrin and Its Use in Biodistribution and Imaging Studies," in preparation.

T.F. Budinger and S.E. Taylor, "In Vivo Assessment of BNCT-Compound Biodistribution," oral reports to the DOE-sponsored Clinical State of Boron Neutron Therapy Workshop, Charlotte, NC, 1997.

physiologically characterized using the BIOLOG system. The study applied, compared, and correlated different microbial community assessment techniques and provided data for a pending major reference research article for future studies.

Microbial ecology and evolution of microorganisms in damaged environments have been emerging areas of research that focus on indigenous microbial communities and their ability to carry out intrinsic bioremediation. Microbial communities in nature are complex, highly integrated, dynamically changing, and diverse assemblies of microbial populations. They offer an unmatched source of biological diversity that is not well documented, because in fact only a small fraction (less than 1%) of naturally occurring microorganisms have been "cultured" and studied using standard selective and enrichment isolation methods. Consequently, new approaches are needed in environmental biotechnology which, combined with new culture techniques, better document microbial diversity. Our work continued to 1) clone and sequence ssrRNA genes isolated directly from the environment for community characterization without need for cultivation, 2) study signature lipid biomarker analysis of the same environmental samples and compare results with that of the ssrRNA gene sequencing, and 3) develop novel isolation techniques and use rapid identification methods. Additional physiological characterization of the new isolates using the BIOLOG system added a new level of comparison to the project.

Use of Gene Sequencing, Signature Lipid Biomarker Analysis, and Microbial Physiology Testing—A Polyphasic Approach to Assess and Monitor Microorganisms in Damaged Environments

Principal Investigators: Stanley Goldman and Tamas Torok

Project No.: 96047

Project Description

This project utilizes small subunit ribosomal (ssr)RNA gene sequencing and signature lipid biomarker analysis to survey and characterize selected microbial ecosystems in damaged environments. Also, newly isolated intrinsic microorganisms were

Accomplishments

Last year we worked with several dozen soil, sediment, and water samples from random sites with different organic matter content, collected from the now closed Alameda Naval Air Station, selenate- and selenite-contaminated agricultural run-offs from the Central Valley in California, and subsurface rock samples from the Test Area North (TAN) site in Idaho. Also, we isolated several microorganisms from an *ex situ* bioreactor that remediates methyl ethyl ketone (MEK).

To isolate large numbers of intrinsic microorganisms, isolation and culturing techniques simulated the natural environment where the sample was collected. Soil and rock extract were prepared from either pristine or contaminated samples or from a standard commercially available potting soil and added to media. Low-nutrient media were often used with low agar or gellan-gum content, which provided a more colloidal growth environment. Additionally, selective

isolation media for actinomycetes, heterotrophic bacteria, sulfur oxidizers, autotrophs, and fungi were chosen. Cultures were incubated in the dark at room temperature or below. After isolation and preliminary screening, cultures were preserved immediately to avoid the potential damage from further subculturing and maintained at -80°C.

Prior to DNA extraction, microorganisms were grown and harvested by centrifugation. Several DNA extraction protocols were adapted. PCR amplification of small subunit rRNA genes was optimized. Primer sequences were derived from *Escherichia coli* for bacteria, and from *Saccharomyces cerevisiae* for eukaryotes. Following cycle sequencing with dye terminators, automatic sequencing was performed with an ABI PRISM 377 DNA Sequencer. Edited ssrRNA gene sequences were analyzed and aligned with the help of the Ribosomal Database Project and other online software protocols.

Sample preparation protocol for fatty acid methylester analysis (FAME) was provided by MIDI, manufacturer of the Microbial Identification System. Sherlock version 2.01 (MIDI) was used for peak naming, database comparison, strain identification, and 2D plot and dendrogram analysis.

Procedures for sample preparation, microbial identification, and relationship analysis using a BIOLOG MicroLog 3 System followed manufacturers' recommendations.

During FY97 dozens of environmental samples were characterized and several hundred strains isolated and preserved. The molecular-level genotypic and phenotypic description of intrinsic microbial communities helped us to better understand the samples, the activity of microorganisms, their fate, and influence. Through collaboration with other projects, six student interns participated, learned, and used new techniques. Important scientific topics, such as the phylogenetic discrimination of close relatives in the nonproliferation project, characterizing rock-inhabiting and TCE-degrading microorganisms or those growing on MEK as the sole carbon source, could be dealt with. The success of this LDRD project is measured by the amount of data collected for a reference manuscript.

This work will continue in FY98, with the application of ssrRNA gene sequences used with a microarray method to survey the environment for the relative abundance of diverse individual sequences in complex DNA samples.

Publications

T. Torok, S. Goldman, and J.C. Hunter-Cevera, "Polyphasic Characterization of Intrinsic Microbial Communities in Damaged Environments," poster presentation to the American Society of Microbiology General Meeting, Miami Beach, FL, May, 1997.

T. Torok, S. Goldman, and J.C. Hunter-Cevera, "Who Is Out There? What Is It Doing? The Pros and Cons of Polyphasic Characterization of Microbial Communities," poster presentation to the 8th European Congress for Biotechnology, Budapest, Hungary, August, 1997.

T. Torok, S. Goldman, and J.C. Hunter-Cevera, "The Pros and Cons of Polyphasic Characterization of Microbial Communities in Damaged Environments," (invited paper) American Chemical Society Meeting, Pittsburgh, PA, September, 1997.

T. Torok, S. Goldman, and J.C. Hunter-Cevera, "Polyphasic Characterization of Microorganisms Isolated from Contaminated Environments," to be submitted to *Applied Environ. Microbiol.*

Large-Scale Computing for Nuclear Physics and High Energy Physics Experiments

Principal Investigators: William Johnston, William Greiman, Gary Hoo, Jason Lee, Stewart Loken, Brian Tierney, Craig Tull, and Douglas Olson

Project No.: 97032

Project Description

Future experiments in high energy and nuclear physics face enormous computing challenges. The STAR experiment at RHIC will collect more than 10^7 events per year, generating more than 10^{14} bytes per year of data. Data sets for the LHC experiments will be larger. Models for handling large volumes of data and making them available to members of a worldwide collaboration are still under development—a common element between high energy and nuclear physics. It is expected that the data will be distributed to a collection of regional centers. This project was to develop a Particle Data Storage Facility (PDSF) as one of these centers. Large amounts of CPU power are

needed for simulation of these experiments. The current PDSF can contribute a substantial fraction of this for STAR and ATLAS. Computer code for this next generation of experiments will require a paradigm shift from the present structure to an object-oriented approach that will permit extensive software reuse. This pilot project utilized PDSF processor farm to address issues of tracking in the BaBar, STAR, and ATLAS experiments.

Immediate effective exploitation of the PDSF is essential if it is to have any long-term future. By concentrating in the short term on operating a successful system that is used by physicists from outside of Berkeley Lab, the basis for future expansion and exploitation can be established. Such outside support is vital if long-term funding from DOE is to be obtained. There is an immediate demand for CPU cycles for simulation work on ATLAS and STAR and for analysis of NA49 data. PDSF can satisfy a significant portion of this demand. The development of a data distribution model is aimed at satisfying the demand from high energy and nuclear physics experiments for an efficient system of data distribution to many geographically distributed collaborators. It is essential that the model be scalable to the very large collaborations for the LHC. Finally, we also investigated emerging technologies for the development of large, reusable software systems. We developed codes to address specific tracking problems and then worked to abstract these into object libraries.

Accomplishments

The physics data handling experiment is divided into several parts and specifically was applied to a realistic application environment called STAR Analysis Framework (STAF). In the first part we are trying to model the analysis environment. In a production configuration, it is expected that several hundred processors will operate in parallel, each on a single experiment "event" (1–10 megabytes of data). The data archive query interface will select a set of tapes and records on the tertiary storage system. The current model has the storage system interface being 3–5 high-speed tape drives operating in parallel (each of which delivers about 9 megabytes/s). This data is written to a Distributed-Parallel Storage System (DPSS) from which STAF accesses the data.

Performance for the STAF application accessing data in the cache was measured using a DPSS configuration of three disk servers with two disks per server. STAF requests that data be loaded into

memory-resident objects that are defined by serialized (XDR-encoded) records. Deserializing, in turn, causes data requests to be made through the DPSS file semantics interface which collects blocks from the DPSS servers, buffers them, and provides access to the buffer. The throughput rates are measured as data is delivered to the STAF physics analysis modules, a path that includes translating the data to the appropriate machine format and structuring it in memory (both of which are very fast operations). With a single instance of STAF running on a Sun E4000 system with an OC-12 (622 megabytes/s) ATM interface, a data rate of 22 megabytes/s is achieved for reading data, and 30 megabytes/s for writing data.

Another area examined was an experiment in high-speed, wide-area distributed data handling with many clients.

We saw that the first-level data from the instrument system flows from the instrument, through the network, to a receiving cache. The DPSS is used for this cache, the servers of which may be located at one site, or (as in the MAGIC testbed) distributed across many sites. The first level of processing can be done directly out of the cache. The first-level data is also moved from cache to tertiary storage, and the results of this processing can be used to optimize data placement on tertiary storage. (As noted above, the write rates into the DPSS should be sufficient for this approach.)

It is our contention that in the time frame of the next generation of physics experiments (2000–2005 AD), wide-area networks will be easily capable of distributing the instrument output data stream anywhere in the U.S. (and probably to Europe).

Distributing experimental data has two potential advantages. The first-level processing (which is easily parallelized) can be done using resources at the collaborators' sites (each experiment typically involves 5–10 major institutions). Second, large tertiary storage systems exhibit substantial economies of scale. Using a large tertiary storage system at a supercomputer center, for example, should result in more economical storage, better access (because of much larger near-line systems—e.g., lots of tape robots), and better media management, especially in the long term, than can be obtained in local systems.

We tested the wide-area aspects of the framework in the following experiment. The NTON network testbed that connects Berkeley Lab and Lawrence Livermore National Laboratory (LLNL) can be

configured for a 2000 km, OC-12 path (by using the 16 OC-12 SONET paths that make up the 400 km underlying network). A high-speed workstation that has a collection of STAR events stored on its disks is located at LLNL and connected to NTON. This workstation will emit events at the same rate as the STAR detector, and this data will be cached on the DPS at Berkeley Lab. The Lab's computing cluster will process data out of the cache (doing "reconstruction") and those results will be written back to the cache. A storage manager will migrate data to tertiary storage (or a "null" system that has the same throughput characteristics, as there is little point in actually storing this synthetic data).

Except that the computing cluster will not have sufficient compute capacity to do all of the required processing at the operating data rates, once this scenario works as expected, it should demonstrate the feasibility of wide-area processing of this type of real-time data. The experiment is illustrated in Figure 1.

Publications

W.E. Johnston, W. Greiman, G. Ho, J. Lee, B. Tierney, C. Tull, and D. Olson, "High Performance Networking and Computing," Proceedings of ACM/IEE SC97, San Jose, CA, November 12-15, 1997.

W. Johnston, G. Jin, C. Larsen, J. Lee, G. Hoo, M. Thompson, B. Tierney, and J. Terdiman, "Real-Time Generation and Cataloguing of Large Data-Objects in Widely Distributed Environments," to be published in *International Journal of Digital Libraries*, special issue on "Digital Libraries in Medicine." Available at <http://www-itg.lbl.gov/WALDO>.

W. Greiman, W. E. Johnston, C. McParland, D. Olson, B. Tierney, and C. Tull, "High-Speed Distributed Data Handling for HENP," International Conference on Computing in High Energy Physics, Berlin, Germany, April, 1997. Also available at <http://www-itg.lbl.gov/STAR>.

D. Olson, C. McParland, W. Johnston, and W. Greiman, "HENP Data Analysis Requirements," http://www-rnc.lbl.gov/computing/ldrd_fy97/html/star_reqs.htm.

W. Greiman, W. E. Johnston, C. McParland, D. Olson, B. Tierney, and C. Tull, "High Speed Distributed Data Handling for HENP," http://www-rnc.lbl.gov/computing/ldrd_fy97/henpdata.htm.

C. Tull, W. Greiman, D. Olson, D. Prindle, and H. Ward, "The STAR Analysis Framework Component Software in a Real-World Physics Experiment," International Conference on Computing in High Energy Physics, Berlin, Germany, April, 1997.

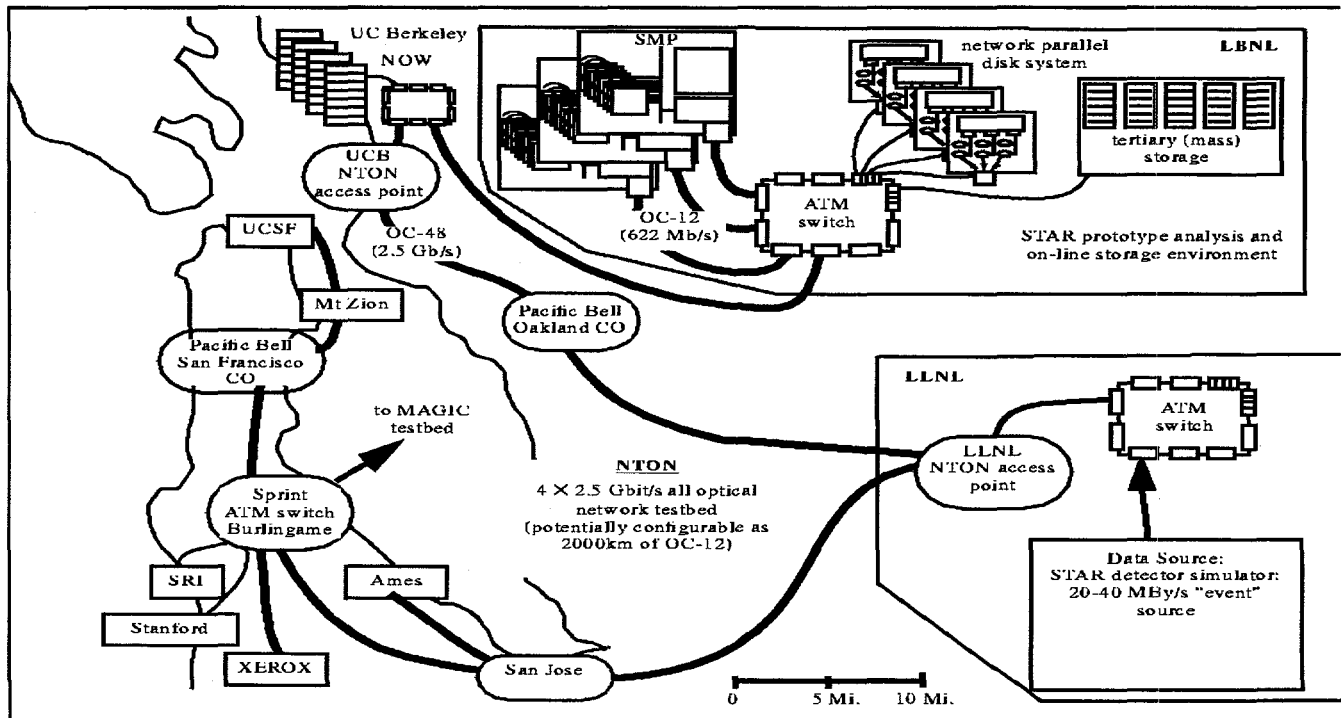


Figure 1. The distributed processing experiment.

Acronyms and Abbreviations

| | | | |
|-------|--|-----------|---|
| AFM | atomic force microscopy | LLNL | Lawrence Livermore National Laboratory |
| ALS | Advanced Light Source | MAD | multiwavelength anomalous diffraction |
| APT | automated patrol telescope | MAR | matrix attachment region |
| ASIC | application-specific integrated circuit | MC | Monte Carlo |
| ATWR | analog transient waveform recorder | MCD | molecular circular dichroism |
| BLISS | Building Lifecycle Information Systems | MCP | microchannel plate |
| BNCT | boron neutron capture therapy | MD | molecular dynamics |
| BNL | Brookhaven National Laboratory | MIR | multiple isomorphous replacement |
| BOPP | boronated protoporphyrin | MPP | massively parallel processors |
| bp | base pairs | MRI | magnetic resonance imaging |
| CAC | chromatin assembly complex | MSCD | multiple scattering in cluster diffraction |
| CAF | chromatin assembly factor | NASA | National Aeronautics and Space Administration |
| CCD | charge-coupled device | NERSC | National Energy Research Scientific Computing Center |
| CDF | collider detector at Fermilab | NIH | National Institutes of Health |
| CERN | European Organization for Nuclear Research | NOW | network of workstations |
| CFD | computational fluid dynamics | NMR | nuclear magnetic resonance |
| CLPP | community-level physiological profile | NSF | National Science Foundation |
| CMT | computed microtomography | OSHA | Occupational Safety and Health Administration |
| CMB | cosmic microwave background | OTT | Office of Transportation Technologies, DOE |
| COMPS | computing on clusters of multiprocessor systems | PAH | polycyclic aromatic hydrocarbon |
| CPU | central processing unit | PCR | polymerase chain reaction |
| DNA | deoxyribonucleic acid | PDSF | particle data storage facility |
| DOD | Department of Defense | PDT | photodynamic therapy |
| DOE | Department of Energy | PEEM | photoemission electron microscopy |
| DOS | density of states | PIC | particle in cell |
| DPSS | distributed parallel storage systems | PNNL | Pacific Northwest National Laboratory |
| DSP | digital signal processor | PVM | parallel virtual machine |
| EA | electron affinity | rf | radio frequency |
| ECM | extracellular matrix | RHIC-STAR | Relativistic Heavy-Ion Collider—Solenoidal Tracker at RHIC. |
| ECR | electron cyclotron resonance | rRNA | ribosomal ribonucleic acid |
| EPA | Environmental Protection Agency | SAMS | self-assembled monolayers |
| ESNet | Energy Sciences Network | SELECT | a computer framework |
| EPR | electron paramagnetic resonance | SETAC | Society of Environmental Toxicology and Chemistry |
| ETC | equal thickness contour | SMD | single molecule detection |
| EXAFS | x-ray absorption fine structure spectroscopy | SMP | symmetric multiprocessor |
| FAME | fatty acid methyl ester | SMS | single molecule spectroscopy |
| FG | ferrofluid for guiding liquids | SSC | Superconducting Super Collider |
| FTSI | Fourier transform spectral interferometry | SFG | sum frequency generation |
| GAs | genetic algorithms | SPFM | scanning polarization force microscopy |
| GRB | gamma-ray burst | spFRET | single-pair fluorescence resonance energy transfer |
| GRO | gamma-ray observatory | SQUID | superconducting quantum interference device |
| HIF | heavy-ion fusion | | |
| IC | integrated circuit | | |
| JPL | Jet Propulsion Laboratory | | |
| LBNL | Lawrence Berkeley National Laboratory ("Berkeley Lab") | | |
| LDRD | Laboratory Directed Research and Development | | |
| LHC | Large Hadron Collider | | |

| | | | |
|-------|--|-------|---|
| STAF | STAR Analyzer Framework | U-Net | Cornell University's network interface |
| SXEER | soft-x-ray endstation for environmental research | U.S. | architecture |
| TEM | transmission electron microscopy | URL | United States |
| TPPE | two-photon photoemission | UV | universal resource locator |
| UHV | ultra-high vacuum | VIA | ultraviolet |
| UCB | University of California, Berkeley | VUV | virtual interface architecture |
| UCSD | University of California, San Diego | XANES | vacuum ultraviolet |
| UCSF | University of California, San Francisco | | x-ray absorption near-edge spectroscopy |
| U.K. | United Kingdom | XM | microprobe |
| | | | x-ray microscopy |